

THE IMAGE-ENHANCED OPERATING ENVIRONMENT IN  
ROBOT ASSISTED LAPAROSCOPIC PARTIAL  
NEPHRECTOMY

Archie Hughes-Hallett BMBS, BMedSci, MRCS

The Department of Surgery and Cancer, Division of Surgery,  
St Mary's Hospital, Imperial College London

Doctor of Philosophy (PhD) 2015

Supervisors: Professor the Lord Darzi of Denham, Dr Philip Pratt, Mr Erik Mayer and Mr  
Justin Vale

## DECLARATION OF ORIGINALITY

This thesis is submitted to Imperial College of Science, Technology and Medicine in partial fulfilment of the requirements for the degree of Doctor of Philosophy. Except for where indicated, it presents entirely my own work and describes the results of my own research.

The copyright of this thesis rests with the author and is made available under a Creative Commons Attribution Non-Commercial No Derivatives licence. Researchers are free to copy, distribute or transmit the thesis on the condition that they attribute it, that they do not use it for commercial purposes and that they do not alter, transform or build upon it. For any reuse or redistribution, researchers must make clear to others the licence terms of this work.



*“Surgeons without anatomy are like moles: they work in the dark and the work of their hands are molehills”*

Friedrich Tiedmann (1781-1861)

## ABSTRACT

In the last twenty-five years surgical practice has undergone radical change. Although this change has heralded improved patient outcomes it has also presented a new set of problems centred around the reduction in sensory inputs received by the modern surgeon. A potential solution to mitigate for this sensory loss is image guidance.

The thesis has its heart four guiding aims:

- 1) *To define the window of opportunity for the development of an image guidance platform for intra-abdominal MIS.*
- 2) *To establish whether there is a user need for image guidance in RAPN.*
- 3) *To better understand the fundamental safety and behavioural implications of the implementation of an IEOE.*
- 4) *To develop and validate a novel approach to image guidance in partial nephrectomy, utilising the preceding evidence base to inform this development.*

The first of these aims was met, through the development of a novel metric of innovation, with the growth potential of image guidance in abdominal surgical oncology subsequently examined. The second was addressed using a qualitative survey of robotic urologists. These two studies demonstrated that image guidance in intra-abdominal surgery lies in a period of rapid innovation growth, and that demand exists for image guidance in partial nephrectomy amongst the target population.

In order to meet the third of the outlined aims, two potential drawbacks of augmenting the surgeon's intraoperative view were examined, namely: inattention blindness, and the reliability and accuracy of the most commonly used method of image preparation: segmentation.

Prior to the development of the platform the limitations of existing research platforms were examined and the problems needing to be addressed for efficacious image guidance were defined as part of a systematic review into image guidance in RAPN. These problems can be distilled down to issues pertaining to: *image preparation, registration, deformation compensation, and display.*

Informed by this review and the findings of the previous thesis chapters a dual modality platform was developed capitalising on the respective strengths of pre- and intraoperative

imaging to deliver an image guidance solution offering significant benefit for both planning and execution phases.

Overall, this thesis has systematically devised, and evidenced a first generation dual modality image guidance platform for partial nephrectomy, meeting the differing guidance needs for specific operative steps.

## ACKNOWLEDGEMENTS

*Teamwork is the ability to work together toward a common vision. The ability to direct individual accomplishments toward organizational objectives. It is the fuel that allows common people to attain uncommon results.*

Andrew Carnegie (1835 - 1919)

Like any academic endeavour the work presented in this thesis has not been undertaken in isolation. I would like to take this opportunity to thank those who have helped and supported me along the way. Although there are many people who have been involved a few deserve specific mention.

First and foremost, I would like to thank Erik Mayer, Justin Vale and Ara Darzi who have allowed me to achieve that which I set out to do three years ago, both as an academic and clinician, through the opportunities they have presented to me. I would also like to offer particular thanks to Philip Pratt, without whose engineering wizardry, clinical focus and patience the development of the platform outlined herein would not have been possible. I am forever indebted to them for their supervision, guidance and support.

To the clinical collaborators who have been involved in this project, in particular Alex Mottrie and Bijan Khoubehi. Without their cases and feedback the tablet-based guidance platform would not have got the stage of development that it has.

I would also like to offer a special thanks to my office colleagues and collaborators: Hani Marcus, Thomas Cundy and Richard Kwasnicki. Without the discussion and collaboration that has taken place within the confines of the office my thesis would have been of considerably poorer quality. Their input has been invaluable and their company has been, without fail, excellent.

To my parents who are a source of constant support and inspiration, they have shown remarkable patience over the course of my thesis (and life) listening to me talk for hours about subjects of which they have limited understanding and even less interest.

Finally, to my girlfriend Sophie who has put up with my moments of frustration and elation over the course of the data collection and write-up phases of this project and in-so-doing has demonstrated an amazing ability to feign interest and excitement over my achievements.

## PUBLICATIONS ARISING FROM THIS THESIS

1. **Hughes-Hallett, A.**, Mayer, E. K., Marcus, H. J., Cundy, T. P., Pratt, P. J., Darzi, A. W, Vale, J. A. (2014). Augmented reality partial nephrectomy: Examining the current status and future perspectives. *Urology*, 83(2), 266-273
2. **Hughes-Hallett, A.**, Mayer, E. K., Marcus, H. J., Cundy, T. P., Pratt, P. J., Parston, G., Darzi, A. W. (2014). Quantifying Innovation in Surgery. *Annals of Surgery*, 260(2), 205-211.
3. **Hughes-Hallett, A.**, Mayer, E., Pratt, P., Vale, J., Darzi, A. (2015). Quantitative analysis of technological innovation in minimally invasive surgery. *British Journal of Surgery*. (Epub ahead of print)
4. **Hughes-Hallett, A.**, Mayer, E. K., Pratt, P., Mottrie, A., Darzi, A., & Vale, J. (2014). The current and future use of imaging in urological robotic surgery: A survey of the European Association of Robotic Urological Surgeons. *International Journal of Medical Robotics and Computer Assisted Surgery*
5. **Hughes-Hallett, A.**, Mayer, E., Marcus, H., Pratt, P., Mason, S., Darzi, A., Vale, J. (2015). Inattention Blindness in Surgery. *Surgical Endoscopy*. (Epub ahead of print)
6. **Hughes-Hallett, A.**, Pratt, P., Mayer, E., Clark, M., Vales, J., Darzi A. (2015). Using preoperative imaging for intraoperative guidance: A case of mistaken identity. *International Journal of Medical Robotics and Computer Assisted Surgery*. (Epub ahead of print)
7. **Hughes-Hallett, A.**, Pratt, P., Mayer, E., Martin, S., Darzi, A., & Vale, J. (2014). Image guidance for all - Tilepro display of 3-dimensionally reconstructed images in robotic partial nephrectomy. *Urology*, 84(1), 237-242.
8. **Hughes-Hallett, A.**, Pratt, P., Mayer, E., Martin, S., Darzi, A., & Vale, J. (2014). Reply. *Urology*, 84(1), 243.
9. **Hughes-Hallett, A.**, Pratt, P., Mayer, E., Di Marco, A., Yang, G. -Z., Vale, J., Darzi, A. (2014). Intraoperative ultrasound overlay in robot-assisted partial nephrectomy: First clinical experience. *European Urology*, 65(3), 671-672.
10. Pratt, P., Jaeger, A., **Hughes-Hallett, A.**, Mayer, E., Vale, J., Darzi, A., ... & Yang, G. Z. (2015). Robust ultrasound probe tracking: initial clinical experiences during robot-assisted partial nephrectomy. *International journal of computer assisted radiology and surgery*, 10(12), 1905-1913.

11. Pratt, P., **Hughes-Hallett, A.**, Zhang, L., Patel, N., Mayer, E., Darzi, A., & Yang, G. Z. (2015). Autonomous Ultrasound-Guided Tissue Dissection. In *Medical Image Computing and Computer-Assisted Intervention--MICCAI 2015* (pp. 249-257).

## OTHER PUBLICATIONS ARISING FROM WORK RELATED TO THIS THESIS

1. Sridhar, A. N., **Hughes-Hallett, A.**, Mayer, E. K., Pratt, P. J., Edwards, P. J., Yang, G. -Z., Vale, J. A. (2013). Image-guided robotic interventions for prostate cancer. *Nature Reviews Urology*, 10(8), 452-462. (joint first author)
2. **Hughes-Hallett, A.**, Mayer, E., Pratt, P., Mottrie, A., Darzi, A., & Vale, J. (2014). A census of robotic urological practice and training: a survey of the robotic section of the European Association of Urology. *Journal of Robotic Surgery*.
3. Marcus, H. J., Cundy, T. P., **Hughes-Hallett, A.**, Yang, G. -Z., Darzi, A., & Nandi, D. (2014). Endoscopic and keyhole endoscope-assisted neurosurgical approaches: A qualitative survey on technical challenges and technological solutions. *British Journal of Neurosurgery*, 28(5), 606-610.
4. Marcus, H. J., **Hughes-Hallett, A.**, Cundy, T. P., Di Marco, A., Pratt, P., Nandi, D., Yang, G. -Z. (2014). Comparative Effectiveness of 3-Dimensional vs 2-Dimensional and High-Definition vs Standard-Definition Neuroendoscopy: A Preclinical Randomised Crossover Study. *Neurosurgery*, 74(4), 375-380.
5. Marcus, H. J., Pratt, P., **Hughes-Hallett, A.**, Cundy, T. P., Marcus, A. P., Yang, G-Z., Darzi, A., Nandi, D. Comparative effectiveness and safety of image guidance systems in neurosurgery: a preclinical randomised study. *Journal of Neurosurgery*. [Epub ahead of print]
6. Marcus, H. J., **Hughes-Hallett, A.**, Kwasnicki, R., Darzi, A., Yang, G. Z., Nandi, D. (2015) Technological innovation in neurosurgery: a quantitative study. *Journal Neurosurgery*, 123(1):174-81
7. Marcus, H. J., Payne, C. J., **Hughes-Hallett, A.**, Gras, G., Leibrandt, K., Nandi, D., & Yang, G. Z. (2015). Making the Leap: the Translation of Innovative Surgical Devices From the Laboratory to the Operating Room. *Annals of surgery*.



## ORAL PRESENTATIONS ARISING FROM THIS THESIS

1. **Hughes-Hallett, A.**, Pratt, P., Novara, G., Vale, J., Mottrie, A., Darzi, D., Mayer, E. Image-guided robot assisted partial nephrectomy: An assessment of efficacy. European Association of Urology Congress (EAU) 2015
2. **Hughes-Hallett, A.**, Pratt, P., Mayer, E., Vale, J., Darzi, A., Augmented reality ultrasound guided tumour resection in partial nephrectomy. Division of Surgery and Cancer, Imperial College London, Annual Research Afternoon, December 2014.  
\*\*Winner best oral presentation
3. **Hughes-Hallett, A.**, Pratt, P., Mayer, E., Vale, J., Darzi, A., Augmented reality partial nephrectomy. Travelling surgical society. October 2014.
4. **Hughes-Hallett, A.**, Pratt, P., Mayer, E., Vale, J., Darzi, D., Augmented reality in robotic partial nephrectomy utilizing intraoperative ultrasound. European Robotic Urology Congress (ERUS) 2014
5. **Hughes-Hallett, A.**, Mayer, E., Pratt, P., Vale, J., Darzi, D., Quantifying Innovation in Robotic Surgery. Hamlyn Symposium on Medical Robotics '14
6. Marcus, HJ., **Hughes-Hallett, A.**, Pratt, P., Clark, J., D Nandi, Darzi, A., Yang, GZ.. Operative Working Spaces in Keyhole Neurosurgery: An MRI Study. Hamlyn Symposium on Medical Robotics 2013
7. Pratt, P., **Hughes-Hallett, A.**, Di Marco, A., Cundy, T., Mayer, E., Vale, J., Darzi, A., Yang, GZ. Multimodal Reconstruction for Image-Guided Interventions. Hamlyn Symposium on Medical Robotics 2013

## ORAL PRESENTATIONS ARISING FROM WORK RELATED TO THIS THESIS

1. **Hughes-Hallett, A.**, Mayer, E., Cundy, T., Pratt, P., Mottrie, A., Darzi, A., Vale, J. Determining satisfaction of training needs for robotic surgery: A predictive model. European Robotic Urology Congress (ERUS) 2014 \*\* Winner best abstract and presentation
2. Di Marco, A., Pratt, P., Jeyakumar, J., **Hughes-Hallett, A.**, Cundy, T., Yang, G-Z., Darzi, A., Validation of a Novel Stereoscopic Viewer for Transanal Endoscopic Microsurgery. American College of Surgeons 2013

## EXACT DETAILS OF CONTRIBUTIONS

All of the work carried out in this thesis was undertaken by me, however as part of the process of developing the proposed image guidance platform and in performing the outlined studies other individuals were involved. The details of their contributions are below. The thesis was overseen by my supervisors Professor the Lord Ara Darzi, Mr Justin Vale, Mr Erik Mayer and Dr Philip Pratt.

CHAPTER 4: The illustrative case was performed by Mr Justin Vale and the software utilised to generate the image overlay was written by Dr Philip Pratt

CHAPTER 7: The software component of the platform was written by Dr Philip Pratt. Clinical cases were performed by Mr Justin Vale, Dr Alex Mottrie (OLV clinic, Aalst, Belgium) and Mr Bijan Khoubehi (Chelsea and Westminster NHS trust, London, UK).

CHAPTER 8: *Intraoperative ultrasound overlay in RAPN*: Software and algorithms were written for the platform by Dr Philip Pratt and Alex Jager. Clinical cases performed by Mr Justin Vale.

*Augmented reality freehand 3D ultrasound*: Software and algorithms for the platform were written by Philip Pratt.

# TABLE OF CONTENTS

<b>DECLARATION OF ORIGINALITY</b>	<b>2</b>
<b>ABSTRACT</b>	<b>4</b>
<b>ACKNOWLEDGEMENTS</b>	<b>6</b>
<b>PUBLICATIONS ARISING FROM THIS THESIS</b>	<b>8</b>
<b>OTHER PUBLICATIONS ARISING FROM WORK RELATED TO THIS THESIS</b>	<b>10</b>
<b>ORAL PRESENTATIONS ARISING FROM THIS THESIS</b>	<b>11</b>
<b>ORAL PRESENTATIONS ARISING FROM WORK RELATED TO THIS THESIS</b>	<b>12</b>
<b>EXACT DETAILS OF CONTRIBUTIONS</b>	<b>13</b>
<b>LIST OF FIGURES</b>	<b>19</b>
<b>LIST OF ACRONYMS</b>	<b>25</b>
<b>CHAPTER 1: INTRODUCTION</b>	<b>27</b>
1.1 PROLOGUE	28
1.2 INNOVATING IN SURGICAL TECHNOLOGY AND IMAGE GUIDANCE	30
1.3 HAPTIC REPLACEMENT	34
1.4 IMAGE-ENHANCED OPERATING ENVIRONMENT	36
1.4.1 SAFETY OF IMAGE GUIDANCE AND THE IMAGE-ENHANCED OPERATING ENVIRONMENT	37
1.5 CURRENT CLINICAL APPLICATIONS OF IMAGE-ENHANCED OPERATING ENVIRONMENT	38
1.5.1 NEUROSURGERY	38
1.5.2 INTRA-ABDOMINAL IMAGE GUIDANCE	38
1.5.3 PARTIAL NEPHRECTOMY	39
1.6 THESIS OVERVIEW, AIMS AND OBJECTIVES	42
<b>CHAPTER 2: ASSESSMENT OF INNOVATION POTENTIAL</b>	<b>44</b>
2.1 INTRODUCTION	45
2.2 METHODS	46
2.2.1 PATENT AND PUBLICATION DATA COLLATION	46
2.2.2 NORMALISATION OF DATA	46

2.2.3	PATENT CODES	49
2.2.4	ESTABLISHING THE TOP PERFORMING AND EMERGING TECHNOLOGY CLUSTERS	49
2.2.5	QUALIFYING GROWTH IN IMAGE-GUIDED SURGERY	51
2.2.6	STATISTICAL ANALYSIS	51
<b>2.3</b>	<b>RESULTS</b>	<b>51</b>
2.3.1	DATA ON PATENTS AND PUBLICATIONS	51
2.3.2	TOP PERFORMING TECHNOLOGY CLUSTERS	52
2.3.3	SUB-ANALYSIS OF IMAGE GUIDANCE CLUSTER	53
<b>2.4</b>	<b>DISCUSSION</b>	<b>63</b>
2.4.1	PRINCIPAL FINDINGS	63
2.4.2	GROWTH IN IMAGE GUIDANCE	64
2.4.3	COMPARISON WITH OTHER STUDIES	65
2.4.4	STUDY LIMITATIONS	67
<b>2.5</b>	<b>CONCLUSIONS</b>	<b>68</b>
 <b><u>CHAPTER 3: THE CURRENT AND FUTURE USE OF IMAGING IN UROLOGICAL ROBOTIC SURGERY: A SURVEY OF THE EUROPEAN ASSOCIATION OF ROBOTIC UROLOGICAL SURGEONS</u></b>		<b>69</b>
<b>3.1</b>	<b>INTRODUCTION</b>	<b>70</b>
<b>3.2</b>	<b>METHODS</b>	<b>72</b>
3.2.1	RECRUITMENT	72
3.2.2	SURVEY DESIGN AND ADMINISTRATION	72
3.2.3	SURVEY CONTENT	73
<b>3.3</b>	<b>RESULTS</b>	<b>75</b>
3.3.1	DEMOGRAPHICS	75
3.3.2	CONTEMPORARY USE OF IMAGING IN ROBOTIC SURGERY	75
3.3.3	DESIRE FOR AUGMENTED REALITY	82
<b>3.4</b>	<b>DISCUSSION</b>	<b>82</b>
3.4.1	PRINCIPAL FINDINGS	82
3.4.2	COMPARISON WITH OTHER STUDIES	83
3.4.3	STUDY LIMITATIONS	84
<b>3.5</b>	<b>CONCLUSIONS</b>	<b>85</b>
 <b><u>CHAPTER 4: ASSESSING THE IMPACT OF IMAGE GUIDANCE ON SURGICAL INATTENTION BLINDNESS</u></b>		<b>86</b>
<b>4.1</b>	<b>LITERATURE REVIEW</b>	<b>87</b>

4.1.1	METHODS	87
4.1.2	RESULTS	88
4.1.3	DISCUSSION	92
4.1.4	CONCLUSIONS	93
<b>4.2</b>	<b>INATTENTION BLINDNESS IN SURGERY: THE EFFECTS OF COGNITIVE LOAD AND IMAGE GUIDANCE</b>	<b>95</b>
4.2.1	INTRODUCTION	95
4.2.2	METHODS	95
4.2.3	RESULTS	99
4.2.4	DISCUSSION	103
4.2.5	CONCLUSIONS	107
<b>CHAPTER 5: PREOPERATIVE IMAGING AND GUIDANCE</b>		<b>108</b>
<b>5.1</b>	<b>INTRODUCTION</b>	<b>109</b>
<b>5.2</b>	<b>METHODS</b>	<b>110</b>
5.2.1	STATISTICAL ANALYSIS	113
<b>5.3</b>	<b>RESULTS</b>	<b>113</b>
5.3.1	OVERALL	113
5.3.2	RATER EXPERIENCE AND SEGMENTATION ACCURACY	114
5.3.3	TUMOUR TYPE AND SEGMENTATION ACCURACY	117
5.3.4	LOCATION OF BOUNDARY MISIDENTIFICATIONS	117
<b>5.4</b>	<b>DISCUSSION</b>	<b>119</b>
5.4.1	PRINCIPAL FINDINGS	119
5.4.2	COMPARISON WITH OTHER STUDIES	120
5.4.3	STUDY LIMITATIONS	120
<b>5.5</b>	<b>CONCLUSIONS</b>	<b>121</b>
<b>CHAPTER 6: AUGMENTED REALITY PARTIAL NEPHRECTOMY: EXAMINING CURRENT STATUS AND FUTURE PERSPECTIVE</b>		<b>122</b>
<b>6.1</b>	<b>INTRODUCTION</b>	<b>123</b>
<b>6.2</b>	<b>LITERATURE SEARCH</b>	<b>124</b>
6.2.1	SEARCH STRATEGY	124
<b>6.3</b>	<b>PRINCIPLES OF REGISTRATION</b>	<b>126</b>
6.3.1	SURFACE-BASED REGISTRATION	127
6.3.2	3D-CT STEREOSCOPIC IMAGE REGISTRATION	132
6.3.3	ORGAN TRACKING	133

6.3.4	INTRA-OPERATIVE IMAGING AND FIDUCIAL-BASED REGISTRATION	137
<b>6.4</b>	<b>CONCLUSIONS</b>	<b>139</b>
<b>CHAPTER 7: A NOVEL TABLET-BASED IMAGE GUIDANCE PLATFORM</b>		<b>140</b>
<b>7.1</b>	<b>INTRODUCTION</b>	<b>141</b>
<b>7.2</b>	<b>METHODS</b>	<b>142</b>
7.2.1	<i>EX-VIVO</i> RANDOMISED CROSSOVER STUDY	142
7.2.2	CLINICAL PLATFORM DESIGN	145
7.2.3	CASE-CONTROL SERIES	148
7.2.4	STATISTICAL ANALYSIS	150
<b>7.3</b>	<b>RESULTS</b>	<b>153</b>
7.3.1	RANDOMISED CROSSOVER STUDY	153
7.3.2	CASE SERIES	155
<b>7.4</b>	<b>DISCUSSION</b>	<b>160</b>
7.4.1	PRINCIPAL FINDINGS OF <i>EX-VIVO</i> RANDOMISED CONTROL STUDY	160
7.4.2	PRINCIPAL FINDINGS OF <i>IN-VIVO</i> CASE-CONTROL SERIES	160
7.4.3	COMPARISON TO OTHER STUDIES	161
7.4.4	<i>EX-VIVO</i> RANDOMISED CROSSOVER STUDY LIMITATIONS	163
7.4.5	CASE SERIES LIMITATIONS	163
7.4.6	FUTURE WORK	164
<b>7.5</b>	<b>CONCLUSION</b>	<b>165</b>
<b>CHAPTER 8: ULTRASOUND-GUIDED TUMOUR RESECTION</b>		<b>166</b>
<b>8.1</b>	<b>INTRAOPERATIVE ULTRASOUND OVERLAY IN ROBOT ASSISTED PARTIAL NEPHRECTOMY: SYSTEM OUTLINE AND FIRST CLINICAL EXPERIENCE</b>	<b>167</b>
8.1.1	INTRODUCTION	167
8.1.2	METHODS	168
8.1.3	DISCUSSION	177
8.1.4	CONCLUSION	178
<b>8.2</b>	<b>AUGMENTED REALITY FREEHAND THREE-DIMENSIONAL ULTRASOUND GUIDED TUMOUR RESECTION IN ROBOT ASSISTED PARTIAL NEPHRECTOMY</b>	<b>179</b>
8.2.1	INTRODUCTION	179
8.2.2	METHODS	179
8.2.3	RESULTS	186
8.2.4	DISCUSSION	190

8.2.5	CONCLUSIONS	193
<b>CHAPTER 9: CONCLUSIONS AND FUTURE WORK</b>		<b>195</b>
<b>9.1</b>	<b>SUMMARY OF ACHIEVEMENTS</b>	<b>196</b>
9.1.1	TO DEFINE OF THE WINDOW OF OPPORTUNITY FOR THE DEVELOPMENT OF AN IMAGE GUIDANCE PLATFORM FOR INTRA-ABDOMINAL MIS.	196
9.1.2	TO ESTABLISH WHETHER THERE IS A USER NEED FOR IMAGE GUIDANCE IN RAPN.	196
9.1.3	TO BETTER UNDERSTAND THE FUNDAMENTAL SAFETY AND BEHAVIOURAL IMPLICATIONS OF THE IMPLEMENTATION OF AN IEOE.	196
9.1.4	TO DEVELOP AND VALIDATE A NOVEL APPROACH TO IMAGE GUIDANCE IN ROBOT ASSISTED PARTIAL NEPHRECTOMY, UTILISING THE PRECEDING EVIDENCE BASE TO INFORM THIS DEVELOPMENT.	197
<b>9.2</b>	<b>FUTURE WORK</b>	<b>199</b>
9.2.1	FURTHER DEVELOPMENT OF THE IMAGE-ENHANCED OPERATING ENVIRONMENT	199
9.2.2	SAFETY AND SURGICAL IMAGE GUIDANCE	203
9.2.3	PATIENT SPECIFIC SIMULATION	204
9.2.4	SURGICAL AUTOMATION	205
<b>9.3</b>	<b>CONCLUSIONS</b>	<b>208</b>
<b>REFERENCES</b>		<b>209</b>
<b>APPENDICES</b>		<b>225</b>
<b>APPENDIX 1. – THE USE OF IMAGING IN ROBOTIC SURGERY QUESTIONNAIRE</b>		<b>226</b>
<b>APPENDIX 2. – ETHICS DOCUMENTATION</b>		<b>227</b>
A2.1	STUDY PROTOCOL	227
A2.2	PARTICIPANT INFORMATION SHEET	233
A2.3	CONSENT FORM	238
<b>APPENDIX 3. – INATTENTION BLINDNESS IN SURGERY DATA COLLECTION TOOL</b>		<b>239</b>
<b>APPENDIX 4. – CREATION OF A HIGH FIDELITY KIDNEY PHANTOM FOR SIMULATING ULTRASOUND GUIDED PARTIAL NEPHRECTOMY</b>		<b>244</b>
A4.1	RENAL CAST PRODUCTION	244
A4.2	CRYOGEL	244
A4.3	CREATION OF PARTIAL NEPHRECTOMY PHANTOM	245



## LIST OF FIGURES

Figure 1.1.1 – Harold Hopkins rod-lens endoscope.....	29
Figure 1.2.1 – Diffusion of hybrid corn in various American states. From Ryan and Gross. <sup>12</sup> .....	33
Figure 1.2.2 – The S-shaped diffusion curve in this figure demonstrates the 3 phases of growth in any technological innovation (incubation, exponential growth and diffusion saturation) and matches them to the characteristics of the individual members of the adopting population. <sup>13</sup> .....	33
Figure 1.3.1 – Pneumatic feedback system. Sensors within the instrument jaws cause inflatable pads over the surgeon’s fingers to inflate, resulting an understanding of the pressure being exerted by the instrument. From King <i>et al.</i> <sup>20</sup> .....	35
Figure 1.3.2 – VerroTouch vibration based haptic feedback system. Vibration sensors are placed on the robotic instruments with actuators and speakers feeding this information back to the surgeon. From Bark <i>et al.</i> <sup>23</sup> .....	35
Figure 1.5.1 Partial nephrectomy. a) Tumour is initially resected along dotted line. Prior to resection the renal artery (and vein) are clamped resulting in warm ischaemia. b) Following removal of the lesion internal renorrhaphy is undertaken in which the renal collecting system and any exposed vessels are closed. c) In the final phase, external renorrhaphy is performed, closing the parenchyma totally; this is often done ‘off-clamp’ in order to minimise ischaemic nephron damage. ....	41
Figure 2.2.1 – Rise in patent counts year-on-year (1950-2010). The left hand axis relates to the <i>innovation index</i> for patents, while the right relates to those pertaining to surgery. R <sup>2</sup> values of exponential curves demonstrated better goodness of fit than those for linear relationships.....	47
Figure 2.2.2 – Rise in publication counts year-on-year (1950-2010). The left hand axis relates to the <i>innovation index</i> for publications, while the right relates to those pertaining to surgery. R <sup>2</sup> values of exponential curves demonstrated better goodness of fit than those for linear relationships.....	48
Figure 2.3.3 – Original counts and the corrected <i>innovation index</i> for publications year-on-year related to surgery (1980-2010).....	56
Figure 2.3.4 – Year-on-year <i>innovation index</i> for patent and publications within image-guided surgery. ..	57
Figure 2.3.5 – Year-on-year <i>innovation index</i> for patent and publications within robotic surgery.....	58
Figure 2.3.6 – Year-on-year <i>innovation index</i> for patent and publications within MIS.....	59
Figure 2.3.7 – Year-on-year <i>innovation index</i> for patent and publications within surgical staplers. Left y-axis pertains to <i>innovation index</i> for publications and the right for patents. Data was initially analysed from 1980-2010, in post hoc analysis this was extended back to 1950. The bounding year of 1980 is represent on the graph by a black line.....	60
Figure 2.3.8 – Year-on-year <i>innovation index</i> for patent and publications within ophthalmic surgery. Left y-axis pertains to <i>innovation index</i> for publications and the right for patents. ....	61
Figure 2.3.9 – Year-on-year <i>innovation index</i> for publications within the image guidance cluster, sorted by surgical site. The y-axis on the left pertains to the innovation index for abdominal and neurosurgery and the right to orthopaedic surgery .....	62
Figure 2.4.1 - Innovation Curve. 1) Period of technological incubation 2) Period of widespread innovation and technological adoption 3) Period of technological refinement.....	66

Figure 3.1.1 – Röntgen's first X-ray of the human hand, 1885.....	71
Figure 3.2.1 – A still taken from a video of augmented reality robot assisted partial nephrectomy. Here the tumour has been painted into the operative view allowing the surgeon to appreciate the relationship of the tumour to the surface of the kidney. ....	74
Figure 3.3.1 – Geographical distribution of surgeons responding to questionnaire.....	77
Figure 3.3.2 – Chart demonstrating responses to the question - Do you use intraoperative ultrasound for robotic partial nephrectomy .....	78
Figure 3.3.3 – Chart demonstrating responses to the question - In robotic partial nephrectomy which parts of the operation do you feel augmented reality image overlay would be of assistance.....	79
Figure 3.3.4 – Chart demonstrating responses to the question - In robotic prostatectomy which parts of the operation do you feel augmented reality overlay technology would be of assistance? .....	80
Figure 3.3.5 – Chart demonstrating responses to the question - In robotic cystectomy which parts of the operation do you feel augmented reality would be of assistance?.....	81
Figure 4.1.1 – PRISMA diagram for the search: [(augmented reality) OR (image guid*) OR (image fusion) OR (image overlay) OR (soft tissue navigation)] AND [(inattention* blindness) OR (awareness) OR (attention* tunnelling) OR (safety) OR (work load) OR (task load)] AND surg* .....	89
Figure 4.2.2 – A frame from the study video demonstrating the presence of the gorilla at the centre of the scene in Simons and Chabris's paper. <sup>33</sup> (taken from Simons and Chabris, 1999).....	105
Figure 5.1.1 – The same dataset represented as a volume rendered and segmented reconstruction (left to right). The image on the right displays an axial CT slice during the process of segmentation. ....	109
Figure 5.2.1 – In the diagram at the top of the figure the ground truth is represented bounded in black with the rater segmentation bounded in red. Segmentation a) high PPV and sensitivity (minimal normal parenchyma removed, minimal tumour left <i>in-vivo</i> . b) demonstrates a high PPV and low sensitivity (no normal parenchyma removed, significant residual tumour left <i>in-vivo</i> ), c) low PPV and high sensitivity (tumour removed intact with significant amount of normal parenchyma), and d) low PPV and sensitivity (significant normal parenchyma removed, significant tumour left <i>in-vivo</i> ). The confusion matrix that makes up the second part of the figure outlines how PPV and sensitivity are calculated.....	112
Figure 5.3.2 – Overall sensitivity of tumour segmentation grouped by experience. <i>Whiskers were calculated as the 75<sup>th</sup> percentile plus 1.5 x IQR and 25<sup>th</sup> percentile minus 1.5 x IQR. Outliers were defined as values falling outside this range.</i> ....	115
Figure 5.3.3 – Overall extent of maximum boundary excursion of tumour segmentation grouped by experience. <i>Whiskers were calculated as the 75<sup>th</sup> percentile plus 1.5 x IQR and 25<sup>th</sup> percentile minus 1.5 x IQR. Outliers were defined as values falling outside this range.</i> .....	116
Figure 5.3.4 – Overall extent of maximum boundary incursion of tumour segmentation grouped by experience. <i>Whiskers were calculated as the 75<sup>th</sup> percentile plus 1.5 x IQR and 25<sup>th</sup> percentile minus 1.5 x IQR. Outliers were defined as values falling outside this range.</i> .....	116
Figure 5.3.5 – Example incursions and excursions of individual raters when compared to the STAPLE derived consensus. Top row, raters experienced in imaging and segmentation; middle row, raters experienced in imaging and bottom row, raters experienced in neither. The red end of the scale	

represents the maximum incursion while the blue represents the maximum excursion in millimetres.....	118
Figure 6.2.1– PRISMA diagram. Search was performed using a combination of the following key words and MeSH terms: “augmented reality” OR “image guidance” OR “image-guided” OR “image fusion” OR “image overlay” OR “soft tissue navigation” AND “nephrectomy” OR “renal cell carcinoma” .....	125
Figure 6.3.2 – A. Intrinsic tracking using the joint positions of the da Vinci robotic arms. The errors in calculation of joint positions compound as you pass down the kinematic chain. B. Optical tracking. Optical tracer is mounted to instrument, tracking system tracks the motion of tracer and requires continuous direct line of sight. C. System proposed by Herrell <i>et al.</i> <sup>143</sup> and Kwartowitz <i>et al.</i> <sup>144,145,149</sup> . Optical tracking is used to ascertain the position of the passive joints, shortening the kinematic chain thereby reducing the error at the instrument tip. D. Electromagnetic tracking. Tracers are attached to the instrument (or organ <sup>146</sup> ) and tracked using an EM tracking plate. No line of sight required, so tracking device can, theoretically, be placed inside patient.....	131
Figure 6.3.3 – From top left: Kidney model including main vessels; tumour localisation; surface of kidney painted away to reveal partially endophytic tumour; exposure of vena cava and renal vein. Pratt <i>et al.</i> <sup>19</sup> .....	134
Figure 6.3.4 – The stereoscopic overlay registration algorithm proposed by Su <i>et al.</i> <sup>153</sup> The chart demonstrates the steps required to perform accurate overlay and tracking. (From Su <i>et al.</i> 2009) .....	135
Figure 7.2.1 – Experimental setup and endoscopic image orientations.....	143
Figure 7.2.2 – Console view and registration process .....	143
Figure 7.2.3 – System set up; the trolley behind the console houses a HP Z820 server that is connected to the TilePro™ inputs of the console. The iPad™ was mounted on the console as shown.....	144
Figure 7.2.4 – System schematic: The host institution inserts a CD containing preoperative imaging into a HP Z820 server, the data was then retrieved via a secure network connection by the research team at Imperial College London. Subsequent to this the images were processed and the guidance server updated remotely. On the day of the case, the workstation is connected via 2 DVI cables to the da Vinci console stereo TilePro™ inputs (one for each eye feed). The system utilises a wireless iPad™ interface (the iPad™ is mounted onto the side of the console), with the image visible in the console also visible on the iPad™ screen (left eye console feed). The surgeon is able to manipulate images on the iPad™ with the reconstructions also visible in stereo in the TilePro™ function of the console (image viewing is also possible on the iPad). All image rendering is undertaken on the workstation. ....	146
Figure 7.2.5 – iPad™ display interface. The toolbar™ on the left can be used to select the imaging state required and then minimised. The surgeon is then able to manipulate the image on the iPad™ screen. Intraoperatively, the main image is also visible in the TilePro™ view on the console. In the image above blue represents venous anatomy, red arterial anatomy, yellow renal cyst and green target tumour.....	147
Figure 7.2.6 – Different viewing options available to the surgeon and their respective benefits and shortcomings. ....	151

Figure 7.2.7 – The console view with TilePro™ enabled. A) The complex hilar vascular anatomy is seen within the image allowing the surgeon to better appreciate the anatomy seen in the operative view. B) The surgeon is able to plan tumour resection by making the surface of the kidney a wireframe mesh while keeping the tumour solid.....	152
Figure 7.3.2 – Box-Whisker plot illustrating NASA-TLX score. Whiskers were calculated as the 75 <sup>th</sup> percentile plus 1.5 x IQR and 25 <sup>th</sup> percentile minus 1.5 x IQR. Outliers were defined as values falling outside this range. ....	154
Figure 8.1.2 – From top, left to right: CAD illustration of ultrasound probe and clip passing through 12mm port. Ultrasound probe design and manufactured probe clip with scale.....	170
Figure 8.1.3 – Left image corresponds to asymmetrical circular dot pattern, while right is the previously utilised chessboard pattern (blooming and smudging can be seen in this image).....	172
Figure 8.1.4 – Real time tracking and registration process.....	172
Figure 8.1.5 – Region of interest tracking. $d$ = distance, $S_v$ = velocity x scaling factor.....	173
Figure 8.1.7 – The different modes of image display available to the surgeon. From left to right: Solid overlay, transparent overlay and cutaway view, all displays included a 1mm ruler. The modes are demonstrated on a PVA cryogel phantom (See Appendix 4).....	176
Figure 8.2.1 – Segmentation process. From left to right: a) Raw DICOM data from Hitachi Aloka Prosound ALPHA 10 scanner, with contrast enhancement. b) Same image with ITK-SNAP edge attraction pre-segmentation applied. c) Post the implementation of supervised region growing algorithm. a) 3D volume generated by process.....	180
Figure 8.2.2 – High fidelity phantom for the simulation of partial nephrectomy. A) Phantom B) Axial section through phantom, phantom tumour can be seen in the centre of the section C) Ultrasound view of tumour within kidney phantom (narrow field of view due to the physical limitations of the probe used).....	181
Figure 8.2.3 – Process map for freehand 3D resection guidance. Two processes occur in parallel and in the same coordinate system: The first of dense stereo scene reconstruction in outlined in the top row and comprises stereo video capture followed by a dense stereo scene reconstruction and finally texture coordinate generation. The second process is that of freehand 3D ultrasound, which is outlined on the lower part of the image. These two datasets are then combined in the same coordinate system and displayed to the surgeon, in stereo via an on-demand peddle at the console. <i>Green and blue lines correspond to right and left camera feeds respectively.</i> .....	184
Figure 8.2.4 – Augmented reality view displayed to the surgeon. Two modalities of viewing were available: a) Surface reconstruction and tumour volume b) Surface reconstruction and tumour volume overlaid onto the operative view. The surgeon was able to control the virtual camera orientation and position when viewing images .....	185
Figure 8.2.6 – Planning time by surgeon (each colour representing a different surgeon).....	188
Figure 8.2.7 – Resection time by surgeon (each colour representing a different surgeon).....	189
Figure 8.2.8 – Time to task completion (not including processing time) by surgeon (each colour representing a different surgeon) .....	189

## LIST OF TABLES

Table 1.2.1 – Innovation qualities, as defined by Everett Rogers <sup>13</sup> applied to technological innovations in surgery.....	31
Table 1.2.2 - Key recommendations for research design at each IDEAL phase <sup>11</sup> .....	32
Table 2.2.1 – PubMed and PatentInspiration search strategies.....	49
Table 2.2.2 – Pubmed search strategies for image guidance sub-analysis.....	51
Table 2.3.1 – Top 30 patent codes amalgamated into technology clusters (patent counts are normalised). Clusters in <b>bold</b> were those selected for in-depth analysis .....	54
Table 3.3.1 – Which preoperative imaging modalities do you use for surgical planning and diagnosis.....	76
Table 3.3.2 – How do you typically view preoperative imaging in the operating room (3D recons = Three dimensional reconstructions) .....	76
Table 4.1.1 – Study design and target organ or procedure type. <i>RCT = Randomised control trial RXT = Randomised cross over trial</i> .....	90
Table 4.1.2 – NASA-TLX scores. Unless otherwise stated number in brackets is the standard deviation (SD). Numbers in <b>bold</b> denote a statistically significant reduction in the NASA-TLX score.....	91
Table 4.1.3 – Number of participants noting the presence of a foreign body on the operative scene on prompting. Items in <b>bold</b> denote decrease in the ability to identify a foreign body in the operative scene .....	91
Table 4.2.1 – Effect of cognitive load on inattention blindness.....	99
Table 4.2.2 – Effect of modality of image guidance style on inattention blindness.....	101
Table 4.2.3 – Effect of image guidance on inattention blindness.....	101
Table 4.2.4 – Effects of prompting on inattention blindness.....	102
Table 5.3.1 – Analysis of variables according to rater experience and tumour type. Standard deviations in brackets. PPV = Positive predictive value .....	114
Table 6.3.1 – Proposed augmented reality systems by registration type - = not reported. TRE = target registration error, EM = electromagnetic, DOF =degrees of freedom, 3D = 3-dimension.....	129
Table 6.3.2 – Target registration error the available augmented reality systems, 3D = 3-dimensions TRE = target registration error.....	136
Table 7.3.1 – Comparison of iPad and 3D mouse interfaces, values shown are medians. 3D = three dimensional IQR = Interquartile range *Measure of rotational accuracy in all three axes, a value of 2 represents the maximum error possible and 0 would represent a perfect alignment.....	153
Table 7.3.2 - Patient parameters, clinical outcomes, subjective benefit and greatest contribution to case difficulty.....	156
Table 7.3.3 – Comparison of image-guided and non-image-guided procedures. Unless otherwise stated values are medians. *Calvien-Dindo .....	159
Table 8.1.1 – Ultrasound system specifics.....	174
Table 8.2.1 – Freehand registered 3D ultrasound versus conventional 2D ultrasound guided resection. <i>Where not stated numbers are medians.</i> .....	187
Table 9.2.1 - Key recommendations for research design at each IDEAL phase <sup>11</sup> .....	200

Table 9.2.2 – Innovation qualities, as defined by Everett Rogers<sup>13</sup> applied to technological innovations in surgery..... 201

## LIST OF ACRONYMS

<b>ANOVA</b>	–	Analysis of variance
<b>AR</b>	–	Augmented reality
<b>CAD</b>	–	Computer assisted design
<b>CKD</b>	–	Chronic kidney disease
<b>CT</b>	–	Computerised Tomography
<b>DICOM</b>	–	Digital imaging and communications in medicine
<b>DOCDB</b>	–	European patent database
<b>DOF</b>	–	Degree of freedom
<b>DVI</b>	–	Digital visual interface
<b>EAU</b>	–	European Association of Urology
<b>ERUS</b>	–	European symposium of robotic urological surgeons
<b>EM</b>	–	Electromagnetic
<b>ENT</b>	–	Ear, nose and throat
<b>EPO</b>	–	European patent office
<b>IB</b>	–	Inattention blindness
<b>IDEAL</b>	–	Idea, Development, Exploration, Assessment, Long-term follow-up
<b>IEOE</b>	–	Image-enhanced operating environment
<b>IQR</b>	–	Inter-quartile range
<b>IRCAD</b>	–	Research Institute Against Cancers of the Digestive System
<b>ITK-SNAP</b>	–	Imaging tool kit
<b>MeSH</b>	–	Medical subject headings
<b>MIS</b>	–	Minimally invasive surgery
<b>MRI</b>	–	Magnetic resonance imaging
<b>NASA-TLX</b>	–	National Aeronautics and Space Administration - Task Load Index
<b>NPV</b>	–	Negative predictive value
<b>PADUA</b>	–	Preoperative aspects and dimensions used for anatomical classification renal tumors
<b>PPV</b>	–	Positive predictive value
<b>PRISMA</b>	–	Preferred items for systematic reviews and meta-analysis
<b>PVA</b>	–	Polyvinyl alcohol
<b>PVA-C</b>	–	Polyvinyl alcohol cryogel
<b>RALP</b>	–	Robot assisted laparoscopic prostatectomy
<b>RAPN</b>	–	Robot assisted laparoscopic partial nephrectomy

<b>REC</b>	–	Research ethics committee
<b>RCT</b>	–	Randomised control trial
<b>RXT</b>	–	Randomised cross over trial
<b>SDI</b>	–	Serial digital interface
<b>STAPLE</b>	–	Simultaneous truth and performance level estimation algorithm
<b>TRE</b>	–	Target registration error
<b>UK</b>	–	United Kingdom
<b>US</b>	–	Ultrasound
<b>USA</b>	–	United States of America
<b>WIPO</b>	–	World intellectual property office
<b>WIT</b>	–	Warm ischaemic time
<b>2D</b>	–	Two-dimensional
<b>3D</b>	–	Three-dimensional



## CHAPTER 1: INTRODUCTION

## 1.1 Prologue

In 1959, Harold Hopkins patented a device that drove a seismic change in surgical practice: the rod lens endoscope (Figure 1.1.1).<sup>1</sup> The inception of this single device resulted in the well documented shift from maximally to minimally invasive surgery (MIS). Although the advent of MIS has conferred many advantages to the patient, reducing post-operative pain, wound complications, hospital length of stay and overall postoperative recovery,<sup>2-4</sup> it has also created a more challenging environment in which the surgeon has to operate.<sup>5</sup>

Intra-abdominal MIS is generally performed through a series of ports in a patient's abdomen, with long instruments passed through these ports to manipulate tissue. The use of ports and rigid shaft based instruments both limits the degrees of freedom with which a surgeon can operate, and introduces a confounding fulcrum. In addition, the use of a 2D camera results in the loss of the depth perception offered by binocular vision.<sup>6</sup> These problems are further compounded by the reduction in non-visual cues to the operative anatomy with the surgeon's haptic sense markedly reduced.<sup>7,8</sup>

A number of technology-based solutions to these problems has been proposed and subsequently adopted into practice, with 3D endoscopes and robot assistance mitigating for the loss of binocular vision and reduction in the degrees of freedom, respectively. However, the problem of haptic loss remains underexplored, with the solutions that have been proposed failing to gain traction amongst either the research or wider surgical community.<sup>7,9</sup>

This loss of haptics affects both the appreciation of anatomy on a microscopic scale, for definition of the normal tissue to tumour interface, but also on a macroscopic level with the surgeon less capable of defining subsurface anatomical structures such as veins, arteries and nerves.<sup>7</sup> This deficit has been further exacerbated by robot-assisted surgery, with the most widely utilised robotic platform, the da Vinci surgical system (Intuitive Surgical, Sunnyvale, CA, USA), offering no haptic compensation. Without addressing this deficit in robotic surgery, and more broadly within MIS, patients with more challenging anatomy may find themselves subjected to conventional open surgery, or radical rather than organ preserving surgeries, due to the sensory limitations of MIS.<sup>10</sup>

June 28, 1966

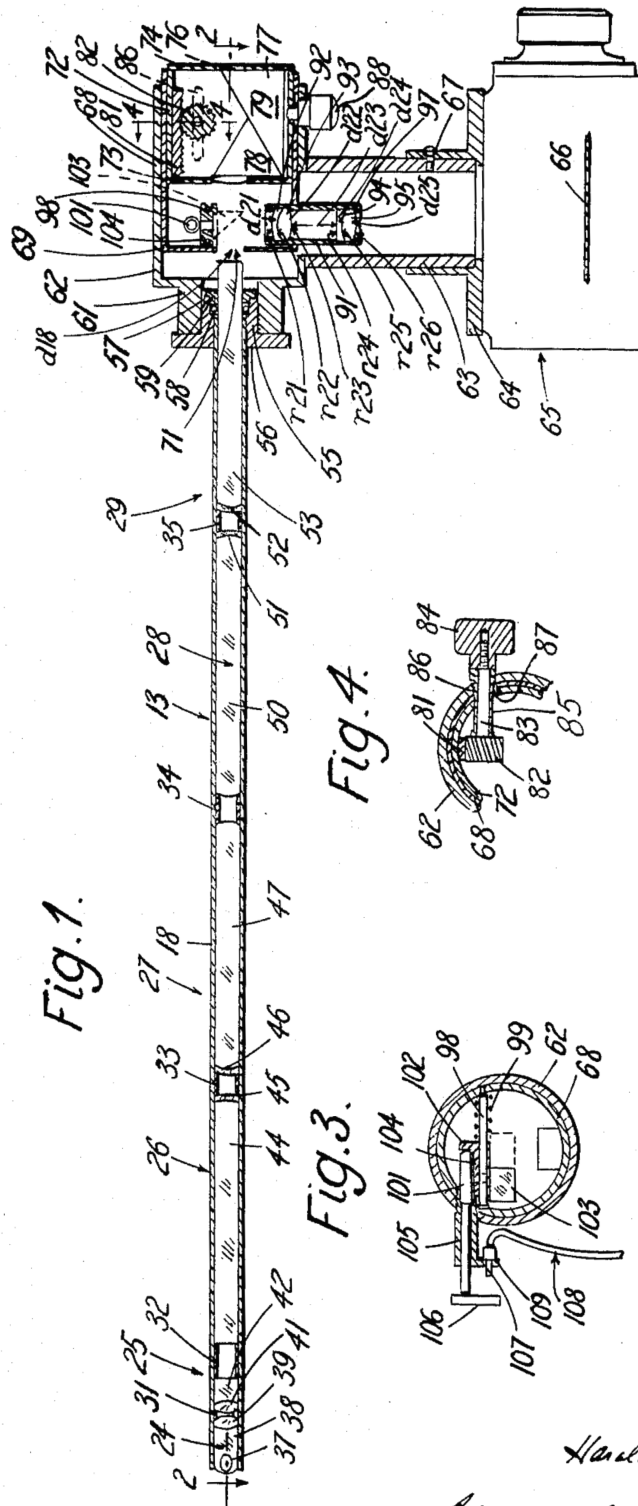
H. H. HOPKINS

3,257,902

OPTICAL SYSTEM HAVING CYLINDRICAL ROD-LIKE LENSES

Filed July 14, 1960

4 Sheets-Sheet 1



INVENTOR

Harold Horace Hopkins

By Watson, Cole, Grindle & Watson  
ATTORNEYS

Figure 1.1.1 – Harold Hopkins rod-lens endoscope.

## 1.2 Innovating in surgical technology and image guidance

In 2009 the Idea, Development, Exploration, Assessment and Long-term follow-up collaboration (IDEAL) published their framework for surgical innovation suggesting a more rigorous and methodical approach was needed in surgical research.<sup>11</sup> This consensus document suggested that innovations pass through five stages of development, with each stage involving a greater barrier to progression (Table 1.2.2). With the collaboration's findings heralding a new era of potentially expensive randomised control trials, surgeons and researchers must look to maximise the chance of a given innovation's adoption by the target population, rather than relying on luck and intuition alone.

The study of innovation outside the field of medicine began in the 1940s with Ryan and Gross's seminal work on the diffusion of hybrid corn through the farming population of rural Iowa.<sup>12</sup> This hybrid version of corn offered unquestionably better crop yields and pest resistance than its precedent. Despite this fact Ryan and Gross noted that it was not adopted instantaneously by all farmers, but rather according to a very predictable pattern of sigmoidal growth (Figure 1.2.1). It was soon after this initial paper that Everett Rogers founded innovation science in his book "Diffusion of Innovations".<sup>13</sup> In this he proposed that all innovations follow this same pattern of sigmoid growth, and that adopters can be classified according to four types according to when they adopt a technology on this growth curve (Figure 1.2.2).

Outside of the healthcare literature this theory of innovation diffusion has been extensively used both to study the history of innovations, and to predict how likely an innovation is to succeed.<sup>14-16</sup> However, the application of the theory within healthcare technology is less well explored and has been limited to largely qualitative research.<sup>17-19</sup> The development of a quantitative predictive measure of innovation in surgical technology would allow surgeons to better assess innovations in the *idea* and *development* stages of the IDEAL framework,<sup>11</sup> and would help to minimise time wasted on innovations that are unlikely to diffuse into the target surgical community.

This thesis will propose and validate a novel metric, offering a quantitative measure with which to document and predict the levels of innovation within a given technology cluster. This metric will be developed with the objective of applying it to intra-abdominal MIS to assess this technology cluster's *innovation potential* to ensure it represents an area of market and research interest.

Beyond assisting in the setting of research and funding agendas, Everett Roger's theory offers a framework with which to assess all innovation to help understand why it has (or has not) diffused through a target population. The simple *innovation sieve* that Roger's gives up is made up of five separate assessment factors: *trialability*, *compatibility*, *relative advantage*, *complexity* and *observability* (Table 1.2.1).<sup>13</sup>

When using these to assess image guidance in MIS it becomes evident why image guidance platforms in intra-abdominal MIS have been limited to small volume case series in academic institutions.<sup>7,9</sup> The reasons can be classified according to failures in the steps of: *image acquisition*, *preparation*, *compensation* and *display related factors*.

Simply speaking the proposed platform must be easy to use, require minimal engineering input, be relatively low cost and must be compatible with existing theatre equipment, in addition to offering the surgeon an advantage over the status quo. The platform proposed in this thesis will draw on these user related factors, as defined by Everett Rogers, as a central guiding dogma in order to deliver a solution that has the maximum diffusion potential.

<b>Factor</b>	<b>Definition</b>
<b>Relative advantage</b>	How improved a technological innovation is over the previous generation?
<b>Compatibility</b>	The level of compatibility with existing surgical hardware/how easily can the innovation be integrated into the surgical workflow
<b>Complexity</b>	How difficult is the technology to use?
<b>Trialability</b>	Can the technology be easily tested?
<b>Observability</b>	Is the technological innovation be visible to other surgeons (publication, display at conferences etc.)?

Table 1.2.1 – Innovation qualities, as defined by Everett Rogers<sup>13</sup> applied to technological innovations in surgery

<b>IDEA Professional Innovation Database</b>	<b>DEVELOPMENT Prospective Development Studies</b>	<b>EXPLORATION Phase IIS Study</b>	<b>ASSESSMENT Surgical RCT</b>	<b>LONG TERM MONITORING Prospective Registries</b>
Compulsory reporting of all new innovations	Detailed description of selection criteria	To evaluate technique prospectively and co-operatively	RCT – question agreed in Phase IIS	Should monitor indications as well as outcomes
Confidential entry allowed to encourage reporting of failed innovations (similar to CHRP system)	Detailed technical description	To develop a consensus over definition of the procedure, quality standards and indications	Use power calculations from Phase IIS	SPC used for quality control (Shewart charts, CUSUM, VLAD)
Hospital or institution to be informed separately as a professional duty	Prospective account of ALL cases consecutively, including those NOT treated with new technique/device	To gather data for power calculations	Use learning curve data to decide entry points for clinicians	
	Clear STANDARDISED definitions of outcomes reported	To evaluate and monitor learning curves	Use phase IIS consensus to define operation, quality control AND outcome measures	
	Description of ALL modifications, and when they were made during the series	To achieve consensus on the trial question	Use modified RCTs or recognised alternative if RCT not feasible:	
	Registration of PROTOCOL before study starts	To develop a multi-centre randomised trial (RCT)	Feasibility RCT Expertise-based RCT Cohort multiple RCT Step-wedge design Controlled-interrupted time series	
	Use of Statistical Process Control (SPC) methods to evaluate progress			

Table 1.2.2 - Key recommendations for research design at each IDEAL phase<sup>11</sup>

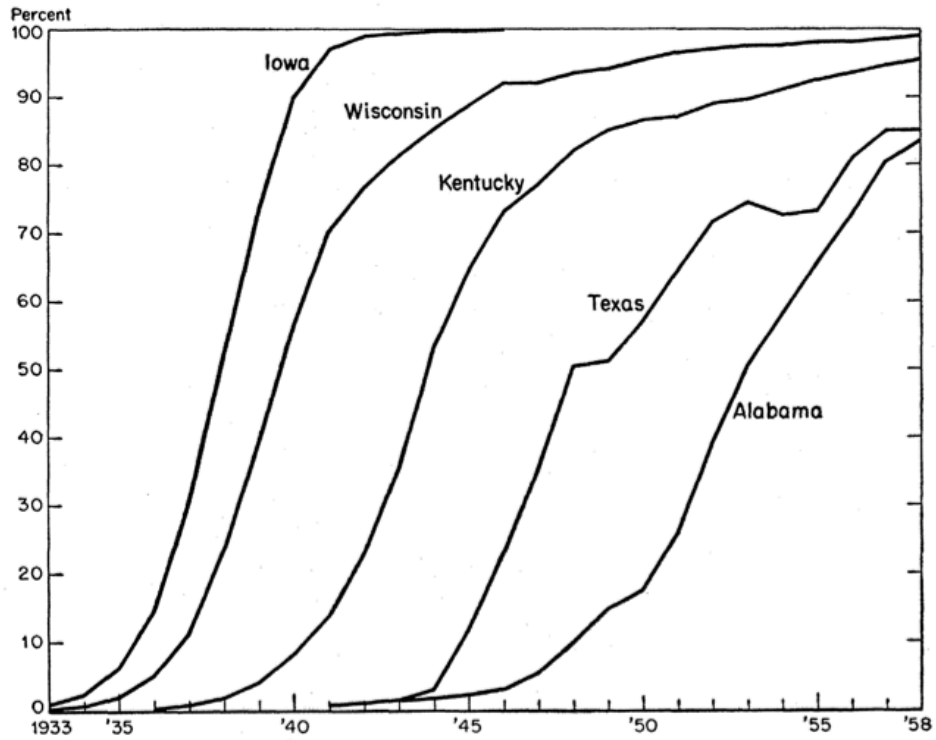


Figure 1.2.1 – Diffusion of hybrid corn in various American states. From Ryan and Gross.<sup>12</sup>

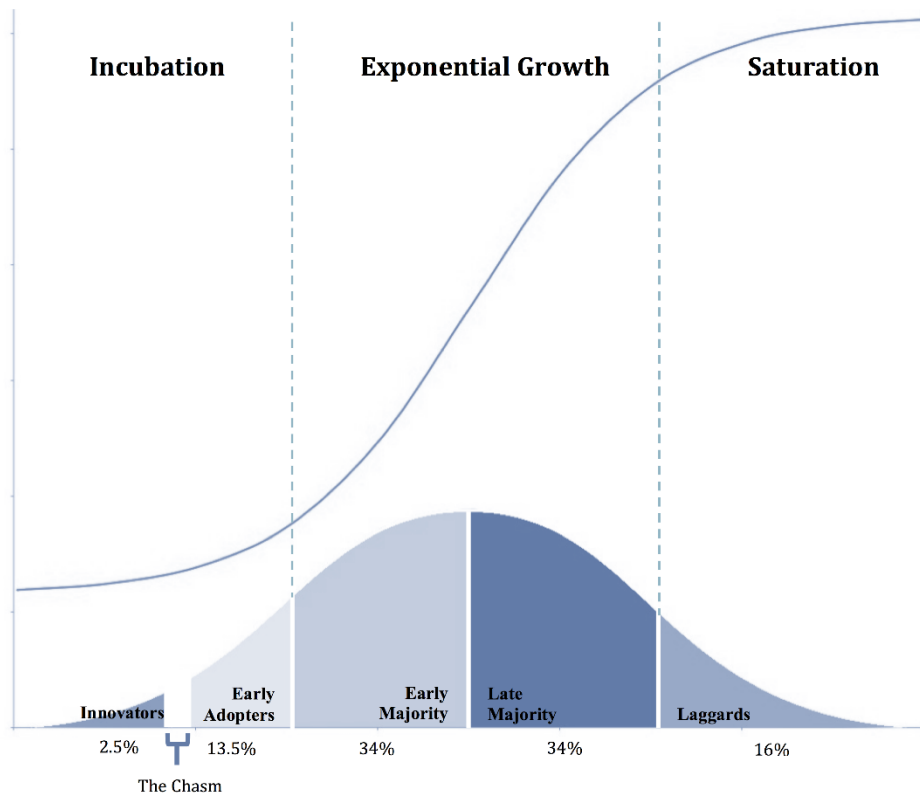


Figure 1.2.2 – The S-shaped diffusion curve in this figure demonstrates the 3 phases of growth in any technological innovation (incubation, exponential growth and diffusion saturation) and matches them to the characteristics of the individual members of the adopting population.<sup>13</sup>

### 1.3 Haptic replacement

Historically, two solutions to sensory loss have been proposed in the surgical and medical engineering literature: haptic replacement and the enhancement of the surgeon's view with relevant patient specific imaging, henceforth referred to as an *Image-Enhanced Operating Environment* (IEOE).

The augmentation of surgical tools with haptic sensing and feedback devices seems to be the intuitive solution to the problem of haptic loss, as it replaces like with like. Two approaches have been attempted: in the first a sensor is deployed at the instrument tip, or end effector,<sup>20,21</sup> (Figure 1.3.1) while in the second a sensor is placed outside the patient on the instrument shaft (Figure 1.3.2).<sup>21,22</sup> The use of haptic feedback devices in MIS although of interest, has failed to gain significant traction amongst surgeons, in part due to the limitations of the systems proposed, but also due to a number of more fundamental problems.

Perhaps the greatest of these more fundamental limitations is inherent to the instruments themselves; with laparoscopic tools having a relatively small surface area when compared to the human hand. This reduction in surface area severely limits the amount of information even the most perfect haptic sensor could confer, thereby limiting any potential benefits of the sensing device.

Although the like-for-like approach seems intuitive, it falls short of offering the resolution of information that can be gained from a human's innate sensory mechanisms, offering only a relatively crude representation of the torsional or compressive force being exerted on tissue. This serves at best to prevent force-related tissue and suture damage, but falls short of offering an understanding of subsurface anatomy.



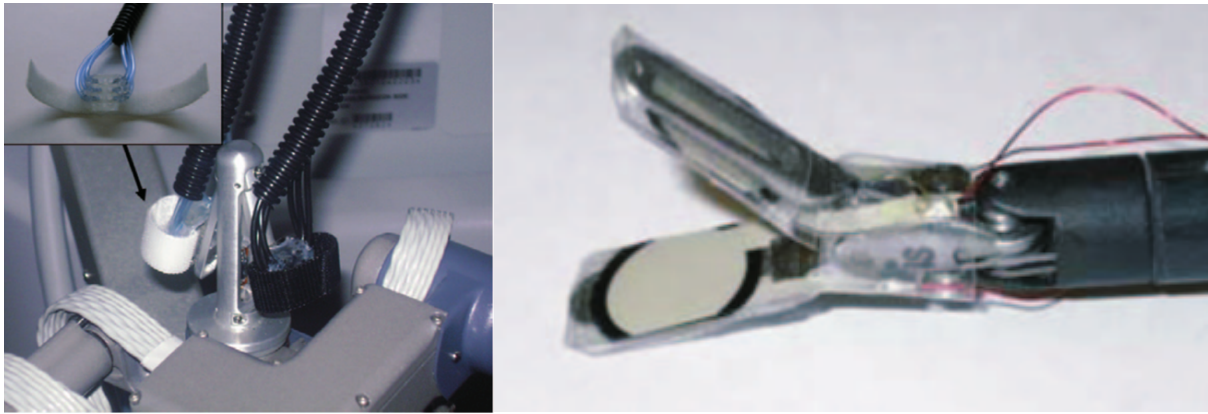


Figure 1.3.1 – Pneumatic feedback system. Sensors within the instrument jaws cause inflatable pads over the surgeon’s fingers to inflate, resulting an understanding of the pressure being exerted by the instrument. From King *et al.*<sup>20</sup>

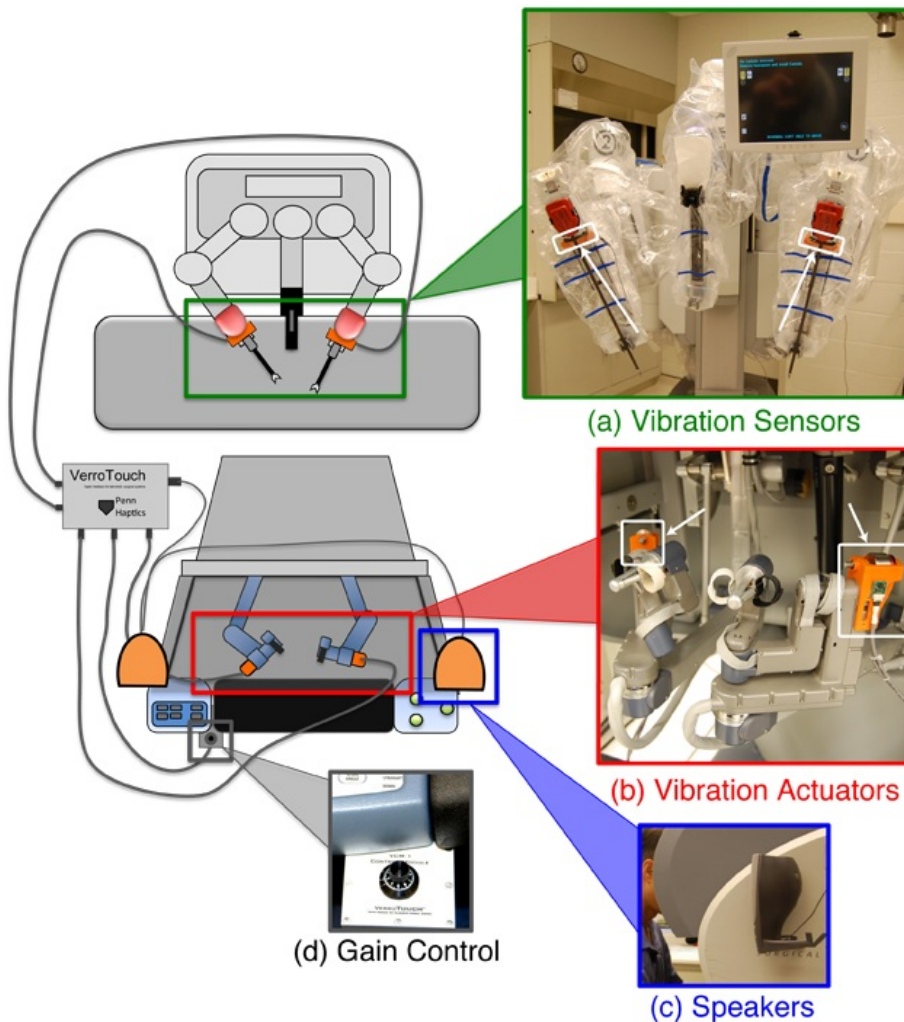


Figure 1.3.2 – VerroTouch vibration based haptic feedback system. Vibration sensors are placed on the robotic instruments with actuators and speakers feeding this information back to the surgeon. From Bark *et al.*<sup>23</sup>

## 1.4 Image-enhanced operating environment

An IEOE can be defined as an operative environment which is augmented with a patient-specific imaging dataset displayed alongside or superimposed onto the surgical field of view. In the past image guidance solutions have utilised a single modality of imaging in order to solve all of the problems faced by the contemporary minimally invasive surgeon. The concept of the IEOE is to capitalise on the strengths of a particular imaging type, delivering more focused guidance solutions for specific surgical tasks. This may include more than a single modality of imaging.

The multimodal approach to image guidance contrasts with the majority of platforms developed to date, which attempt to use a single imaging format to solve all of the intraoperative problems. The source datasets used can be both pre and intraoperative, allowing the surgeon to simultaneously assimilate important visual information from the operative field with imaging modalities (e.g. ultrasound, CT or MRI) that usually play a passive or absent role within the operating room.

While research surrounding haptic replacement has been limited to a small number of studies, image-guided MIS is an area of significant research growth.<sup>24</sup> The reasons behind the comparative success of image guidance in robotics are probably related to the lower computational requirements; the human eye is unable to process information at greater than approximately 60 frames per second, a fraction of the 1kHz refresh rate of the hand and fingers.<sup>25</sup> This is in addition to its greater breadth of benefit when compared to haptic replacement alone.

The increased breadth of benefit is related to the broader appreciation of the patient's anatomy afforded by an imaging dataset. Rather than just an understanding of the anatomy that lies in the surgeon's immediate operating window, as would be the case with a haptic interface, imaging can be used to garner a wider sense of the patient's anatomy. As well as the greater anatomical understanding, image based guidance has the added potential to be used to build automated safety mechanisms into the operative work flow; for instance in the active constraint of the surgeon to a safe operative window.<sup>26</sup>

Although the use of imaging appears preferable to haptic replacement, applying image overlay technology to intra-abdominal organs presents unique challenges. Intra-abdominal organs are

not constant in their relationship to the anatomical landmarks that surround them.<sup>27</sup> Moreover, their size and shape can vary due to the surgeon's manipulation of the organ and tissue dissection, as well as patient factors such as respiration and the cardiac cycle.<sup>28</sup> These problems are further compounded by the tendency to use preoperative imaging for intraoperative guidance, a further and significant source of inaccuracy.<sup>29</sup> This thesis aims to capitalise on the breadth of potential benefit gleaned from intraoperative image guidance while attempting to compensate for its inherent limitations .

#### **1.4.1 Safety of image guidance and the image-enhanced operating environment**

Although the potential benefits of image guidance cannot be understated, the potential safety implications of guidance platforms must also be understood prior to their dissemination into practice. Work has been done both in the aviation<sup>30-32</sup> and social science literature<sup>31,33</sup> to establish the nature and impact of these drawbacks. However, only a handful of studies has been published in the medical literature.

The most significant of these concerns relates to the failure to notice salient features or events. This failure to perceive an unexpected object when attention is diverted to another object or task is commonly termed *inattention blindness*.<sup>33,34</sup> Its effects have been well noted in other industries involving highly complex tasks, with focus on the task having been observed to result in a failure to notice critical changes to the environment within which the task takes place.<sup>30</sup> It has been particularly well studied in the military, aviation and space industries, in particular in the context of head-up-displays (HUDs).<sup>30,32</sup> The parallels between HUDs and the IEOE are obvious but the medical literature has, as yet, left the effects of augmenting the operator's view largely unexplored.

As well as the potential impact of the display of imaging and inattention, the literature is also limited in its exploration of the accuracy of the source data for many image guidance platforms, e.g. models generated from segmented cross sectional imaging.<sup>35,36</sup> Prior to the development of the IEOE proposed in this thesis, studies were undertaken to gain an improved understanding of the impact of inattention blindness and image preparation on the safety of image guidance platforms.

## 1.5 Current clinical applications of image-enhanced operating environment

The desire and need for image guidance in soft tissue surgery is greatest under three conditions: *impaired sensory feedback reduction* (as discussed previously), *complex and/or varied target organ anatomy*, and *limited organ resection* (where an emphasis is put on the minimisation of positive oncological margins while maximising the amount of normal tissue spared). When applying these criteria to the different organ systems there are three frontrunners for the use of image guidance: neurosurgery,<sup>37</sup> hepatic resection,<sup>9</sup> and nephron-sparing partial nephrectomy.<sup>9</sup>

### 1.5.1 Neurosurgery

The most developed field with regards to image guidance in surgery is without question neurosurgery. Stereotactically-guided neurosurgery, using CT or MRI imaging, has been a mainstay of practice for neurosurgeons for the last two decades.<sup>38</sup> The reason for this widespread adoption probably relates to a number of factors: First, the paramount need for *limited organ resection*, with a neuron-sparing approach crucial for the best post-operative functional outcomes.

The second reason for the rapid adoption of image guidance in neurosurgery is likely to be related to a relatively low technical barrier to implementation. The intra-abdominal viscera are only loosely related to a patient's surface anatomy with patient position and pneumoperitoneum significantly altering organ position.<sup>7,9,39</sup> In contrast, the relationship of the brain and skull is close enough to be assumed constant. This allows radio and MRI-opaque fiducials to be placed on the skull, prior to scanning the patient, with subsequent manual registration of the patient and scan in theatre using these fiducials. This relationship between brain and skull allows for the high levels of registration accuracy required for stereotactic neurosurgery. Although lessons can be learnt from neurosurgical image guidance practice, the barriers to adoption are smaller due to the ease of image registration; perhaps explaining the disproportionate adoption within this subspecialty.

### 1.5.2 Intra-abdominal image guidance

Within the context of intra-abdominal surgery, two procedures meet the criteria laid out above (*limited organ resection*, *complex and/or variable anatomy* and *impairment of sensory feedback*): limited hepatic resection and partial nephrectomy.<sup>9</sup> The problems faced in these two

procedures are similar. Both require a solution that can inform the surgeon of the target organ vascular anatomy and the location of the tumour-to-normal tissue interface, in the context of the dynamic environment of the insufflated abdomen.

Partial nephrectomy was chosen as the index procedure for this thesis rather than hepatic resection for a number of reasons. The most significant of these relate to the widespread use of the da Vinci robot for this procedure; specifically, the combination of the da Vinci's detrimental effect on haptic feedback, and the fact that the stable stereoscopic camera reduces the significant challenges faced when designing an image guidance platform for minimally invasive intra-abdominal surgery. In addition to these important robot-related factors, many urologists already utilise both CT reconstruction and intraoperative US in their routine practice for partial nephrectomy.

### **1.5.3 Partial nephrectomy**

Partial nephrectomy is the gold standard treatment for T1a and amenable T1b renal cell carcinomas (RCC).<sup>40,41</sup> The procedure aims to maximally spare functioning nephrons while achieving a complete resection of the renal tumour and is, under normal circumstances, undertaken with warm ischaemia (i.e. with the renal artery and/or vein clamped), in order to reduce bleeding (Figure 1.5.1). The period of warm ischaemia must be kept to a minimum to reduce ischaemic nephron loss.<sup>42</sup> Partial nephrectomy has been shown to reduce the incidence of chronic kidney disease (CKD) when compared to radical nephrectomy<sup>43</sup> due to the nephron-sparing nature of the procedure. CKD is associated with an increased risk of cardiovascular disease<sup>44,45</sup> and partial nephrectomy has been shown to reduce this risk in addition to increasing post-operative survival when compared to radical nephrectomy.<sup>46-49</sup> These benefits are achieved with no negative impact on oncological outcome.<sup>50,51</sup>

Historically, the operation has been performed largely via an open technique with a laparoscopic approach being potentially underutilised despite improvements in post-operative recovery time.<sup>52</sup> This is likely to be down to two factors: first, the difficulty of the procedure; and second, the loss of haptics.

The first of these problems has been addressed, at least in part, by the advent of robot-assisted laparoscopic partial nephrectomy (RAPN) which has reduced the technical difficulty of laparoscopic suturing.<sup>53</sup> This reduction in difficulty has seen the plateau phase of a surgeon's

learning curve for warm ischaemic time (WIT) fall from greater than 200 cases for the conventional laparoscopic approach,<sup>54</sup> to less than 30 cases for the robot-assisted approach.<sup>55</sup> In turn, this has resulted in a minimally invasive approach to partial nephrectomy becoming more accessible to surgeons who did not previously have the required skill set.<sup>56</sup>

Although the advent of robot assistance has mitigated for the technical difficulties associated with laparoscopic suturing in a time critical environment, it has further exacerbated the problem of haptic loss.<sup>8</sup> In an open approach the surgeon has the ability to palpate the tumour helping them to accurately define the interface between tumour and normal parenchyma, in addition to other subsurface anatomical detail.<sup>7</sup> This tactile feedback is lost entirely in a robot-assisted approach, forcing the surgeon to use visual cues to define the interface. The clinical corollary is a potential impact on the quality and safety of surgical resection, particularly in cases of cystic or endophytic tumours. This haptic sacrifice may well be the driving factor behind the tendency for surgeons to perform open partial nephrectomy or laparoscopic radical nephrectomy for complex T1a and T1b renal tumours, rather than the gold standard partial nephrectomy.<sup>10,57-59</sup>

Image guidance in combination with robot assistance may offer a solution to this underutilisation giving surgeons the confidence and information necessary to tackle more T1a and T1b RCC using a minimally invasive approach to partial nephrectomy. In addition to the *loss of haptics* and *limited organ resection* required in RAPN, the *vascular anatomy of the target organ is highly variable*, thereby meeting the third condition needed to maximise the efficacy of a surgical image guidance platform.

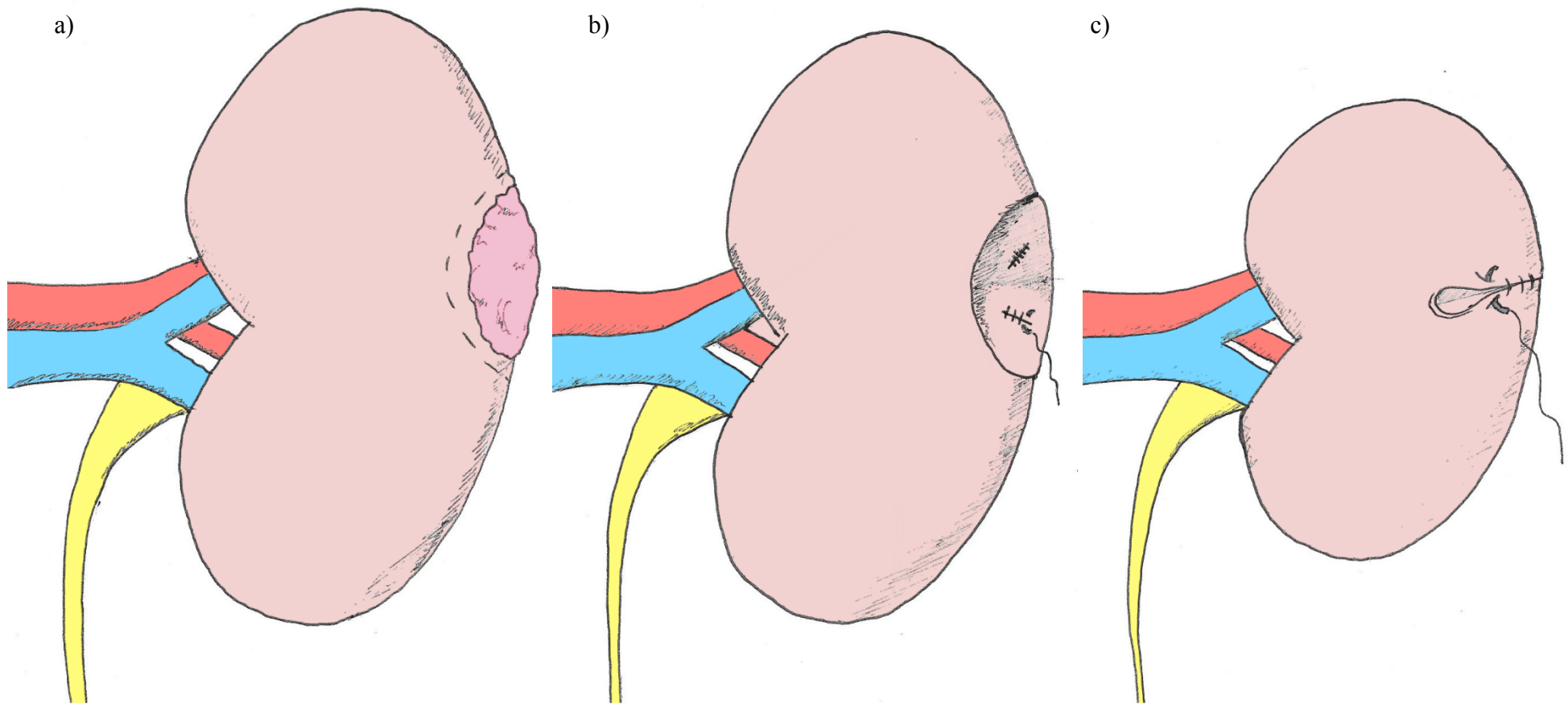


Figure 1.5.1 Partial nephrectomy. a) Tumour is initially resected along dotted line. Prior to resection the renal artery (and vein) are clamped resulting in warm ischaemia. b) Following removal of the lesion internal renorrhaphy is undertaken in which the renal collecting system and any exposed vessels are closed. c) In the final phase, external renorrhaphy is performed, closing the parenchyma totally; this is often done 'off-clamp' in order to minimise ischaemic nephron damage.

## 1.6 Thesis overview, aims and objectives

The following thesis has a number of central aims around which it has been structured. The first of these was *to define the window of opportunity for the development of an image guidance platform for intra-abdominal MIS*. This was undertaken in order to ensure that the endeavours of the thesis were both timely and relevant. In order to meet this aim a number of objectives were set, the first of these was to develop a novel, quantitative, and predictive measure of innovation within surgery. Once developed this metric was then applied to image guidance to establish the growth characteristics of the IEOE, and within which surgical fields this growth was occurring.

The third chapter of the thesis looked to further define this window and *to establish whether there was a user need for image guidance in RAPN*. The objective derived from this overarching aim was to undertake a consensus gathering questionnaire study to establish where, and how an image guidance solution would be of most use in RAPN. As a supplementary objective the questionnaire was to establish the problems that a surgeon faces when performing a RAPN, and which of these problems could potentially be mitigated for with image-guidance.

Subsequently the thesis looks *to better understand the fundamental safety and behavioural implications of the implementation of an IEOE*. The objectives derived from this aim were to establish the impact of inattention blindness in the context of image guidance. Further to this the thesis will also endeavour to establish the quality and reliability of image segmentation of pre-operative cross sectional images, to establish whether this offers the accuracy and reproducibility required to provide high level image-guidance for tasks such as tumour resection.

After determining *a window of innovation opportunity, establishing user need and examining the potential safety and behavioural implications* for the IEOE in minimally invasive abdominal surgery, an understanding of the status quo is presented in chapter six. In this chapter a systematic review of the literature relating to image guidance in RAPN was undertaken with the primary objectives being to gain a better understanding of the problems faced, and the solutions previously proposed to these problems.



In the final two technical chapters of the thesis the knowledge gained from previous work was used to inform *the development of a novel approach to image guidance in partial nephrectomy*. This platform was derived using an iterative, evidence and surgeon feedback led approach, the objectives of this platform were four fold: 1) That it should be safe, 2) of benefit to the surgeon and patient, 3) feasible, and 4) it should have a low barrier to adoption by the target community; in order to maximise its chances of adoption into routine practise. RAPN is performed (in the clinical setting) using the da Vinci surgical system (Intuitive Surgical, Sunnyvale, CA) and as such this thesis will focus on the augmentation of this platform in order to maximise adoption by the target population of renal surgeons.

In summary the thesis has at its centre four principal aims:

- 1) *To define the window of opportunity for the development of an image guidance platform for intra-abdominal MIS.*
- 2) *To establish whether there is a user need for image guidance in RAPN.*
- 3) *To better understand the fundamental safety and behavioural implications of the implementation of an IEOE.*
- 4) *To develop and validate a novel approach to image guidance in robot-assisted laparoscopic partial nephrectomy, utilising the preceding evidence base to inform this development.*

## CHAPTER 2: ASSESSMENT OF INNOVATION POTENTIAL<sup>†</sup>

---

<sup>†</sup> Content from this chapter was published as:

**Hughes-Hallett, A.**, Mayer, E. K., Marcus, H. J., Cundy, T. P., Pratt, P. J., Parston, G., Darzi, A. W. (2014). Quantifying Innovation in Surgery. *Annals Of Surgery*, 260(2), 205-211.

**Hughes-Hallett, A.**, Mayer, E., Pratt, P., Vale, J., Darzi, A. (2015). Quantitative analysis of technological innovation in minimally invasive surgery. *British Journal of Surgery*. (Epub ahead of print)

Content from this chapter was presented as:

**Hughes-Hallett, A.**, Mayer, E., Pratt, P., Vale, J., Darzi, D., Quantifying Innovation in Robotic Surgery. Hamlyn Symposium on Medical Robotics '14

## 2.1 Introduction

In order to understand whether any technological innovation, and in particular innovation in healthcare, is likely to be successful two facets of the technology must first be understood; the innovation potential and the user needs.<sup>60</sup> In the initial part of this chapter a novel approach to understanding the innovation within a surgical technology cluster is proposed, and subsequently utilised to assess image guidance.

Innovation in healthcare technology generally, and more specifically within surgery, can be defined as a dynamic and continuous process involving the introduction of a new technology or technique that initiates a change in clinical practice.<sup>61,62</sup> Innovation has been unrelenting in surgery since the introduction of aseptic technique and anaesthesia in the late 19<sup>th</sup> century, and has been spasmodic in line with the advent of novel and enabling technologies, most recently the advent of intra-abdominal MIS.<sup>63</sup>

The study of innovation is a relatively mature academic field in social science and industry. It stems from seminal work undertaken by Ryan and Gross in the 1940s that related to the adoption of agricultural products,<sup>12</sup> and has become universal in its theoretical application.<sup>13,62,64,65</sup> Although there has been increasing interest in innovation theory and its application within healthcare,<sup>18,63,66–69</sup> a robust method or framework for quantitative analysis is missing. Progress across all healthcare disciplines has been limited by this lack of appropriate and easily accessible metric for innovation.<sup>19,62</sup>

The genesis of technological innovation is often identified as an original patent. A patent can be defined as “the right to exclude others from making, using, offering for sale, or selling an invention”,<sup>70</sup> and represents a relevant, reliable, and readily accessible potential tool for measurement of technology development.<sup>62</sup> A more recognised alternative to patent data is the bibliometric analysis of peer-reviewed publications.<sup>71</sup> These metrics have both been proposed as measures of healthcare research output.<sup>72</sup>

Surgery has seen a recent paradigm shift in practice due to the development of intra-abdominal MIS, which has been facilitated by technological innovations. In this chapter

this shift in surgical practice has been used to validate the use of patent and publications as metrics of healthcare technology and innovation and to assess their potential as predictors of future areas of innovation growth. These novel innovation metrics were then used to elucidate the areas of greatest contemporary innovation in surgery and to establish whether surgical image guidance lay among the areas of greatest innovation growth.

## 2.2 Methods

### 2.2.1 Patent and publication data collation

Patent data were collated using the proprietary software *PatentInspiration* (AULIVE, Ypres, Belgium) which searches the “DOCDB” patent database using bibliographic data from over 90 countries.<sup>73</sup> Granted patents (titles, abstracts, and descriptions) were searched from 1980 to 2010 using the following Boolean search strategy: (“surgeon” OR “surgical” OR “surgery”). The search results were limited to single members of patent families to prevent duplication of data. Using the same strategy, a PubMed (National Library of Medicine, Maryland, USA) search was performed to extract publication data for the same period.

### 2.2.2 Normalisation of data

Over the course of time, both overall patent and publication counts have been rising exponentially (Figure 2.2.1 and Figure 2.2.2). In order to normalise for this background rise innovation was assumed to be a global constant allowing for both patent and publication counts to be normalised using for using the total patent and publication counts from 2010 (the year reporting the greatest number of patent and publications).

$$II_i^{normalised} = \frac{II_i^{original}}{c_i}$$

$$c_i = \frac{t_i}{t_{2010}}$$

Here,  $t_i$  is the total number of patents granted by the United States patenting office, or publications indexed on PubMed and  $c_i$  is the innovation constant for a given year,  $i$ ,

and  $II_i$  denotes the innovation index (defined as the number of patents or publications within a specific domain). This approach to scaling data has been previously utilised for analysis of patent data<sup>74,75</sup> but has not yet been applied to publication data, though the same principles apply.

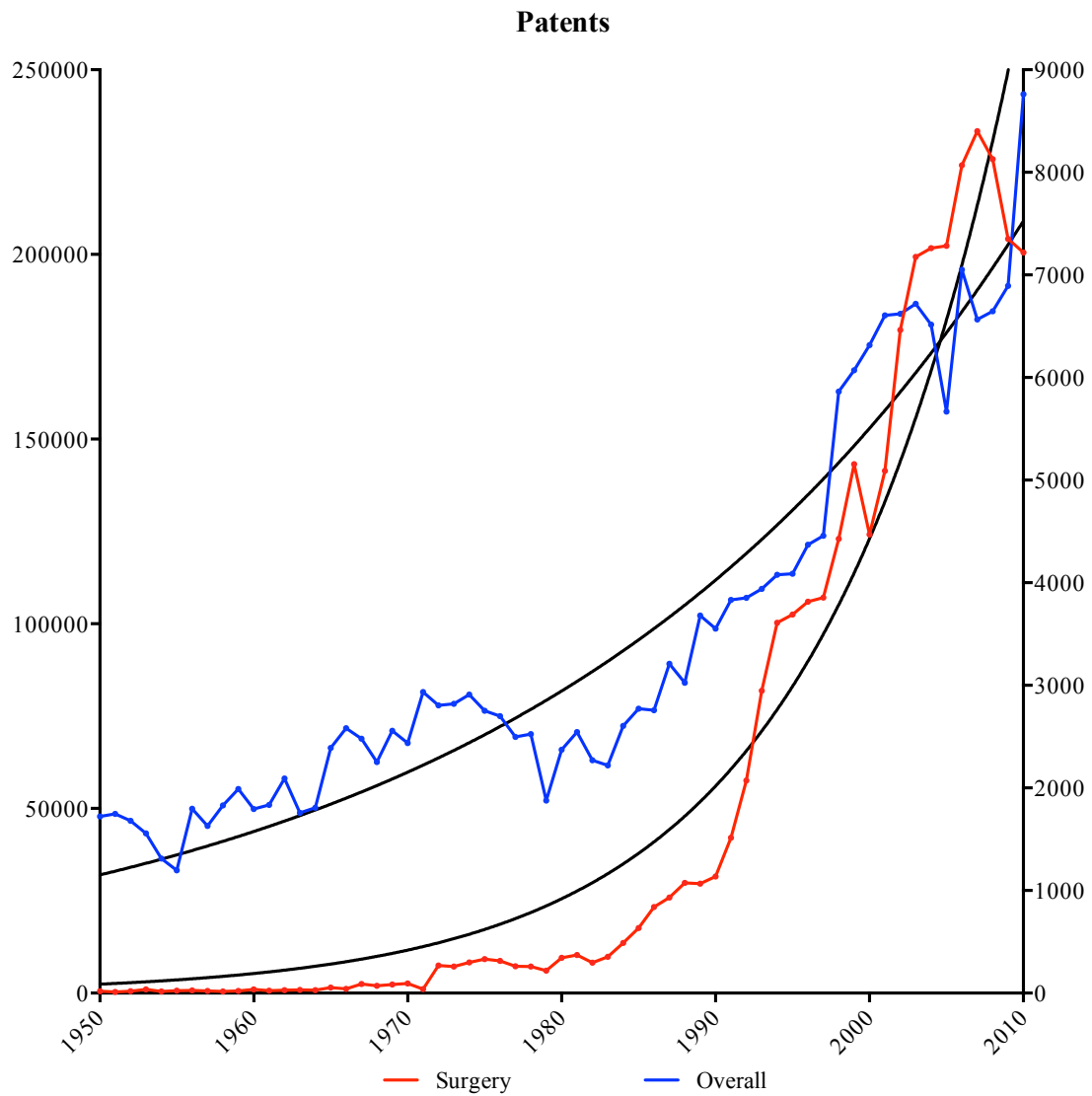


Figure 2.2.1 – Rise in patent counts year-on-year (1950-2010). The left hand axis relates to the *innovation index* for patents, while the right relates to those pertaining to surgery.  $R^2$  values of exponential curves demonstrated better goodness of fit than those for linear relationships.

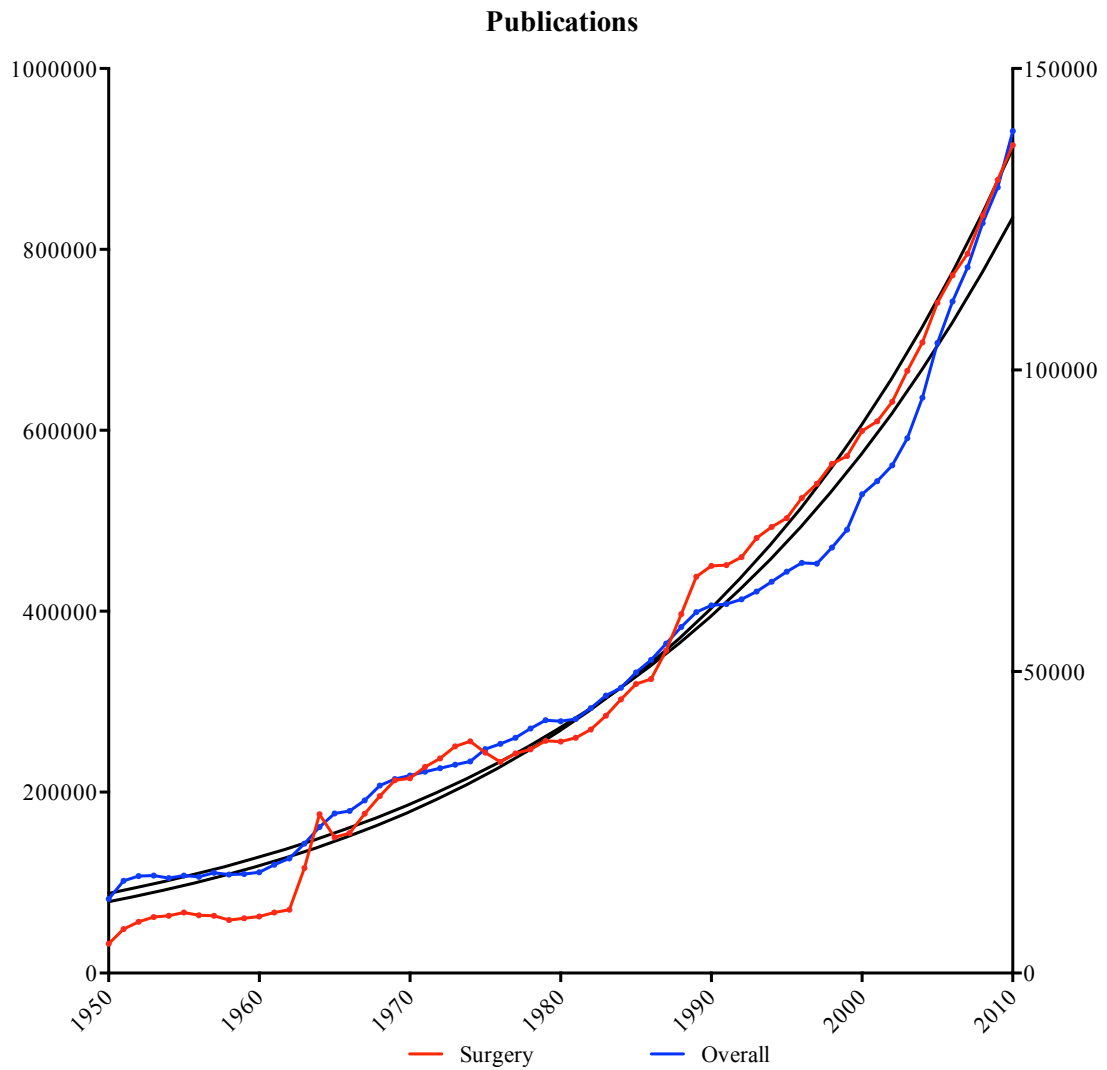


Figure 2.2.2 – Rise in publication counts year-on-year (1950-2010). The left hand axis relates to the *innovation index* for publications, while the right relates to those pertaining to surgery.  $R^2$  values of exponential curves demonstrated better goodness of fit than those for linear relationships.

### 2.2.3 Patent codes

All patents are identified by a series of codes; these allow patents pertaining to similar technologies to be grouped together. The code structure is pyramidal with the most descriptive codes lying at the base of the hierarchy (Figure 2.2.3). These descriptive codes were used when performing the analysis of patent performance, as outlined below.

### 2.2.4 Establishing the top performing and emerging technology clusters

Following compilation of the dataset, the top 30 performing patent codes (those patent codes under which the greatest number of patents had been applied for) were extracted. Codes were subsequently grouped into clusters of related surgical technologies (Figure 2.2.3) by two authors with any disagreement arbitrated by a third author.

Patent Group	Search Strategy
Image guidance and imaging	("image guidance" OR "image-guided" OR "augmented reality") AND (surgery OR surgical OR surgeon)
Surgical robots	(robot OR robotic OR daVinci OR "da Vinci") AND (surgery OR surgeon OR surgical)
MIS	("minimally invasive" OR laparoscopic OR laparoscopy OR "minimal access" OR "key hole") AND (surgery OR surgical OR surgeon)
Ophthalmic Surgery	(cornea OR eye OR ophthalmic OR ocular) AND (surgery OR surgeon OR surgical)
Surgical Staplers	(stapler OR staple) AND (surgery OR surgical OR surgeon)

Table 2.2.1 – PubMed and PatentInspiration search strategies

In order to identify the patents granted within these technology clusters, but not captured within the top 30 patent codes, a Boolean search, specific to each cluster, was undertaken of the patent database (see Table 2.2.1 for specific search strategies). The same strategies were then used to search PubMed in order to acquire a measure of publication activity. Searches were limited to the well-defined areas of technological innovation; these were determined by two authors, with any disagreement, again, arbitrated by a third author. This process was undertaken to acquire a measure of technology and innovation year-on-year.

The above methodology was then repeated while limiting the search period to 2000-2010. Reframing the data to a more recent time period generated a contemporary list of the top 30 patent codes. The comparison of the two datasets allowed areas of recent technology expansion to be explored.

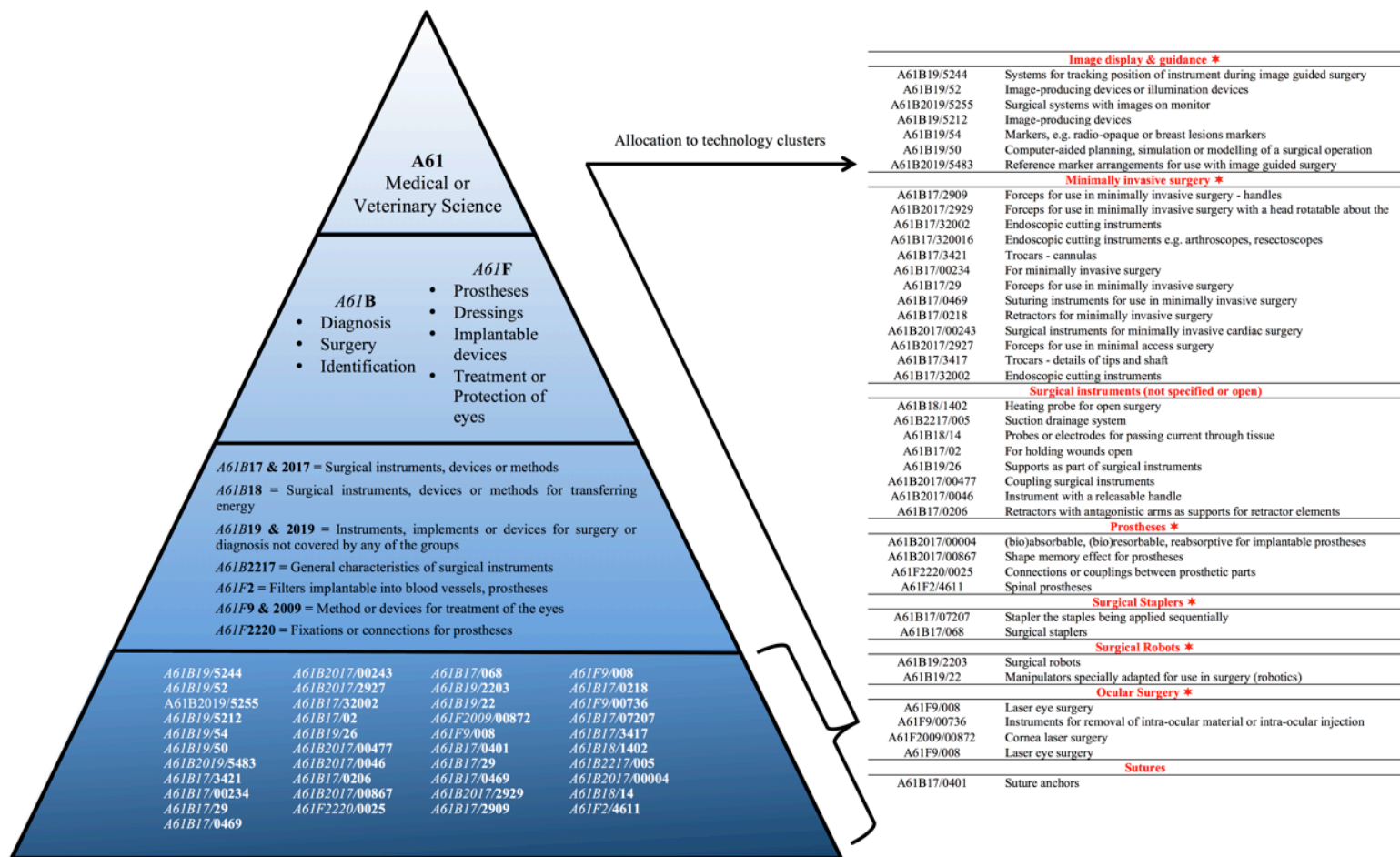


Figure 2.2.3 – Hierarchy of top 30 performing patent codes retrieved by the search “Surgery OR Surgical OR Surgeon” between 1980 to 2010 and 2000 to 2010. On the left hand side of the figure the patent codes and their cluster allocation in elucidated. \* Denotes clusters chosen for in-depth analysis



## 2.2.5 Qualifying growth in image-guided surgery

After the validation of the metric and the determination of correlation between patent and publication an additional step of analysis was undertaken to allow a better understanding of innovation growth in image guidance within different anatomical regions – specifically for orthopaedic, neurosurgical and abdominal pathology, three areas in which image guidance technology has been employed. The patent codes do not offer the level of granularity to establish the target organ and as such this step employed further systematic searches of the Medline database alone. The search strategies used can be seen in Table 2.2.2.

Group	Search Strategy
Abdominal Surgery	((("image guidance" OR "image-guided" OR "augmented reality") AND (("minimally invasive" OR laparoscopic OR laparoscopy OR "minimal access" OR "key hole" OR abodme*)) AND (surgery OR surgical OR surgeon)) NOT (neurosurg* OR brain OR ortho* OR knee OR hip)
Neurosurgery	((("image guidance" OR "image-guided" OR "augmented reality") AND (neurosurg* OR brain) AND (surgery OR surgical OR surgeon)) NOT (("minimally invasive" OR laparoscopic OR laparoscopy OR "minimal access" OR "key hole" OR abodme*) OR ortho* OR knee OR hip)
Orthopaedic Surgery	((("image guidance" OR "image-guided" OR "augmented reality") AND (ortho* OR knee OR hip) AND (surgery OR surgical OR surgeon)) NOT (("minimally invasive" OR laparoscopic OR laparoscopy OR "minimal access" OR "key hole" OR abodme*) OR neurosurg* OR brain)

Table 2.2.2 – Pubmed search strategies for image guidance sub-analysis

## 2.2.6 Statistical analysis

Patent and publication data were plotted against one another to determine the nature of their relationship. If their relationship was monotonic, Pearson’s (r) or Spearman’s rank (r<sub>s</sub>) correlation coefficient was utilised, depending on whether the association was linear or non-linear, respectively. Statistical analysis was undertaken using *GraphPad Prism* (GraphPad Software Inc, CA, USA).

## 2.3 Results

### 2.3.1 Data on patents and publications

The initial search of patent data retrieved a total of 52,046 patents. The largest proportion of patents was accounted for by the USA, representing 28% of the data pool

(Figure 2.3.1). The initial search of the PubMed database retrieved a total of 1,801,075 publications. The original and normalised patent and publication data are illustrated in Figure 2.3.2 and Figure 2.3.3, with surgical patenting activity exhibiting an overall upward trajectory over time in contrast to publication activity which appeared to peak in 1997, followed by a subsequent decline toward a baseline level.

### **2.3.2 Top performing technology clusters**

The top performing technology clusters over the last 30 years are summarised in Table 2.3.1. The largest cluster was MIS, accounting for 40.1% of patents granted during the period studied. The four other technology clusters selected for in-depth analysis were image-guided surgery, robot-assisted surgery, surgical staplers, and ophthalmic surgery (Table 2.3.1).

When the same analysis was performed on patents from 2000 to 2010, there was re-arrangement in ordering of the top-performing technology clusters. Image guidance represented the most dominant group accounting for 27.4% of patents. Robot-assisted surgery, which did not feature in the initial 30-year analysis, also emerged as an important technology cluster (Table 2.3.1).

As can be seen in Figure 2.3.4 and Figure 2.3.5, the rapid growth in both robot-assisted surgery and image guidance appears to be closely related, with patent and publication rate very strongly correlated ( $r_s = 0.98$  and  $0.94$  respectively,  $p < 0.001$ ). As an established technology cluster, MIS had a unique patent and publication signature amongst those selected for analysis (Figure 2.3.6). The period from 1990 to 1994 saw a rapid rise in MIS patent and publication counts. This initial rise was followed by a sustained period of slower growth in publications and patents. Similarly, high correlation was seen between patent and publication counts within MIS ( $r_s = 0.95$ ,  $p < 0.001$ ). Surgical staplers (Figure 2.3.7) and ophthalmic surgery (Figure 2.3.8) were the oldest of the technologies evaluated<sup>76,77</sup> and demonstrated a relatively constant rate of both patent and publication counts over the 30-year period examined, with poor correlation of these metrics ( $r_s = 0.30$ ,  $p = 0.10$  and  $0.46$   $p=0.009$ ).

Further post-hoc analysis of surgical stapler and ophthalmic surgery data was undertaken to investigate the observed flat and poorly correlated growth pattern. The analysis period was extended to span from 1950 to 2010 such that longer-term trends could be determined (Figure 2.3.7 and Figure 2.3.8). This revealed sigmoid shaped growth curves followed by prolonged plateau phases for both technology clusters. Correlation of the stapler and ophthalmic surgery datasets over this period of time improved to 0.65 ( $p < 0.001$ ) and 0.84 ( $p < 0.001$ ) respectively.

### 2.3.3 Sub-analysis of image guidance cluster

As can be seen in Figure 2.3.9, if publication growth within image guidance is subdivided into the target organ sets, differing patterns of growth can be seen. Within neurosurgery and orthopaedics, publication growth stalls and plateaus in the late 1990s. In contrast a longer and shallower, exponential growth curve is seen within image guidance in intra-abdominal surgery.

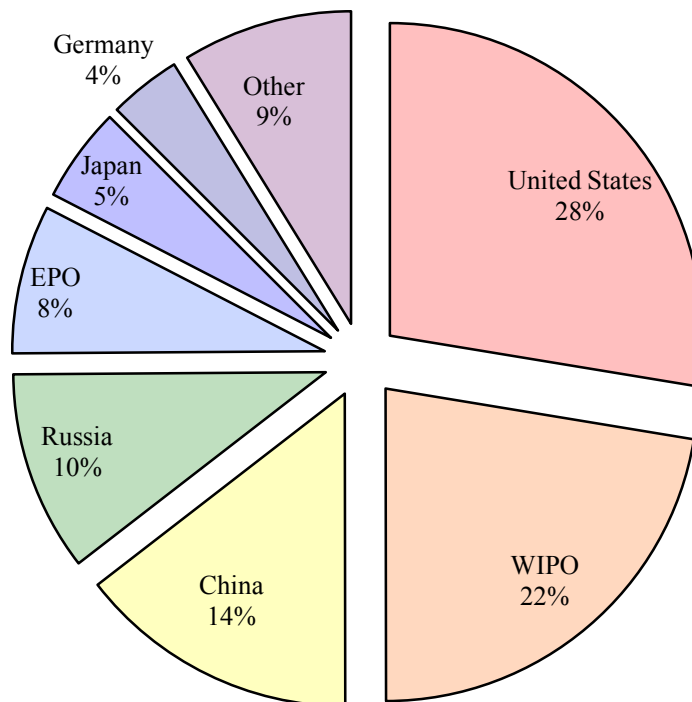


Figure 2.3.1 – Patenting offices by percentage of total patents filed relating to surgery, data from the United States patenting office was used for the normalisation of data. *WIPO = World intellectual property organisation, EPO = European patent office*

Rank	Technology Cluster	No. Codes	No. Patents	%
<i>1980-2010</i>				
<b>1</b>	<b>MIS</b>	<b>11</b>	<b>9806</b>	<b>40·1</b>
2	Surgical instruments*	8	6069	24·8
<b>3</b>	<b>Image guidance</b>	<b>4</b>	<b>3612</b>	<b>14·8</b>
<b>4</b>	<b>Ophthalmic surgery</b>	<b>3</b>	<b>3621</b>	<b>8·3</b>
5	Prostheses	2	1373	5·6
6	<b>Surgical staplers</b>	1	849	3·5
7	Sutures	1	677	2·8
<i>2000-2010</i>				
<b>1</b>	<b>Image guidance</b>	<b>7</b>	<b>3978</b>	<b>27·4</b>
<b>2</b>	<b>MIS</b>	<b>8</b>	<b>3911</b>	<b>27·0</b>
3	Surgical instruments*	5	2520	17·4
4	Prostheses	3	1099	7·6
<b>5</b>	<b>Surgical staplers</b>	<b>2</b>	<b>899</b>	<b>6·2</b>
<b>6</b>	<b>Surgical robotics</b>	<b>3</b>	<b>881</b>	<b>6·1</b>
<b>7</b>	<b>Ophthalmic surgery</b>	<b>2</b>	<b>803</b>	<b>5·5</b>
8	Sutures	1	415	2·9

Table 2.3.1 – Top 30 patent codes amalgamated into technology clusters (patent counts are normalised).

Clusters in **bold** were those selected for in-depth analysis

## Patents

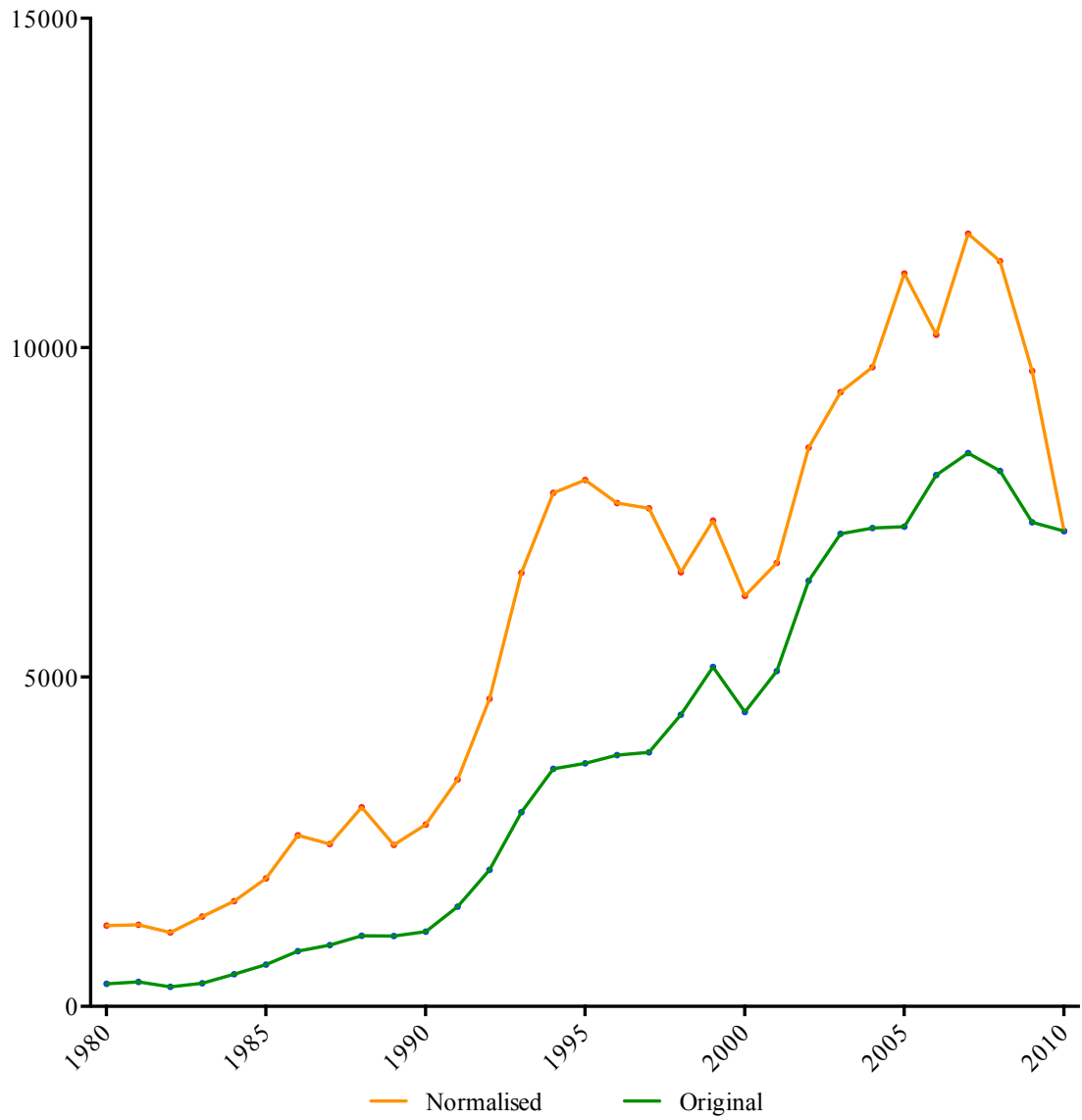


Figure 2.3.2 – Original counts and the corrected *innovation index* for patents year-on-year related to surgery (1980-2010).

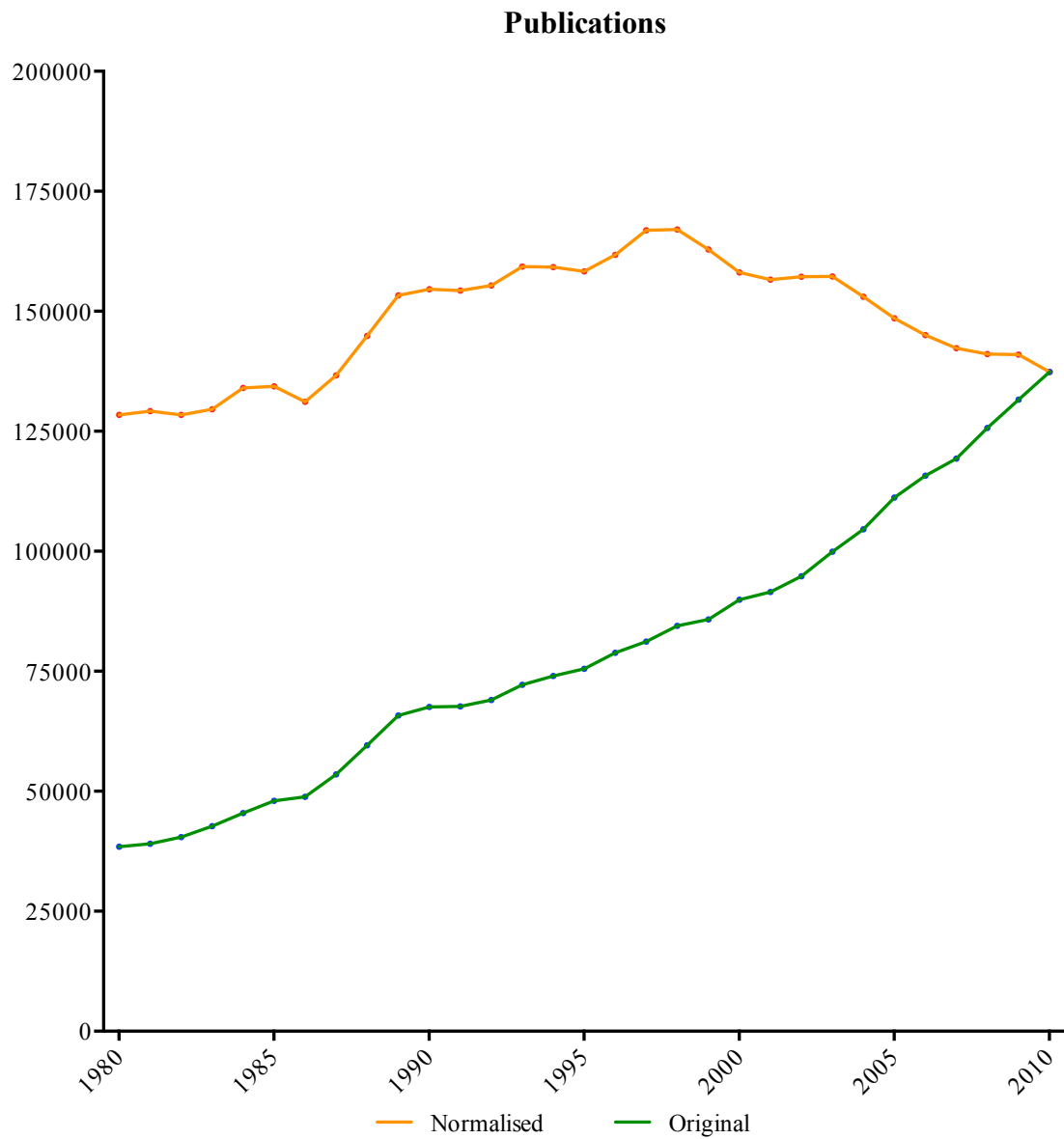


Figure 2.3.3 – Original counts and the corrected *innovation index* for publications year-on-year related to surgery (1980-2010).

### Image Guided Surgery 1980-2010

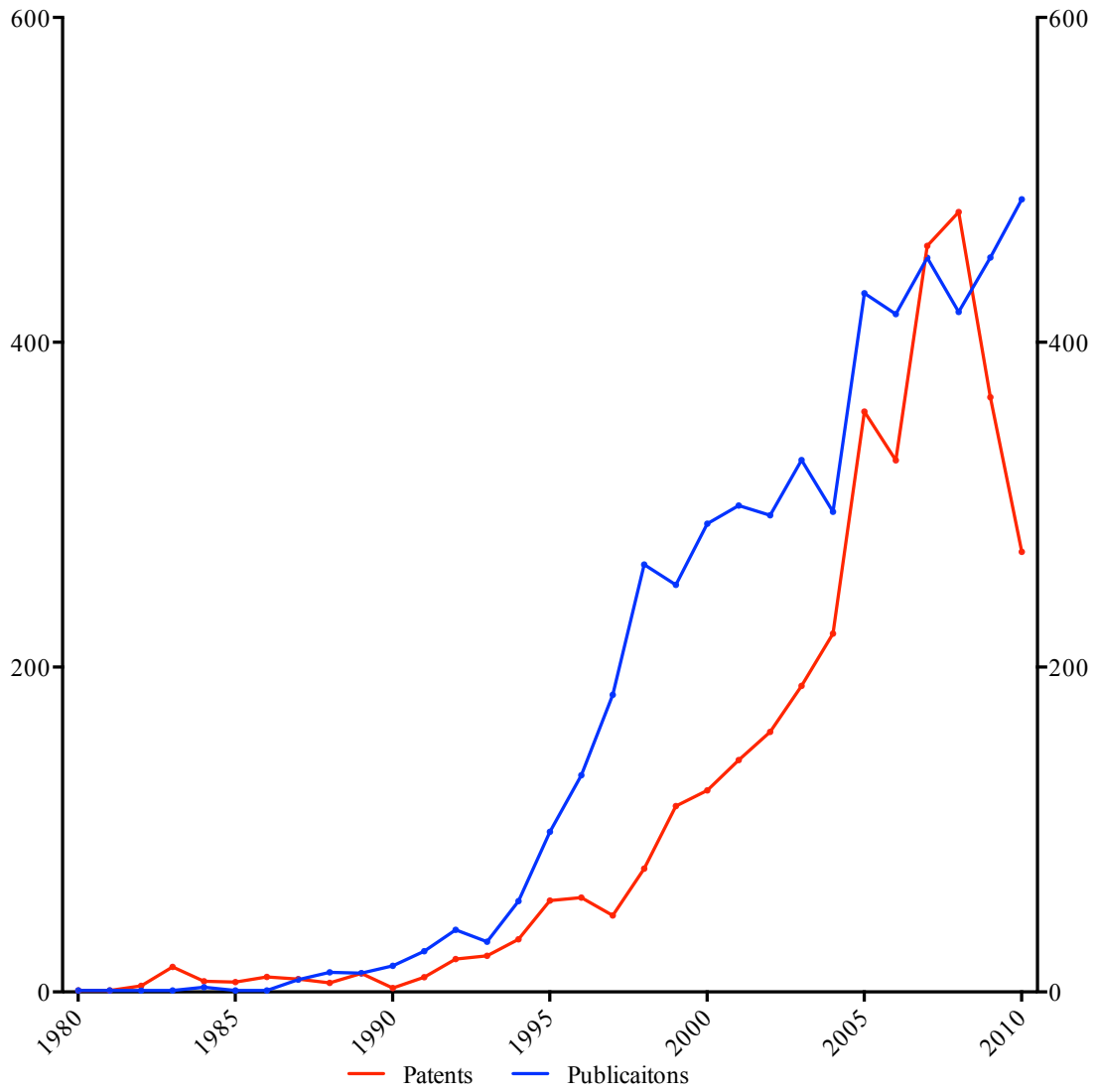


Figure 2.3.4 – Year-on-year *innovation index* for patent and publications within image-guided surgery.

### Robotic Surgery 1980-2010

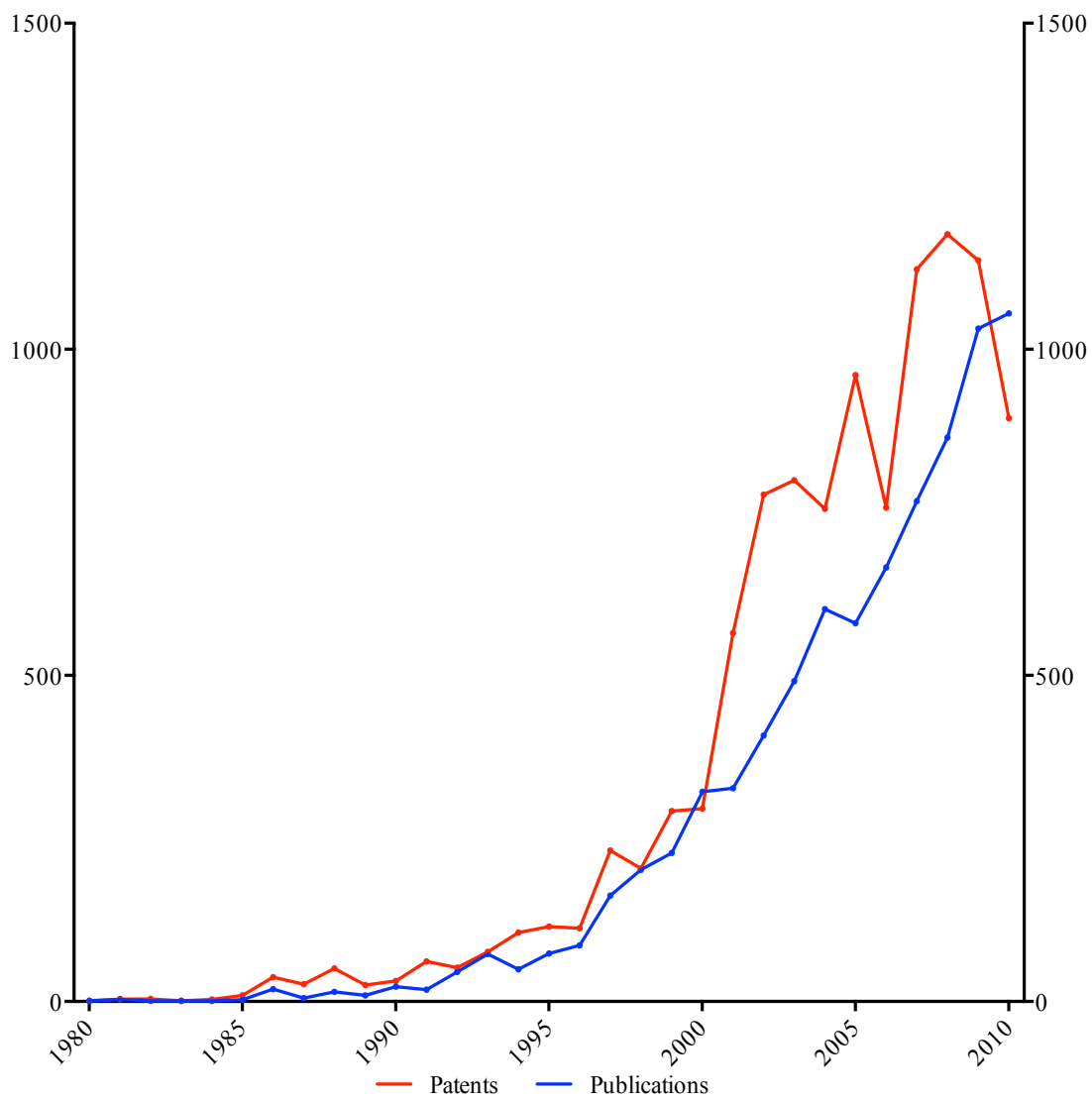


Figure 2.3.5 – Year-on-year *innovation index* for patent and publications within robotic surgery.



### Minimally Invasive Surgery 1980-2010

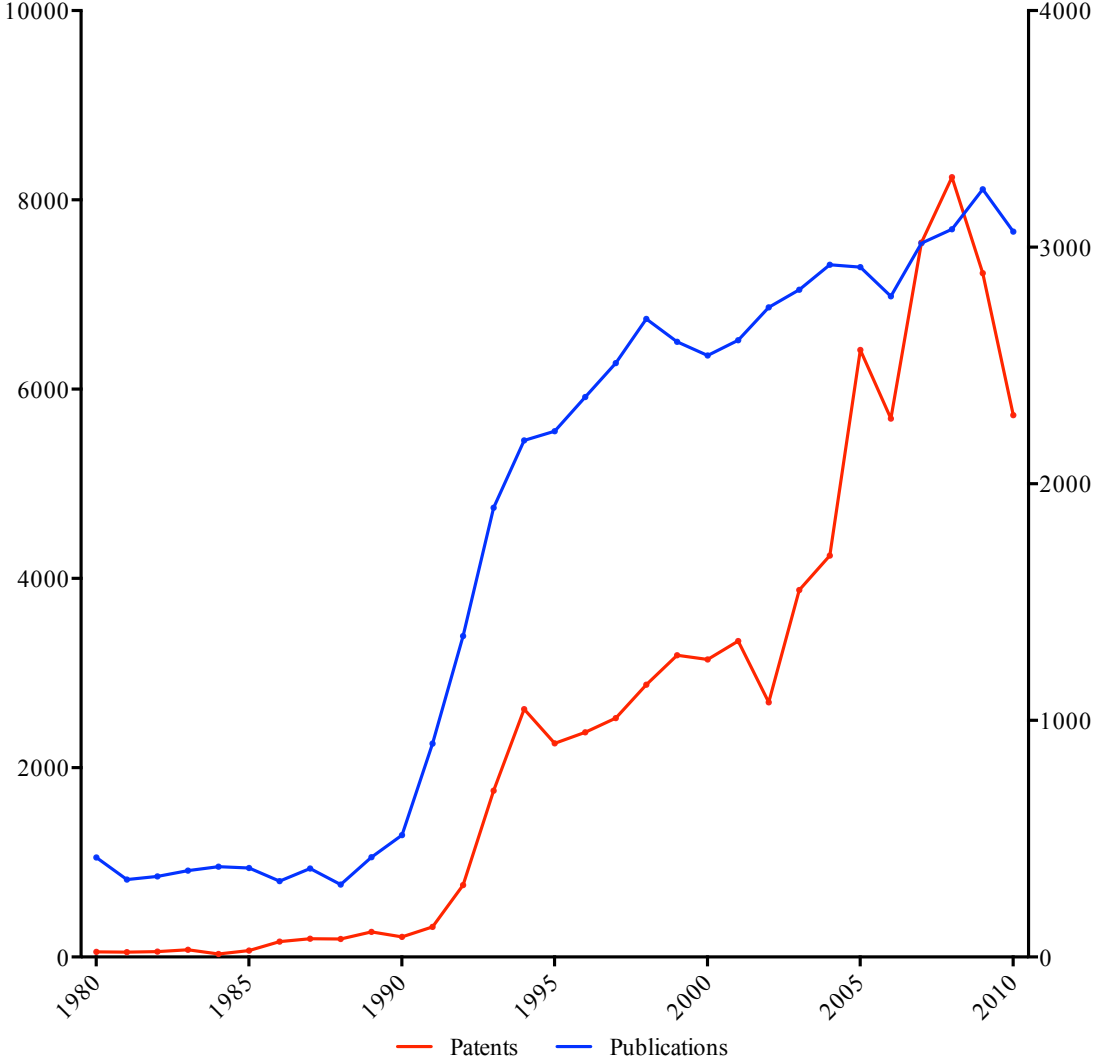


Figure 2.3.6 – Year-on-year *innovation index* for patent and publications within MIS.

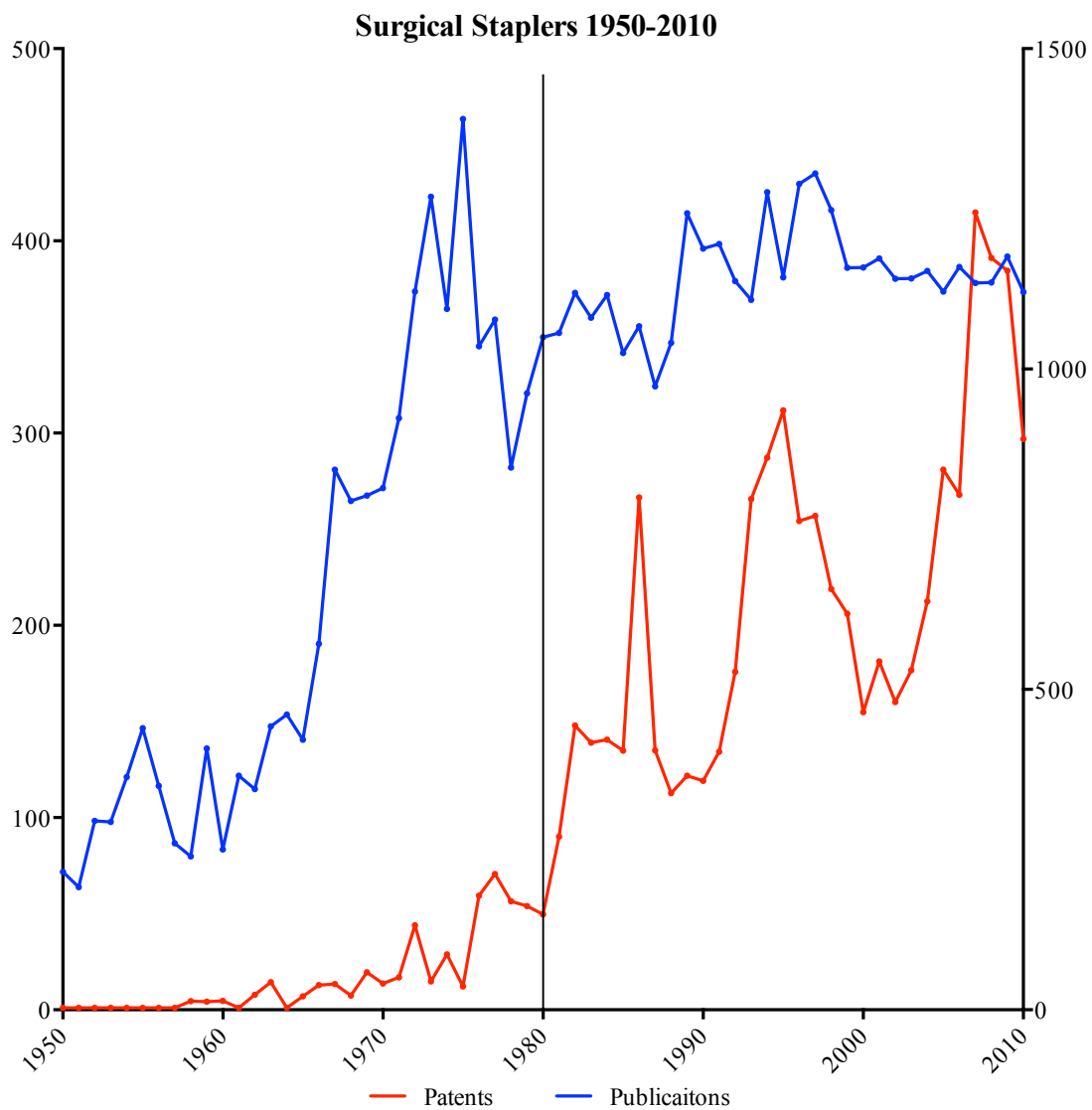


Figure 2.3.7 – Year-on-year *innovation index* for patent and publications within surgical staplers. Left y-axis pertains to *innovation index* for publications and the right for patents. Data was initially analysed from 1980-2010, in post hoc analysis this was extended back to 1950. The bounding year of 1980 is represent on the graph by a black line.

### Ophthalmic Surgery 1950-2010

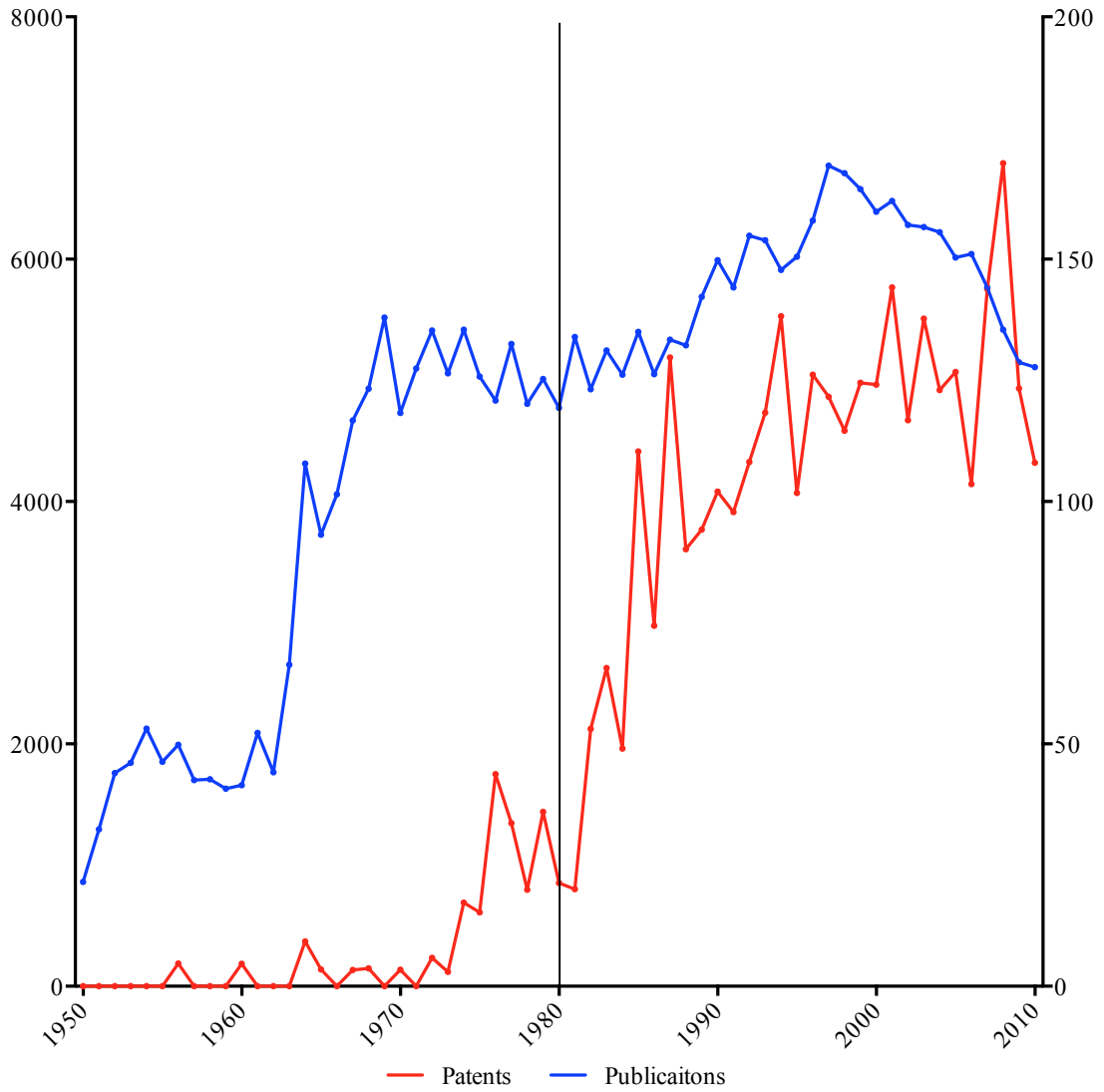


Figure 2.3.8 – Year-on-year *innovation index* for patent and publications within ophthalmic surgery. Left y-axis pertains to *innovation index* for publications and the right for patents.

### Image guidance publications by target organ group

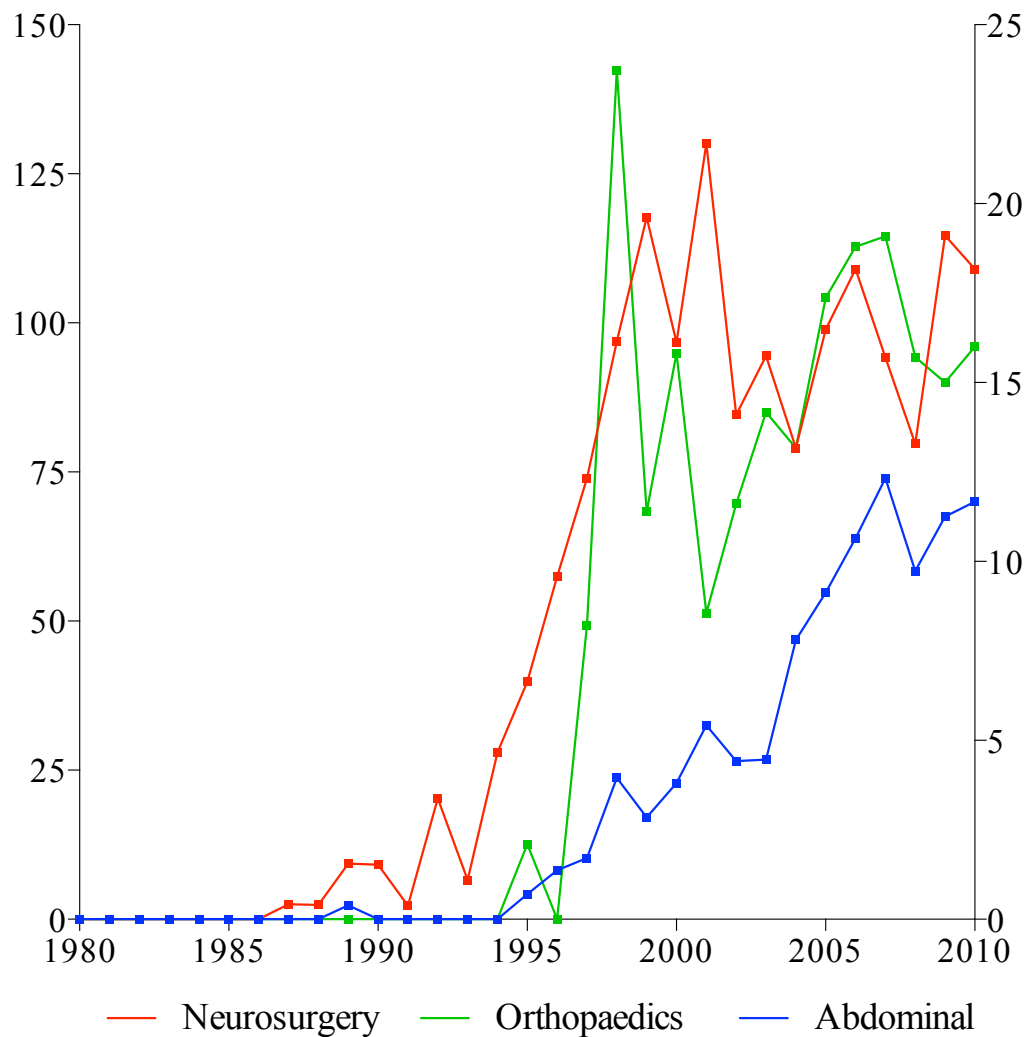


Figure 2.3.9 – Year-on-year *innovation index* for publications within the image guidance cluster, sorted by surgical site. The y-axis on the left pertains to the innovation index for abdominal and neurosurgery and the right to orthopaedic surgery

## 2.4 Discussion

### 2.4.1 Principal findings

In this study a quantitative analysis of healthcare technology and innovation has been performed using a novel framework combining international patent and publication data. Using surgery as an exemplar, major technology clusters of influence and their respective patterns over time have been identified. Minimally invasive surgery was found to be the most significant innovation to have occurred over the past 30 years, with notable peaks in overall publication and patent counts corresponding closely with its progress of adoption into clinical practice. Looking forward, recent trends in these metrics suggest that image guidance and robotics will play an increasingly important role in the near future. The distinctly steep upward trajectories for publication and patent counts of these emerging technology clusters highlights future value in using these metrics as forecasting tools for clinical impact potential.

Rogers' *Diffusion of Innovations* theory describes the adoption curve of a technology as 'S-shaped'.<sup>13</sup> Attitudes and responses of potential adopters towards any given innovation vary along different portions of the curve, and this influences their status and timing of adoption.<sup>13</sup> This curve does not apply exclusively to the adopters. As evidenced by the data presented in this study, the theory can also be applied to specific innovation clusters themselves.<sup>64</sup>

Between 1980 and 2010 three phases of publication and patent activity were seen amongst the technology clusters selected for in-depth analysis: a correlated exponential rise (i.e. image guidance, robotics and pre-1994 MIS), a plateau (i.e. MIS post-1994), and finally a poorly correlated plateau in both patents and publications (i.e. surgical staplers and ophthalmic surgery post-1980). These phases correspond to the different periods of innovation highlighted in Figure 2.4.1. The first phase is one of incubation in which there is take-off in growth corresponding to early patenting and publication activity.<sup>78</sup> The patents and publications filed in this stage are likely to be 'high value' due to their seminal nature and as such are likely to be highly cited. This incubation phase is followed by a phase of *exponential growth*<sup>78</sup> corresponding to maximal innovation reflected by a high innovation output by both surgeons (reflected in

publication counts) and institutions and industry (reflected in patent counts). In the final phase of the curve, patent and publication numbers plateau, representing the point of *diffusion saturation*. At this point patent and publication counts are sustained by technological refinement<sup>65,78</sup> but the period of maximal innovation has passed.

Within the cluster of surgical staplers and ophthalmic surgery, the poorly correlated and comparatively flat trends in patent and publication counts were inconsistent with the other clusters examined and the expected sigmoid shaped growth curves. This plateau-like pattern may relate to the maturity of the technologies.<sup>76,77</sup> Similar poorly correlated flat growth trends have been documented outside of the medical literature as being indicative of a mature technology in which industry leaders incrementally refine patents to maintain market share.<sup>65</sup> The extended post-hoc analysis confirmed these plateaus to be the tail-end of a prolonged classical S-shaped innovation curve.<sup>13</sup>

Another curious trend is the decrease in number of patents granted from 2008 to 2010 across all datasets examined. There are two possible explanations for this. First, that innovation in surgery is currently in a state of *lapsed activity*, perhaps as a consequence of the recent global economic crisis. The second, and possibly more likely explanation, is that this downturn in patenting is a result of the *delay* between a patent being applied for and it being granted.<sup>64</sup>

#### **2.4.2 Growth in image guidance**

When examining the growth in image guidance, a further sub analysis of the data, by organ system was undertaken, looking to establish the context in which this growth was occurring. This analysis revealed two distinct categories of growth. The first was a period of rapid exponential growth occurring in the late 1990s, and occurred within the image-guided neuro- and orthopaedic surgery clusters. This probably corresponds to the widespread adoption of stereotactic image-guided surgery in these subspecialties in the early to mid 1990s.<sup>79,80</sup> In contrast, image guidance in abdominal surgery continues to be in a phase of slower trajectory, exponential growth that seems to have passed the crucial diffusion chasm (Figure 1.2.2). This ‘chasm’ represents the moment where a technology moves from the innovators to early adopters and is the point at which most

innovations fail, with the diffusion chasm representing the greatest hurdle in the path to widespread adoption.<sup>13</sup>

The nature of image-guided surgery in abdominal surgery, largely related to greater difficulties with image registration and deformation, means it poses numerous and complex engineering challenges when compared to the more rigid structures faced in neuro- and orthopaedic surgery. The increased difficulty of accounting for these factors within the deformable environment of the abdomen has almost certainly resulted in a slower rate of development, and may well explain the two distinct patterns of growth observed.

### **2.4.3 Comparison with other studies**

Historically, research examining healthcare innovation has almost exclusively focused on the *qualitative* analysis of isolated case examples.<sup>18,63,67,81</sup> Within the wider healthcare context, much of the literature is orientated towards the generalisable process of adoption rather than innovations or technology clusters themselves.<sup>66,69,82,83</sup> The status of scientific study in healthcare innovation is therefore restricted in scope to assess performance of medical or surgical technologies objectively, or forecast future growth and potential for clinical impact. This study has addressed this restriction providing a *quantitative* framework, based on patent and publication data, with which to assess the impact of past, and potential impact of emerging areas of healthcare innovation.

The use of patent library data as a tool to measure healthcare innovation is under-utilised and under-investigated. Trajtenberg described a method for equating patent citations and counts with innovation value, and reported that these metrics were indicative of patent *value* within the then novel and expanding technology field of CT imaging.<sup>62,84</sup> This work demonstrated that patent counts, weighted by citations, were symptomatic of the value of innovation within the technology cluster of CT scanners. In addition to establishing relationships between patent citations and innovation, it was also postulated that simple patent counts were a good measure of the amount of research and development occurring within a given field.

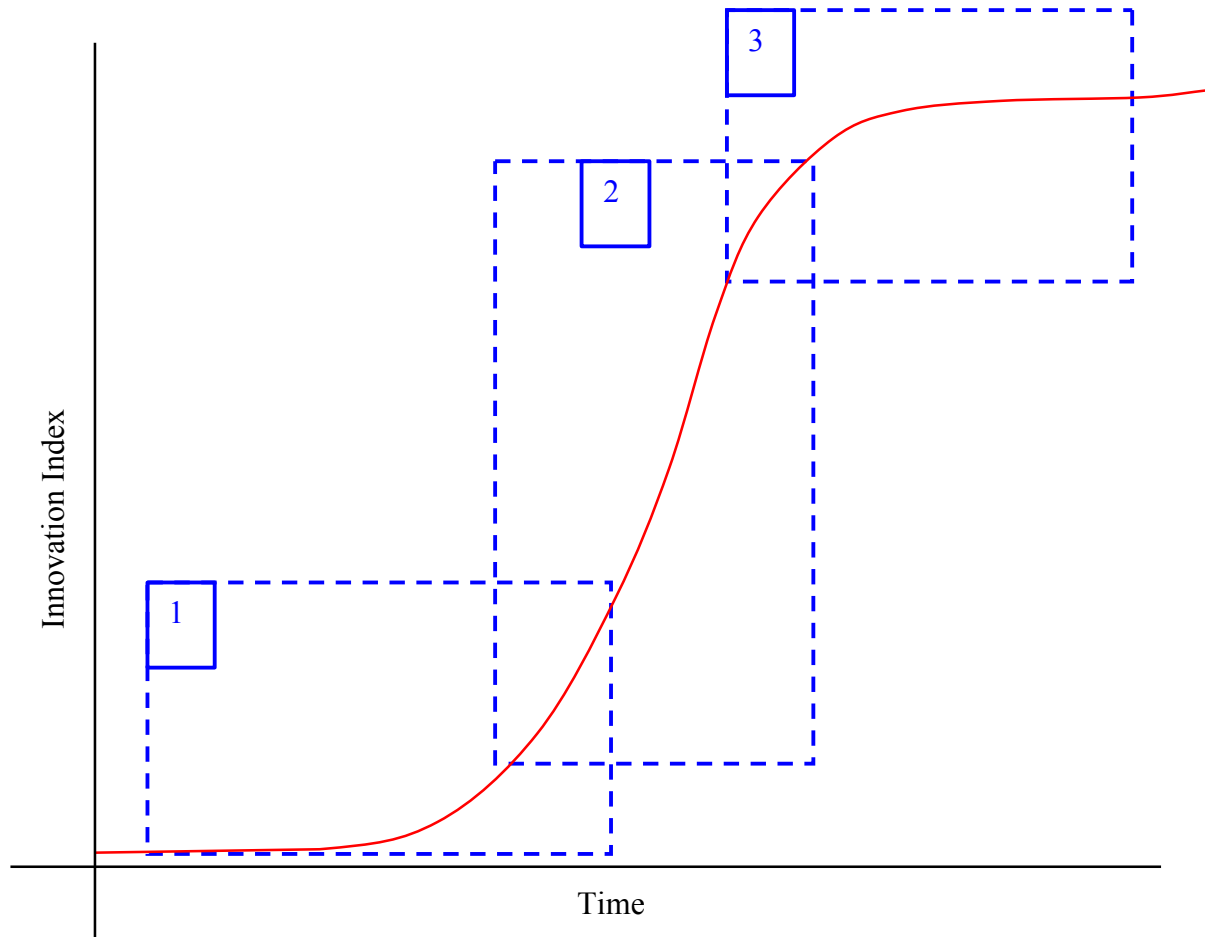


Figure 2.4.1 - Innovation Curve. 1) Period of technological incubation 2) Period of widespread innovation and technological adoption 3) Period of technological refinement



Outside the healthcare literature, a number of other studies have also described a quantitative approach to analysis of innovation.<sup>64,65,85</sup> Bengisu *et al.* examined the use of patent and publication data to forecast emerging technologies across a wide range of disciplines and demonstrated similar findings to this study.<sup>65</sup> Their findings were that technologies demonstrating a high correlation between patents and publications were most likely to become key technologies for industry in the future, while technologies that had relatively flat growth and low correlation had reached maturation, with developers minimising risk by reducing investment in the product.<sup>65</sup>

#### **2.4.4 Study limitations**

In addition to being metrics of innovation, both patents and publications may themselves act as adjuncts to innovation. Both exist on publically available databases that are accessed as a matter of routine by ‘innovators’ as a repository of knowledge acting to inspire the development of novel ideas and technologies. As such, a rise in patents and publications may positively re-enforce the diffusion of innovation within a particular technology cluster. Although of interest, this feedback loop does not alter the efficacy of patent and publication counts as innovation metrics since the end product, innovation growth, is left unaffected.

Although this study offers a novel quantitative approach to assessment of healthcare innovation, it is not without limitations. Patents may ignore the output of independent inventors who do not have the financial resources to patent. A similar problem relates to an artificial publication lag, with developers potentially employing a strategy of deliberate academic publication delay until a patent has been granted. There are two further factors that may limit the predictive capacity of the model: firstly, the methodology prevents recognition of a valuable innovation in its nascence; and secondly, there is unavoidable time lag between an original patent application and patent granting.

## **2.5 Conclusions**

Publicly available patent and publication data can be used to both identify and, to some extent, forecast technological innovation in healthcare.<sup>62,65</sup> Within this chapter, these metrics have been utilised to empirically map 30 years of surgical history. In addition to establishing the influential technology clusters of the past, the results offer insight into the future landscape for surgical technology, with the fields of surgical image guidance and robotics undergoing exponential growth. This exponential growth in image guidance, and more specifically within intra-abdominal image guidance, suggests that it lies within the phase of continued rapid adoption and as such represents an area of research growth and market interest.

CHAPTER 3: THE CURRENT AND FUTURE USE OF  
IMAGING IN UROLOGICAL ROBOTIC SURGERY: A SURVEY  
OF THE EUROPEAN ASSOCIATION OF ROBOTIC  
UROLOGICAL SURGEONS<sup>†</sup>

---

<sup>†</sup> Content from this chapter was published as:

**Hughes-Hallett, A.**, Mayer, E. K., Pratt, P., Mottrie, A., Darzi, A., & Vale, J. (2014). The current and future use of imaging in urological robotic surgery: A survey of the European Association of Robotic Urological Surgeons. (2015) *International Journal of Medical Robotics and Computer Assisted Surgery*. *11(1)*. 8-14

### 3.1 Introduction

Since Röntgen first utilised X-rays to image the carpal bones of the human hand in 1895 (Figure 3.1.1), medical imaging has evolved and is now able to provide a detailed representation of a patient's intracorporeal anatomy, with recent advances allowing for 3D reconstructions. The visualisation of anatomy in 3D has been shown to improve the ability to localise structures when compared to 2D with no change in the amount of cognitive loading.<sup>86</sup> This has, in turn, allowed imaging to move from a largely diagnostic tool to one that can be used for both diagnosis and operative planning.

One potential interface to display 3D images, to maximise its potential as a tool for surgical guidance, is to overlay them onto the endoscopic operative scene. This addresses, in part, a criticism often levelled at robotic surgery, the loss of haptic feedback. Augmented reality has the potential to mitigate for this sensory loss by enhancing the surgeon's visual cues with information regarding subsurface anatomical relationships.<sup>7</sup>

Augmented reality surgery is in its infancy for intra-abdominal procedures due in large part to the difficulties of applying static preoperative imaging to a constantly deforming intraoperative scene.<sup>87</sup> There are case reports and *ex-vivo* studies in the literature examining the technology in minimal access prostatectomy<sup>87-90</sup> and partial nephrectomy,<sup>91-94</sup> but there remains a lack of evidence determining whether surgeons feel there is a role for the technology and if so for what procedures they feel it would be efficacious.

A questionnaire-based study was designed to assess: firstly, the pre- and intraoperative imaging modalities utilised by robotic urologists; secondly, the current use of imaging intraoperatively for surgical planning; and finally, whether there is a desire for augmented reality amongst the robotic urological community.

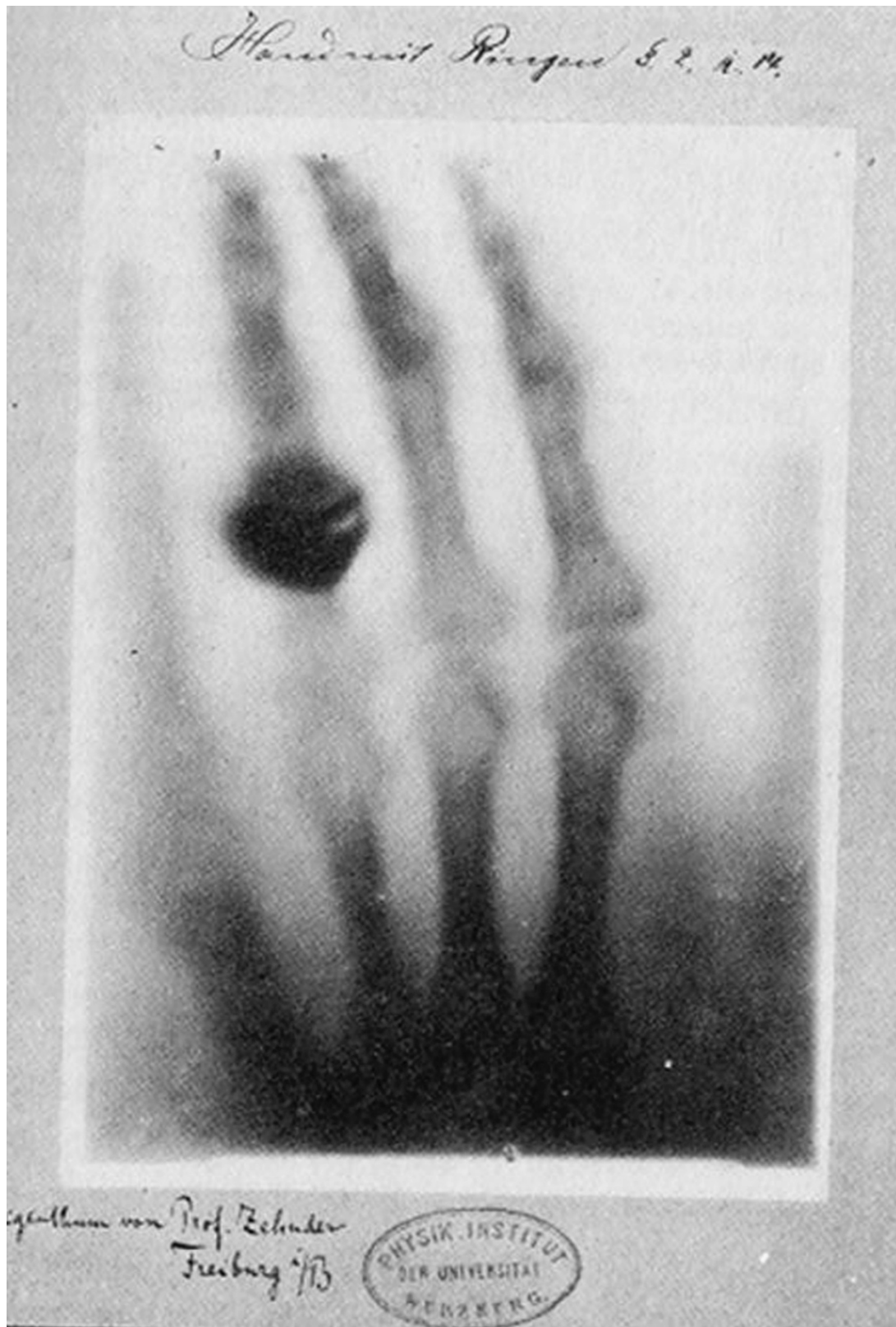


Figure 3.1.1 – Röntgen's first X-ray of the human hand, 1895

## **3.2 Methods**

### **3.2.1 Recruitment**

A web-based survey instrument was designed and sent out to members of the EAU Robotic Urology Section (ERUS). Only independently practising robotic surgeons performing RALP, RAPN and/or robotic cystectomy were included in the analysis. Those surgeons exclusively performing other procedures were excluded. Respondents were offered no incentives to reply. All data collected was anonymous.

### **3.2.2 Survey design and administration**

An anonymous web based questionnaire (Appendix 1) was distributed to the mailing list of the robotic section of the European Association of Urology (EAU). The survey was designed in accordance with the available recommendations for web-based surveys<sup>95,96</sup> and constituted part of a larger survey of robotic urologists. Prior to distribution, it was trialled by both native and non-native English speakers and feedback was obtained from six urologists; two trainees and four consultant surgeons.

The questionnaire was designed using LimeSurvey ([www.limesurvey.com](http://www.limesurvey.com)) and hosted on their website. A link to the survey website was embedded in the covering letter and responses were captured using an automated process. The questionnaire was dynamic with the number and nature of the responses tailored towards the individual based on their previous answers. The questionnaire was open for one month, with a single reminder sent out after initial dissemination.

A survey request was considered valid if the potential participant opened the email containing the link to the survey. A valid respondent was defined as an individual who had answered at least the first five questions of the questionnaire. The response rate was calculated as the ratio between valid respondents to valid requests.<sup>95</sup> Incomplete but valid responses were not excluded.

When computing fractions or percentages, the denominator was the number of respondents to answer the question. This number is variable due to the dynamic nature of the questionnaire.

### **3.2.3 Survey Content**

#### **3.2.3.1 *Demographics***

All respondents to the survey were asked in what country they practised and what robotic urological procedures they performed. In addition to what procedures they performed surgeons were asked to specify the number of cases they had undertaken for each procedure.

#### **3.2.3.2 *Current imaging practice***

Procedure-specific questions in this group were displayed according to the operations the respondent performed. A summary of the questions can be seen in Appendix 1. Procedure non-specific questions were also asked. Participants were asked whether they routinely used the TilePro™ function of the da Vinci console (Intuitive Surgical, Sunnyvale, USA) and whether they routinely viewed imaging intraoperatively.

#### **3.2.3.3 *Augmented reality***

Prior to answering questions in this section, participants were invited to watch a video demonstrating an augmented reality platform during RAPN, performed by our group at Imperial College London. A still from this video can be seen Figure 3.2.1 They were then asked whether they felt augmented reality would be of use as a navigation or training tool in robotic surgery.

Once again, in this section, procedure-specific questions were displayed according to the operations the respondent performed. Only those respondents who felt augmented reality would be of use as a navigation tool were asked procedure-specific questions. Questions were asked to establish where in these procedures they felt an augmented reality environment would be of use.

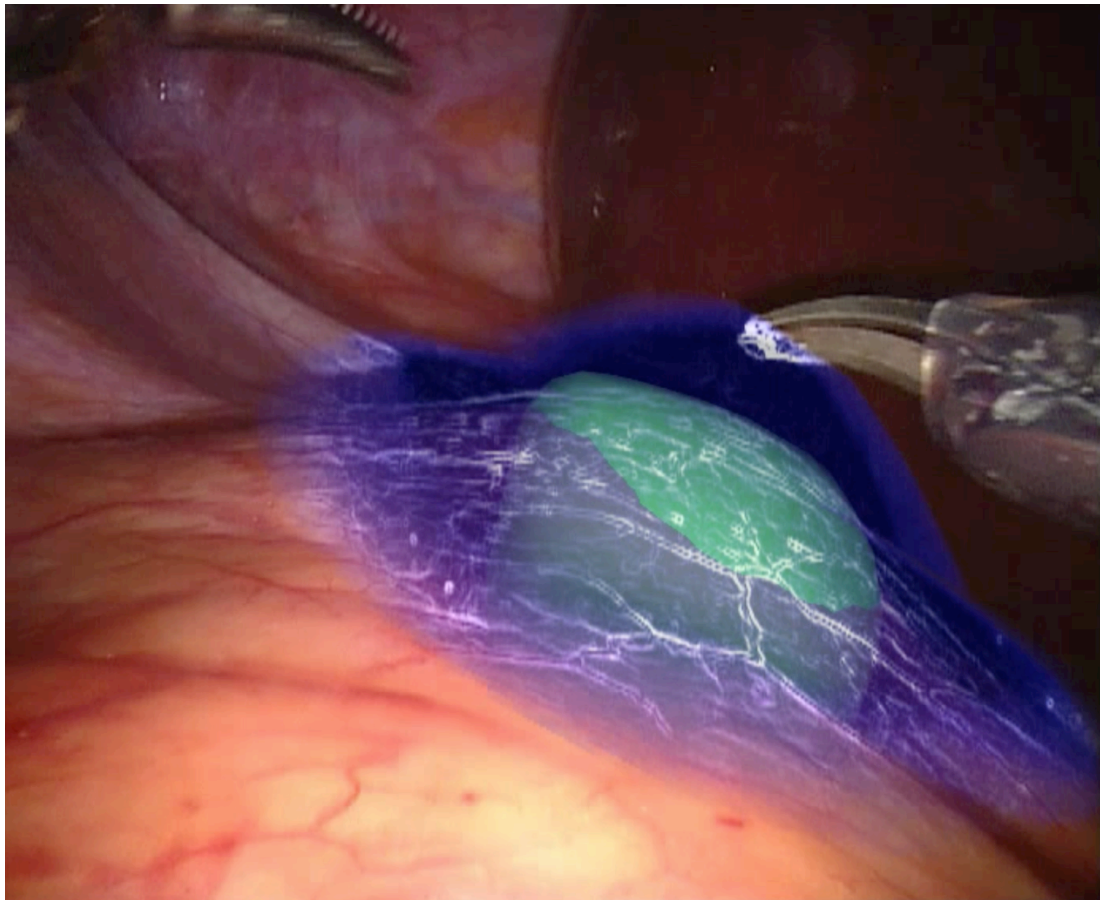


Figure 3.2.1 – A still taken from a video of augmented reality robot assisted partial nephrectomy. Here the tumour has been painted into the operative view allowing the surgeon to appreciate the relationship of the tumour to the surface of the kidney.



## **3.3 Results**

### **3.3.1 Demographics**

The survey was distributed to a total of 1,423 surgeons, of these 828 opened the invitation email with 239 individuals completing the larger survey, giving a response rate of 29%. Of the 239 respondents completing the larger survey 117 were independently practising robotic surgeons and were therefore eligible for analysis.

The majority of surgeons had both trained (210/239, 87.9%) and worked in Europe (215/239, 90.0%). The median numbers of cases undertaken by those surgeons reporting their case volume were: 120 (6 - 2000), 9 (1 – 120) and 30 (1 – 270), for RALP, Robot-assisted cystectomy and RAPN respectively.

### **3.3.2 Contemporary use of imaging in robotic surgery**

When enquiring about the use of imaging for surgical planning, the majority of surgeons (57%, 65/115) routinely viewed preoperative imaging intraoperatively with only 9% (13/137) routinely capitalising on the TilePro™ function in the console to display these images. When assessing the use of TilePro™ amongst surgeons who performed RAPN, 13.8% (9/65) reported using the technology routinely.

Of all the imaging modalities available in theatre, the majority of surgeons performing RALP (74%, 78/106) reported using MRI with an additional 37% (39/106) reporting the use of CT for preoperative staging and/or planning. For surgeons performing RAPN and robot-assisted cystectomy there was more of a consensus with 97% (68/70) and 95% (54/57) of surgeons, respectively, using CT for routine preoperative imaging (Table 3.3.1).

Those surgeons performing RAPN were found to have the most diversity in the way they viewed preoperative images in theatre, routinely viewing images in sagittal, coronal and axial slices (Table 3.3.2). The majority of these surgeons also viewed the images as 3D reconstructions (54%, 38/70).

The majority of surgeons used ultrasound intraoperatively in RAPN (51%, 35/69) with a further 25% (17/69) reporting they would use it if they had access to a ‘drop-in’ ultrasound probe (Figure 3.3.2).

	<b>CT</b>	<b>MRI</b>	<b>USS</b>	<b>None</b>	<b>Other</b>
<b>RALP (n=106)</b>	39.8% (39)	73.5% (78)	2% (3)	15.1% (16)	8.4% (9)
<b>RAPN (n=70)</b>	97.1% (68)	42.9% (30)	17.1% (12)	0% (0)	2.9% (2)
<b>Cystectomy (n=57)</b>	94.7% (54)	26.3% (15)	1.8% (1)	1.8% (1)	5.3% (3)

Table 3.3.1 – Which preoperative imaging modalities do you use for surgical planning and diagnosis

	<b>Axial slices</b>	<b>Coronal slices</b>	<b>Sagittal slices</b>	<b>3D recons.</b>	<b>Do not view</b>
<b>RALP (n=106)</b>	49.1% (52)	44.3% (47)	31.1% (33)	9.4% (10)	31.1% (33)
<b>RAPN (n=70)</b>	68.6% (48)	74.3% (52)	60% (42)	54.3% (38)	0% (0)
<b>Cystectomy (n=57)</b>	70.2% (40)	52.6% (30)	50.9% (29)	21.1% (12)	8.8% (5)

Table 3.3.2 – How do you typically view preoperative imaging in the operating room (3D recons = Three dimensional reconstructions)

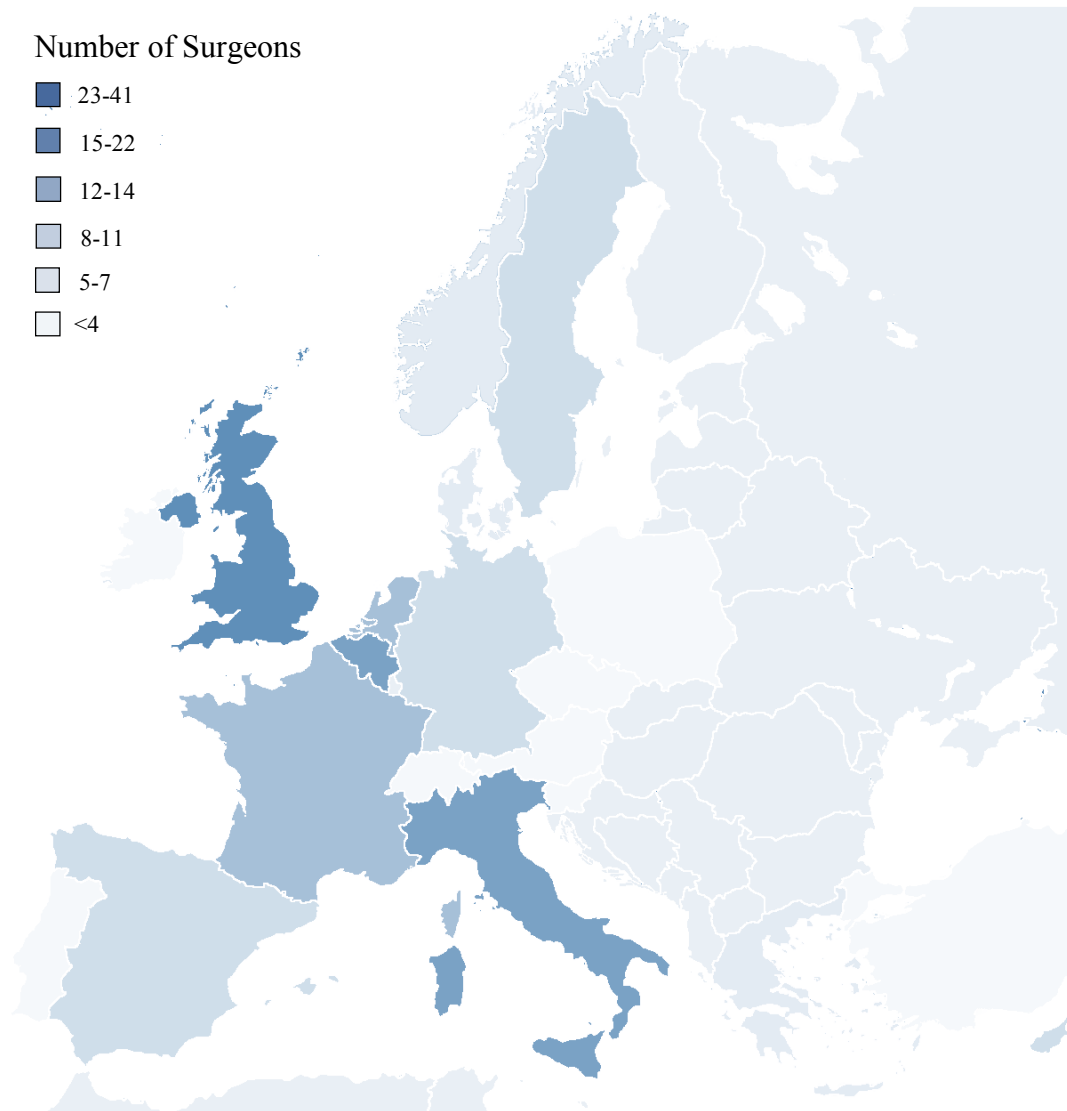


Figure 3.3.1 – Geographical distribution of surgeons responding to questionnaire

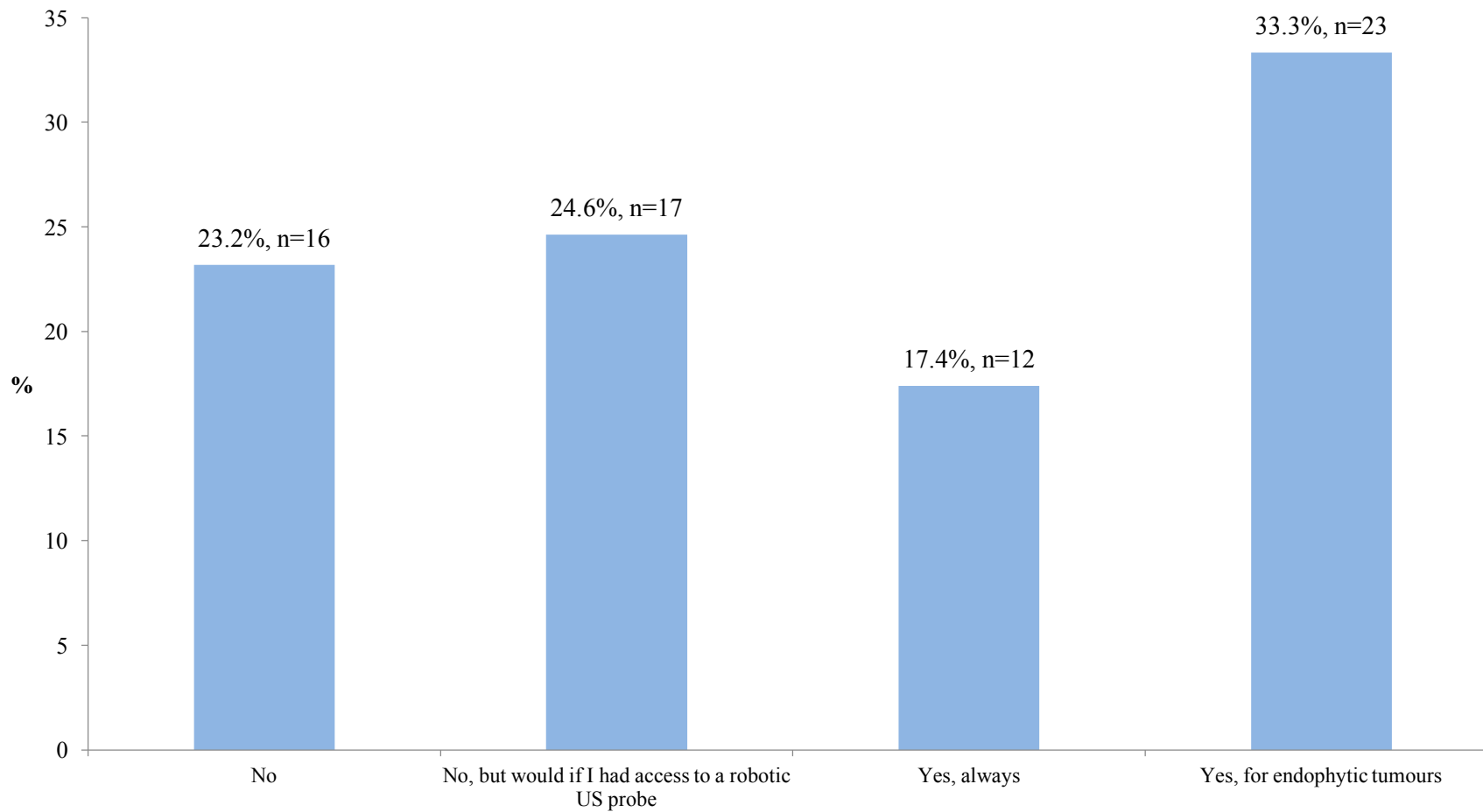


Figure 3.3.2 – Chart demonstrating responses to the question - Do you use intraoperative ultrasound for robotic partial nephrectomy

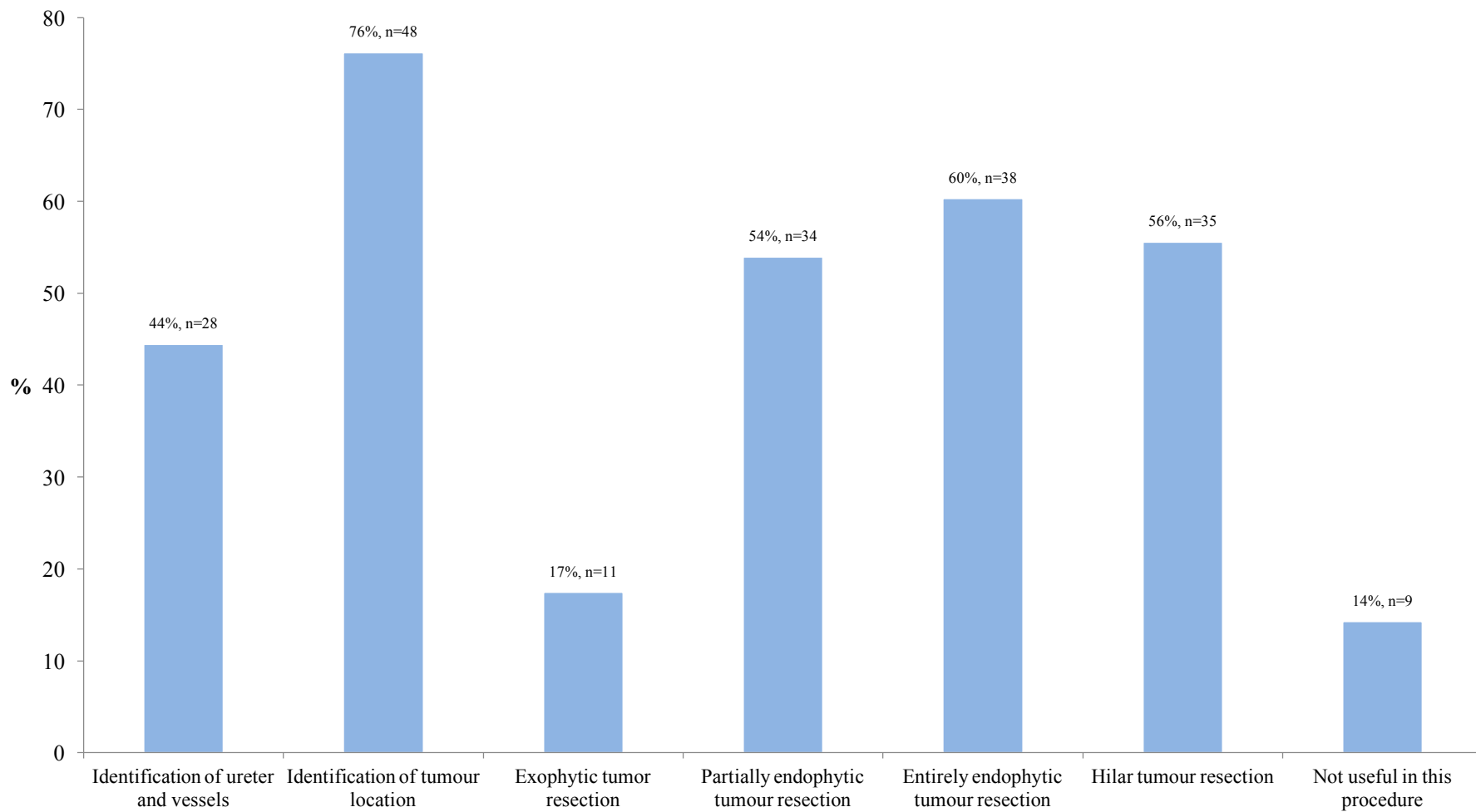


Figure 3.3.3 – Chart demonstrating responses to the question - In robotic partial nephrectomy which parts of the operation do you feel augmented reality image overlay would be of assistance

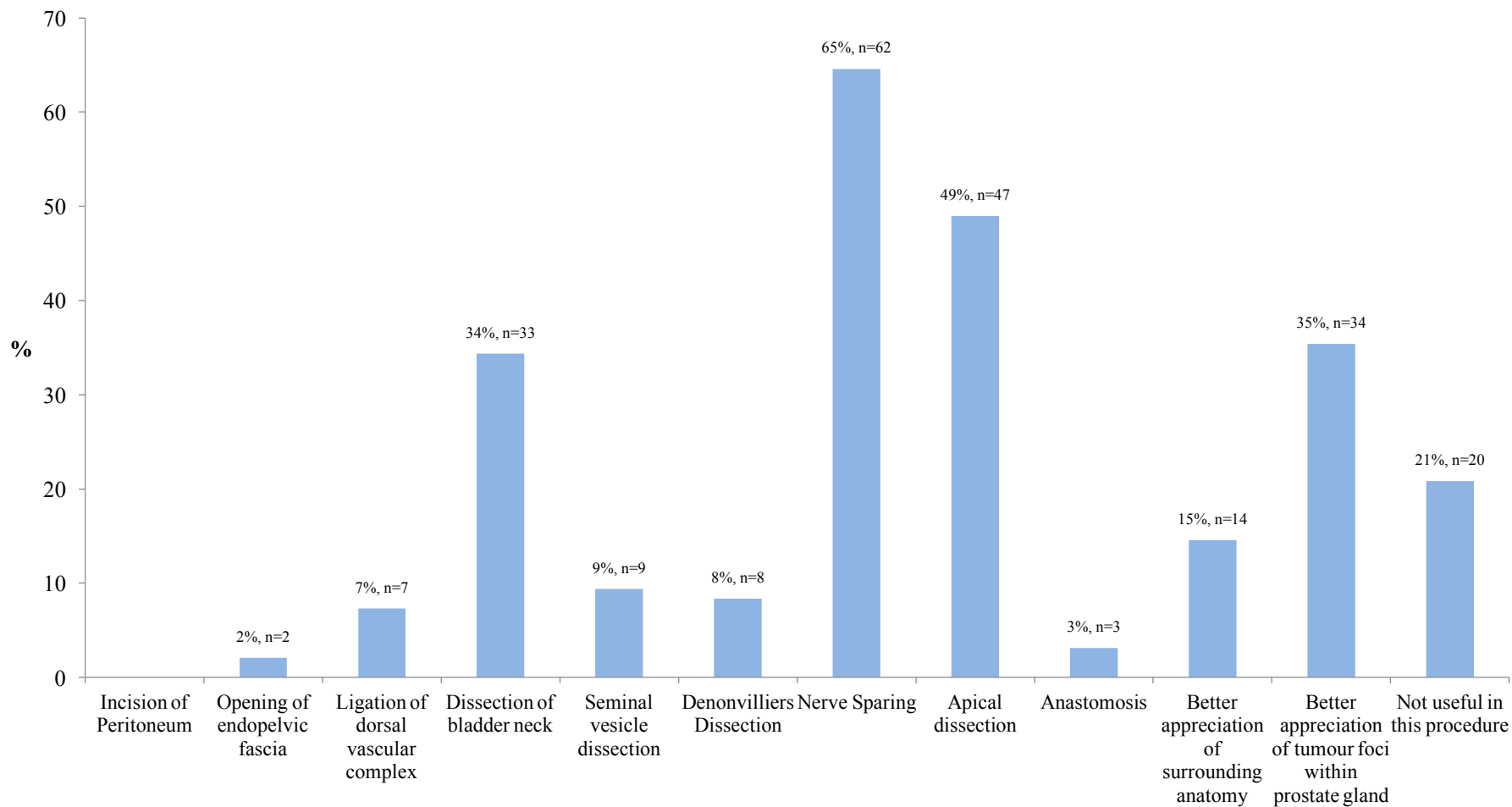


Figure 3.3.4 – Chart demonstrating responses to the question - In robotic prostatectomy which parts of the operation do you feel augmented reality overlay technology would be of assistance?

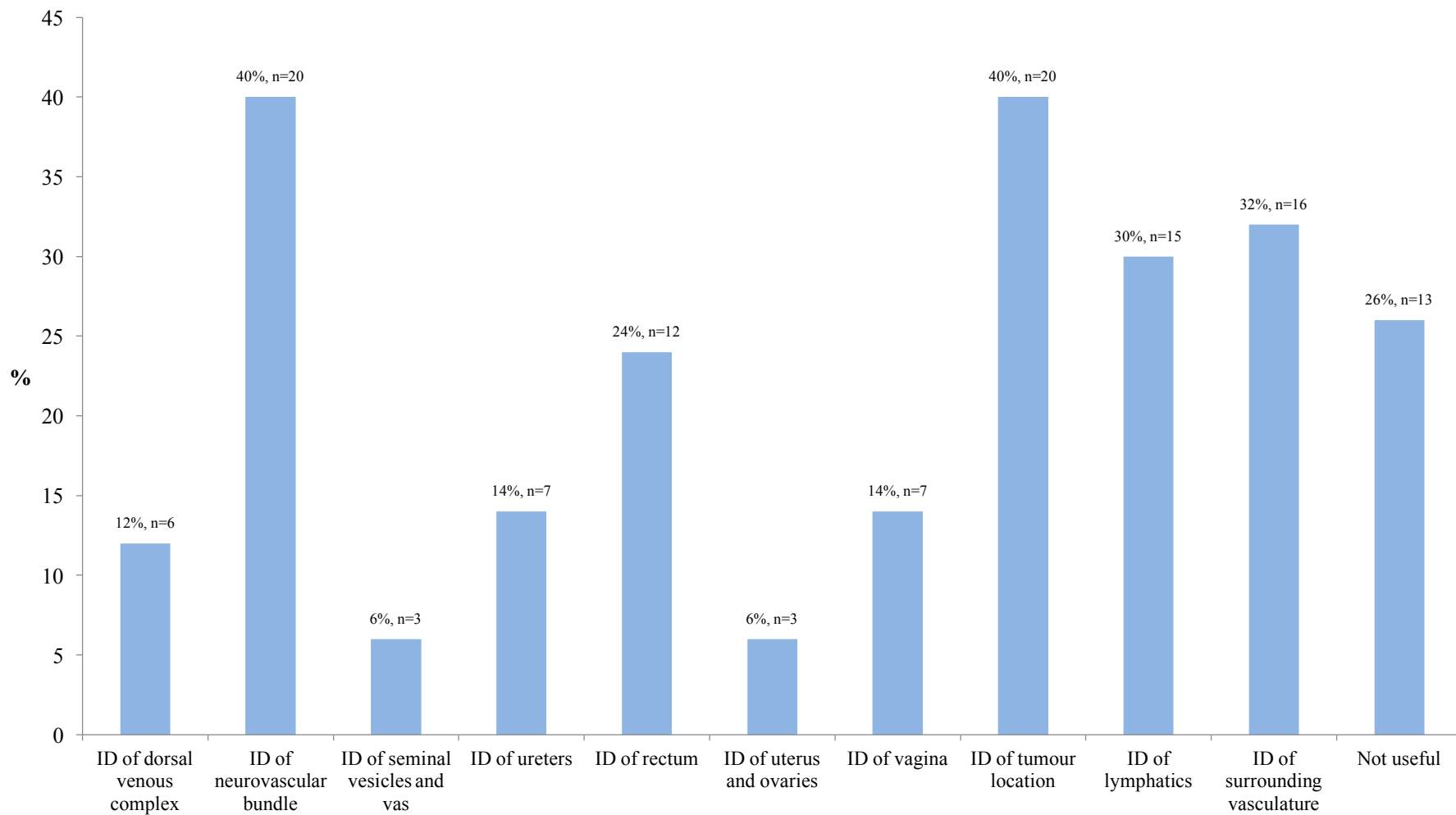


Figure 3.3.5 – Chart demonstrating responses to the question - In robotic cystectomy which parts of the operation do you feel augmented reality would be of assistance?

### **3.3.3 Desire for augmented reality**

In all 87% of respondents envisaged a role for augmented reality as a navigation tool in robotic surgery and 82% (88/107) felt that there was an additional role for the technology as a training tool.

The greatest desire for augmented reality was amongst those surgeons performing RAPN with 86% (54/63) feeling the technology would be of use. The largest group of surgeons felt it would be useful in identifying tumour location, with significant numbers also feeling it would be efficacious in tumour resection (Figure 3.3.3).

When enquiring about the potential for augmented reality in Robot-Assisted Laparoscopic Prostatectomy (RALP), 79% (20/96) of respondents felt it would be of use during the procedure, with the largest group feeling it would be helpful for nerve sparing 65% (62/96) (Figure 3.3.4). The picture in cystectomy was similar with 74% (37/50) of surgeons believing augmented reality would be of use, with both nerve sparing and apical dissection highlighted as specific examples (40%, 20/50) (Figure 3.3.5). The majority also felt that it would be useful for lymph node dissection in both RALP and robot assisted cystectomy (55% (52/95) and 64% (32/50), respectively).

## **3.4 Discussion**

### **3.4.1 Principal findings**

The results from this study suggest that the contemporary robotic surgeon views imaging as an important adjunct to operative practice. The way these images are being viewed is changing; although the majority of surgeons continue to view images as 2D slices a significant minority have started to capitalise on 3D reconstructions to give them an improved appreciation of the patient's anatomy.

This study has highlighted surgeons' willingness to take the next step in the utilisation of imaging in operative planning, augmented reality, with 87% feeling it has a role to play in robotic surgery. Although there appears to be a considerable desire for augmented reality, the technology itself is still in its infancy with the limited evidence demonstrating clinical application reporting only qualitative results.<sup>8,87,97,98</sup>



### 3.4.2 Comparison with other studies

There are a number of significant issues that need to be overcome before augmented reality can be adopted in routine clinical practice. The first of these is registration. This process has been performed both manually and using automated algorithms with varying degrees of accuracy.<sup>7,9</sup> The second issue pertains to the use of static preoperative imaging in a dynamic operative environment; in order for the preoperative imaging to be accurately registered it must be deformable. This problem remains as yet unresolved.

Live intraoperative imaging circumvents the problems of tissue deformation and in RAPN 51% of surgeons reported already using intraoperative ultrasound to aid in tumour resection. Cheung *et al.*<sup>93</sup> have published an *ex-vivo* study highlighting the potential for intraoperative ultrasound in augmented reality partial nephrectomy. They report the overlaying of ultrasound onto the operative scene to better the surgeon's appreciation of the subsurface tumour anatomy. This improvement in anatomical appreciation resulted in greater resection quality over conventional ultrasound guided resection.<sup>93</sup> Building on this work the first *in-vivo* use of overlaid ultrasound in RAPN has recently been reported.<sup>94</sup> Although good subjective feedback was received from the operating surgeon, the study was limited to a single case demonstrating feasibility and as such was not able to show an outcome benefit.<sup>94</sup>

RAPN also appears to be the area in which augmented reality would be most readily adopted with 86% of surgeons claiming they see a use for the technology during the procedure. Within this operation there are two obvious phases to augmented, one of *planning* in which anatomical identification is undertaken (in particular vessel identification to facilitate both routine 'full clamping' and for the identification of secondary and tertiary vessels for 'selective clamping'<sup>99</sup>) and one of *execution*, in which tumour resection takes place. These two phases have different requirements from an augmented reality platform; the first phase of identification requires a gross overview of the anatomy without the need for high levels of registration accuracy. However, tumour resection necessitates sub-millimetre accuracy in registration and needs the system to account for the dynamic intraoperative environment. The step of anatomical identification is amenable to the use of non-deformable 3D reconstructions of

preoperative imaging while that of image-guided tumour resection is perhaps better suited to augmentation with live imaging such as ultrasound.<sup>7,93,100</sup>

For RALP and robot-assisted cystectomy, the steps in which surgeons felt augmented reality would be of assistance were those of neurovascular bundle preservation and apical dissection. The perceived relative efficacy of augmented reality in these steps correlates with previous examinations of augmented reality in RALP.<sup>101,102</sup> Although surgeon preference for utilising AR while undertaking robotic prostatectomy has been demonstrated, Thompson *et al.* failed to demonstrate an improvement in oncological outcomes.<sup>102</sup>

Both nerve sparing and apical dissection require a high level of registration accuracy and a necessity for either live imaging or the deformation of preoperative imaging to match the operative scene. Achieving this level of registration accuracy is made more difficult by the mobilisation of the prostate gland during the operation.<sup>101</sup> These problems are equally applicable to robot-assisted cystectomy. Although guidance systems have been proposed in the literature for RALP,<sup>87-89,98,101</sup> none has achieved the level of accuracy required to provide assistance during nerve sparing. Additionally, there are still imaging challenges that need to be overcome. Although multiparametric MRI has been shown to improve decision making in opting for a nerve sparing approach to RALP<sup>103</sup>, the imaging is not yet able to reliably discern the exact location of the neurovascular bundle. This said significant advances are being made with novel imaging modalities on the horizon that may allow for imaging of the neurovascular bundle.<sup>104</sup>

### **3.4.3 Study limitations**

The study may have been limited by the response rate of 29%. This may indicate an element of self-selection bias with surgeons with an interest in the area being more likely to respond than those without. However, when examining response rates from similar studies in the past these were found to be similar.<sup>105-107</sup> A further limitation relates to the self-reported nature of the questionnaire, leaving it open to the potential for recall bias. This limitation is true of all studies based on self reporting and was impossible to mitigate for within the study design.

### **3.5 Conclusions**

This survey depicts the contemporary robotic surgeon to be comfortable with the use of imaging to aid in intraoperative planning. Furthermore, it highlights a significant interest amongst the urological community in augmented reality operating platforms.

Short to medium term development of augmented reality systems in robotic urology surgery would be best performed using RAPN as the index procedure. Not only was this the operation where surgeons saw the greatest potential benefits, but it may also be the operation where it is most easily achievable by capitalising on the respective benefits of technologies the surgeons are already using: preoperative CT for anatomical identification and intraoperative ultrasound for tumour resection.

## CHAPTER 4: ASSESSING THE IMPACT OF IMAGE GUIDANCE ON SURGICAL INATTENTION BLINDNESS<sup>†</sup>

---

<sup>†</sup> Content from this chapter was published as:

**Hughes-Hallett, A.**, Mayer, E. K., Marcus, H. J., Pratt, P., Mason, S., Darzi, A., Vale, J., (2015).  
Inattention blindness in surgery. *Surgical Endoscopy*. [Epub ahead of print]

## **4.1 Literature review**

Historically much has been written about the potential benefits of image guidance in intra-abdominal MIS. However, the body of evidence examining the potential negative impact of image guidance on the awareness and loading of the surgeon remains less well documented with no apparent defined consensus in the literature.

When looking for studies examining the effects of the image-enhanced environment outside of medicine, and even more specifically surgery, a number of concerns have been raised.<sup>30,32,108,109</sup> The majority of this research has taken place within the aviation<sup>30,32,108</sup> and social science literature<sup>31,33</sup> and has highlighted two specific potential detrimental effects of augmenting the view of an operator, namely: inattention blindness (IB, defined as the failure to perceive an unexpected object when attention is focused on another object or task.<sup>33,34</sup>) and an increase in cognitive loading.

This systematic review of the medical and surgical literature aims to establish the extent of investigation that has taken place into the effect of surgical image guidance on these two factors.

### **4.1.1 Methods**

A systematic review of the literature was performed of the Medline and Embase databases with the following search criteria: [(augmented reality) OR (image guid\*) OR (image fusion) OR (image overlay) OR (soft tissue navigation)] AND [(inattention\* blindness) OR (awareness) OR (attention\* tunnelling) OR (safety) OR (work load) OR (task load)] AND surg\*. The results were limited to English language articles. Two reviewers independently identified articles, any disagreements were arbitrated by a third reviewer. The primary search strategy was supplemented by reviewing the reference lists of retrieved articles and using the PubMed related articles feature.

The inclusion criteria were as follows: comparative studies of intraoperative image guidance versus no image guidance and/or those studies assessing the impact of image guidance on situational awareness and/or task load. Reviews and conference abstracts were excluded from analysis.

## 4.1.2 Results

The search revealed 96 articles, of which seven met the inclusion and exclusion criteria (Figure 4.1.1). Of the seven studies identified two assessed for IB<sup>110,111</sup> and the remainder assessed task load (one utilising physiological parameters and the remaining studies using the National Aeronautics and Space Administration – Task Load Index (NASA-TLX)) assessment of task load.<sup>112–116</sup> No other markers of awareness or task load were found by the search.

As can be seen in Table 4.1.1, studies five focused on endoscopic skull or sinus surgery, one on mastoidectomy and one on endoscopic neurosurgery. No studies examining the effects of image guidance in minimally invasive abdominal surgery were found. All studies used some form of image overlay to display guidance.

### 4.1.2.1 Task load

Of those studies reporting on the NASA-TLX, three<sup>113–115</sup> broke the index down into its constituent elements of mental demand, physical demand, temporal demand, performance and frustration (Table 4.1.2) and one reported the mean TLX score across all groups.<sup>112</sup> Two of the studies identified found task load to be increased when undertaking a task with no image guidance.<sup>113,114</sup> The remaining studies demonstrated no significant difference in task performance between the image guidance and no image guidance groups.<sup>112,115</sup> In the studies of Luz *et al.*<sup>112</sup> and Theodoraki *et al.*<sup>116</sup> studies, physiological (heart rate, respiratory rate and blood pressure) as well as subjective measures of load were collected. In both studies a non-significant increase was seen in physiological parameters in the no image guidance group on performing the simulated surgical task.

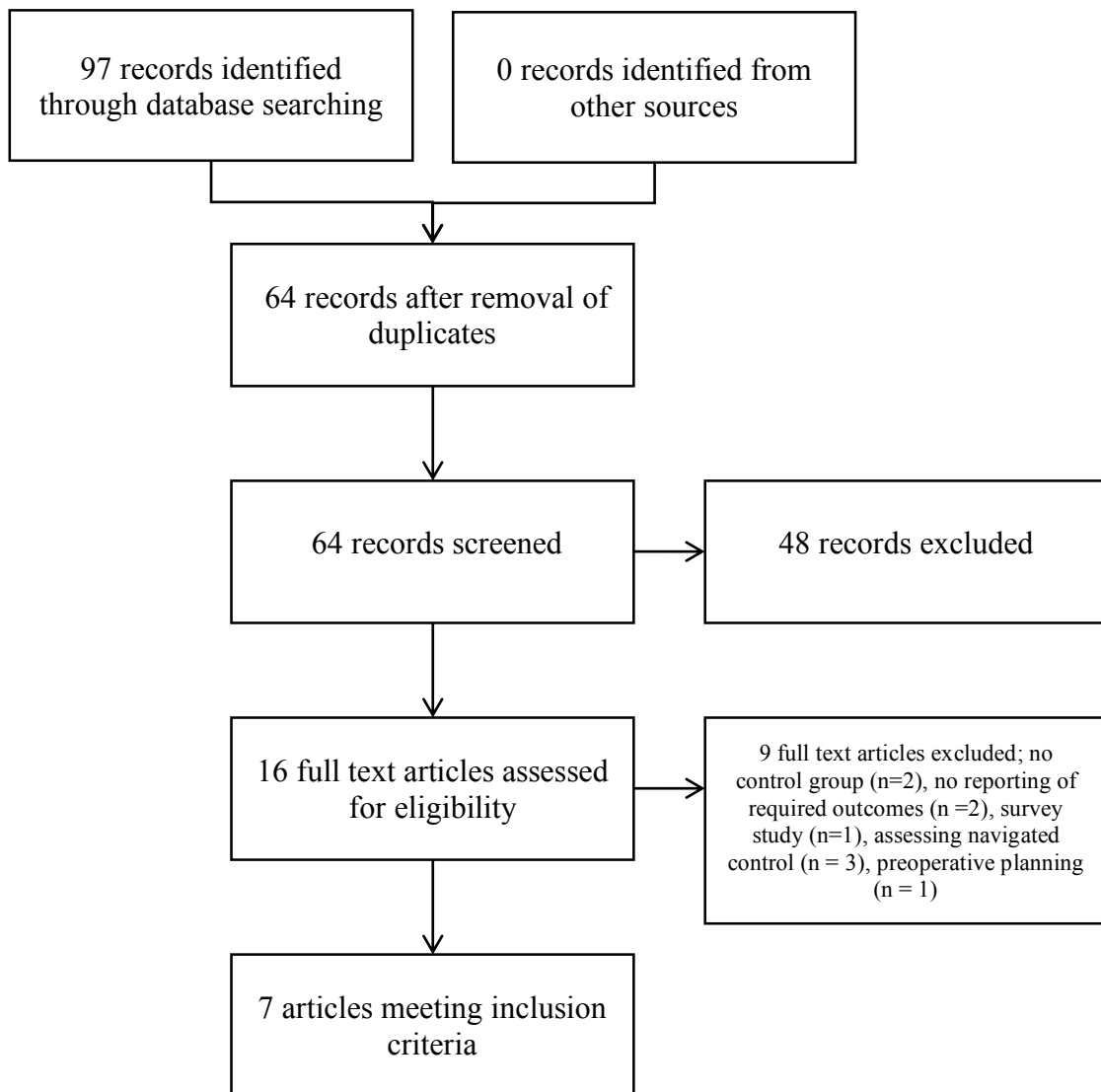


Figure 4.1.1 – PRISMA diagram for the search: [(augmented reality) OR (image guid\*) OR (image fusion) OR (image overlay) OR (soft tissue navigation)] AND [(inattention\* blindness) OR (awareness) OR (attention\* tunnelling) OR (safety) OR (work load) OR (task load)] AND surg\*

<b>Paper</b>	<b>Study design</b>	<b>Organ/Procedure</b>
Marcus <i>et al.</i> '15 <sup>110</sup>	<i>Ex-vivo</i> RCT	Endoscopic brain surgery
Luz <i>et al.</i> '15 <sup>112</sup>	<i>Ex-vivo</i> RCT	Mastoidectomy
Theodoraki <i>et al.</i> '15 <sup>116</sup>	<i>In-vivo</i> RCT	Endoscopic sinus surgery
Haerle <i>et al.</i> '15 <sup>115</sup>	Prospective case series	Endoscopic skull base surgery
Dixon <i>et al.</i> '13 <sup>111</sup>	<i>Ex-vivo</i> RCT	Endoscopic sinus surgery
Dixon <i>et al.</i> '12 <sup>114</sup>	<i>Ex-vivo</i> RXT	Endoscopic sinus surgery
Dixon <i>et al.</i> '11 <sup>113</sup>	<i>Ex-vivo</i> RXT	Endoscopic skull base surgery

Table 4.1.1 – Study design and target organ or procedure type. *RCT* = *Randomised control trial* *RXT* = *Randomised cross over trial*



Paper	Control (SD)	Guidance (SD)
<b>Mental demand</b>		
Haerle <i>et al.</i> 2015 <sup>115</sup>	6 (3.8) (n = 5)	8 (3-16) (n = 11)
<b>Dixon <i>et al.</i> 2012<sup>114</sup></b>	<b>8.5 (4.4) (n = 8)</b>	<b>7 (3.9) (n = 8)</b>
<b>Dixon <i>et al.</i> 2011<sup>113</sup></b>	<b>7.96 (4.38) (n = 12)</b>	<b>4.58 (3.60) (n = 12)</b>
<b>Physical demand</b>		
Haerle <i>et al.</i> 2015 <sup>115</sup>	7 (3-9)	10.5 (4-15)
Dixon <i>et al.</i> 2012 <sup>114</sup>	5 (2.4)	4.4 (2.2)
Dixon <i>et al.</i> 2011 <sup>113</sup>	4.67 (2.90)	4.13 (3.13)
<b>Temporal demand</b>		
Haerle <i>et al.</i> 2015 <sup>115</sup>	7 (4-8)	9.5 (4-14)
<b>Dixon <i>et al.</i> 2012<sup>114</sup></b>	<b>4.6 (2.6)</b>	<b>3.3 (2.2)</b>
Dixon <i>et al.</i> 2011 <sup>113</sup>	5.29 (3.56)	4.67 (3.66)
<b>Performance</b>		
Haerle <i>et al.</i> 2015 <sup>115</sup>	2 (2-4)	2.5 (2-7)
<b>Dixon <i>et al.</i> 2012<sup>114</sup></b>	<b>6.9 (3.9)</b>	<b>4.8 (2.9)</b>
<b>Dixon <i>et al.</i> 2011<sup>113</sup></b>	<b>10.12 (3.22)</b>	<b>6.46 (5.85)</b>
<b>Effort</b>		
Paper	Control	Guidance
Haerle <i>et al.</i> 2015 <sup>115</sup>	7 (Range 5-14)	12 (Range 3-15)
<b>Dixon <i>et al.</i> 2012<sup>114</sup></b>	<b>8.6 (3.4)</b>	<b>5.1 (3.1)</b>
<b>Dixon <i>et al.</i> 2011<sup>113</sup></b>	<b>9.08 (4.54)</b>	<b>3.67 (2.06)</b>
<b>Frustration</b>		
Haerle <i>et al.</i> 2015 <sup>115</sup>	5 (3-9)	5 (2.5-12)
<b>Dixon <i>et al.</i> 2012<sup>114</sup></b>	<b>7.4 (3.8)</b>	<b>3.6 (2.3)</b>
<b>Dixon <i>et al.</i> 2011<sup>113</sup></b>	<b>7.67 (3.66)</b>	<b>3.38 (2.88)</b>
<b>Overall</b>		
Luz <i>et al.</i> 2015 <sup>112</sup> (mean score)	10.6 (n = 8)	11.6 (n = 16)

Table 4.1.2 – NASA-TLX scores. Unless otherwise stated number in brackets is the standard deviation (SD). Numbers in **bold** denote a statistically significant reduction in the NASA-TLX score

Paper	Control	Guidance
<b>Marcus <i>et al.</i> 2015<sup>110</sup></b>	<b>9/10 (90%)</b>	<b>14/40 (35%)</b>
<b>Dixon <i>et al.</i> 2013<sup>111</sup></b>	<b>12/17 (70.6%)</b>	<b>1/15 (6.7%)</b>

Table 4.1.3 – Number of participants noting the presence of a foreign body on the operative scene on prompting. Items in **bold** denote decrease in the ability to identify a foreign body in the operative scene

#### **4.1.2.2 *Inattention blindness***

The remaining two papers assessed the impact of image guidance platforms on IB (Table 4.1.3).<sup>110,111</sup> Both of these studies demonstrated a significant increase in IB in the group undertaking a simulated task with image guidance engaged.<sup>110,111</sup>

### **4.1.3 Discussion**

Although there are well-recognised problems with image overlay and guidance outside of the medical literature<sup>30,32,108,109</sup> the examination of these factors in the surgical literature remains limited with only seven eligible studies identified by this literature review. These studies focused on areas in which image guidance has become relatively commonplace, namely: neurosurgery and ear, nose and throat surgery (ENT). In addition no study examined the effect of both cognitive load and image guidance simultaneously preventing a direct comparison of these two contributing factors.

#### **4.1.3.1 *Cognitive load***

In all of the studies in question the task used to induce the cognitive load was a simulated (or in one case a real world) procedure. These tasks all involved the location of subsurface anatomy and as such, it is perhaps unsurprising that providing the participants with a ‘road-map’ elucidating this location reduced the cognitive loading on the participants. Of note, no study examined the effect of loading on inattention blindness but rather examined the effect of image guidance on cognitive load when performing a location-defining task.

The reduction in cognitive load on participants is perhaps made even less surprising bearing in mind that in all but one of the studies, participants were trainees.<sup>112,114,116</sup> In the study in which experts were used, no difference in cognitive load was seen.<sup>115</sup> Trainees are perhaps more likely to derive benefit from image guidance than experts, due to their inferior operative experience and understanding of the underlying anatomy. This may explain why the positive finding of the novice and intermediate studies were not replicated by the experts.

#### **4.1.3.2 Inattention blindness**

The potentially more interesting finding of those studies examined was regarding augmented reality induced IB.<sup>110,111</sup> In the two studies by Dixon *et al.*<sup>111</sup> and Marcus *et al.*<sup>110</sup>, participants were asked to undertake a task with AR image guidance. In both of these studies a foreign body was present in the scene at the time of procedure. Post procedurally, participants were asked whether they had noted any foreign bodies within the operative scene. Both found that in those groups in which image guidance was used, a significant increase in IB for the unexpected item was seen. In the study of Marcus *et al.* study, this assessment of IB was extended beyond just a single modality of image display with the effects of different types of display examined (including conventional image guidance where the image was displayed on a separate screen). No statistically significant difference was found when looking at differences in IB between the different modalities of display.

This failure to see items within the operative scene raises concerns regarding a surgeon's impaired ability to pick up adverse events occurring within the operative field when augmented reality is engaged. Questions remain regarding whether it is the image guidance or the increased cognitive load associated with operating an image system that results in this impairment. But its presence, in *ex-vivo* simulation at least, is cause for concern.

#### **4.1.4 Conclusions**

When looking to the to the military and aviation literature the increasing cognitive load and the augmentation of an operator's view are repeatedly referenced as having a detrimental impact on their ability to identify salient factors within their field of view.<sup>30-33,108</sup> This review has highlighted a deficit, with regards the investigation of these factors, in the surgical image guidance literature, with a failure to explore the potential negative impact of image guidance platforms on surgical practice. The limited evidence that does exist suggests that these platforms improve task performance; with a positive impact on the load experienced while undertaking a task requiring knowledge of the subsurface anatomy. However, they also appear to impair the ability of the surgeon to identify foreign bodies in the operative scene.

The following section of this chapter presents a study that attempts to determine the effect of augmented reality image guidance and cognitive load (independent of the operation of the image guidance platform) on inattention blindness. In addition, the study looks to establish whether the modality of the display has any influence on the level of inattention blindness.

## **4.2 Inattention blindness in surgery: The effects of cognitive load and image guidance**

### **4.2.1 Introduction**

Inattention blindness (IB) can be defined as the failure to perceive an unexpected object when attention is focused on another object or task.<sup>33,34</sup> This principle, if applicable to surgery, has the potential to influence adverse event and error detection, but as yet remains under-examined in the surgical and broader medical literature. Although the effects of IB have been poorly investigated in the context of surgery, with only a handful of studies investigating its prevalence,<sup>111</sup> within the social sciences<sup>31,33</sup> and specifically the aviation literature<sup>30,32,108</sup> it is well established. Two relevant factors have consistently been identified as contributing to levels of IB: firstly, cognitive load<sup>31,117</sup> and secondly, any augmentation of an individual's visual field with task-relevant information.<sup>30,32</sup> Until relatively recently, only the first of these factors has played a significant role in surgical practice but with the recent growth in image-guided and intra-abdominal MIS<sup>118</sup>, the future is likely to see that both have influence. The primary objectives of the study were to assess the impact of both cognitive load and AR intraoperative image overlay on operative IB.

### **4.2.2 Methods**

A randomised control study design was utilised. Participants recruited to the trial were all consultant surgeons or trainees. Informed consent was obtained from all participants. Demographic data (age, sex and number of postgraduate years' experience) was recorded for all participants.

A segment of video (one minute and 42 seconds in length) was retrospectively taken from a robot assisted laparoscopic partial nephrectomy. Ethics and consent was obtained prior to the collecting of data (REC reference 07/Q0703/24, see Appendix 2). The video was selected to fulfil a number of criteria: first, a corresponding patient specific reconstructed CT dataset was required in order to create the AR overlay; and second, the video needed to contain two foreign bodies, one in the centre of the operative scene and a second in the periphery of vision. As can be seen in Figure 4.2.1,

within the video the two foreign bodies visible in the operative scene were: a swab or surgical sponge, for a total of 40 seconds (39.2% of the video) within the periphery of vision; and a suture, visible for a total of three seconds in the centre of the operative scene (2.9% of the video). The video was viewed in 2D on a standard computer display.

Two levels of block randomisation were undertaken to ensure an adequate number of participants in each group. The first randomisation step allocated participants to either a high or low cognitive load group. At the second randomisation step, participants were randomised to one of three AR subgroups: wireframe overlay, solid overlay, and a control group in which no overlay was displayed (Figure 4.2.1). This process resulted in a total of six groups. Image overlay was undertaken using a previously published semi-automated registration technique.<sup>92</sup> The same video was viewed, with differing AR overlays, by all participants.

For the high cognitive load cohort, participants were asked to count the number of instrument movements that occurred during the course of the video. This step involved keeping a count of the movements of two separate surgical instruments. The use of simultaneous counting is a well-validated cognitive loading tool in the assessment of IB<sup>33</sup> and was selected as it forced participants to concentrate on the area of operative focus, replicating the direction of true intraoperative attention. If the instrument count was more than three standard deviations from the mean, the participant was excluded from the study on the basis that their focus had not been sufficiently maintained. In the low cognitive load group participants were only asked to view the footage with no counting task.

Data were collected using a computer-based tool (Appendix 3). All participants were asked to answer the following questions to assess the degree of IB. Q1 assessed *unprompted* attention while Q2 and 3 assessed *prompted* attention:

Q1) 'Did you see any items in the operative field other than the robotic surgical instruments or assistant's suction device (i.e. foreign bodies, other surgical instruments or devices)? If so what did you see?'

Q2) 'Did you see a swab in the operative field?'

Q3) ‘Did you see a suture and thread in the operative field?’ Each question appeared on a different page of the tool to prevent the retrospective alteration of data by participants. The approach used to assess IB has previously been validated in the social science literature.<sup>33</sup> Participants were asked to complete a National Aeronautics and Space Administration – Task Load Index (NASA-TLX) in order to assess the level of task loading they experienced during the video.<sup>119</sup>

Participants allocated to the image overlay subgroups were also asked to rate their agreement to the following statements according to a seven point Likert scale: ‘The image overlay impaired my ability to appreciate all features in the operative environment’; and ‘I believe image overlay would improve the accuracy of tumour resection’. Likert score ratings were converted to a numbered scale to allow analysis, where one represented ‘strongly disagree’, two represented ‘disagree’, and so on.

#### **4.2.2.1 Pilot study**

An initial pilot study was undertaken to allow a power calculation to be performed; the study was powered to establish whether an increase in cognitive load increased surgical inattention blindness for the swab. In the pilot, participants were allocated to either high or low cognitive load groups. Eight participants were allocated to each group. None of the participants in the high cognitive load group reported seeing the swab compared with 50% of participants in the low cognitive load group. The power calculation was therefore performed with anticipated incidences of 0% and 50% for swab inattention in the high and cognitive load groups respectively. This calculation demonstrated the need for 11 participants per group to show a statistically significant difference at the 5% level for 80% power.

#### **4.2.2.2 Statistical analysis**

All statistical analysis was performed using GraphPad Prism (GraphPad Software Inc, CA, USA). Analysis of binary categorical data was performed using Fisher’s exact test. Analysis of independent continuous data was performed using the Mann-Whitney *U* test. The Bonferroni correction was applied as and when serial comparisons were undertaken.

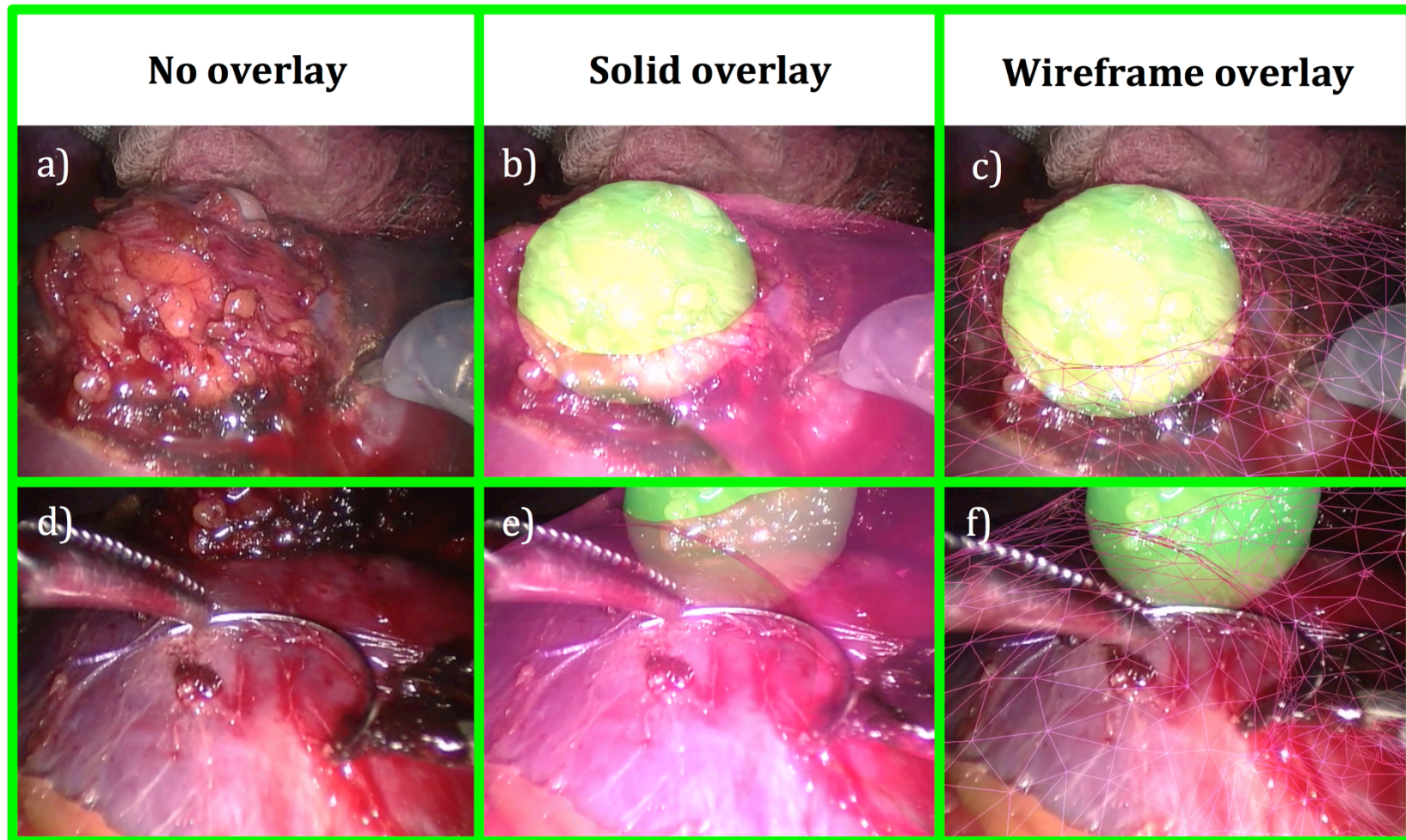


Figure 4.2.1 – Differing styles of image display, no overlay, solid and wireframe (left to right) a-c) show a view with the swab visible d-e) show a view with the suture and needle visible



### 4.2.3 Results

In total, 73 surgeons with an average of eight years of post-graduate experience were recruited to take part in the study. No significant difference in experience was observed across all six groups ( $p = 0.59$ ). The mean number of instrument movements observed was 35.7, with a standard deviation of 10.02. A single participant was excluded from analysis as the instrument count was more than three standard deviations from the mean.

#### 4.2.3.1 Overall inattention blindness

When combining all groups the level of prompted inattention blindness was seen to be 74% (54 of 73) and 10% (7 of 73) for the swab and suture respectively (all results are for prompted attention unless otherwise stated). When examining the levels of IB within the control group (i.e. low level of cognitive load and no image overlay) the levels of inattention were found to be similarly high (5 of 11, 45%) for the swab while comparatively lower for the suture (1 of 11, 9%).

		High Cognitive Load (%)	Low Cognitive Load (%)	p-value
<b>Subjects</b>		39	34	
<b>Unprompted</b>	<b>Noted Swab</b>	2 (5)	12 (32)	0.002
	<b>Noted Suture</b>	25 (64)	23 (68)	0.808
<b>Prompted</b>	<b>Noted Swab</b>	3 (8)	16 (47)	< 0.001
	<b>Noted Suture</b>	35 (90)	31 (91)	1.000

Table 4.2.1 – Effect of cognitive load on inattention blindness

#### 4.2.3.2 The effect of cognitive load on inattention blindness

When comparing the low and high cognitive load groups, the high load group had a significantly higher NASA-TLX score (69.7 versus 48.0,  $p = 0.04$ ) and also demonstrated significantly higher IB for the swab (95% versus 68%,  $p = 0.002$ , Table 4.2.1). No significant difference was seen between the groups for detection of the suture, with all groups demonstrating a relatively low level of inattention.

#### **4.2.3.3     *The effect of image overlay on inattention blindness***

When looking at the effects of display modality on IB no significant difference was seen between the two image guidance groups (wireframe and solid), for prompted attention of the swab or suture (Table 4.2.2). The same was true when amalgamating the two image guidance groups and comparing with the control group (no image overlay), regardless of cognitive load (Table 4.2.3).

Subjectively, however, participants felt that having an image overlay impacted on their ability to appreciate the operative environment (median Likert score of six) with only a marginal increase in their understanding of the subsurface anatomy (median Likert score of five). Again, there was no significant difference between the different types of image display ( $p = 0.80$  and  $0.57$ , respectively).

#### **4.2.3.4     *The effect of prompting on inattention blindness***

As can be seen in Table 4.2.4, the effects of prompting on inattention for the swab and the suture appear to be dichotomous, with no apparent effect on inattention for the swab (19% versus 26%,  $p = 0.429$ , for unprompted and prompted groups, respectively) but a marked effect on inattention for the suture (65% versus 90%,  $p = 0.001$ , for unprompted and prompted groups, respectively) regardless of cognitive load or image guidance.

		<b>Wireframe (%)</b>	<b>Solid (%)</b>	<b>p-value</b>
<b>Subjects</b>		24	25	
<b>Unprompted</b>	<b>Noted Swab</b>	4 (17)	4 (16)	1.000
	<b>Noted Suture</b>	11 (46)	19 (76)	0.042
<b>Prompted</b>	<b>Noted Swab</b>	7 (29)	5 (20)	0.520
	<b>Noted Suture</b>	22 (92)	22 (88)	1.000

Table 4.2.2 – Effect of modality of image guidance style on inattention blindness

		<b>No image guidance (%)</b>	<b>Image guidance (%)</b>	<b>p value</b>
<b>Subjects</b>		24	49	
<b>Unprompted</b>	<b>Noted Swab</b>	6 (25)	8 (16)	0.528
	<b>Noted Suture</b>	18 (75)	30 (61)	0.300
<b>Prompted</b>	<b>Noted Swab</b>	7 (29)	12 (24)	0.778
	<b>Noted Suture</b>	22 (92)	44 (90)	1.000

Table 4.2.3 – Effect of image guidance on inattention blindness

		Unprompted (%)	Prompted (%)	p-value
Low cognitive load	Noted Swab	12 (32)	16 (47)	0.460
	Noted Suture	23 (68)	31 (91)	0.033
High Cognitive Load	Noted Swab	2 (5)	3 (8)	1.000
	Noted Suture	25 (64)	35 (90)	0.014
No Image guidance	Noted Swab	6 (25)	7 (22)	1.000
	Noted Suture	18 (75)	22 (92)	0.245
Image guidance	Noted Swab	8 (16)	12 (24)	0.452
	Noted Suture	30 (61)	44 (90)	0.002
Overall	Noted Swab	14 (19)	19 (26)	0.429
	Noted Suture	48 (65)	66 (90)	0.001

Table 4.2.4 – Effects of prompting on inattention blindness

#### 4.2.4 Discussion

##### 4.2.4.1 *Principal findings*

The principal finding of this study is that regardless of cognitive load and image overlay, the level of IB for items at the periphery of vision is relatively high. When prompted, even those surgeons under low cognitive load and with no image overlay displayed exhibited 45% inattention for the swab, despite the fact it was present for 39% of the operative video. Furthermore, with increasing cognitive, load participants demonstrated a deterioration in their ability to register events occurring outside of their working space, potentially experiencing a *tunnelling of focus*. It seems that with the same increase in cognitive load, the ability to detect occurrences within this tunnel remain unaffected. Finally, the results of this study would suggest that the effect of AR on IB is negligible when compared to cognitive load.

The concept of a *tunnelling of focus* and increasing IB under increasing cognitive load is not new. Groups outside of the surgical and wider medical literature have previously demonstrated its occurrence<sup>31</sup>, but this has previously remained relatively under examined in the medical literature. The implications of this focus are numerous, but two are worth specific mention. The first, and perhaps most important, is that unnecessary cognitive loading of the operating surgeon must at all times be kept to a minimum, particularly during critical operative steps. This is pertinent in view of previous work demonstrating that the number of distractions in theatre runs at approximately one every three minutes.<sup>120</sup>

Although *tunnelling of focus* is almost certainly a major contributing factor in increasing surgical inattention, there are other confounders that may have also had an effect on inattention for the swab, an example of which being how visually salient the offending object is. More work is needed to establish the effect of these other contributing factors on inattention.

Secondly, in addition to minimising the cognitive load for the surgeon, the level of surgical experience must also be taken into consideration. A surgeon with little experience is likely to have greater tunnelling of focus than one with greater experience,

due to the higher levels of cognitive load experienced when undertaking the same task.<sup>121</sup> This reinforces the need for supervised training, both for the benefit of the trainee and the patient, with the lower cognitively loaded and more experienced trainer, if present, able to warn the operating trainee of complications occurring outside of their tunnel of focus. In addition, it also underpins the value of an experienced surgical assistant, as the lower cognitively loaded surgeon, in identifying potential complications.

A supplementary, and interesting observation was the effect of prompting on surgical inattention. The level of pick up for the item at the centre of the surgeon's tunnel of focus was improved by prompting, suggesting that a significant minority of surgeons registered the presence of the item at a subconscious level and then disregarded its existence as irrelevant. Interestingly, this same finding was not observed for the swab. The difference is perhaps most likely explained by an under-powering of the data in this respect, as fewer participants overall noted the swab's presence. The decrease in inattention blindness through participant prompting is well documented in the wider literature and as such it is no surprise that its existence has been demonstrated here.<sup>34</sup> Its presence does however raise interesting questions regarding how the brain determines what to 'notice' and what to disregard, and whether this is affected by factors such as surgical experience or in theatre distraction.

#### **4.2.4.2 Comparison with other studies**

Perhaps the best-known demonstration of inattention blindness is in Simons and Chabris's paper entitled 'Gorillas in our midst' (Figure 4.2.2).<sup>33</sup> In this study, participants were asked to count the number of passes of a basketball between team members. During this task, a man in a gorilla costume walked across the scene. Grossly speaking these findings tally with those presented here, namely that with increasing task complexity the level of IB increased. However, there is a subtle difference that warrants further discussion. In Simons and Chabris's paper the gorilla was present in the centre of the screen rather than at the periphery, akin to the suture in this study. In the data presented herein there was little IB for the suture in any of the groups, and no significant difference in levels of IB with a change in cognitive load. The reason behind this difference may well relate to the interaction with the suture or gorilla. In the Simons

*et al.* paper the gorilla is passive, not taking part in the task on which the participant was being asked to focus. This is in direct contrast to the suture with which the surgical instruments interact during the course of the video, and it is perhaps this interaction that forces this foreign body to the forefront of attention.



Figure 4.2.2 – A frame from the study video demonstrating the presence of the gorilla at the centre of the scene in Simons and Chabris’s paper.<sup>33</sup> (taken from Simons and Chabris, 1999)

In addition to correlating with Simons and Chabris’s seminal paper, the data presented here also correlates with social science, and neuroscience literature more generally, with regards attentional tunnelling. More specifically, the findings here, and in the wider literature suggest that with increasing cognitive load comes a tangible reduction in an individual’s functional field of view,<sup>31</sup> with a corresponding increase in IB.<sup>33,117</sup>

As well as examining the effects of cognitive load on perceptual blindness, the social science literature has looked extensively at the effects of image overlays. This investigation has focused largely on the use of head-up-displays (HUDs) in the military and aviation industries.<sup>30,32,108,109</sup> A meta analysis examining the effects of HUDs on pilot performance in 2000 found that there was little or no effect on IB, with the

exception of entirely unexpected events during final approach.<sup>30</sup> Again these findings align with those of the work presented here and with Liu *et al.*'s work examining the effect of HUD in anaesthesia,<sup>122</sup> with no significant difference seen between image guidance and control groups.

When looking to the literature surrounding IB in surgery the findings of this study contradict, to some extent, those of Dixon *et al.*<sup>111</sup> and Marcus *et al.*<sup>110</sup> who demonstrated that IB was significantly increased with surgical image guidance. This difference may relate to an increase in cognitive load, independent from the overlay itself. In both studies participants used an operative image guidance platform, which required them to maintain the optically tracked probe and reference arc in line of sight of the camera. Achieving this, particularly for individuals not familiar with the system, could potentially impose a level of cognitive load sufficient to induce IB, independent of the image overlay, thereby confounding the results. Other potential confounders in Dixon *et al.*'s study included the use of a screw, as the foreign body, in a cadaver.<sup>111</sup> The finding of a screw within a normal operative field would be unusual, bringing into question the relevance of IB for this object, with evidence in the social science and neuroscience literature suggesting that levels of IB are higher for items outside the normal context of an environment.<sup>30,33,123</sup>

This study attempted to address these confounders firstly by using a pre-recorded operative video, as a result of which the scene was identical to that seen in operative practice and was standardised across all participants. In addition there was no requirement to operate an image guidance system, thereby mitigating for any associated loading effects. The use of operative video also allowed for the assessment of IB for objects that are routinely visible in the operative scene, again making the findings more relevant to operative practice.

Although the data presented here have shown non-significance with regards image overlay and inattention blindness, participants did raise subjective concerns regarding the impact of AR on a surgeon's ability to sufficiently appreciate the operative scene. This limitation of AR image guidance needs to be taken into consideration when designing and utilising platforms based on this technology, with image overlay rationalised and limited to situations where there is a demonstrable benefit.



#### **4.2.4.3 Study Limitations**

This study has identified cognitive load as the driving factor in surgical IB, with any potential effect induced by AR operating environments likely to be relatively small. This said, the study is not without its limitations. The majority of these relate to the video having been obtained retrospectively rather than being engineered specifically for the study. Perhaps the most important of these video-related limitations was the relevance of the ability to identify a swab or suture, as these are surrogates for the subject of real interest which is the ability, or lack thereof, to identify adverse events occurring outside of the surgeon's tunnel of focus. Secondly, although this study comes closer to operative reality than the existing literature, it is still not directly examining intraoperative IB. In particular, the task participants were asked to perform was an approximation of intraoperative cognitive load, and utilised calculation rather than a motor task to simulate this load. Although this is true, the consensus within the literature is that IB is the result of exhaustion of attentional capacity with perceptual load, and as both motor and counting tasks impact this load, their effects should be similar.<sup>117,124</sup>

#### **4.2.5 Conclusions**

Inattention blindness is an important and under-investigated part of error and adverse event detection in operative surgery. In this study, all groups, regardless of cognitive load, demonstrated relatively high levels of inattention for items outside of their tunnel of focus. Furthermore, increasing the level of cognitive loading significantly increased this inattention. Consistent with the non-medical literature, the effect of AR overlays on IB was found to be relatively insignificant. Although AR may not have a significant effect on IB *per se*, it is possible that the cognitive load required to operate image guidance systems may do so, and this should be considered when designing future platforms.

## CHAPTER 5: PREOPERATIVE IMAGING AND GUIDANCE<sup>†</sup>

---

<sup>†</sup> Content from this chapter was published as:

**Hughes-Hallett, A.,** Pratt, P., Mayer, E., Clark, M., Vales, J., Darzi A. (2015). Using preoperative imaging for intraoperative guidance: A case of mistaken identity. *International Journal of Medical Robotics and Computer Assisted Surgery*. (Epub ahead of print)

## 5.1 Introduction

Surgical image guidance systems for laparoscopic and robotic platforms in intra-abdominal MIS have, to date, focused largely on creating an *augmented reality* by overlaying 3D reconstructions of preoperative data onto the endoscopic view. These have historically been generated in one of two ways (Figure 5.1.1). The first utilises manual or semi-automated image segmentation. Manual segmentation involves partitioning individual CT or MRI slices into multiple segments and then amalgamating the slices to create a series of distinct 3D volumes (Figure 5.1.1). Automation utilises supervised region-growing algorithms that operate in 3D space. In contrast, volume rendering is an automated process mapping each voxel to an opacity and colour. The voxels are then compounded along rays through each screen pixel.<sup>125</sup>

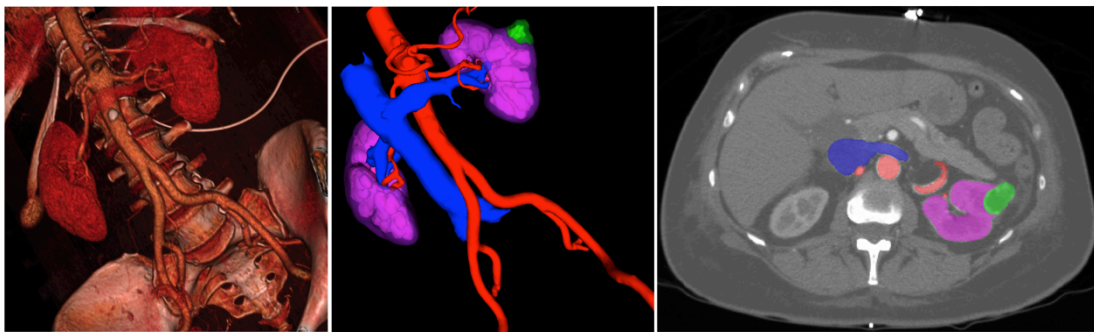


Figure 5.1.1 – The same dataset represented as a volume rendered and segmented reconstruction (left to right). The image on the right displays an axial CT slice during the process of segmentation.

Although both of these modalities of reconstruction have respective benefits, segmentation has proved more popular for intraoperative image guidance,<sup>7,9</sup> for two reasons.<sup>126</sup> First, the individual undertaking the segmentation can be selective about what they reconstruct, allowing a stylised and easier to interpret version of the anatomy to be displayed. Secondly, and perhaps more importantly, context specific knowledge can be used to inform the viewer as to anatomical structures that are unclear in the imaging dataset.

Much of the literature surrounding augmented reality and image-guided operating environments has focused on the registration and deformation of segmented reconstructions to the live operative scene.<sup>7,9,87,127,128</sup> This process makes the

assumption that the initial segmentation is accurate. The potential impact of this is particularly pertinent when utilising image guidance for tasks such as tumour resection. In this situation the reconstruction, registration and deformation must adhere to the highest levels of accuracy.<sup>7</sup>

The primary aim of this chapter was to establish the quality and degree of variability in the segmentation of tumour anatomy. This was achieved utilising a previously published tool<sup>35</sup> for the assessment of segmentation accuracy and the inter rater variability of soft tissue tumour segmentation. In addition, the level of segmentation or pathology-specific imaging expertise was assessed to establish the respective influences of this on accuracy and variability.

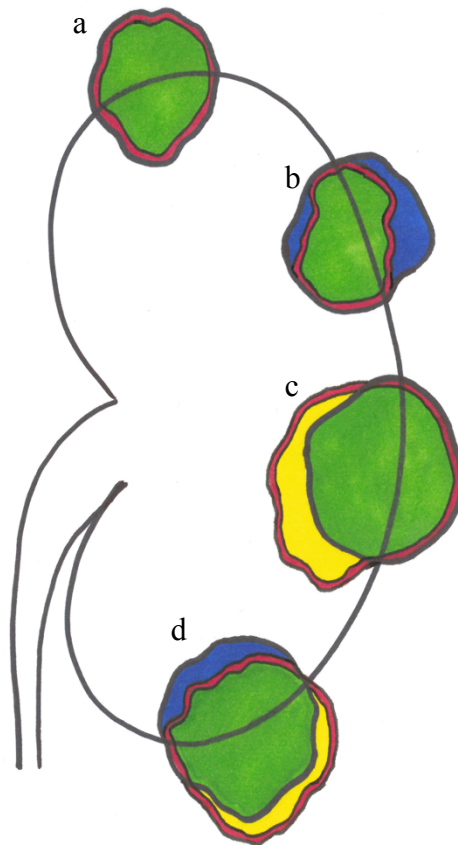
## 5.2 Methods

Computerised tomography scans from 10 patients who had undergone partial nephrectomy in our institution over the last 12 months were obtained. Consent and ethical approval for their use existed as part of a larger study examining image-guided partial nephrectomy (REC reference 07/Q0703/24). Nine raters (five surgical trainees, two surgical consultants, a consultant radiologist and an image guidance software engineer with over five years of experience in medical imaging for this pathology) were asked to undertake a manual segmentation of the 10 tumours using an industry-standard, open-source image segmentation software package ITK-SNAP.<sup>129</sup> Raters were subdivided into three groups according to both clinical and segmentation experience (experienced in segmentation and image interpretation, experienced in image interpretation, and experienced in neither segmentation nor image interpretation for renal cell carcinoma, these groups will henceforth be referred to as experts, intermediates and novices respectively). The order in which raters were asked to undertake the segmentations was electronically randomised ([www.random.org](http://www.random.org)) in order to minimise any software learning curve effect. Those participants not previously familiar with the software were asked to undertake an ITK-SNAP tutorial (<http://www.itksnap.org/>) prior to performing the segmentations, again in order to minimise this effect. In addition to being classified by rater, the images were also

classified according to tumour type (cystic or solid) to establish if this had any effect on segmentation accuracy.

Once the segmentations were completed, a gold standard segmentation was generated using the previously validated STAPLE (Simultaneous Truth And Performance Level Estimation) algorithm.<sup>35</sup> The algorithm computes a consensus segmentation based on the established mathematical principle that the individual judgements of a population can be modelled as a probability distribution, with the population mean centred near the true mean.<sup>130</sup>

Any deviation from the STAPLE gold standard was quantified using the sensitivity and positive predictive value (PPV) of that segmentation (Figure 5.2.1). In this context the specificity of segmentation is relatively meaningless as the majority of the datasets are made up of tumour negative voxels and as such the sensitivity will always be close to one. For a segmentation to be considered to have reliably accurate reproducibility, it must demonstrate a high PPV and sensitivity in addition to non-significant variability in the same variables.<sup>36</sup> In addition to establishing the PPV and sensitivity of segmentations the maximum excursion (excess segmentation of parenchyma) and incursion (failure to segment tumour voxels) from the consensus tumour boundary were calculated (Figure 5.2.1) and the locations (either endo or exophytic) collected using the open-source academic software, meshmetric3D (<http://www.nitrc.org/projects/meshmetric3d/>).



█ Segmentation Boundary  
█ Tumour Boundary

	Gold standard positive	Gold standard negative	
Rater Positive	True positive	False positive (Excursion)	<b>PPV =</b> $\frac{\sum \text{True positive}}{\sum (\text{True positive} + \text{False positive})}$
Rater Negative	False negative (Inursion)	True negative	
	<b>Sensitivity =</b> $\frac{\sum \text{True positive}}{\sum (\text{True positive} + \text{False negative})}$	<b>Specificity =</b> $\frac{\sum \text{True negative}}{\sum (\text{True negative} + \text{False positive})}$	

Figure 5.2.1 – In the diagram at the top of the figure the ground truth is represented bounded in black with the rater segmentation bounded in red. Segmentation a) high PPV and sensitivity (minimal normal parenchyma removed, minimal tumour left *in-vivo*). b) demonstrates a high PPV and low sensitivity (no normal parenchyma removed, significant residual tumour left *in-vivo*), c) low PPV and high sensitivity (tumour removed intact with significant amount of normal parenchyma), and d) low PPV and sensitivity (significant normal parenchyma removed, significant tumour left *in-vivo*). The confusion matrix that makes up the second part of the figure outlines how PPV and sensitivity are calculated.

### 5.2.1 Statistical Analysis

Statistical analysis of the results was performed in GraphPad Prism (GraphPad Software Inc, CA, USA). The population mean for participant error was assumed to be centred on a normal distribution. Significant differences between raters and segmentations for continuous data were assessed using the one-way analysis of variance (ANOVA). For the same variables subgroup analysis according to rater experience and tumour type was performed using a two-way ANOVA and student t-test, respectively. Analysis of categorical data was performed using the Chi-Squared test. A threshold  $\alpha \leq 0.05$  was used as the marker of statistical significance in all instances, with the exception of multiple pairwise comparisons where the Bonferroni correction was applied ( $n = 3$ , adjusted  $p \leq 0.017$ ).

## 5.3 Results

### 5.3.1 Overall

Average sensitivity and PPV were 0.902 and 0.891, respectively. Across all segmentations and raters (Table 5.3.1), when assessing for variability between raters for PPV and sensitivity, statistically significant differences were seen in both variables ( $p < 0.001$ ). The variability between the segmentations of different tumours however, failed to meet significance for either PPV or sensitivity ( $p = 0.080$  and  $0.101$  respectively).

When looking to establish inconsistencies in the definition of the tumour boundary the mean maximum excursion from this boundary was found to be 3.14 mm. A significant difference was seen when comparing individual raters and tumours ( $p = 0.018$  and  $< 0.001$ , respectively). The mean maximum incursion into the consensus boundary was 3.33 mm. Again a significant difference was seen when comparing individual raters and tumours ( $p = 0.029$  and  $< 0.001$ , respectively).

	PPV	Sensitivity	Incursions (mm)	Excursions (mm)
<b>Overall</b>				
	0.891 (0.092)	0.902 (0.094)	3.33 (1.28)	3.14 (0.85)
<b>Stratified by Experience</b>				
<b>Expert</b>	0.958 (0.046)	0.876 (0.047)	3.663 (1.12)	2.156 (1.21)
<b>Intermediate</b>	0.911 (0.033)	0.917 (0.040)	2.838 (1.30)	2.909 (1.09)
<b>Novice</b>	0.842 (0.041)	0.903 (0.038)	3.543 (1.68)	3.802 (1.06)
<i>p-value</i>	<i>&lt;0.001</i>	<i>0.398</i>	<i>0.068</i>	<i>0.007</i>
<b>Stratified by Tumour Type</b>				
<b>Cystic</b>	0.884 (0.023)	0.886 (0.032)	2.603 (0.32)	2.684 (0.29)
<b>Solid</b>	0.896 (0.019)	0.912 (0.016)	3.823 (0.21)	3.372 (0.35)
<i>p-value</i>	<i>0.657</i>	<i>0.472</i>	<i>0.007</i>	<i>0.151</i>

Table 5.3.1 – Analysis of variables according to rater experience and tumour type. Standard deviations in brackets. PPV = Positive predictive value

### 5.3.2 Rater experience and segmentation accuracy

Rater experience was seen to be a significant predictor of PPV but not sensitivity (Figure 5.3.1, Figure 5.3.2 and Table 5.3.1). When undertaking multiple pairwise comparisons within the PPV group across all tumours, no significant difference was seen between experts and intermediates ( $p = 0.150$ ). However, a significant difference was seen between the expert and intermediate groups when compared to the novices, who had little or no experience of renal tumours ( $p < 0.001$  and  $p = 0.006$ , respectively, Figure 5.3.1).

When comparing the difference in the mean maximum excursion between raters grouped by experience, a significant difference was seen again ( $p = 0.007$ , Table 5.3.1). After undertaking further multiple pairwise comparisons of participants grouped by experience, a significant difference was only seen between experts and novices ( $p = 0.007$ , Figure 5.3.3). In contrast, only a trend towards significance was seen when comparing the maximum incursion by rater experience ( $p = 0.068$ , Table 5.3.1 and Figure 5.3.3), with no significant difference found on a multiple pairwise comparison.



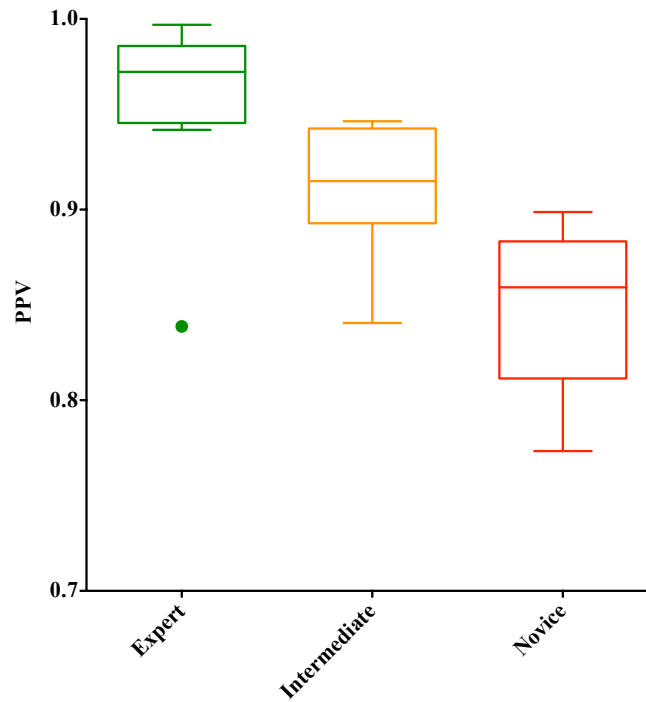


Figure 5.3.1 – Overall PPV of tumour segmentation grouped by experience. Whiskers were calculated as the 75<sup>th</sup> percentile plus 1.5 x IQR and 25<sup>th</sup> percentile minus 1.5 x IQR. Outliers were defined as values falling outside this range.

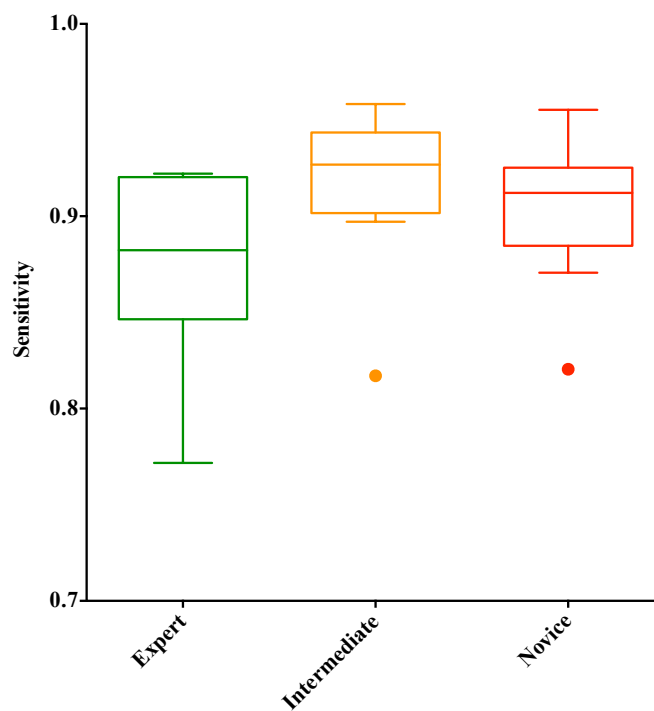


Figure 5.3.2 – Overall sensitivity of tumour segmentation grouped by experience. Whiskers were calculated as the 75<sup>th</sup> percentile plus 1.5 x IQR and 25<sup>th</sup> percentile minus 1.5 x IQR. Outliers were defined as values falling outside this range.

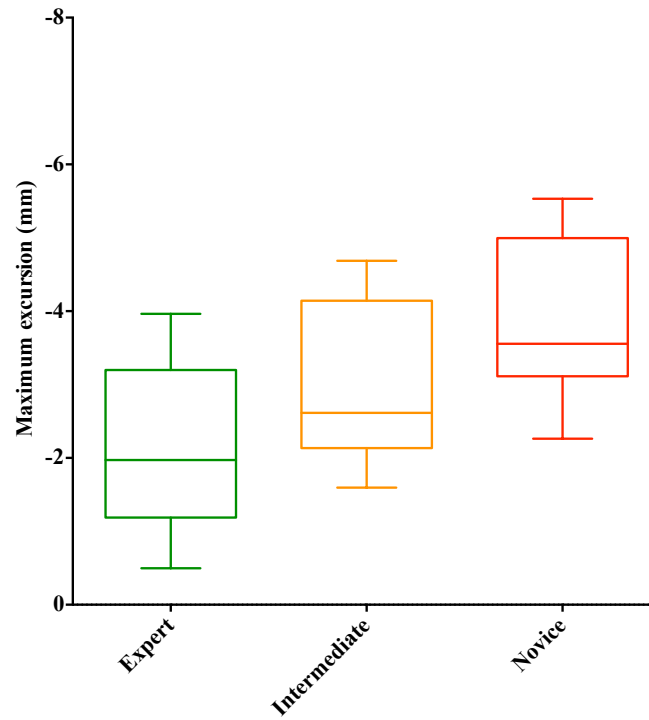


Figure 5.3.3 – Overall extent of maximum boundary excursion of tumour segmentation grouped by experience. *Whiskers were calculated as the 75<sup>th</sup> percentile plus 1.5 x IQR and 25<sup>th</sup> percentile minus 1.5 x IQR. Outliers were defined as values falling outside this range.*

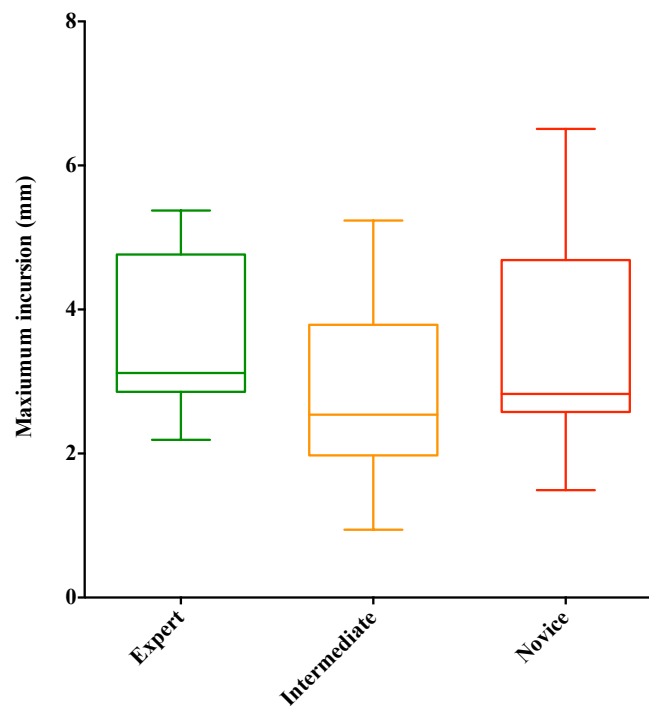


Figure 5.3.4 – Overall extent of maximum boundary incursion of tumour segmentation grouped by experience. *Whiskers were calculated as the 75<sup>th</sup> percentile plus 1.5 x IQR and 25<sup>th</sup> percentile minus 1.5 x IQR. Outliers were defined as values falling outside this range.*

### **5.3.3 Tumour type and segmentation accuracy**

No significant difference was seen between rater accuracy when comparing cystic and solid tumours for PPV, sensitivity or maximum excursions (Table 5.3.1). However, a significantly greater mean incursion of 3.82 mm into the consensus tumour was seen in solid tumours when compared to the mean incursion of 2.60 mm seen in the cystic tumour group ( $p = 0.007$ , Table 5.3.1).

### **5.3.4 Location of boundary misidentifications**

Significantly more of the maximum incursions and excursions from the consensus boundary were on the endophytic rather than the exophytic border (120 and 60 respectively,  $p < 0.001$ ). Of the incursions, 64 were endophytic and 26 exophytic, ( $p < 0.001$ ) and of the excursions, 56 were endophytic and 34 exophytic ( $p = 0.001$ ). This data was also represented graphically in three dimensions, an example of which is given in Figure 5.3.5.

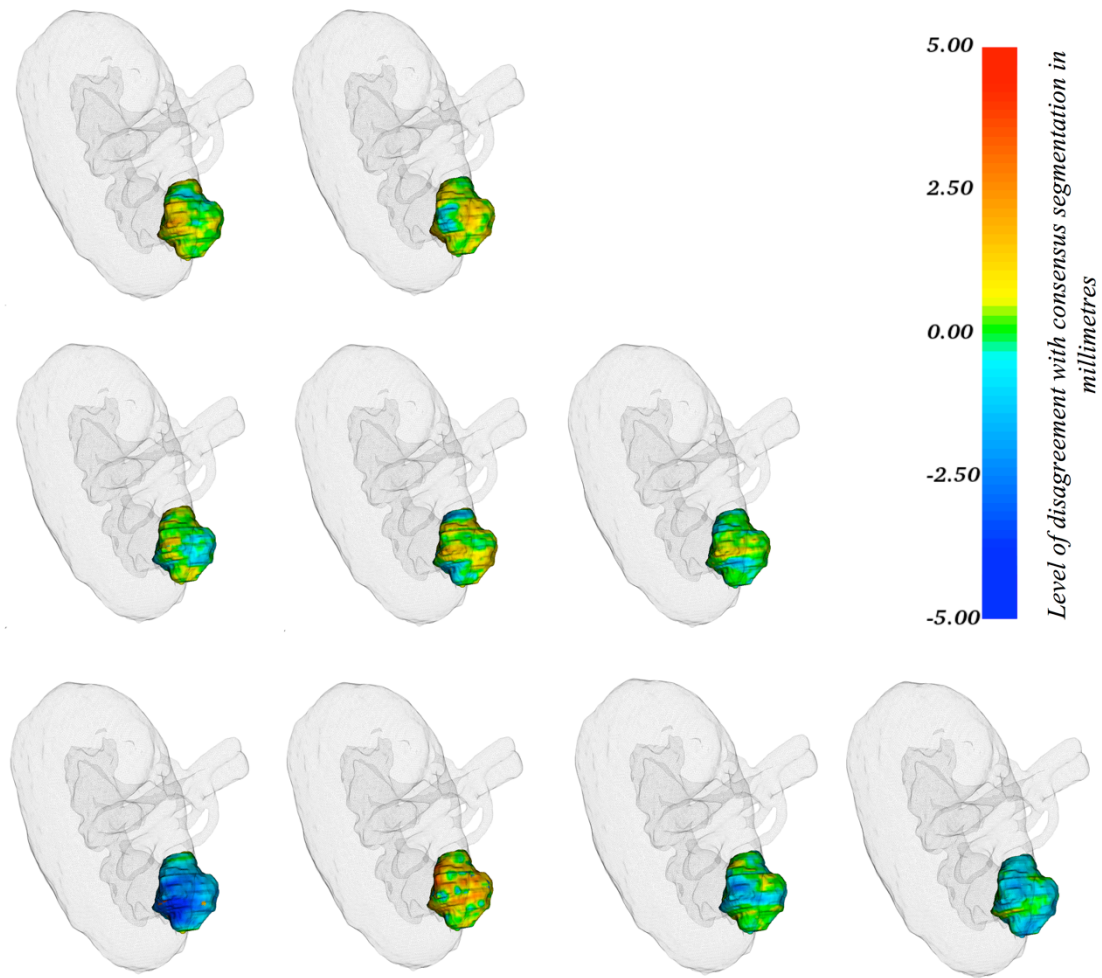


Figure 5.3.5 – Example incursions and excursions of individual raters when compared to the STAPLE derived consensus. Top row, raters experienced in imaging and segmentation; middle row, raters experienced in imaging and bottom row, raters experienced in neither. The red end of the scale represents the maximum incursion while the blue represents the maximum excursion in millimetres.

## 5.4 Discussion

### 5.4.1 Principal findings

This chapter has elucidated the degree of variability and inaccuracy from segmentation-derived tumour volumes. The data presented herein has shown there is a statistically significant variation in the quality of segmentation. This quality appears to be related to the segmentation and pathology specific imaging experience of the rater, with those with more experience generally performing better. This said, even amongst the most experienced group significant levels of error were still seen.

In recent years, there has been significant growth in image-guided surgical research<sup>9,87,118</sup> with much of this research focused on the registration<sup>8,9,89,92</sup> and deformation<sup>28,131</sup> of preoperative segmented reconstructions to fit the intraoperative scene. This application of segmentation for high precision guidance has been reported in *ex* and *in-vivo* studies in a large number of surgical subspecialties,<sup>132</sup> including hepatobiliary surgery,<sup>9</sup> neurosurgery<sup>133</sup> and urology.<sup>7,87</sup> The data presented here brings into question the validity of segmented images for this type of guidance due to the not insignificant error in combination with the significant variability in segmentation quality.

Although generally speaking the quality of segmentation was insufficiently accurate those participants with pathology specific imaging experience were found to be better raters than those with no experience. More specifically, these raters were seen to be less conservative in their approach when compared to the inexperienced group, with a more radical approach achieved without an increase in the amount of tumour left unsegmented.

This demonstrates, perhaps unsurprisingly, that with experience comes an improved ability to define structural borders. This disparity may be the result of inexperienced raters attempting to compensate by ‘erring on the side of caution’ when there was any debate regarding whether a voxel represented tumour or normal tissue. The impact of this on clinical practice, if these segmentations were used for tumour resection

guidance, would be more normal tissue being left removed if an individual with relevant experience prepared the imaging. As such the experience of the individual creating the images is crucial and should be taken into consideration when preparing any dataset for image guidance.

Another important consideration is the loci of inaccuracies. The observed greater endophytic boundary inaccuracy suggests it is more difficult to differentiate the normal parenchyma to tumour interface, than the tumour to extra renal fat boundary. The level of this inaccuracy is also clinically significant with an average maximum incursion of over 3 mm into the tumour. This is in itself unsurprising, but its demonstration brings into further question the use of segmentation for high precision image guidance tasks such as tumour resection, as it is this endophytic boundary that the image guidance is being used to define.

#### **5.4.2 Comparison with other studies**

When looking to the literature regarding the assessment of segmentation accuracy, two approaches have been taken.<sup>134</sup> In the first, performance evaluation against a ground truth, compares the performance of an individual against an algorithm derived gold standard segmentation.<sup>35,36,135</sup> Although this approach has previously been used for assessing the definition of specific organs<sup>35,36</sup> it has, up until this point, not been utilised to assess the accuracy of intra-visceral tumour anatomy segmentation. The second approach to the assessment of segmentation accuracy is cruder and assesses the variation in the segmented volume without first knowing or establishing an estimation of ground truth.<sup>134,136</sup> This has the propensity to misrepresent any inaccuracy as it only takes into account the number of voxels segmented, rather than their number and location. As such, this technique fails to take into account the important factor of boundary misidentification.

#### **5.4.3 Study Limitations**

Although this chapter has demonstrated that segmented images are subject to significant inter rater variability and inaccuracy, it is not without its limitations. The largest of these is the STAPLE algorithm itself. The degree of disagreement with STAPLE established ground truth was the parameter used to determine and

performance benchmark each participant. If this algorithm does not truly represent the ground truth, then this benchmarking is invalid. However, the algorithm is well validated and even if some inaccuracy is assumed the variation between raters alone make segmentations an inappropriate image preparation technique for high precision surgical image guidance. In addition, only the segmentation of renal tumours has been assessed and although these findings can be extrapolated to other solid organs any inferences must be exercised with caution.

## **5.5 Conclusions**

This paper has demonstrated that the image interpretation required during the segmentation of preoperative imaging introduces significant inconsistency and inaccuracy into this initial dataset. These failings make surgical image guidance based on segmentation safe only for gross anatomical appreciation. Future work is needed to develop novel approaches to image guidance, perhaps utilising intraoperative ultrasound overlay<sup>93,94</sup> or immunofluorescence,<sup>137</sup> that offer the levels of accuracy in preparation, registration and deformation required for image-guided tumour resection and other surgical tasks necessitating similarly high levels of precision.

CHAPTER 6: AUGMENTED REALITY PARTIAL  
NEPHRECTOMY: EXAMINING CURRENT STATUS AND  
FUTURE PERSPECTIVE<sup>†</sup>

---

<sup>†</sup>Content from this chapter was published as

**Hughes-Hallett, A.**, Mayer, E., Marcus, H., Cundy, T., Pratt, P., Darzi., Vale, J., (2014) Augmented Reality Partial Nephrectomy: Examining the Current Status and Future Perspectives. *Urology*, 83(2), 266-273.



## 6.1 Introduction

As outlined in the introductory chapter open surgery permits the surgeon to engage all sensory faculties to acquire an intimate understanding of tissue appearance, texture, and consistency amongst many other important distinguishing characteristics. One of the major criticisms of minimal access surgery for partial nephrectomy has been the impairment of haptic feedback for detailed discrimination and delicate intervention of the target operative anatomy.<sup>8</sup> This may impact the quality and safety of surgical resection, particularly in cases of cystic or endophytic tumours. Image guidance, and more specifically augmented reality, is forecast to play a major enabling role in the future of minimal access partial nephrectomy by integrating enhanced visual information to supplement the loss of force and tactile sensations.<sup>118</sup>

An AR operating environment allows a surgeon to simultaneously assimilate important visual information from the operative field with imaging modalities (e.g. ultrasound, CT or MRI) that usually play a passive or absent role within the operating room. Applying this image overlay technology to intra-abdominal organs presents unique challenges in registration and deformation that are difficult to overcome.<sup>27,28</sup>

During partial nephrectomy there are two stages in which an AR environment offers a potential clinical advantage. First, to facilitate rapid and accurate anatomical identification of important neighbouring structures such as the major vessels and the renal vasculature; and secondly, to assist in unambiguous dissection during tumour resection ensuring negative surgical margins while achieving a maximally nephron-sparing operation. While the latter requires high accuracy and precision, the former does not.

In this chapter, the literature has been critically appraised to examine the current status-quo, existing challenges and future research agendas for AR in minimal access partial nephrectomy.

## **6.2 Literature search**

### **6.2.1 Search strategy**

A systematic review of literature was performed using the Medline, Embase and PubMed databases. These databases were searched between January 2000 - February 2013, using combinations of the following search terms; ‘augmented reality’, ‘image guid\*’’, ‘image fusion’, ‘image overlay’, ‘soft tissue navigation’, ‘nephrectomy[Mesh]’, and ‘renal cell carcinoma[MeSH]’. An English language restriction was applied. Two reviewers independently identified articles. The study selection process is described in the Preferred Items for Systematic Reviews and Meta-analysis (PRISMA) diagram (Figure 6.2.1)

The primary search strategy was supplemented by reviewing the reference lists of retrieved articles and using the PubMed related articles feature.

#### **6.2.1.1 Eligibility criteria**

Titles and abstracts were screened to identify publications that, 1) featured the use of an augmented reality system, and 2) described the application in minimally invasive partial nephrectomy, whether *in-vivo* or *ex-vivo*. Studies were excluded if they related exclusively to focal ablative therapies or computer-assisted stereotactic procedures.

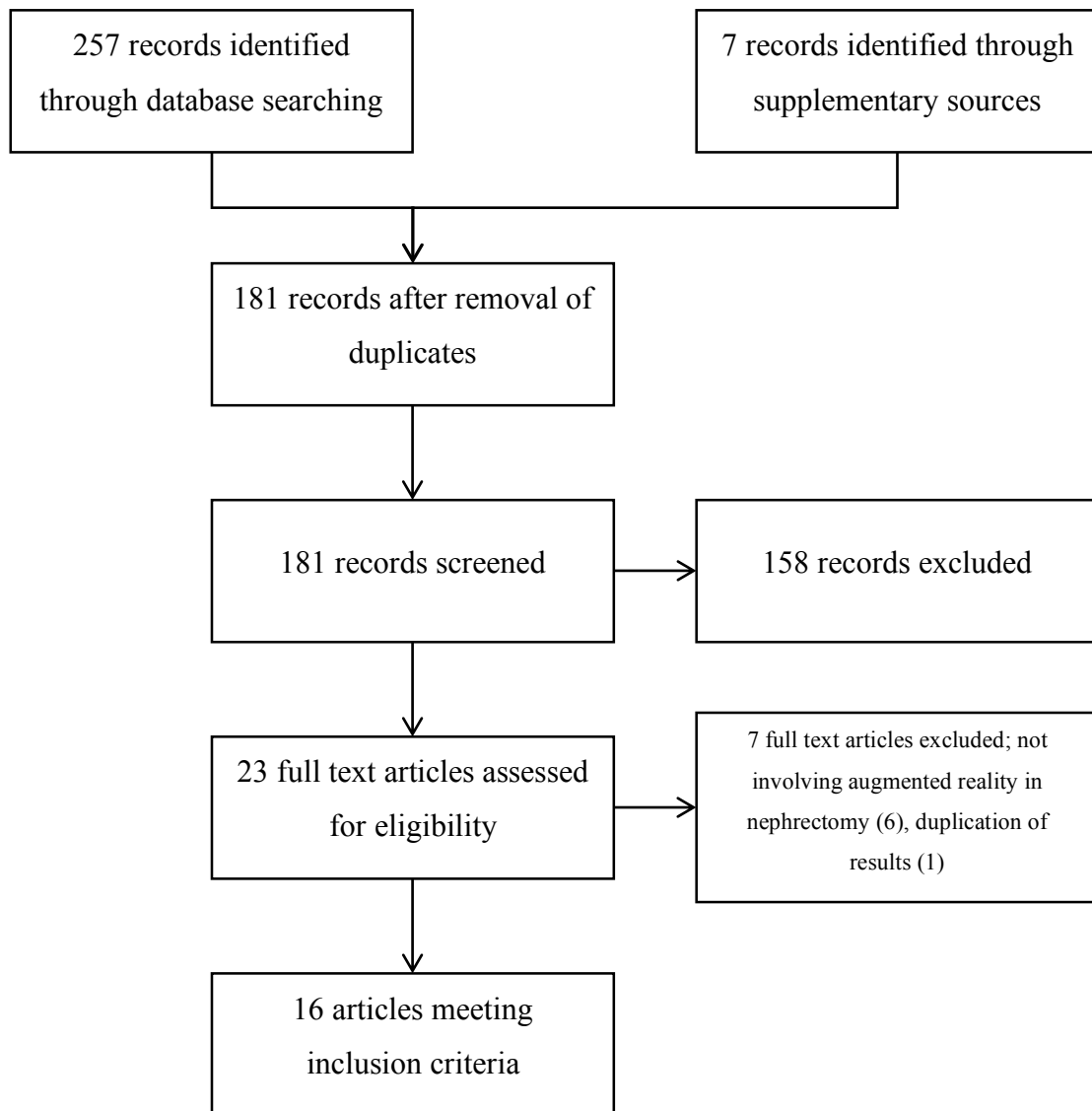


Figure 6.2.1– PRISMA diagram. Search was performed using a combination of the following key words and MeSH terms: “augmented reality” OR “image guidance” OR “image-guided” OR “image fusion” OR “image overlay” OR “soft tissue navigation” AND “nephrectomy” OR “renal cell carcinoma”

### 6.3 Principles of registration

Image registration is needed for all image overlays, be it live intraoperative imaging or the overlay of preoperative reconstructed imaging. Registration is the process by which multiple datasets spatially are aligned in a single coordinate system such that the locations of corresponding points match as best as possible.<sup>28,138</sup> To understand and apply the principles of registration in the context of partial nephrectomy it is useful to consider the procedure in two phases. Firstly, an intraoperative *planning phase* involving anatomy definition and localization and secondly an *execution phase* of tumour resection.

Within the *planning phase*, the surgeon may utilise image guidance to better appreciate neighbouring anatomical structures, in particular the orientation of the hilar vasculature, the spatial characteristics of the tumour, and its relationship to the collecting system (especially in the case of partially or entirely endophytic tumours). This stage relies on the image being overlaid in order to enable the surgeon to appreciate detailed anatomy at a gross scale. As such, a millimetre level of registration accuracy may not be fundamentally important in this phase, unlike during tumour resection where high accuracy of registration is important for maximal preservation of healthy parenchyma while maintaining adequate resection margins of 5-7mm.<sup>139,140</sup>

In its simplest form, registration is performed manually using the surgeon's innate knowledge of human anatomy combined with the ability of the human brain to align two objects in 3D space (Figure 6.3.1). Applied to image-guided surgery, this method of registration offers a level of accuracy sufficient to provide a 'road map' of the anatomical relationships (*planning phase*) but lacks the accuracy to allow image-guided resection (*execution phase*). Three groups have reported human *in-vivo* experience using manually overlaid 3D reconstructions for minimal access partial nephrectomy (Table 6.3.1).<sup>8,97,98</sup> Although these studies did not report objective data, positive surgeon feedback was noted.<sup>8</sup>

Systems, such as those proposed, offering manually registered images represent a relatively low barrier to entry and allow the surgeon to have a better understanding of both: hilar vascular anatomy, offering increased clarity when dissecting and clamping

the hilar vessels;<sup>141</sup> and tumour extent, allowing improved resection planning, potentially minimising positive surgical margins while maximally preserving renal parenchyma.<sup>142</sup>

### 6.3.1 Surface-based registration

Surface-based registration is the method of image alignment that has been best described in robotic partial nephrectomy.<sup>28,143–147</sup> In this form of image registration, computer-based algorithms are used to achieve higher levels of accuracy than are possible using manual registration alone. One of the most commonly applied forms of computer-aided registration aligns surface features within the real and virtual scenes.

In the papers examining the use of surface-based registration in renal models, a tracked instrument has been used as a topography defining stylus<sup>28,143,145,147</sup> to create an accurate intraoperative model of the surface anatomy of the kidney (Figure 6.3.1). Surface anatomy is then matched to the surface of a segmented reconstruction generated from pre-operative images. This method of registration has been used both in tissue-mimicking models<sup>28,143,147</sup> and human subjects<sup>28</sup> during robotic partial nephrectomy (Table 6.3.1).

Herrell *et al.* reported a reduction in the normal parenchyma-to-tumour ratio (resection ratio) when AR was used in a phantom model mimicking renal tumour resection (resection ratio of 3.26 vs. 9.01;  $p < 0.01$ ).<sup>143</sup> In an *in-vivo* setting, Altamar *et al.*<sup>28</sup> demonstrated good qualitative alignment of predetermined markers with intended targets, although quantitative measures of accuracy were not investigated and the system was not used to perform image-guided tumour excision.

The studies by Altamar *et al.*<sup>28</sup> and Herrell *et al.*<sup>143</sup> both utilised a tracked da Vinci→ Surgical System instrument (Intuitive Surgical, Sunnyvale, USA) as a topography defining stylus, which requires accurate knowledge of the positions of the robotic arms in order to calculate instrument tip location in 3D space. This data can be acquired either intrinsically or extrinsically. The intrinsic method utilises the kinematic chain of the robot along with the robotic cart joint positions (Figure 6.3.2).<sup>148</sup> This approach is limited by the accuracy of measurements of da Vinci→ passive and active robotic joint

positions. Inaccuracies in measured angular position of the passive and active joints compound, as they pass down the kinematic chain (including both active and passive joints), leading to large errors in the computed position of the instrument tip, reported at  $10.6 \pm 22\text{mm}$ .<sup>145</sup> This far exceeds the accepted 5-7mm tolerance for partial nephrectomy margins.<sup>139,140</sup>

Herrell *et al.*<sup>143</sup> and Kwartowitz *et al.*<sup>144,145,149</sup> combined both intrinsic and extrinsic tracking systems (extrinsic tracking utilises commercially available electro-magnetic or optical tracking systems to ascertain the positions of the instruments and camera in three dimensional space) to capitalise on the benefits of both while mitigating respective drawbacks. In their system, an optical tracking system was used to determine the position of the passive setup joints of the robot while continuing to use intrinsic localisation for the active robotic joints. Using this system the observed intra arm error was reduced from, 10.6mm to <2mm (Figure 6.3.2).<sup>145</sup>

This use of a tracked robotic instrument as a topography-defining stylus is the most widely published method of endoscopic surface-based registration. However, laser range finders have also been used to map organ surfaces, with success in *ex-vivo* renal models.<sup>147,150</sup> Although these *ex-vivo* studies represent proof of concept, a suitable laparoscopic laser range finder is yet to be trialled in renal surgery.

There are a number of inherent problems with surface-based registration that need to be overcome before it can be applied to the operating room environment. The most apparent of these is the need for extrinsic tracking. Most of the literature to date has focused on the use of external optical tracking of the robotic instruments or arms. Optical tracking requires a continuous direct line of sight for motion capture (Figure 6.3.2), which is difficult to achieve due to the continuous flow of staff and equipment in a normal operating room environment. A further issue relates to the presence of perinephric fat preventing easy access to the renal capsule. Benincasa *et al.*<sup>147</sup> calculated that a minimum of 28% of the surface area of the kidney needs to be exposed for accurate surface-based registration. In clinical practice, this necessitates stripping large areas of perinephric fat in order to perform a sufficiently accurate surface-based registration.

<b>Manual Registration</b>				
		n	Study Description	Outcomes
Nakamura <i>et al.</i> 2010 <sup>97</sup>	<i>In-vivo</i>	2	3D volume rendered images fused with live operative view.	Demonstration of feasibility.
Teber <i>et al.</i> 2009 <sup>8</sup>	<i>In-vivo</i>	10	Projection of intra-abdominal anatomy onto patient skin to aid in port placement. Manual registration of segmented reconstruction onto live operative view.	No complications. No positive margins. Good feedback from operating surgeon.
Ukimura <i>et al.</i> 2008 <sup>151</sup>	<i>In-vivo</i>	1	Four-colour-coded-zonal navigation. Augmented reality used to aid surgical resection by highlighting in green the 'safe' 5mm resection margin zone.	Demonstration of feasibility.
<b>Surface-based registration</b>				
Altamar <i>et al.</i> 2011 <sup>28</sup>	<i>In-vivo/Ex-vivo</i>	-	Assessment of surface-based registration.	Good qualitative alignment of images in <i>in-vivo</i> cases. TRE of 1.4mm in <i>ex-vivo</i> cases.
Herrell <i>et al.</i> 2009 <sup>143</sup>	<i>Ex-vivo</i>	13	Used optical tracking to track robotic instruments, allowing instruments to be used as stylus to map kidney surface.	Reduced normal parenchyma to tumour ratio seen in AR group. Reduction in resection time in AR group.
Benincasa <i>et al.</i> 2008 <sup>147</sup>	<i>Ex-vivo</i>	1	Compared surface-based registration to fiducial gold standard.	Established that 28% of kidney surface needs to be scanned for reliably accurate surface registration.
<b>Fiducial Based Registration</b>				
Teber <i>et al.</i> 2009 <sup>8</sup>	<i>Ex-vivo</i>	10	3D cone beam imaging used to create 3D reconstruction of organ which was subsequently registered to real time image	TRE of 0.5mm in image registration
Nakamoto <i>et al.</i> 2008 <sup>146</sup>	<i>Ex-vivo</i>	1	Image registered using fiducial markers and then organ tracking preformed using wireless magnetic tracking	Successfully registered and tracked resected tumour but with high level of inaccuracy. TRE of 3-5mm
Baumhauer <i>et al.</i> 2008 <sup>152</sup>	<i>Ex-vivo</i>	3	3D cone beam imaging used to register pre-op CT to intraoperative image	System was able to register images in 97% (maximum TRE of 0.89mm) of the 700 frames chosen randomly from the video feed of three cases
<b>3D-CT stereoscopic image registration</b>				
Pratt <i>et al.</i> 2012 <sup>92</sup>	<i>In-vivo/Ex-vivo</i>	3/20	A single feature is selected in the left and right images, this pins the reconstruction to one point in the source image, surgical assistant must then complete the registration	TRE of the system on a phantom organ revealed a TRE of 1.6mm. The system when trialled <i>in-vivo</i> received positive feedback from the operating surgeon
Su <i>et al.</i> 2009 <sup>153</sup>	Post-procedural	2	Applied a novel automated 3D registration and tracking algorithm to a post procedural video	TRE of <1mm. Reported a 4 frame latency and a refresh rate of 10Hz

Table 6.3.1 – Proposed augmented reality systems by registration type - = not reported. TRE = target registration error, EM = electromagnetic, DOF =degrees of freedom, 3D = 3-dimension

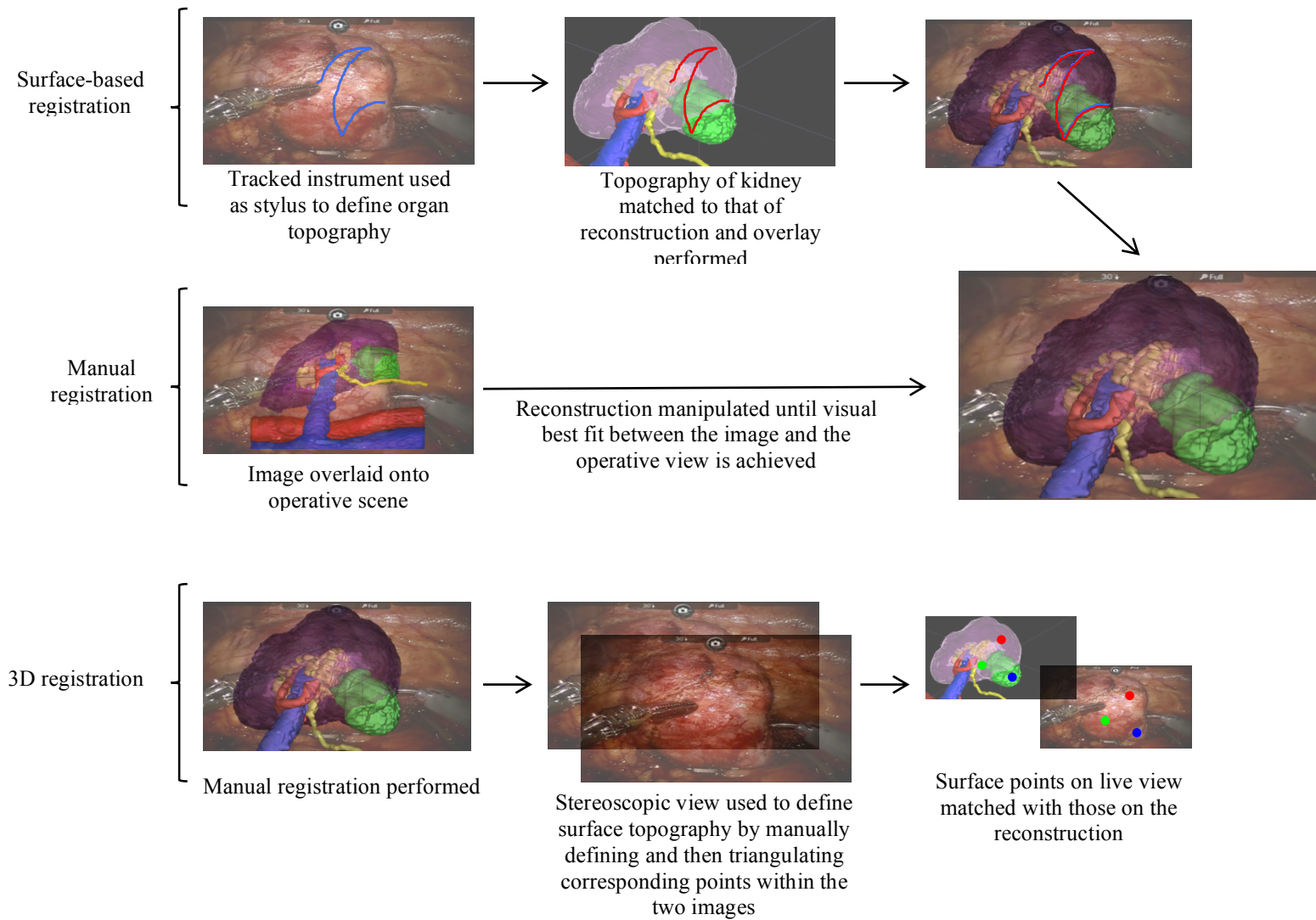


Figure 6.3.1 – Flowchart displaying the various approaches to image registration



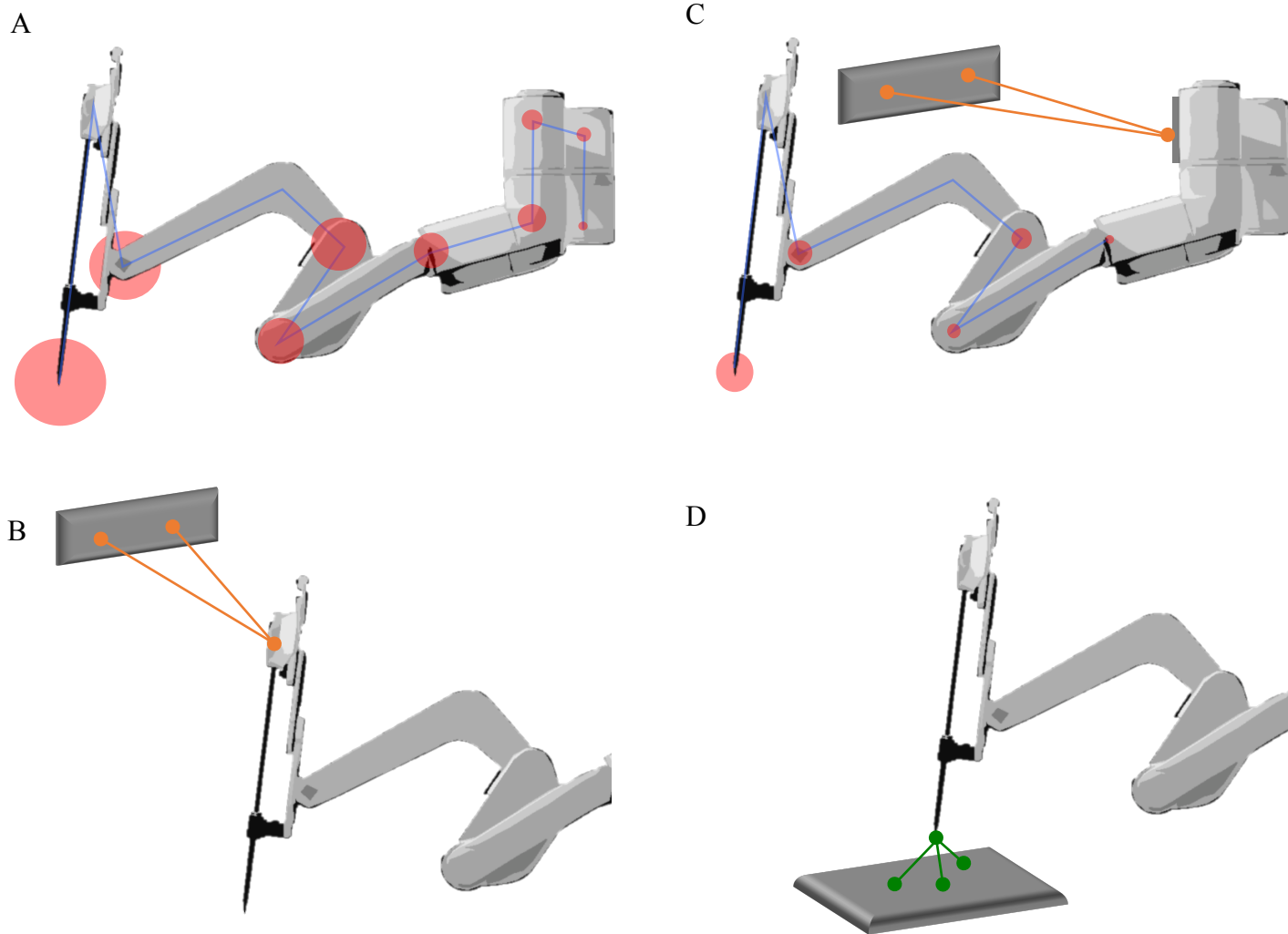


Figure 6.3.2 – A. Intrinsic tracking using the joint positions of the da Vinci robotic arms. The errors in calculation of joint positions compound as you pass down the kinematic chain. B. Optical tracking. Optical tracer is mounted to instrument, tracking system tracks the motion of tracer and requires continuous direct line of sight. C. System proposed by Herrell *et al.*<sup>143</sup> and Kwartowitz *et al.*<sup>144,145,149</sup>. Optical tracking is used to ascertain the position of the passive joints, shortening the kinematic chain thereby reducing the error at the instrument tip. D. Electromagnetic tracking. Tracers are attached to the instrument (or organ<sup>146</sup>) and tracked using an EM tracking plate. No line of sight required, so tracking device can, theoretically, be placed inside patient.

Although there are problems associated with surface-based tracking it represents a potential improvement over manual tracking alone through automation. This both improves the accuracy of registration, moving one step closer to a system accurate enough for image-guided resection, and takes the task of registration away from the surgeon reducing his/her cognitive work load.

### **6.3.2 3D-CT stereoscopic image registration**

This method of registration uses the disparity in perspective between the two cameras to triangulate where objects are within the camera frame (Figure 6.3.1).<sup>154,155</sup> The need for external instrument tracking is therefore eliminated, avoiding the requirement for optical tracking equipment in the operating room.

A combination of manual and stereoscopic camera-based registration for human *in-vivo* AR in robotic partial nephrectomy has been described by Pratt *et al.* (Figure 6.3.1 and Figure 6.3.3).<sup>92</sup> In this system, a single feature on the surface of the kidney is identified and aligned, through a spatial translation, with the corresponding feature on the surface of a 3D reconstruction of the kidney. Once this point has been isolated it is used as a centre of rotation around which the image is moved until it is coincident with the anatomy being viewed. When validated on a phantom this system showed an average target registration error (TRE) of 1.6mm (Table 6.3.2). A disadvantage to this system is the lack of any camera or organ tracking such that registration has to be repeated each time the camera is moved, potentially impacting on the surgical workflow. Su *et al.* have proposed a similar approach that also performs organ and camera tracking, with TRE reported as <1mm (Figure 6.3.1 and Figure 6.3.4).<sup>153</sup> This approach has been validated in a post-procedural human *ex-vivo* model but is yet to be trialled intra-operatively.

The use of the stereoscopic camera to register an endoscopic image to the preoperative 3D reconstructed CT has many advantages: It requires no external trackers, generates adequately accurate images to assist in resection and permits fast registration. The overall impact on the surgical workflow can be minimised to less than a minute, with Pratt *et al.* reporting mean image registration duration of 48.1 seconds.<sup>92</sup> However, such systems are burdened by high

costs for the stereoscopic camera, image capture hardware and software systems that are able to process large data volumes for image overlay without significant time lag.

### 6.3.3 Organ tracking

Few AR platforms proposed to date have progressed beyond image registration to address the next logical step of camera and organ tracking. In a system that accounts for these factors, the overlaid registered image will be 'locked' to the operative view and synchronously co-aligned with organ (*organ tracking*) and camera (*camera tracking*) movement. Without organ and camera tracking, image registration is only momentarily accurate with inaccuracies being introduced by respiration, soft-tissue deformation, camera movement and other changes to the operative field of view such as bleeding.

Magnetic tracking has received criticism on account of the magnetic field being easily disturbed by ferromagnetic objects such as laparoscopic instruments or operating tables. The maximum error introduced by endoscopic instruments in contact with the transponder has been quantified as 1mm, and  $\leq 0.4\text{mm}$  when the instrument was  $\geq 20\text{mm}$  away.<sup>146</sup> When assessing the registration error of the magnetic tracking system, the error was found to be more significant at 3-5mm; this was further compounded by a registration delay induced by image processing, causing further errors in temporal registration.<sup>146</sup>

Although appealing in some regards, the ability to apply an electromagnetically based tracking system successfully in the surgical environment is debatable. There are abundant ferromagnetic objects in most operating rooms that have the potential to influence tracking distortion. Additionally, the system requires the surgeon to insert transponders into the target organ, a step that is potentially difficult to justify clinically. Arguably the greatest limitation with the system, in its current form, is the misalignment error of up to 5mm. This error is too great to be considered safe and reliable for partial nephrectomy.

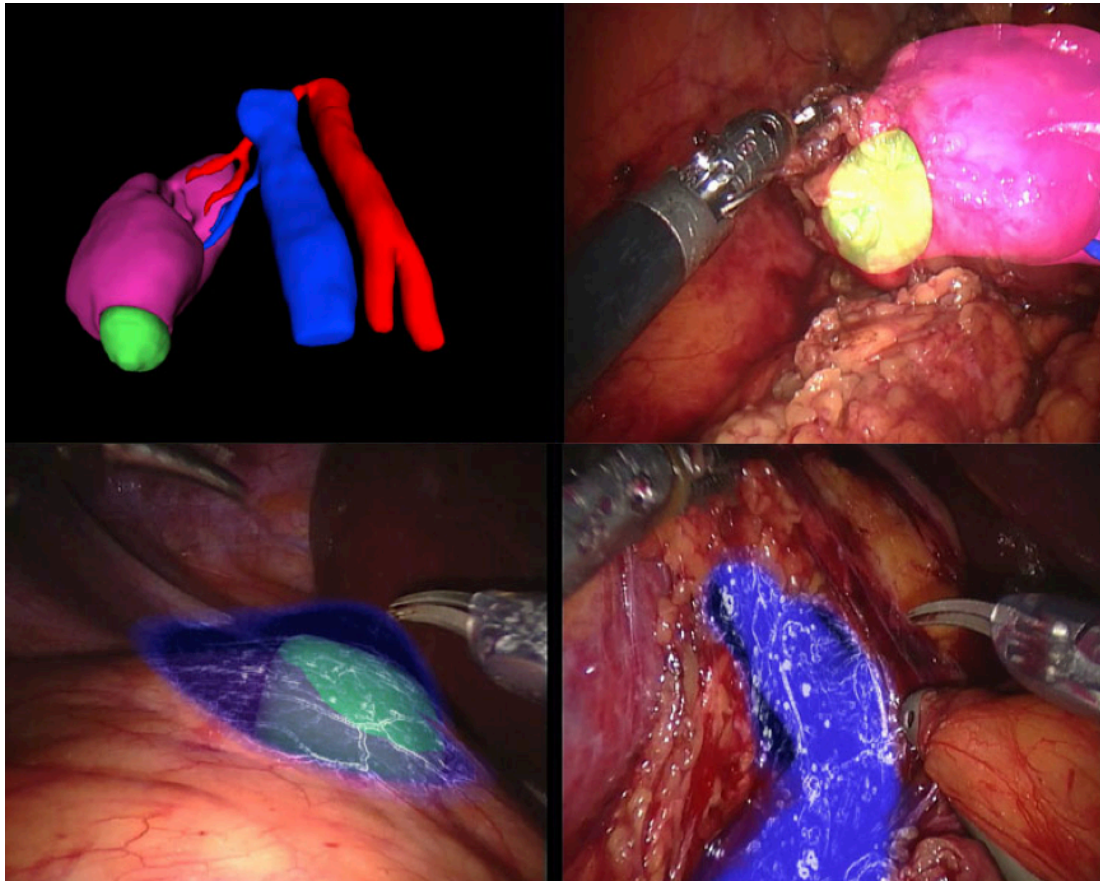


Figure 6.3.3 – From top left: Kidney model including main vessels; tumour localisation; surface of kidney painted away to reveal partially endophytic tumour; exposure of vena cava and renal vein. Pratt *et al.*<sup>19</sup>

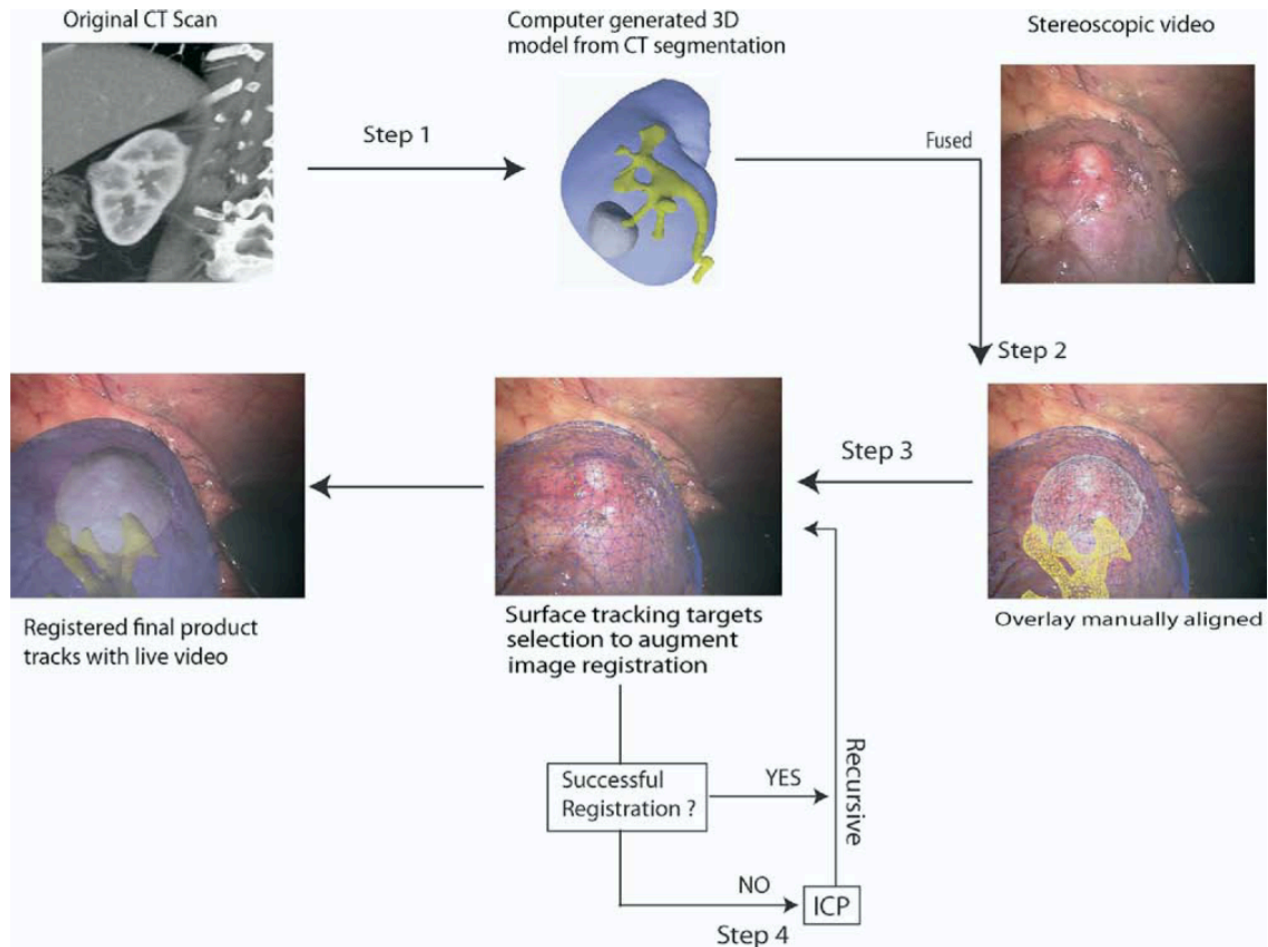


Figure 6.3.4 – The stereoscopic overlay registration algorithm proposed by Su *et al.*<sup>153</sup> The chart demonstrates the steps required to perform accurate overlay and tracking. (From Su *et al.* 2009)

	<b>Imaging Modality</b>	<b>Registration Type</b>	<b>Mean TRE</b>
<b>Yip <i>et al.</i> 2012</b> <sup>156</sup>	-	3D stereoscopic image registration	1.3-3.3mm
<b>Pratt <i>et al.</i> 2012</b> <sup>92</sup>	CT/MRI	3D-CT to stereoscopic image registration	1.6mm
<b>Altamar <i>et al.</i> 2011</b> <sup>92</sup>	CT	Surface-based registration	1.4mm
<b>Glisson <i>et al.</i> 2011</b> <sup>157</sup>	CT	Surface-based registration using laser range finder	4.9mm
<b>Su <i>et al.</i> 2009</b> <sup>153</sup>	CT	Post procedural 3D-CT to stereoscopic image registration	<1mm
<b>Teber <i>et al.</i> 2009</b> <sup>8</sup>	Cone beam CT	Fiducial based registration	0.5mm
<b>Benincasa <i>et al.</i> 2008</b> <sup>147</sup>	CT	Surface-based registration	0.4mm
<b>Baumhauer <i>et al.</i> 2008</b> <sup>152</sup>	CT	Fiducial based registration	0.89mm
<b>Nakamoto <i>et al.</i> 2008</b> <sup>146</sup>	CT	Fiducial based registration and wireless magnetic organ tracking	3-5mm

Table 6.3.2 – Target registration error the available augmented reality systems, 3D = 3-dimensions TRE = target registration error

As well as the previously mentioned system trialled by Su *et al.*,<sup>153</sup> (Figure 6.3.4) further work published by Yip *et al.*<sup>156</sup> has explored using stereo-matched registration and tracking algorithms in a post-procedural model. These algorithms act by triangulating surface features in a stereoscopic scene to perform tissue tracking and the group were able to achieve a 1.3–3.3mm degree of error.<sup>156</sup> This method of tracking, although computationally expensive, is more accurate and less invasive than magnetic tracking and as such represents an attractive alternative.

The literature is limited to two studies that have investigated kidney tissue deformation.<sup>28,158</sup> Most recently Altamar *et al.*<sup>28</sup> published an *ex-vivo* study in which six porcine kidneys, after fiducial placement, were perfused to an arterial pressure of 100mmHg at which point the renal artery and vein were clamped. After CT scanning, an incision was made in the surface of each kidney with a tracked scalpel to allow accurate superimposition of the incision onto the virtual model. Finally, a post-deformation CT scan was performed. The mean shift of the surface fiducials was then calculated. The researchers had two aims: first, to quantify the organ deformation occurring on clamping of the renal vessels and incision of the organ surface, and

second, to develop a model to predict the effects of these two variables. Mean displacement of the fiducials on the organ surface was 4.4mm ( $\pm 2.1$ mm) when the vessels were clamped and the organ surface incised. When comparing the actual deformation in a single kidney (3.2mm) compared with the amount of deformation predicted by the model (6.7mm), the model was able to compensate for approximately 52% of the deformation. Although encouraging, this level of accuracy is not as high as would be desired in the *in-vivo* operative setting. It is also worth highlighting that the validity of this model as a surrogate for a diseased human kidney is unclear, as it was performed in porcine renal tissue, not under pneumoperitoneum and with no simulated lesion.

The second relevant publication by Ong *et al.*<sup>158</sup> describes a smaller series of two porcine kidneys that were scanned before and after clamping of the renal vessels. The group attempted to model for deformation using Biot's model of consolidation.<sup>159</sup>

Tissue deformation represents an area of concern when using preoperative imaging to define tumour anatomy in partial nephrectomy. No viable solution to the problem has yet been identified and without the ability to accurately model for tissue deformation, the use of preoperative imaging remains too inaccurate for guidance of tumour resection.

#### **6.3.4 Intra-operative imaging and fiducial-based registration**

Live intraoperative imaging presents a strategy for avoiding issues related to tissue deformation, as there is no requirement for tissue deformation modelling as the information being obtained is live and dynamic.

Intraoperative ultrasound is an imaging modality that is already used in urology, with several laparoscopic probes available on the market for clinical use. However, the use of ultrasound in an AR environment remains relatively unexplored. Cheung *et al.*<sup>93</sup> examined the application of fused video and ultrasound images in a phantom model for laparoscopic partial nephrectomy. In their system, magnetic trackers with six degrees of freedom were fixed to both the camera and ultrasound probe to identify their respective locations (translation in three perpendicular axes combined with rotation)

(Figure 6.3.2). A simulated partial nephrectomy was then performed on a polyvinyl alcohol renal phantom by an experienced renal surgeon. The surgeon was instructed to resect endophytic tumours with a standard 5mm margin. The ultrasound feed was displayed in three different ways; conventionally on two separate screens, fused images presented in 2-dimensions, and fused images presented in 3-dimensions. The best results were seen in the 2-dimensional fusion group, with a mean minimum margin of 1.1mm compared to 2.1mm in the conventional group and 1.8mm in the 3D fusion group, although this was not subject to statistical analysis.

Cone beam CT is another potential live imaging modality. This technique was developed to allow access to CT in an operating room environment. X-rays are delivered in a cone rather than the conventional fan-shape seen in helical scanners, permitting image acquisition of a large area in a single pass of the C-arm, but at the expense of increased x-ray scatter and a corresponding reduction in image quality.<sup>160</sup> Although initially intended for use by interventional radiologists, intra-operative cone beam CT has also been utilised by surgeons, predominantly for head and neck surgery.<sup>160-162</sup> There has been some experimentation of cone beam CT in *ex-vivo* renal models, involving imaging combined with surgeon-placed navigation aids (fiducials) to assist in the overlay of preoperative CT imaging on live operative video (Table 6.3.1).<sup>8,152</sup> Teber *et al.* further explored the use of 3D cone beam CT to form segmented reconstructions of *ex-vivo* organ, tumour and vasculature, which were then superimposed on the live operative image.<sup>8</sup> Registration was performed using barbed navigation aids inserted into the kidney (Figure 6.3.5)

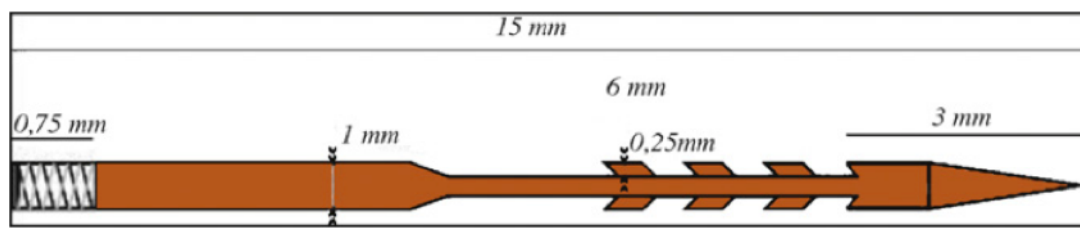


Figure 6.3.5 – Navigation aid proposed by Teber *et al.*<sup>8</sup>

Although promising, the use of cone beam CT is also not without significant limitations. It requires expensive and not widely available imaging technology to be present in the operating room; it subjects both the patient and the operating team to repeated doses of radiation and perhaps most importantly, if the approaches proposed by Teber *et al.*<sup>8</sup> or



Baumhauer *et al.*<sup>152</sup> were applied *in-vivo*, it would involve the insertion of barbed probe tracking aids into the kidney.

## 6.4 Conclusions

There is a growing amount of *ex-vivo* data examining augmented reality in partial nephrectomy but there remains little quantitative evidence investigating the technology's ability to improve patient safety and outcomes. There is a need for more clinically focused research examining the potential impact of AR operating on these patient related factors.

To date, research directed toward AR in minimal access partial nephrectomy has focused on the problems facing the technology and has adopted a 'one-size-fits-all' problem solving approach. This strategy exclusively focuses on single imaging modalities and attempts to use each in isolation to solve all of the current limitations for translation into clinical practice.

As presented in this chapter, a variety of eligible imaging modalities exist, each with respective strengths but also unique drawbacks, for these reasons the platform outlined in the final two chapters of the thesis will take a multi-modality approach to guidance. This approach will combine pre-operative cross sectional imaging with intraoperative ultrasound based guidance for the *planning* and *execution* phases, respectively (outlined Chapters 7 and 8), using the benefits of each imaging modality to target the differing guidance needs of the two phases.

## CHAPTER 7: A NOVEL TABLET-BASED IMAGE GUIDANCE PLATFORM<sup>†</sup>

---

<sup>†</sup> Content from this chapter was published as:

**Hughes-Hallett, A.**, Pratt, P., Mayer, E., Martin, S., Darzi, A., & Vale, J. (2014). Image guidance for all - Tilepro display of 3-dimensionally reconstructed images in robotic partial nephrectomy. *Urology*, 84(1), 237-242

Content from this chapter was presented at:

**Hughes-Hallett, A.**, Pratt, P., Novara, G., Vale, J., Mottrie, A., Darzi, D., Mayer, E. Image-guided robot assisted partial nephrectomy: An assessment of efficacy. European Association of Urology Conference (EAU) '15

## 7.1 Introduction

As outlined in introductory and review chapters of this thesis, the move from open to laparoscopic, and finally to robotic surgery has heralded a progressive decrease in the amount of sensory information received by a surgeon performing a given procedure. The greatest casualty of the increasing sensory distance between surgeon and patient is loss of the ability to determine subsurface anatomical relationships through the palpation of tissue.<sup>7,163</sup> It has been suggested that image-guided surgery represents a major revolution in intra-abdominal MIS, offering the possibility of increased safety with the potential to compensate for the loss of tactile feedback.<sup>164</sup> Whereas traditionally CT and MRI images were viewed as axial slices on two-dimensional monitors, they can now be viewed as 3D reconstructions with relative ease. This representation of patient anatomy results in an improved ability to localise structures with no increase in cognitive load.<sup>86</sup> A potential solution to the loss of haptic feedback is to augment the surgeon's view with these 3D reconstructions providing them with a detailed appreciation of subsurface anatomy, allowing for more informed intraoperative decision making.<sup>165</sup>

This chapter tackles the first of the previously outlined steps of *planning* and *execution*. The pre- and intraoperative *planning* phases in partial nephrectomy focus on the steps of vessel identification and tumour localisation, and are often challenging with both of these factors being highly variable between individuals, and renal tumours often being partially or entirely endophytic.

Initially, a randomised crossover study was undertaken to establish the interface that minimised both the amount of time required to perform a manual image registration, and the error of that registration. Subsequent to this, the largest series of image-guided intra-abdominal surgery to date was undertaken. The presented case-control series represents a IIb study (Table 7.3.1), as defined by the IDEAL collaboration.<sup>11</sup> As such, it had the principal aims of prospectively establishing how beneficial the platform was, for which cases this benefit was greatest and, as a secondary aim, whether the quality of the source imaging affected efficacy.

## 7.2 Methods

### 7.2.1 *Ex-vivo* randomised crossover study

#### 7.2.1.1 *Overview*

The initial randomised crossover study, participants were asked to align pre-recorded endoscopic views of a kidney phantom with a 3D reconstruction of the same kidney. The task was performed on a da Vinci Standard console (first generation) utilising an iPad™ (Apple, Cupertino, USA) or 3D mouse (SpaceNavigator™, 3Dconnexion, Boston, USA) interface. The 3D reconstruction was displayed below the endoscopic view in a fashion akin to the TilePro™ function of the da Vinci S, Si and Xi consoles (Intuitive Surgical, Sunnyvale, USA).

#### 7.2.1.2 *Experimental Design*

Initially a CT scan of a normal kidney was obtained and a segmented reconstruction of the organ created using ITK-SNAP.<sup>129</sup> From this segmentation, a phantom organ was 3D printed (Objet 260 Connex, Stratasys, Minneapolis, USA). The organ phantom was placed in a mannequin orientated in a lateral position similar to that adopted by patients undergoing RAPN. A series of three camera orientations was then recorded.

The rendering of 3D reconstructions was undertaken on a dedicated portable server and fed into the console along with the pre-recorded video from the stereoscopic camera (system architecture previously published by Pratt *et al.*<sup>92</sup>), in order to account for the da Vinci Standard's lack of TilePro™. Software was developed allowing an over-and-under view of the endoscopic feed and 3D reconstruction within the console (Figure 7.2.1).

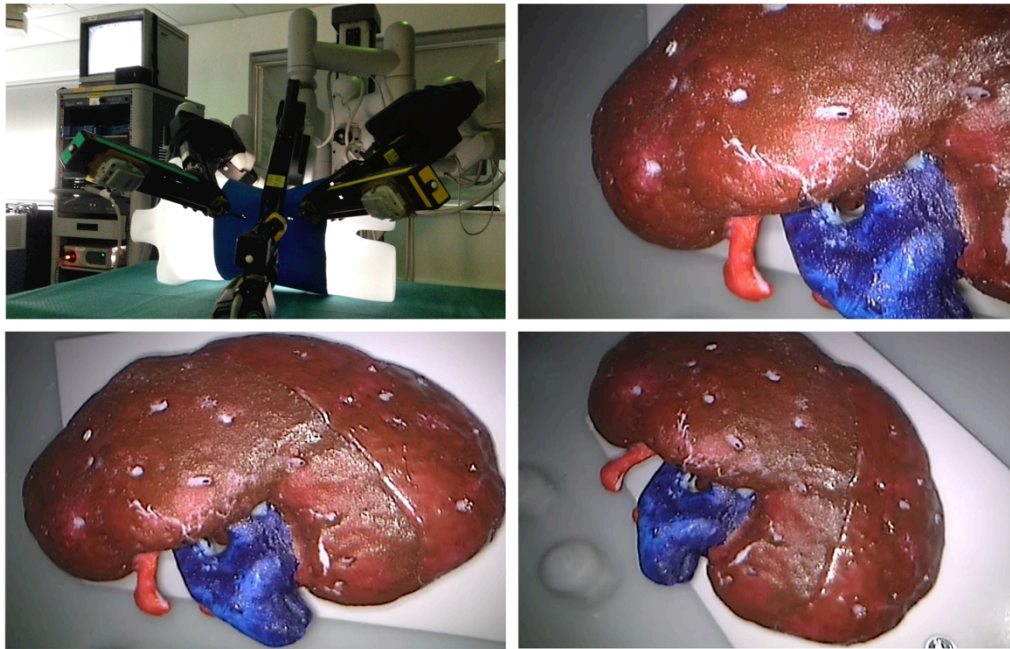
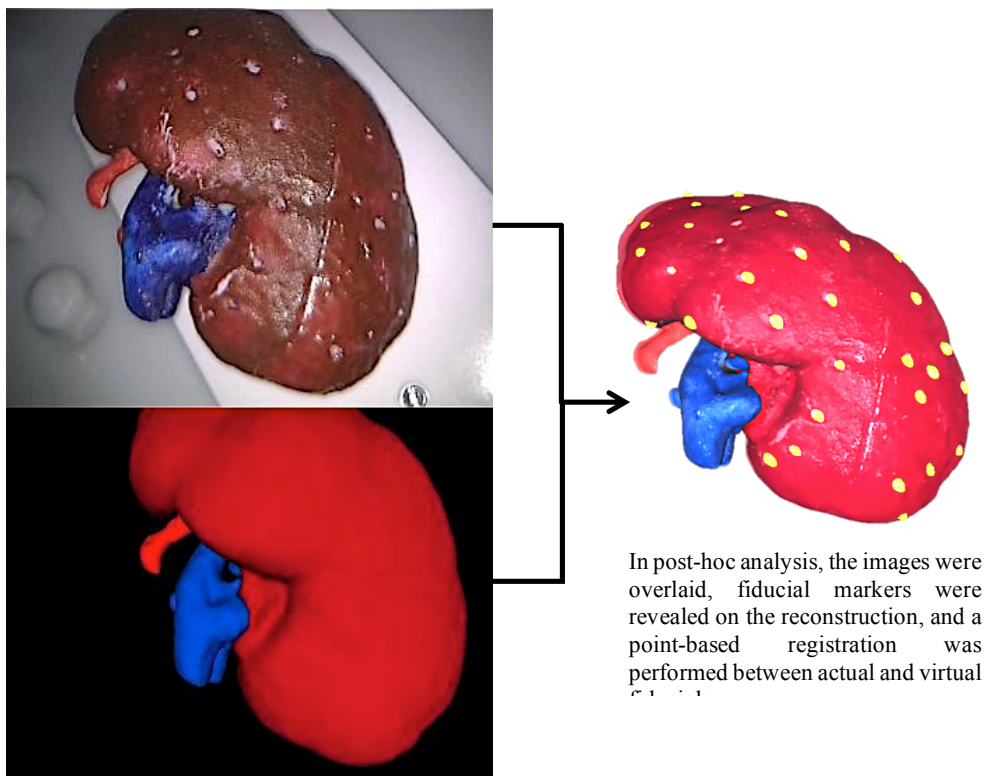


Figure 7.2.1 – Experimental setup and endoscopic image orientations



In post-hoc analysis, the images were overlaid, fiducial markers were revealed on the reconstruction, and a point-based registration was performed between actual and virtual

Image visible from the console. In this view, the subject has completed the alignment task. Note that fiducials are not visible in the reconstruction and therefore cannot be used to aid alignment.

Figure 7.2.2 – Console view and registration process

Fourteen surgical trainees were recruited as participants. Subjects were first given a tutorial in the use of the iPad and 3D mouse interfaces and were subsequently allowed five minutes to familiarise themselves with respective interfaces. In an attempt to replicate the combination of temporal and accuracy-related pressures in theatre, participants were informed that they were being timed, but that accuracy of alignment should be their primary concern. Each subject was asked to perform six alignment tasks - three with each navigation interface (the interface used first was randomised). The tasks consisted of matching the position and orientation of the segmented kidney image with the pre-recorded organ phantom orientation (Figure 7.2.2). The same three endoscopic views were used for all participants and for both the 3D mouse and iPad™ (Figure 7.2.2). The subject ‘stopped the clock’ when they felt they had performed the best possible alignment.

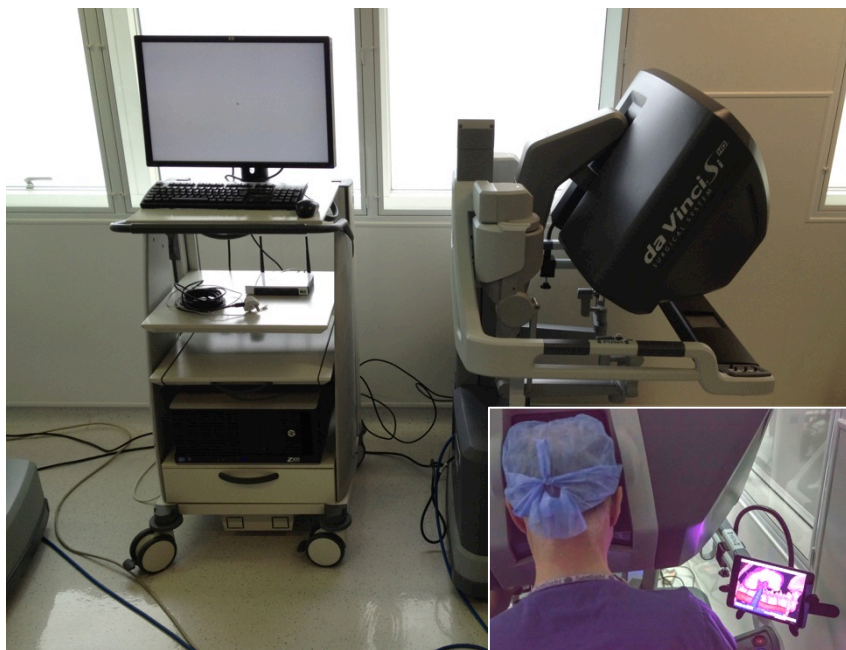


Figure 7.2.3 – System set up; the trolley behind the console houses a HP Z820 server that is connected to the TilePro™ inputs of the console. The iPad™ was mounted on the console as shown

### 7.2.1.3 Outcomes

In order to establish prior familiarity with the respective interfaces subjects were asked whether they had ever used a 3D mouse or iPad™ before. The cognitive load induced by the respective systems was assessed using the NASA-Task Load Index (NASA-TLX) questionnaire <sup>119</sup>. In addition, participants were asked whether they had a preference for a particular interface, and if so which one.

Comparing a participant's alignment to a fiducial-based gold standard, using a closed-form point-based registration,<sup>166</sup> allowed an assessment of the accuracy of alignment (registration can be defined as the transformation from one coordinate system to another such that corresponding objects are optimally aligned). Five separate outcomes were generated: total fiducial registration error, the error in each individual translational axis (x,y and z axes) and rotational error.<sup>167</sup> Rotational inaccuracy was represented as a Frobenius norm. This single number represents the magnitude of the incremental rotation required to translate the 3D reconstruction to the orientation of the renal phantom in all rotational axes. Maximal rotational error is represented by a Frobenius norm of 2 while perfect alignment corresponds to a value of zero.<sup>167</sup>

### **7.2.2 Clinical platform design**

The clinical platform design was based on the results of the initial randomised crossover study. A tablet based system was chosen as it both demonstrated superior subjective and objective performance in this chapter and caused a minimum of cognitive load on the surgeon, an important factor in reducing inattention blindness, as outlined in Chapter 4. The hardware setup of the platform is detailed in Figure 7.2.3 and Figure 7.2.4. The images were available for display to the surgeon as either segmented (segmentation was performed by experts to maximise the accuracy of the reconstructions<sup>29</sup>, Figure 7.2.6) using ITK-SNAP<sup>168</sup>, or volume-rendered reconstructions (Figure 7.2.6, HDVR®, Fovia Inc., Palo Alto, USA), in addition to being available for display as conventional axial, coronal and sagittal slices. The display interface can be seen in Figure 7.2.5. As well as having the reconstructions available, the surgeon also had access to intraoperative ultrasound and Firefly™ fluorescence. The system was designed to be operated without expert engineering input and subsequent to the uploading of patient specific datasets, no input was required.

The clinical platform allows the surgeon to manipulate the position and orientation of the images, adjust the centre of rotation, alter the transfer function of the volumetric rendering (this altering of transfer functions is akin to modifying the window level on a normal 2D grayscale CT), adjust the clipping planes and save application states (including all of the above parameters) for subsequent recall.

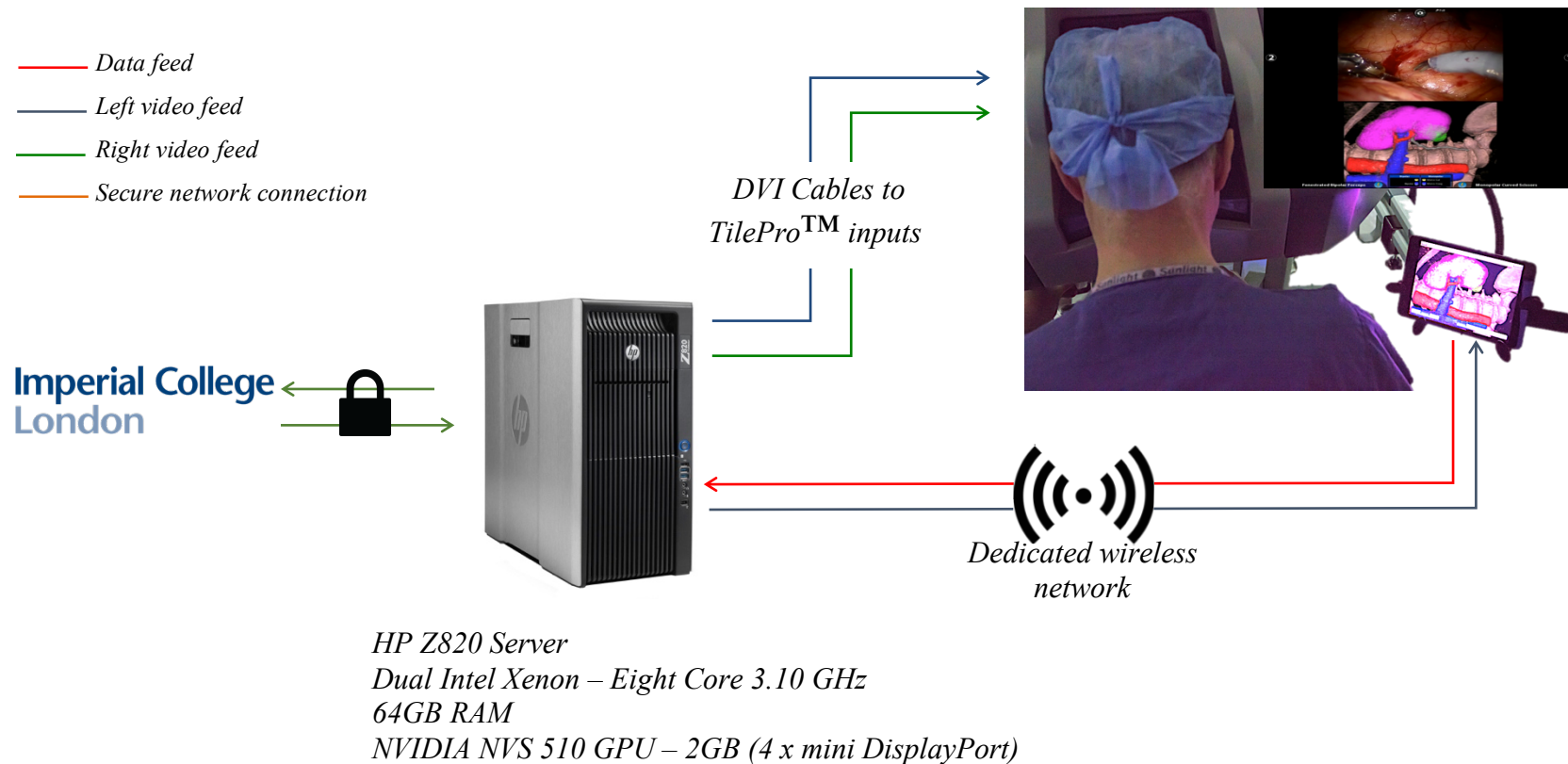


Figure 7.2.4 – System schematic: The host institution inserts a CD containing preoperative imaging into a HP Z820 server, the data was then retrieved via a secure network connection by the research team at Imperial College London. Subsequent to this the images were processed and the guidance server updated remotely. On the day of the case, the workstation is connected via 2 DVI cables to the da Vinci console stereo TilePro™ inputs (one for each eye feed). The system utilises a wireless iPad™ interface (the iPad™ is mounted onto the side of the console), with the image visible in the console also visible on the iPad™ screen (left eye console feed). The surgeon is able to manipulate images on the iPad™ with the reconstructions also visible in stereo in the TilePro™ function of the console (image viewing is also possible on the iPad). All image rendering is undertaken on the workstation.



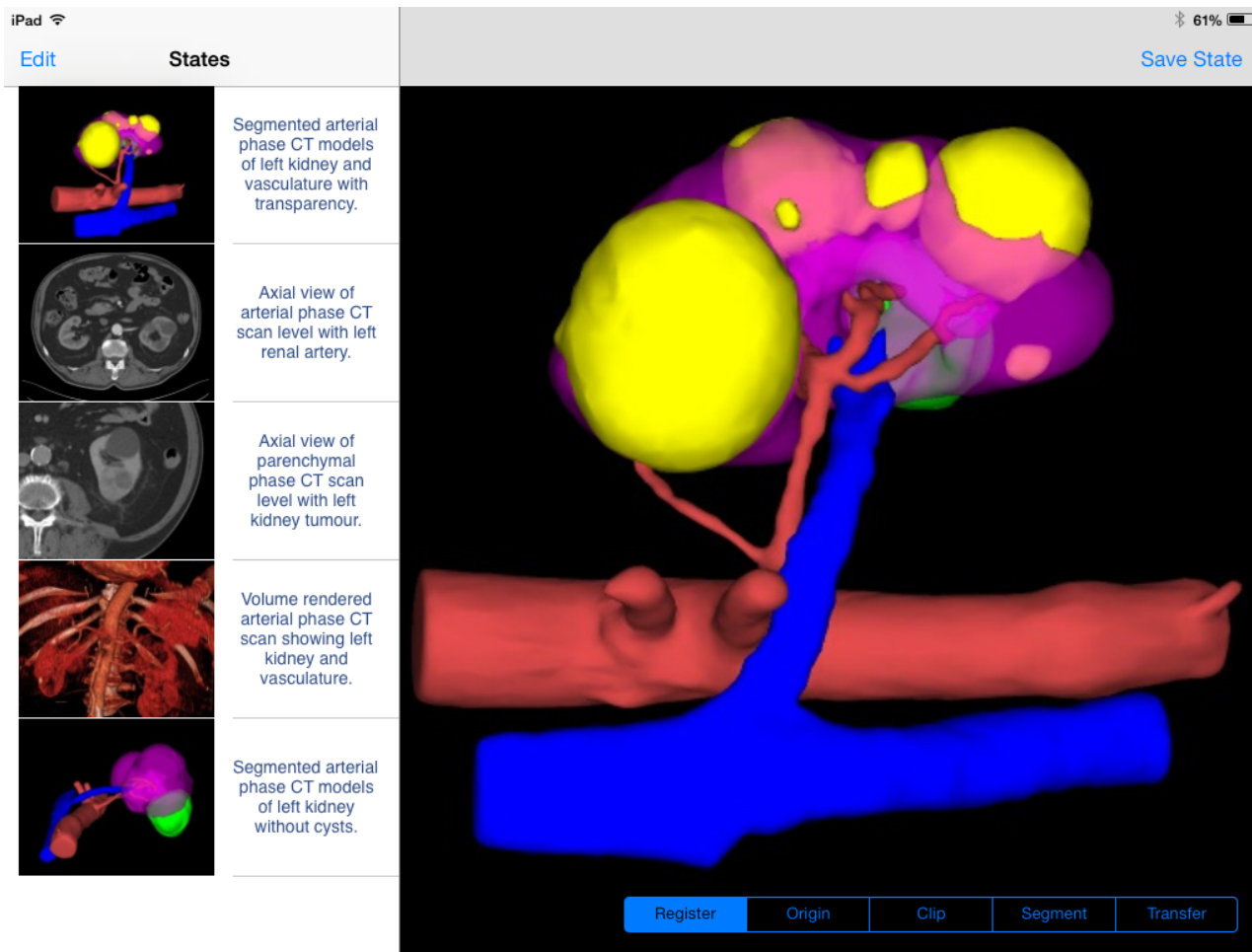


Figure 7.2.5 – iPad™ display interface. The toolbar on the left can be used to select the imaging state required and then minimised. The surgeon is then able to manipulate the image on the iPad™ screen. Intraoperatively, the main image is also visible in the TilePro™ view on the console. In the image above blue represents venous anatomy, red arterial anatomy, yellow renal cyst and green target tumour.

### 7.2.3 Case-control series

Patients undergoing RAPN at a single European institution with access to the system were eligible for inclusion in the study. Ethics approval was sought from the appropriate ethics committee, and granted at both in the UK (REC reference 07/Q0703/24) and at the Belgian site (OLV clinic, Aalst). During these partial nephrectomies, a trifecta of image guidance was employed: the outlined tablet based platform was utilised for the assessment of hilar vascular anatomy and for locating the tumour; Firefly for the assessment of the renal perfusion; and finally intraoperative ultrasound (Analogic, BK ProART ultrasound, Massachusetts, USA) was used to determine the tumour-to-normal parenchyma relationship. There were no specific exclusion criteria.

The planning and image guidance procedure can be divided into the following steps: preoperative planning, anatomical localisation and tumour resection planning. These steps were defined in Chapters 3 and 6. During the *preoperative planning* step the surgeon was able to view the reconstructed images on their iPad™ allowing them to perform mental pre-procedural rehearsal. The surgeon was also able to save application states to which they could return during the procedure.

During the *anatomical localisation* and *tumour resection planning* steps, the reconstruction was viewable in 3D within the TilePro™ function of the console with a copy of the left da Vinci feed viewable on the iPad™ (Figure 7.2.7). Manipulation of the image on the iPad™ was replicated within the console view. The surgeon was able to return to pre-saved application states saved during the preoperative planning step. The system was not utilised for live guidance of tissue dissection.

An anonymised prospective database was kept on a secure server to which the clinical and research teams had access. The data collected was divided into four separate categories: *demographics and operative approach*, *image preparation*, *system efficacy* and *clinical outcomes*.

#### 7.2.3.1 Demographics and operative approach

With regards to demographics a number of data points were collected, namely: age, sex, laterality and, PADUA score<sup>169</sup>. In addition to demographic data, information on

operative approach was also collected including whether or not selective vessel clamping was used (with or without an early unclamping <sup>42</sup>), and whether a trans or retroperitoneal approach to the kidney was employed.

#### **7.2.3.2 *Image Preparation***

The data collected on image preparation was both subjective and objective. Subjectively the researcher preparing the imaging was asked to rate out of 10 their confidence in the reconstructed hilar and tumour anatomy. Where confidence was low they were asked to articulate why this was the case.

Objective data regarding the number of renal arterial branches, the Hounsfield units at the origin of the renal artery (for CT data) and slice thickness were also collected. Hounsfield units and slice thickness were utilised as a surrogate measure of scan quality. These metrics were selected as CT scans with better contrast enhancement allow a greater degree of automation to be used in the segmentation, reducing the potential for rater bias. A standardised CT protocol was not used as much of the imaging was from referring institutions, each with their own imaging protocol.

#### **7.2.3.3 *System efficacy***

Immediately after the procedure, the operating surgeon was asked: How difficult was the case overall on a scale of 1-10 and what was the greatest contributor to case difficulty? Subsequently they were asked a number of questions related to the perceived efficacy of the platform: With regards to the efficacy of the reconstructions the surgeon was asked to rate out of 10 how useful the platform was felt to be: overall, for hilar definition, identification of segmental braches, identification of tumour location and finally the definition of the tumour-to-normal parenchyma interface. Finally, the surgeon was asked whether the reconstructions represented the anatomy seen during the case.

#### **7.2.3.4 *Clinical Outcomes***

Finally, clinical outcomes were assessed. Within this group, a number of different parameters were collected, namely: console time, warm ischaemic time, complications (Clavien-Dindo classification <sup>170</sup>), margin status and histology.

Cases from the study period were matched according to tumour size and PADUA score, with cases from a prospectively collected database of RAPN, and operative and pathological outcomes were compared.

#### **7.2.4 Statistical analysis**

##### **7.2.4.1 *Ex-vivo randomised control study***

Statistical analysis was performed in GraphPad Prism (GraphPad Software, La Jolla, CA, USA). Medians and interquartile ranges were calculated for all values (data were not normally distributed) and the Mann-Whitney *U* test of statistical significance applied. A p-value <0.05 was considered statistically significant.

##### **7.2.4.2 *Case-control series***

To gain an understanding of the impact of the image guidance system on peri and immediate postoperative outcomes, cases were matched using propensity score matching. Patients were matched 1:1 for both PADUA score and clinical size. Matching was undertaken using R.<sup>171</sup> Medians and interquartile ranges were then calculated for all values. When comparing groups, the Mann-Whitney *U* test for statistical significance was used (except for age where means were calculated and an unpaired t-test was used). Where correlation coefficients were computed, Spearman's Rank coefficient of correlation was calculated ( $r_s$ ). Correlation strengths were described using standards previously set in the literature.<sup>172</sup> When assessing efficacy, only cases in which reconstructions represented intraoperative anatomy were analysed.

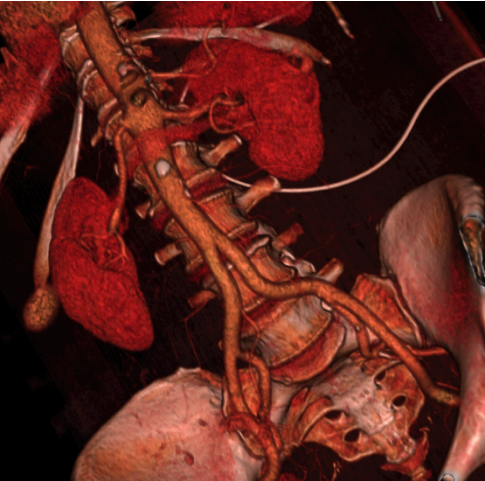
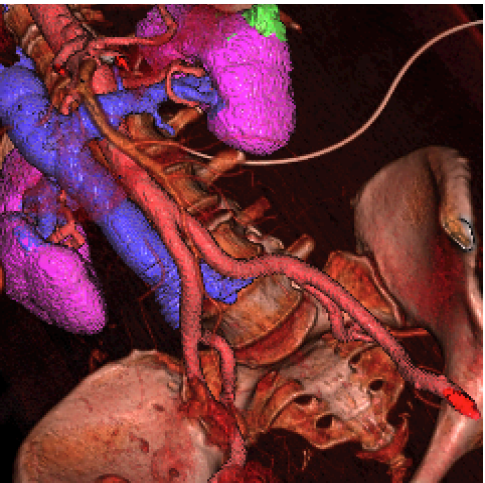

<p style="text-align: center;"><b>Volume Rendered</b></p> <ul style="list-style-type: none"> <li>• No pre-processing required</li> <li>• High level of anatomical detail</li> <li>• Difficult to view subsurface solid organ anatomy</li> <li>• Unable to view only surgically relevant anatomy</li> </ul>	
<p><b>Volume Rendered + Overlaid Segmentation</b></p> <ul style="list-style-type: none"> <li>• Approximately 15 minutes of pre-processing time</li> <li>• Ability to make surfaces transparent allowing the internal anatomy of solid organs to be viewed</li> <li>• Ability to define and view surgically relevant anatomy in addition to landmarks generated by volume rendering</li> <li>• Low image quality of surgeon defined anatomy</li> </ul>	
<p><b>Segmentation displayed as a polygon mesh</b></p> <ul style="list-style-type: none"> <li>• Approximately 30 minutes of pre-processing</li> <li>• Ability to make surfaces transparent allowing the internal anatomy of solid organs to be viewed</li> <li>• Ability to define, and exclusively view, surgically relevant anatomy</li> <li>• High image quality</li> </ul>	

Figure 7.2.6 – Different viewing options available to the surgeon and their respective benefits and shortcomings.

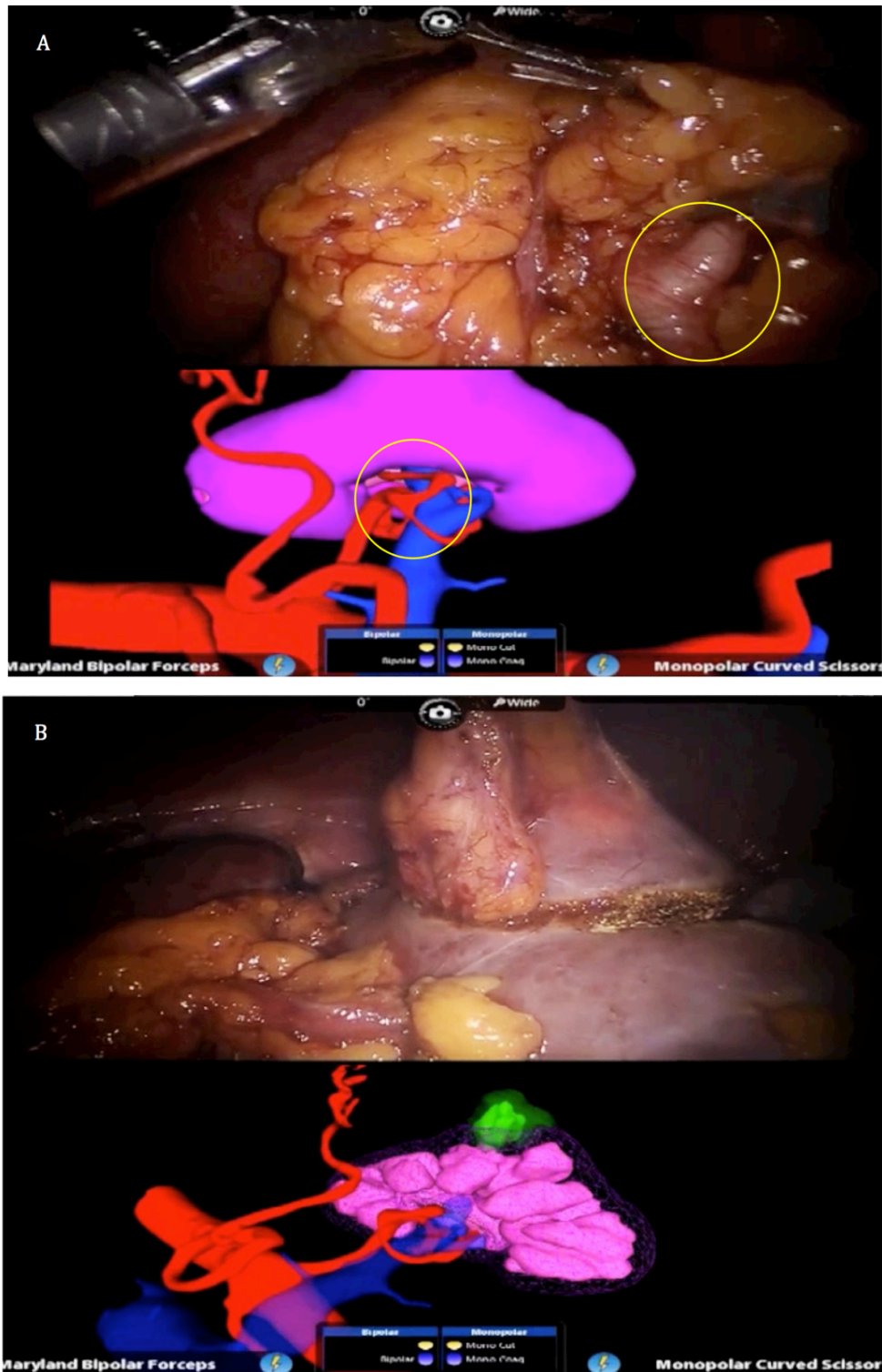


Figure 7.2.7 – The console view with TilePro™ enabled. A) The complex hilar vascular anatomy is seen within the image allowing the surgeon to better appreciate the anatomy seen in the operative view. B) The surgeon is able to plan tumour resection by making the surface of the kidney a wireframe mesh while keeping the tumour solid.

## 7.3 Results

### 7.3.1 Randomised crossover study

In all, 13 out of 14 participants owned an iPad™ and none had previously used a 3D mouse. When comparing the time to task completion (Figure 7.3.1) and NASA-TLX scores (Figure 7.3.2). for the iPad™ and 3D mouse interfaces, the iPad™ was found to have significantly shorter alignment times and a lower cognitive load ( $p < 0.01$  and  $p < 0.01$  respectively, see Table 7.3.1). In total, 79% (n=13) of participants preferred the iPad™, 12% (n=2) the 3D mouse and 6% (n=1) expressed no preference.

When assessing the accuracy of the two systems, no significant difference was seen in the total registration error achieved by the two proposed interfaces ( $p = 0.94$ , Table 7.3.1). For the iPad™-based platform, chosen for use in the clinical system, the greatest error was seen in the z-axis (14.13mm) with lesser errors of 4.31mm and 9.97mm in the x and y-axes respectively. The median rotational error was represented by a Frobenius norm of 0.29.

	<b>3D Mouse (IQR)</b>	<b>iPad™ (IQR)</b>	<b>p-value</b>
<b>x-axis error (mm)</b>	4.98 (4.16)	4.31 (5.26)	0.37
<b>y-axis error (mm)</b>	8.04 (4.82)	9.97 (6.84)	0.05
<b>z-axis error (mm)</b>	15.74 (13.83)	14.13 (12.04)	0.81
<b>Total error (mm)</b>	20.88 (13.30-26.25)	19.66 (11.19)	0.94
<b>Frobenius norm*</b>	0.25 (12.95)	0.29 (0.15)	0.67
<b>NASA- TLX score</b>	56 (15.1)	43.7 (14.8)	<0.01
<b>Time to completion (secs)</b>	67.5 (52.6)	40 (33.3)	<0.01

Table 7.3.1 – Comparison of iPad and 3D mouse interfaces, values shown are medians. 3D = three dimensional IQR = Interquartile range \*Measure of rotational accuracy in all three axes, a value of 2 represents the maximum error possible and 0 would represent a perfect alignment.

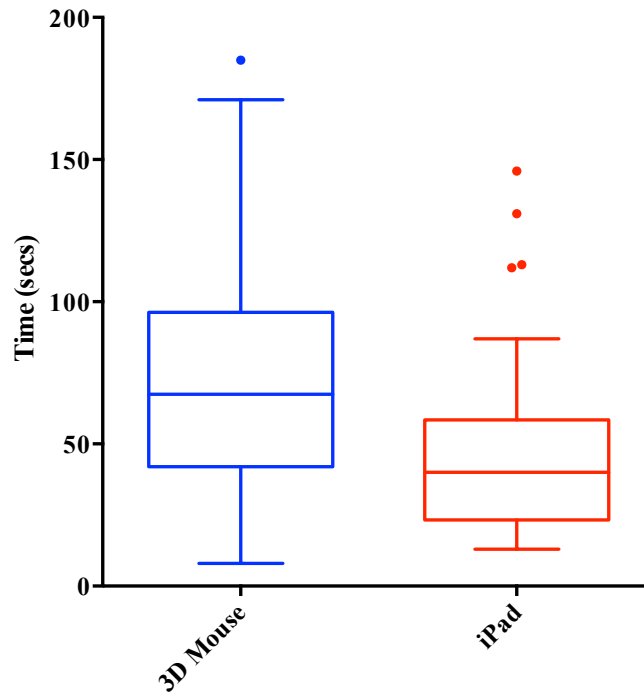


Figure 7.3.1 – Box-Whisker plot illustrating time to task completion. Whiskers were calculated as the 75<sup>th</sup> percentile plus 1.5 x IQR and 25<sup>th</sup> percentile minus 1.5 x IQR. Outliers were defined as values falling outside this range.

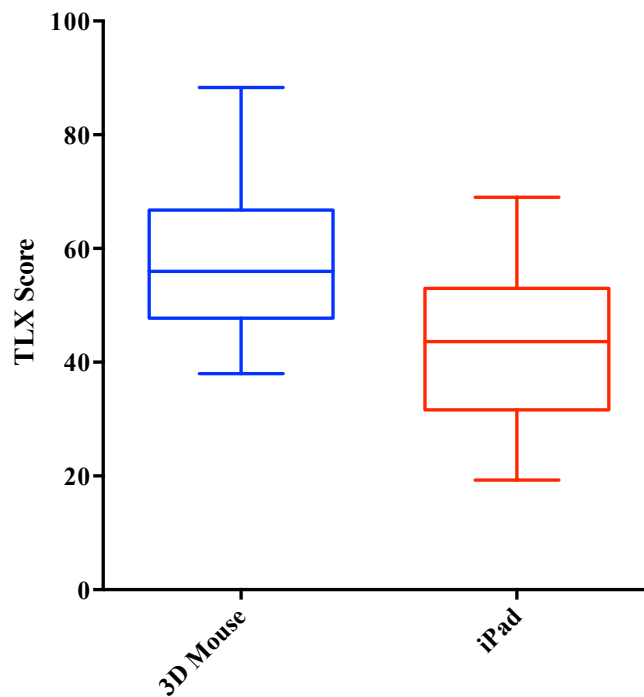


Figure 7.3.2 – Box-Whisker plot illustrating NASA-TLX score. Whiskers were calculated as the 75<sup>th</sup> percentile plus 1.5 x IQR and 25<sup>th</sup> percentile minus 1.5 x IQR. Outliers were defined as values falling outside this range.



## 7.3.2 Case series

### 7.3.2.1 *Demographics and operative approach*

Table 7.3.2 summarises the clinical characteristics, perceived efficacy and the greatest contributor to individual case difficulty within the cohort.

Over a 13-month period 43 robot assisted partial nephrectomies were performed utilising the outlined system, firefly and intraoperative ultrasound was utilised in all of these cases. Median age was 67 years, with the majority of patients being male ( $n = 24$  (55.8%). The majority of tumours ( $n = 25$ , 58.1%) were left sided.

In five cases, a selective clamping technique was employed, in three a no clamp technique was used. In the remaining 35 cases a traditional non-selective clamping approach was taken, with an early unclamping technique employed. Only a single case was undertaken using a retroperitoneal approach.

### 7.3.2.2 *Image preparation*

Confidence in the reconstructions of hilar anatomy demonstrated a positive correlation with the Hounsfield unit value at the base of the renal artery ( $r_s = 0.60$ ,  $p < 0.01$ ), no significant correlation was seen with the confidence in tumour anatomy ( $p = 0.90$ ). Conversely, slice thickness was found to be weakly correlated with confidence in tumour anatomy reconstruction ( $r_s = 0.33$ ,  $p = 0.05$ ), while no significant correlation was seen for hilar reconstruction units ( $p = 0.18$ ).

The reconstructions displayed in the platform accurately failed to represent the intraoperative anatomy in 16.3% of the cases. Of the seven cases in which the anatomy was not felt to be representative, in four there was a failure to identify a polar artery, and in two the tumour was incorrectly segmented. In the four cases in which the hilar vascular anatomy was incorrectly identified the median confidence in the reconstructions was 6.5 compared to 8 overall ( $p = 0.009$ ), the median Hounsfield unit value at the origin of the renal artery was also significantly less than in those in which the anatomy was accurately represented (122 versus 229.5,  $p = 0.031$ ).

<b>Patient parameters and clinical outcomes</b>	
Median age (IQR)	67 (56.3 – 73))
Male (%)	24 (55.8%)
Left kidney (%)	25 (58.1%)
Console time, mins (IQR)	140 (120 – 160)
Warm ischaemic time, mins (IQR)	12.5 (10.7 – 16)
Estimated blood loss, ml (IQR)	200 (100 – 300)
PADUA score (IQR)	9 (8 – 10)
Complications	13
$\geq$ <i>Grade 3</i>	2
$\leq$ <i>Grade 2</i>	11
Positive margins	0
<b>Subjective efficacy (IQR)</b>	
Overall	7 (6.5 – 8)
Hilar definition	8 (7 – 8)
ID of segmental branches	8 (7 – 8)
ID of tumour location	7 (6 – 8)
ID of parenchyma-to-tumour interface	7 (5 - 8)
<b>Greatest contributor to difficulty (%)</b>	
Tumour location	28 (63.6)
Hilar anatomy	2 (4.5)
Tumour size	10 (22.7)
Collecting system	1 (2.3)
Other	3 (6.8)

Table 7.3.2 - Patient parameters, clinical outcomes, subjective benefit and greatest contribution to case difficulty

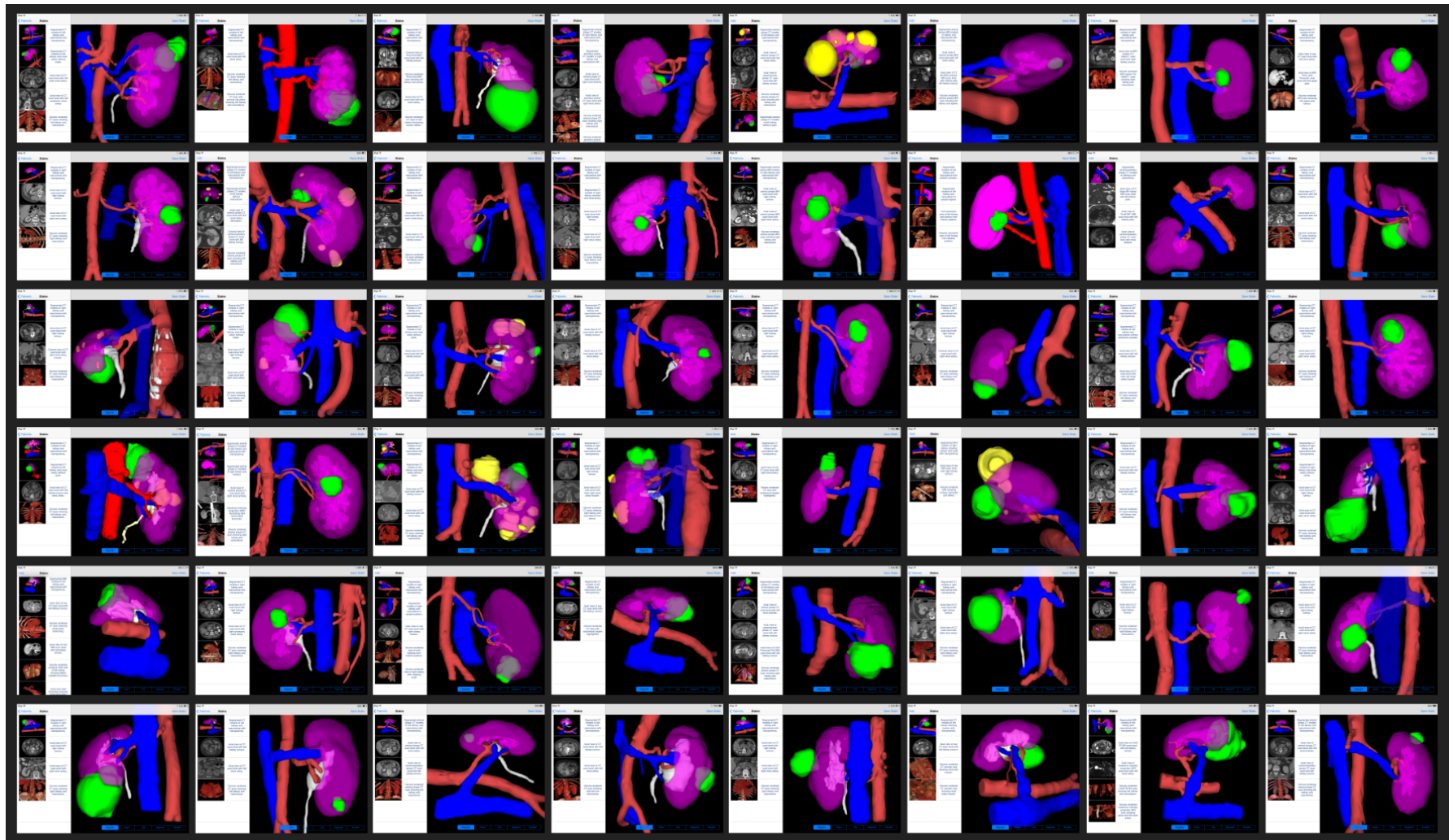


Figure 7.3.3 – Image-guided partial nephrectomies performed to date

### **7.3.2.3      *Clinical outcomes and system efficacy***

With regards complications there were seven (15.6%) grade one complications, four (8.9%) grade two, and two (4.4%) grade three (one early post operative bleed requiring reoperation and one urinoma requiring a nephrostomy). Of lesions resected there were, 32 (75.5%) renal cell carcinomas, seven (15.6%) oncocytomas, two (4.4%) angiomyolipomas, one (2.2%) benign cyst, and one (2.2%) mixed epithelial stromal tumour. No positive margins were observed.

The system was felt to have been of greatest efficacy in the definition of the renal hilum (8/10) and segmental vascular branches (8/10). The greatest contributors to case difficulty were the location and size of the renal tumour.

#### **7.3.2.3.1      *Matched cohort analysis***

The 43 patients in whom an image-guided procedure was undertaken were matched to a historic database containing the details of 129 patients undergoing partial nephrectomy between 2010 and 2012 (this time period was utilised as by this stage the operating surgeon had performed over 100 partial nephrectomies and as such was felt to have overcome his learning curve). In addition, both other imaging modalities, i.e. Firefly and intraoperative ultrasound were already in routine use during this period thereby allowing these variables to be controlled for. Propensity score matching returned a cohort of 86 patients (43 in the image guidance group and 43 in the no guidance group). The final cohort was well matched with a standard mean difference of 6.47%.

No significant differences were seen in any of the parameters measured, with the exception of patient age, which was seen to increase the after advent of image guidance (Table 7.3.3).

	No guidance (IQR)	Guidance (IQR)	p-value
Age (years)	60 (52 – 67)	67 (56.3 – 73))	0.044
Male	28 (65.1%)	24 (55.8)	0.377
Left kidney	19 (44.2%)	25 (58.1)	0.196
Console time (mins)	120 (120 – 150)	140 (120 – 160)	0.509
WIT (mins)	15.5 (12 – 18.3)	12.5 (10.7 – 16)	0.103
EBL (mls)	150 (100 – 200)	200 (100 – 300)	0.058
Complications	9	12	0.451
≥ Grade 3*	1	2	0.557
≤ Grade 2*	8	10	0.596
% Positive margins	2	0	0.152

Table 7.3.3 – Comparison of image-guided and non-image-guided procedures. Unless otherwise stated values are medians. \*Calvien-Dindo

## 7.4 Discussion

### 7.4.1 Principal findings of *ex-vivo* randomised control study

The initial *ex-vivo* study demonstrated that using the tablet interface an acceptable level of error could be achieved in a time (33 seconds) short enough to have a minimal effect on the surgical workflow, with significantly lower cognitive load. This alignment was achieved with a level of registration accuracy that is both safe and clinically useful for improving the surgeon's anatomical awareness but insufficiently accurate to provide guidance for image-guided tumour resection (a function for which the platform was not designed). When interpreting the misalignment errors, it is important to consider the effect inaccuracy in each axis will have on a surgeon's appreciation of the anatomy. Perhaps the most important element of error is rotation, as fairly small errors in rotational alignment will result in a dramatic change in appreciation of anatomical relationships. Rotational error in the alignment tasks performed using both interfaces was small with median Frobenius norms of 0.25 and 0.29 ( $p = 0.67$ ), for the iPad™ and 3D mouse, respectively. Alignment in the translational axes is less important as movement along these axes will only affect the location of the organ in the viewing window leaving the organ orientation and in turn the appreciation of anatomical relationships, unaffected.

### 7.4.2 Principal findings of *in-vivo* case-control series

This chapter has presented the largest case series to date for an image-guided intra-abdominal procedure, demonstrating subjective efficacy and safety. In addition, an objective assessment of an intra-abdominal image guidance platform was carried out for the first time, with non-inferiority seen when compared to a historical control. Subjective efficacy was found to be greatest in the most difficult cases.

A further important finding related to the quality of the source images. In 17.9% of cases the preprocedural, imaging-derived segmentation was not felt to be an accurate representation of the patient. The procedures in which the anatomy was inaccurate were predictable, with those individuals performing the segmentation expressing a relatively low level of confidence in their reconstructions. In addition, the reconstructions in

question also tended to be of a lower spatial resolution with suboptimal contrast enhancement of the renal vasculature (observed as a significantly lower HU value at the origin of the renal artery). This demonstrates that the quality of the source imaging is paramount and in the absence of good quality source imaging (high axial resolution with an arterial phase) the use of image guidance based on preoperative imaging should be abandoned.

### 7.4.3 Comparison to other studies

A system using the TilePro™ function of the da Vinci console has been previously described both for general surgical procedures,<sup>141,173</sup> and for partial nephrectomy specifically.<sup>174</sup> In the image guidance system proposed for partial nephrectomy by Lasser *et al.* pre-operative segmented reconstructions were fed into the Tilepro™ function of the console.<sup>174</sup> This platform was utilised for the specific purpose of tumour resection planning with a preoperative virtual resection undertaken to assist in intraoperative planning. The use of preoperative data to actively guide resection is contentious both due to the inability to account for intraoperative tissue deformation<sup>7</sup> and the relatively poor inter-rater reliability of image segmentation.<sup>36</sup> However, the utilisation of preoperative imaging to assist in the appreciation of anatomical relationships, as has been presented here, has the potential to improve surgical efficiency and, in turn, patient safety.

Volonté *et al.* utilised an OsiriX<sup>168</sup> plug-in that allowed the display of volume rendered images within the console. The translation and rotation of these images could then be altered using the same 3D mouse that was trialled in the *ex-vivo* study of the interface. Although potentially useful, the system has significant limitations. Firstly, as was demonstrated in the feasibility study, the 3D mouse is associated with a relatively high cognitive load and required a median of 55 seconds to achieve alignment. These factors make a 3D mouse interface unattractive for clinical use, particularly bearing in mind the increased inattention blindness demonstrated with increasing cognitive load in Chapter 4.

A further limitation of the previously proposed Osirix based system<sup>141,173</sup> is the reliance on volume rendered images alone. Although volume rendering provides visually attractive reconstructions, it struggles to represent internal solid organ and non-contrast

enhanced anatomy well, and is unable to distinguish between surgically relevant and irrelevant anatomy. In RAPN, an example of this shortcoming is volume rendering's inability to represent graphically the normal parenchyma to tumour interface, potentially limiting its efficacy in tumour resection planning. These factors make a platform based on volume rendering alone an improvement over the status quo, but one that lacks in the anatomical detail required. In the platform proposed, a combination of volume rendered and segmentally reconstructed images (Figure 7.2.6) has been utilised to give the surgeon the best possible appreciation of the anatomy that surrounds their view.

The use of reconstructed imaging for assisting in hilar definition has been proposed before by Ukimura *et al.* and Lasser *et al.* to facilitate renovascular-tumour definition in zero-ischaemia partial nephrectomy.<sup>99,174</sup> In Lasser *et al.*'s work, the images from a desktop computer were displayed within the TilePro function of the console but the surgeon was detached from these, being able to view but not interact with them.<sup>174</sup> This principle was further developed by Isotani *et al.* who utilised the similar reconstructed datasets to assist in preoperative and intraoperative planning, offering a better understanding of possible complications. In addition, they offered a more automated segmentation process allowing the preprocedural image preparation time to be minimised<sup>175</sup>. Although these groups proposed the efficacy of the use of reconstructions they did not offer an ergonomic and demonstrably useful way of displaying the imaging in theatre and presented only a small number of cases, limiting any conclusions to those of feasibility.

Previous surgical image guidance systems have largely focused on image overlay to provide assistance in determining anatomy.<sup>39,87,91,92,142,152,176</sup> The fact the image is being overlaid requires a high level of registration accuracy and achieving this accuracy requires expensive hardware and significant technical expertise in theatre, in addition to assuming no tissue deformation occurs. Although valid this approach provides significant barriers for most surgeons operating outside of large academic institutions. The image guidance system proposed here can be run on an off-the-shelf server and requires no technical expertise in theatre mitigating for the issues that have historically confined image guidance to research environments.



In addition to the issues of expense and expertise, concerns have been raised over the safety of image overlay.<sup>110,111,177</sup> In studies of both Marcus and Dixon *et al.*, examining the effect of image overlay on a surgeon's appreciation of the operative scene, the authors found that surgeons performing a task with overlay engaged were more likely to exhibit inattention blindness.<sup>111</sup> Along with these concerns, the use of image overlay introduces a time lag into the endoscopic video feed meaning performing tissue dissection under truly live guidance is potentially unsafe. The task of intraoperative guidance in our platform was achieved by displaying the intraoperative video feed alongside the 3D volume rendered and segmented reconstructions thereby addressing both of these issues.

#### **7.4.4 *Ex-vivo* randomised crossover study limitations**

The *ex-vivo* randomised crossover study had a number of limitations. The first of these relates to the simplicity of the alignment task; although representative of the alignment that a surgeon performs intraoperatively, the task was idealised with no perinephric fat or surrounding anatomical structures to confuse the alignment. This may have led to improved accuracy. The second criticism pertains to the respective learning curves for each interface. With only five minutes of familiarisation and three alignment tasks for each orientation, it is likely that the plateau phases of the respective learning curves were not reached. This is particularly true for the 3D mouse interface as the majority (13 of 14) of participants owned an iPad™ and were therefore familiar with its use. Although this could be viewed as a limitation, for an image guidance interface to be accepted by surgeons and adopted into routine clinical practice, it needs to be intuitive enough to be learnt in a short amount of time, and as such this criticism becomes less relevant.

#### **7.4.5 Case series limitations**

Although this study goes further in assessing an intra-abdominal platform than those that predated it, it is not without limitations. The largest of these relates to the subjective nature of the outcomes assessed. In addition, the generalisability of our results might be limited by the inclusion of patients treated by a high-volume surgeon with extended experience in the setting of robot-assisted surgery; a less experienced surgeon may well have been able to derive more benefit from the guidance offered by the system.

Although the study design represented a noteworthy limitation, the platform exists within the exploration phase (IIa) as defined by the IDEAL collaboration, and as such a randomised control study would have been premature with this stage of development better suited to uncontrolled studies <sup>11</sup>.

An additional limitation relates to the other forms of image guidance being used by the operating surgeon, namely firefly and intra-operative ultrasound. These imaging adjuncts may have somewhat diminished the overall efficacy of the proposed system. This approach was taken as the consensus view of urologists performing this procedure is that ultrasound, and to a lesser extent firefly, is an integral part operation and as such could not be eliminated from the operative work flow <sup>178</sup>. A pragmatic approach was therefore taken, allowing the surgeon to use the platform as an adjunct to his normal working practice. It is also worth drawing attention to the fact that the vast majority of cases were transperitoneal and as such the efficacy in the retroperitoneal approach to RAPN cannot be commented on.

#### **7.4.6 Future work**

The clinical system itself is not without limitations. Perhaps the most obvious of these is that the surgeon is forced to move their gaze between the TilePro™ and endoscopic views. This introduces the potential for alignment inaccuracies and increased cognitive strain, introducing the possibility of increased IB, as discussed in Chapter 4. TilePro™ also reduces the size of the live operative view, potentially reducing the quality of the surgeon's visual cues; although this was not reported during the clinical experience reported herein.

In addition to the limitations imposed by the system, a further barrier to widespread adoption lies in the preparation of the raw DICOM images, which is both time-consuming and requires a number of labour intensive steps (segmentation, and mesh generation and preparation) to complete. In future iterations of the platform, efforts will be made to simplify and streamline this process making it less time consuming and easier.

## 7.5 Conclusion

With the loss of haptic feedback in robotic surgery, the operating surgeon has come to rely on visual cues in order to appreciate subsurface anatomy. Although the improved visualisation in the da Vinci robotic console mitigates, in part, for this loss of haptics, it is unable to replace it. The search for a solution to the loss of haptic feedback has given rise to increasing research efforts in the field of intraoperative image guidance. The systems proposed to date have required access to technical expertise in theatre and expensive video capture hardware.

This chapter has outlined and demonstrated the efficacy of a platform that capitalises on the TilePro™ function of the robotic console to provide a low cost image guidance solution for the *planning* phase of robot-assisted partial nephrectomy. Now that subjective efficacy and safety have been demonstrated, larger randomised control studies are needed to prospectively establish the impact of image guidance solutions such as this on clinical outcomes and case selection.

## CHAPTER 8:   ULTRASOUND-GUIDED TUMOUR RESECTION†

---

† Content from this chapter was published as:

**Hughes-Hallett, A.**, Pratt, P., Mayer, E., Di Marco, A., Yang, G. -Z., Vale, J., Darzi, A. (2014). Intraoperative ultrasound overlay in robot-assisted partial nephrectomy: First clinical experience. *European Urology*, 65(3), 671-672.

Pratt, P., Jaeger, A., **Hughes-Hallett, A.**, Mayer, E., Vale, J., Darzi, A., ... & Yang, G. Z. (2015). Robust ultrasound probe tracking: initial clinical experiences during robot-assisted partial nephrectomy. *International journal of computer assisted radiology and surgery*, 10(12), 1905-1913.

Content from this chapter was presented as:

**Hughes-Hallett, A.**, Pratt, P., Mayer, E., Vale, J., Darzi, D., Augmented reality in robotic partial nephrectomy utilizing intraoperative ultrasound. European Robotic Urology Congress (European Congress of Robotic Urological Surgeons) 2014

Pratt, P., **Hughes-Hallett, A.**, Di Marco, A., Cundy, T., Mayer, E., Vale, J., Darzi, A., Yang, GZ. Multimodal Reconstruction for Image-Guided Interventions. Hamlyn Symposium on Medical Robotics 2013

Pratt, P., Jaeger, A., **Hughes-Hallett, A.**, Mayer, E., Vale, J., Darzi, A., Peters, T., Yang, G-Z., Robust Ultrasound Probe Tracking: Initial Clinical Experiences During Robot-Assisted Partial Nephrectomy. 6th International Conference on Information Processing in Computer-Assisted Interventions. 2015

## **8.1 Intraoperative ultrasound overlay in robot assisted partial nephrectomy: System outline and first clinical experience**

### **8.1.1 Introduction**

Image-guided surgery is an area of both clinical and research interest<sup>118,179</sup> with the potential to improve operative safety and reduce positive surgical margin rates.<sup>7</sup> To date the majority of image guidance platforms proposed, and in clinical use, utilise preoperative imaging overlaid onto the operative view.<sup>9</sup> Although this approach has potential benefits as a surgical roadmap, as has been highlighted in previous chapters, it falls short of being able to offer truly accurate representations of intraoperative anatomy.<sup>7,87</sup>

This failure is due to two issues: Firstly, imaging is gathered preoperatively and, as such, any change in the anatomy introduces inaccuracy into the guidance.<sup>28</sup> These deviances from preoperative imaging occur for a plethora of reasons including (but not limited to) patient position, respiration, heart beat, arterial/venous clamping and tool tissue interaction; as yet no group has managed to successfully model for these deforming forces in soft tissue surgery.<sup>7</sup> Secondly, the images must be registered to the operative scene, which, again, is a process that is hard to achieve with the speed and accuracy required for clinical use.

In this chapter a potential solution to these problems is proposed, building further on the two-phase (*planning* and *execution*) image guidance solution, with the second phase of *execution* addressed. Utilising a novel approach to optical tracking of an ultrasound probe, the accuracy of registration and the speed of overlay required for intraoperative use can be achieved.<sup>94</sup> The use of intraoperative imaging also renders the problems associated with tissue deformation modelling obsolete as the imaging is contemporaneous and, as such, does not need to be deformed.

Partial nephrectomy represents the ideal index procedure around which to develop an ultrasound based image guidance platform for a number of reasons. Firstly, as highlighted in Chapter four, urologists are already comfortable with intraoperative

ultrasound, with the majority already using it routinely during partial nephrectomy.<sup>178</sup> In addition to this familiarity, partial nephrectomy involves the resection of a tumour from a solid organ in a time critical situation maximising the potential benefits of an image guidance system.

This first study of the chapter presents the use of augmented reality ultrasound overlay in robot-assisted laparoscopic partial nephrectomy, outlining the registration process and system specific details<sup>180</sup> and, subsequently, the first *in-vivo* case of augmented reality ultrasound overlay.

### **8.1.2 Methods**

Registered ultrasound overlay was achieved using a previously described approach. In the paper of Pratt *et al* paper on the use of tracked, registered ultrasound in an *ex-vivo* model for transanal microsurgery.<sup>180</sup> This method of live image registration is best described as a two-step process of probe tracking and image overlay, and has demonstrated a registration accuracy of <0.5mm.<sup>180</sup>

In order to allow the ultrasound probe to be gripped and manipulated with robotic cadere forceps (Intuitive Surgical, Sunnyvale, CA) a custom made ultrasound clip was fabricated. This allowed the probe and clip to fit down a 12mm laparoscopic port. CAD drawings and photographs of the clip, probe and commercially available alternatives can be seen Figure 8.1.1 and Figure 8.1.2.



Figure 8.1.1 – Commercially available robotic ‘drop-in’ ultrasound probes (left to right: BK medical ProART™ and Hitachi Aloka UST-5550-R) alongside the research platform setup of a Aloka Hitachi Aloka UST-533 probe with imperial designed ultrasound clip.



Figure 8.1.2 – From top, left to right: CAD illustration of ultrasound probe and clip passing through 12mm port. Ultrasound probe design and manufactured probe clip with scale.



### **8.1.2.1**      *Ultrasound probe tracking*

For the process of ultrasound probe tracking either a chessboard or, in later iterations of the platform, an asymmetrical dot pattern Keydot® surgical marker (Key Surgical Inc., Eden Prairie, MN, USA) was utilised (Figure 8.1.3). The later iterations of the platform used circular dots rather than the chessboard pattern as they improve probe tracking performance at higher light levels and suboptimal focal distances due to decreased light blooming and smudging, examples of which can be seen in Figure 8.1.3.<sup>181</sup>

#### *8.1.2.1.1*      *Chessboard tracking*

First, the endoscopic image was converted to grayscale. Following this, prominent features were identified in the image. These were characterised by large local variations in pixel intensities. A subsequent Delauney triangulation of these points (seen as red in Figure 8.1.4) reveals geometric structures present in the image, on the assumption that the operative scene will contain few, if any, such structures. As such, the majority will be contained within the image region containing the ultrasound probe and calibration pattern. In the second step of the process, irregular and out-sized triangles were discarded. Triangles satisfying certain neighboring criteria were joined to form quadrilaterals (seen as green in Figure 8.1.4). Sufficiently large groups of quadrilaterals were used to define the location of the chessboard pattern and small groups were discarded.

#### *8.1.2.1.2*      *Circular dot tracking*

In order to achieve circular dot tracking an OpenCV implementation of the simple blob detector was employed.<sup>182</sup> A stepwise process to dot tracking was taken. Initially, the source colour image was converted to greyscale. Subsequent to this connected components were extracted using a contour extraction routine.<sup>183</sup> The blob centres were then grouped by their coordinates across a thresholded image, and then a minimum distance parameter was applied. Sufficiently large groups corresponded to positively identified blobs.

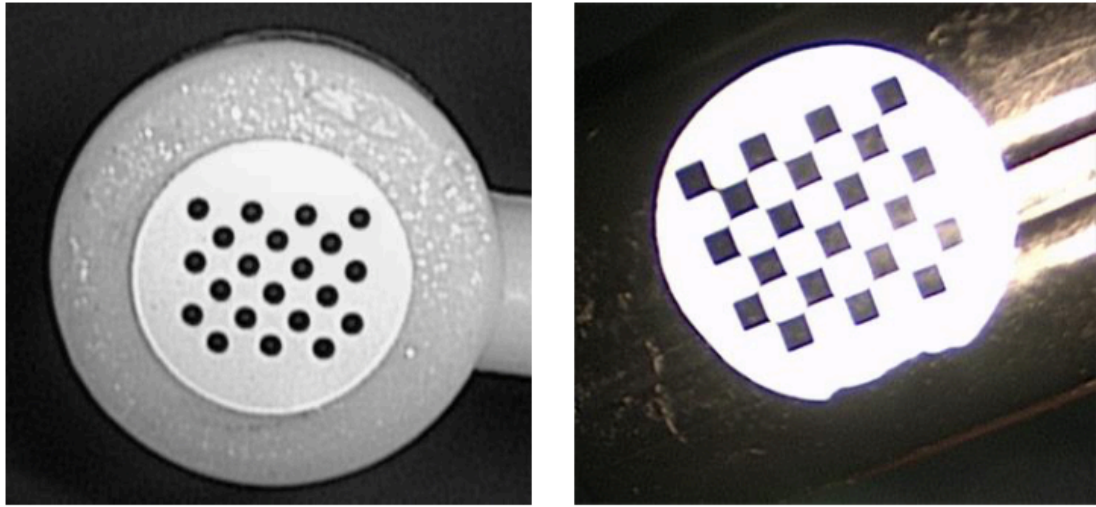


Figure 8.1.3 – Left image corresponds to asymmetrical circular dot pattern, while right is the previously utilised chessboard pattern (blooming and smudging can be seen in this image)

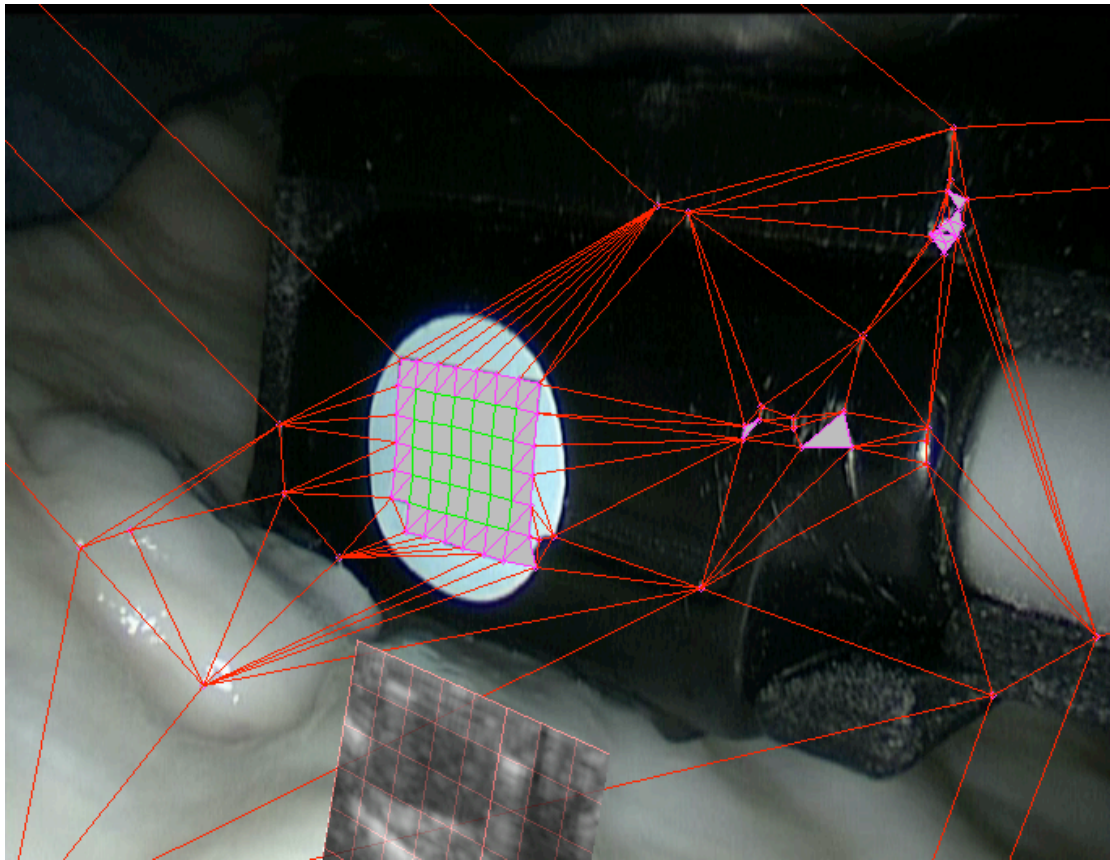


Figure 8.1.4 – Real time tracking and registration process

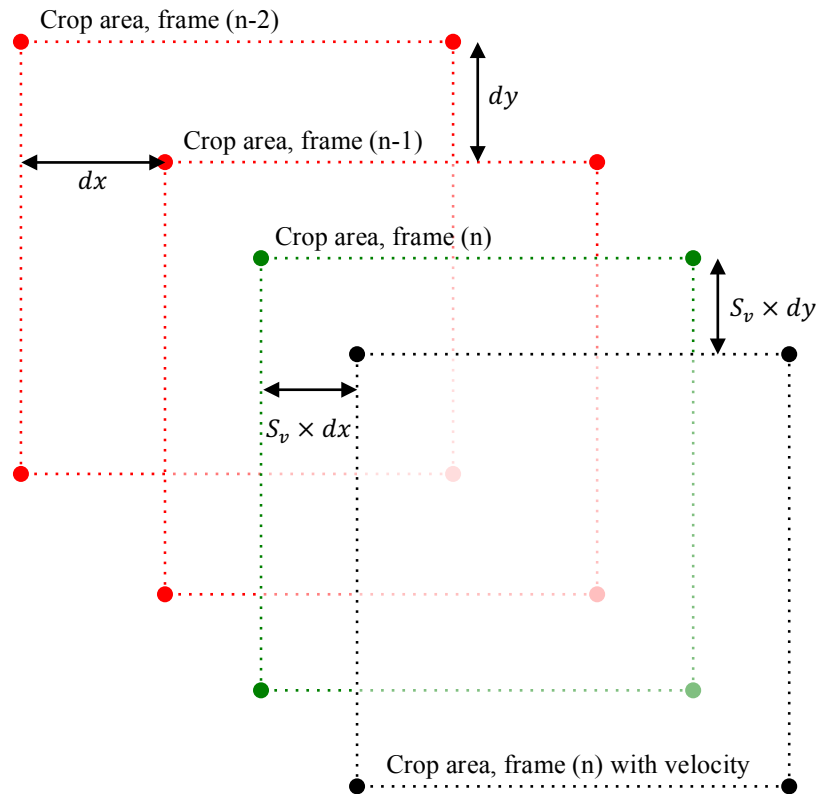


Figure 8.1.5 – Region of interest tracking.  $d$  = distance,  $S_v$  = velocity  $\times$  scaling factor.

### 8.1.2.1.3 Maximising tracking speed – only applies to dot based tracking

In order to maximise the speed of tracking, in particular in high definition environments, a continuous cropping algorithm was applied to minimise the processing time. The algorithm utilised a continuously updating cropping technique to reduce the number of pixels needing to be processed by the tracking algorithm. On detection of the pattern in the original frame, a set of coordinates corresponding to a square proportional to the size of the pattern was determined. This set of coordinates was then used to crop the following frame, thereby reducing the number of pixels needing to be processed. Although the process of cropping improves performance, it also invariably results in a failure of probe detection if the pattern moves too far. In order to improve the reliability of the algorithm a further step was taken to account for the velocity of the pattern. The velocity is estimated by calculating the vector differences between the previous two cropping rectangles. The resultant displacement vector is multiplied by a scaling factor, set empirically to 0.5, and accumulated with the following rectangle. If the tracking fails at any point, the region of interest is reset and the entire image is reprocessed. The process is summarised in Figure 8.1.5.

System Hardware
Portable workstation with NVIDIA Quadro SDI capture and output cards (NVIDIA, Santa Clara, CA, USA)
Hitachi Aloka ProSound ALPHA 10 cart (Hitachi Aloka Medical Ltd., Tokyo, Japan)
Hitachi Aloka UST-533 multifrequency linear array microsurgery probe with attached KeySurgical marker dots (KeySurgical Inc., Eden Prairie, MN, USA)
Custom probe clip 3D printed in sterilisable Cobalt-Chrome-Molybdenum alloy

Table 8.1.1 – Ultrasound system specifics

### 8.1.2.2 *Image overlay and display*

In the final step of the process, the live ultrasound image was superimposed on the stereo console display. This was achieved by estimating its pose relative to the camera coordinate position using the camera’s calibrated intrinsic properties. This transformation was then concatenated with the constant image-to-pattern relationship, allowing calculations of the position and orientation of the ultrasound slice in the operative scene.

The ultrasound image was available for display in three different viewing styles (Figure 8.1.7). The first was a simple overlay, the second an overlay with variable transparency (allowing the surgeon to see the tissue underlying the ultrasound view), while the third enabled a ‘cutaway’ feature. Within this cutaway view the image was displayed as the posterior aspect of a cuboid, allowing the surgeon to appreciate depth more easily.

### 8.1.2.3 *Report of first in-vivo trial*

A single patient with an exophytic renal tumour underwent RAPN. Ethical approval was obtained from the regional ethics committee for the *in-vivo* trial of the image guidance platform (REC reference 07/Q0703/24) and written informed consent was obtained from the patient (Appendix 2). The ultrasound probe and clip were passed through the assistant port and used in a similar fashion to that of a standard and commercially available ‘drop-in’ ultrasound probe. A 3-0 vicryl suture was attached to the probe clip to allow retrieval if it became detached from the probe. The surgeon was able to view both the standard endoscopic image and, as can be seen in Figure 8.1.6, an image including the registered ultrasound overlay in TilePro™ (Intuitive Surgical, Sunnyvale, CA).

The system was used first, to assist in defining the tumour boundary and second to help determine tumour depth. The ultrasound system was disengaged prior to vessel clamping and resection. The system was not used to guide resection as this extended beyond the ethical remit of the study, as such no objective evidence was collected. Subjectively speaking the surgeon reported an improved appreciation of the tumour relationship to the normal parenchymal anatomy when using the probe.

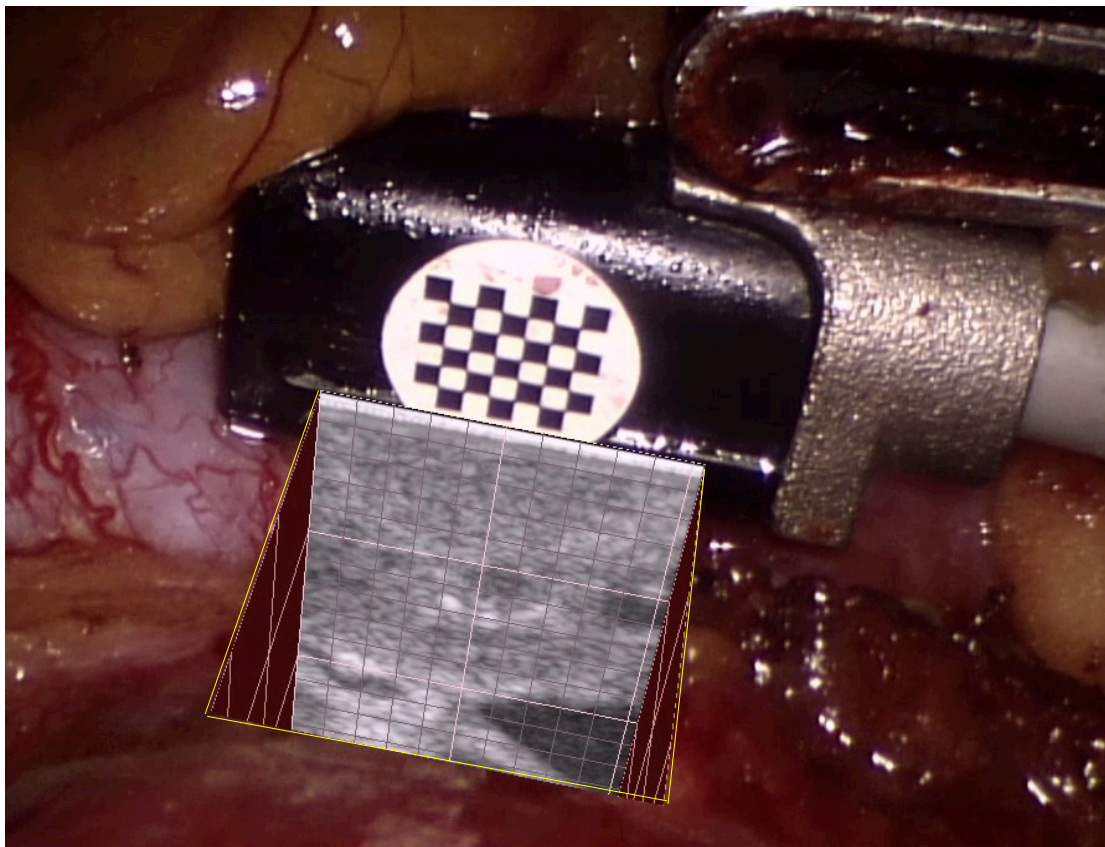


Figure 8.1.6 – First *in-vivo* use of optically tracked ultrasound overlay





Figure 8.1.7 – The different modes of image display available to the surgeon. From left to right: Solid overlay, transparent overlay and cutaway view, all displays included a 1mm ruler. The modes are demonstrated on a PVA cryogel phantom (See Appendix 4)

### 8.1.3 Discussion

#### 8.1.3.1 *Principal findings and comparison to previous studies*

In this section, a method, and the iterative process of its development, for ultrasound probe registration and overlay has been elucidated. Subsequent to this, the first use of registered intraoperative ultrasound overlay *in-vivo* has been outlined (Figure 8.1.6). The use of overlaid ultrasound intra-operatively removes the cognitive registration step that a surgeon needs to undertake during conventional intra-operative ultrasound deployment. This removal of cognitive registration has the potential to reduce the cognitive load placed on the surgeon while offering them a more accurate appreciation of the tumour to normal parenchyma boundary.

The only previous work, by Cheung *et al.*, examining the use of live registered ultrasound, demonstrated the use of an electromagnetically (EM) tracked ultrasound probe to improve resection quality in an *ex-vivo* model.<sup>93</sup> The major difference is that the platform presented here utilises video tracking to establish the probe position, thus removing the need for external optical or electromagnetic (EM) tracking equipment in theatre. It also addresses concerns raised previously over the accuracy of EM tracking due to interference from ferromagnetic objects.<sup>7</sup> The platform removes the requirement on the surgeon to undertake a cognitive registration of the ultrasound image to the real world. This may well lead to improved registration accuracy, with the potential upside of improved resection quality and a reduction in positive surgical margins.

#### 8.1.3.2 *Limitations*

Although the system offers a potential improved appreciation of tumour anatomy, there are still some limitations that needed to be addressed. The most significant is the small time delay introduced by the High Definition video processing. Although this delay has been mitigated for in part by the most recent iteration of the algorithm it still necessitates the need for two views to be displayed simultaneously. In addition, the system still required the surgeon to perform an element of cognitive registration, forcing them to remember the normal paracheyma relationships during resection, as the ultrasound view was not displayed during this operative phase. A further limitation of this system was the overlay itself, which clouds the operative view, making true live

image-guided resection impossible without incurring the safety concerns raised in Chapters 4 and 5.

#### **8.1.4 Conclusion**

Over the course of this initial feasibility study the robustness of a method of live ultrasound tracking and overlay in an in-vivo environment has been demonstrated. Its iterative development has also been highlighted. Although data are required to demonstrate the superiority of the technique over conventional robotic or laparoscopic ultrasound, initial *ex-vivo* data from another group<sup>93</sup> suggests that an image guidance platform based around augmented reality intraoperative ultrasound could potentially improve resection quality. Although initial feasibility has been demonstrated more work is needed to improve the ergonomics of the platform and to develop an evidence base beyond that of feasibility.



## **8.2 Augmented reality freehand three-dimensional ultrasound guided tumour resection in robot assisted partial nephrectomy**

### **8.2.1 Introduction**

In the previous section, a novel approach to ultrasound display for the resection of renal tumours was proposed, and feasibility was demonstrated in a first-in-human trial. Although the technique represents a potential improvement over unregistered ultrasound, it is not without significant limitations.<sup>93</sup> The majority of these relate to the requirement on the surgeon to remember the location of the tumour-to-normal parenchyma interface, rather than having it displayed to them during resection. In addition, the 2D nature of the images represents a further limitation, leading to reliance on a cognitive 3D reconstruction to guide resection, which results in a demonstrably poorer appreciation of the anatomy.<sup>86</sup> Displaying a freehand 3D reconstruction of the ultrasound data overlaid onto the operative view could potentially mitigate for these two problems. This section proposes, and validates, in an *ex-vivo* model such a system and demonstrates its feasibility *in-vivo*.

### **8.2.2 Methods**

#### **8.2.2.1 Phantom development**

The polyvinyl alcohol (PVA) partial nephrectomy phantoms used were similar to those previously developed and validated by Fernandez *et al.*<sup>93,184</sup> (See Appendix 4 and Figure 8.2.2). PVA is a polymer with a tensile strength and elasticity similar to tissue and, as such, makes for an excellent medium for organ phantoms.<sup>185</sup> The rigidity of the material is determined by the number of freeze thaw cycles it is submitted to. In this study, a 10% PVA by weight solution was used. The tumour was submitted to three freeze thaw cycles while the kidney itself was submitted to two – this resulted in tumour that was firmer and less elastic than the surrounding tissue, replicating real-world tumour characteristics. The only ways in which the phantom differed from that previously developed by Fernandez *et al.* were: the addition of red enamel paint (0.8%

by weight) to both tumour and kidney, with the aim of improving the content validity of the model; and the addition of cellulose powder (2% by weight) to the tumour to improve the echogenic contrast between parenchyma and tumour. Neither of these additions impacted the tissue handling characteristics of the model.

To maximise the utility of ultrasound-guided resection all tumours were entirely endophytic and abutted the kidney surface. Two different spherical tumour sizes were used, one 15mm and one 19mm in diameter.

### 8.2.2.2 Platform specifics

The platform outlined in the first part of this chapter was used as the starting point for development. Prior to data capture, the intrinsic and extrinsic parameters of the da Vinci stereo camera were calibrated.<sup>154,182</sup> Initially, the surgeon performed a registered and overlaid ultrasound scan. The orientation and position data, in addition to the image of each slice, from this scan were stored; the technique outlined in the first part of this chapter was used to undertake this step. Once the data had been captured, the image series was imported into ITK-SNAP for post processing; in this step, a supervised region growing algorithm was used to define the tumour volume (Figure 8.2.1).<sup>129</sup> Once the segmentation was completed the resulting mesh file was imported into proprietary software allowing it to be displayed within the da Vinci console.

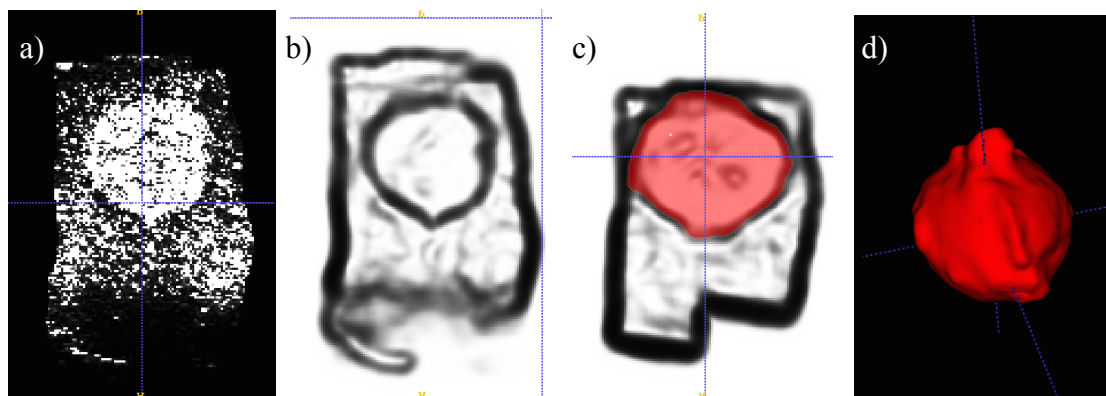


Figure 8.2.1 – Segmentation process. From left to right: a) Raw DICOM data from Hitachi Aloka Prosound ALPHA 10 scanner, with contrast enhancement. b) Same image with ITK-SNAP edge attraction pre-segmentation applied. c) Post the implementation of supervised region growing algorithm. d) 3D volume generated by process.

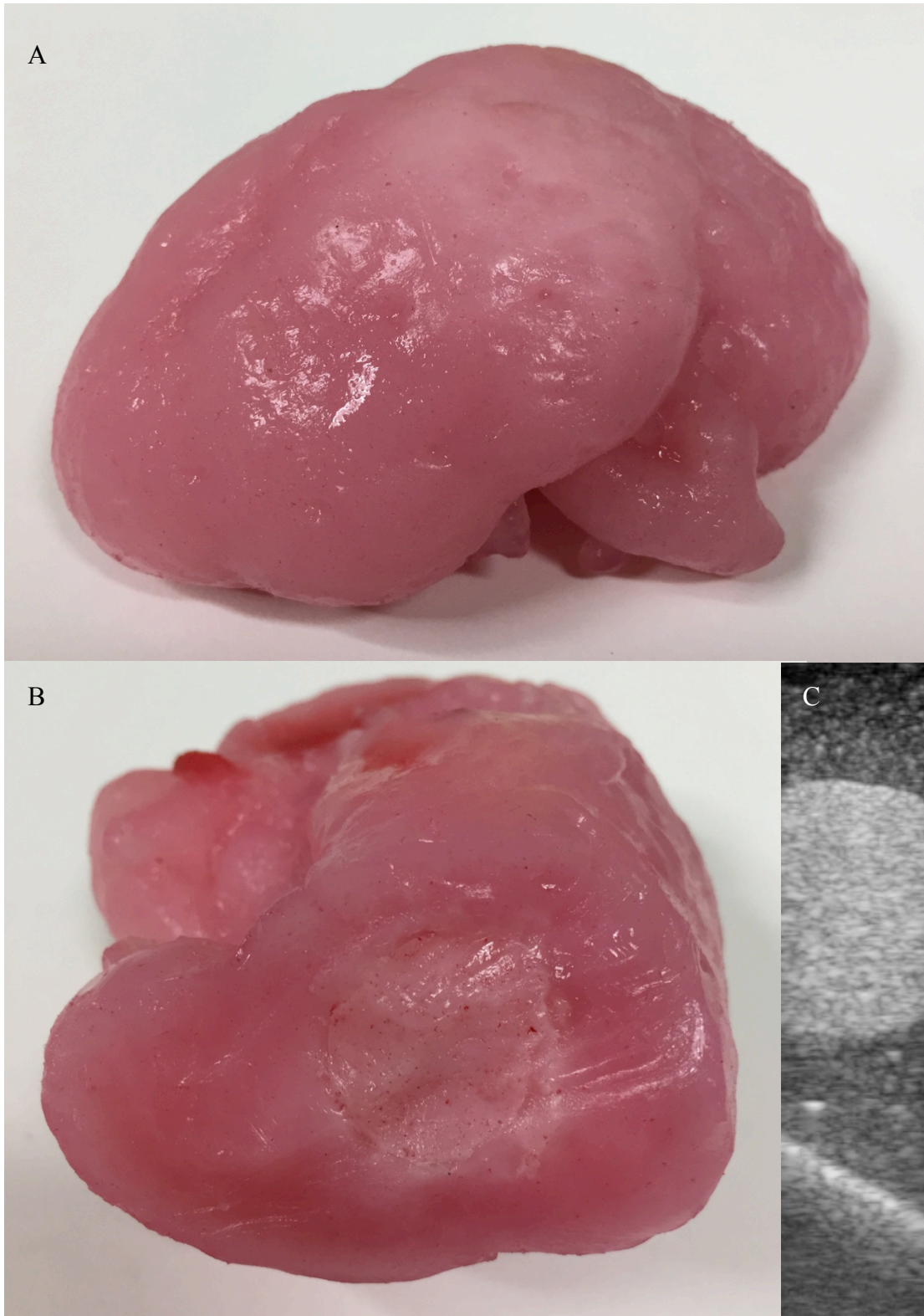


Figure 8.2.2 – High fidelity phantom for the simulation of partial nephrectomy. A) Phantom B) Axial section through phantom, phantom tumour can be seen in the centre of the section C) Ultrasound view of tumour within kidney phantom (narrow field of view due to the physical limitations of the probe used).

To allow the surgeon an appreciation of the tumour's relationship to the kidney surface, a reconstruction of the surface geometry of the kidney was also undertaken using a stepwise process (Figure 8.2.3). First, the stereo camera image was undistorted and rectified. Subsequently a disparity map was created using a semi-global block matching algorithm.<sup>186</sup> This was then reprojected into 3D space and rotated back into the original unrectified camera frame. A mesh was then constructed and simplified using the quadric edge collapse decimation.<sup>187</sup> The mesh was then smoothed and any existing holes were filled. The resulting mesh vertices were then projected, using the camera's intrinsic and distortion parameters, into the current frame, to generate corresponding texture coordinates.

Importantly, both the scene reconstruction and freehand 3D ultrasound were performed simultaneously in the same coordinate system, negating the need for an additional scene to US scan registration.

#### **8.2.2.3 Power calculation**

A power calculation was performed using data from the paper of Cheung *et al.* paper on ultrasound-guided resection of renal tumours.<sup>93</sup> The study was powered for a decrease in planning time of 20%, with a power of 80% and  $\alpha = 0.05$ . In the paper in question, average resection time was  $113 \pm 21.2$  seconds for conventional ultrasound-based guidance.<sup>93</sup> In order to be adequately powered, a sample size of greater than 26 was required with more than 13 resections in each group.

#### **8.2.2.4 Ultrasound-guided resection**

A randomised crossover study design was used to assess the efficacy of the platform. Three participants (all with more than 100 cases experience in robot-assisted urological oncology) were asked to resect tumours from the previously outlined partial nephrectomy phantom kidney.

Participants were asked to perform the resection utilising two approaches to image guidance. In the first, the ultrasound image was displayed as a picture-in-picture (akin to the TilePro™ function in later iterations of the da Vinci platform). This modality of

display was activated via a dedicated foot pedal. In the second group, participants were asked to perform resection while viewing a 3D reconstruction, generated from ultrasound data, of the tumour anatomy overlaid onto the operative view. This was displayed via the same foot pedal used in the display of picture-in-picture, allowing the surgeon to toggle between the augmented reality and unencumbered view (Figure 8.2.4).

Each participant was asked to perform 10 resections, as they would *in-vivo*. Exposure to image guidance and the tumour size were randomised.

A number of outcome measures were collected. The first was planning time (defined as the time from the start of ultrasound collection to first kidney incision minus the processing time). The second was processing time (defined as latent time waiting for image processing to complete). Finally, resection time was collected (defined as first incision to completion of resection). These three metrics were used to compute total time to task completion, which was defined as the sum of planning and resection times.

In addition, to generate a measure of the quality of resection, the ratio of resected tissue volume to tumour volume (resection ratio) was computed. This approach to the assessment of resection quality has been previously utilised in both breast and renal surgery.<sup>143,188</sup> As a further marker of resection quality, the number of breaches to the tumour capsule were counted (positive margins).

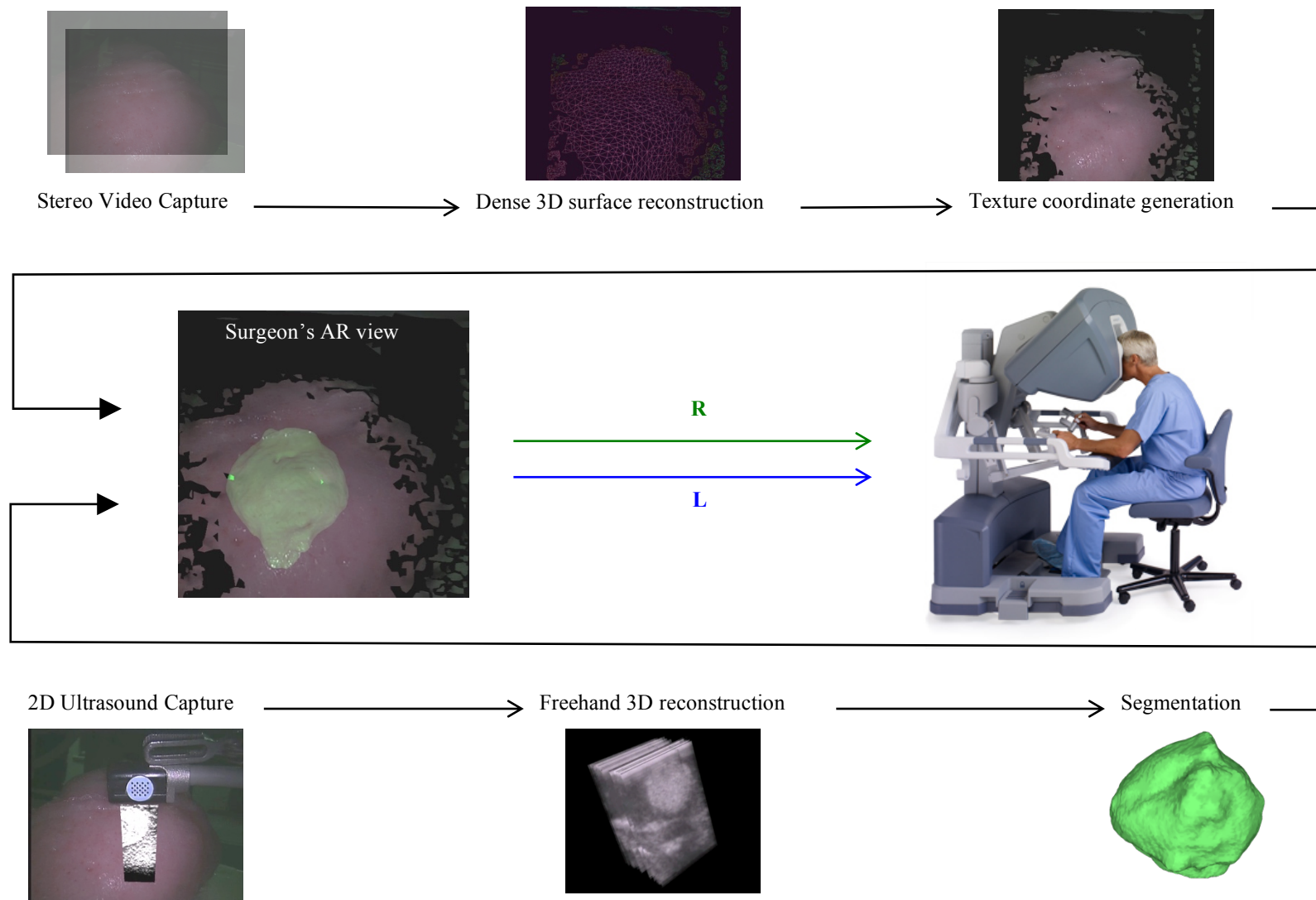


Figure 8.2.3 – Process map for freehand 3D resection guidance. Two processes occur in parallel and in the same coordinate system: The first of dense stereo scene reconstruction in outlined in the top row and comprises stereo video capture followed by a dense stereo scene reconstruction and finally texture coordinate generation. The second process is that of freehand 3D ultrasound, which is outlined on the lower part of the image. These two datasets are then combined in the same coordinate system and displayed to the surgeon, in stereo via an on-demand peddle at the console. *Green and blue lines correspond to right and left camera feeds respectively.*



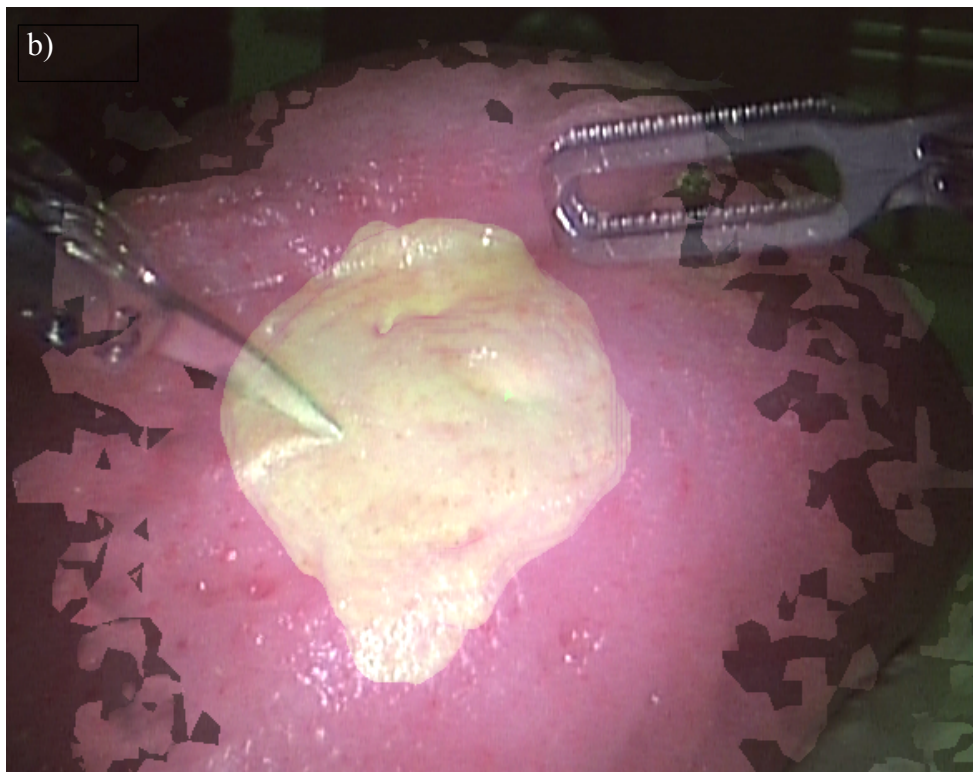
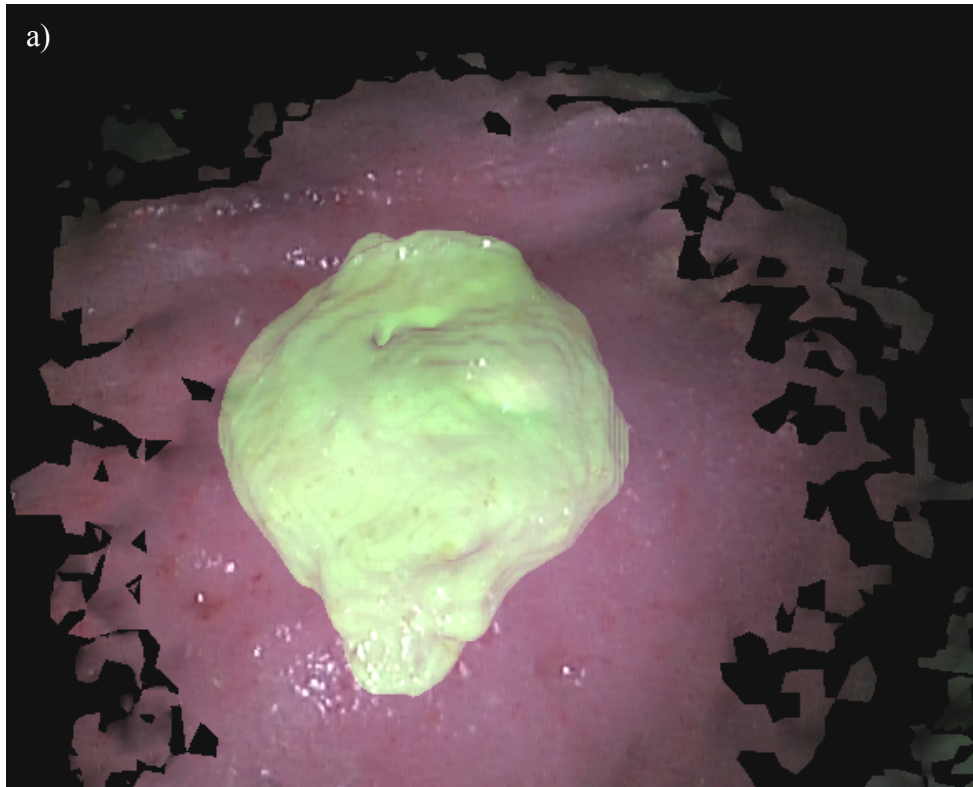


Figure 8.2.4 – Augmented reality view displayed to the surgeon. Two modalities of viewing were available: a) Surface reconstruction and tumour volume b) Surface reconstruction and tumour volume overlaid onto the operative view. The surgeon was able to control the virtual camera orientation and position when viewing images

#### **8.2.2.5 *Statistical analysis***

All statistical analysis was undertaken in GraphPad Prism. When comparing the median task times and resection ratios of two groups, the Mann-Whitney *U* test of statistical significance was used. The Chi-squared test of statistical significance was used to determine significance with regards to tumour capsule breaches. An  $\alpha \leq 0.05$  was deemed to be the marker of statistical significance.

### **8.2.3 Results**

#### **8.2.3.1 *Overall impact of 3D freehand ultrasound guidance on time***

The use of the 3D ultrasound platform was found to decrease the amount of time take to perform the planning phase of the procedure with a 35.9% reduction observed. This trended towards statistical significance ( $p = 0.08$ , Table 8.2.1). The difference in overall time to task completion was found to be insignificant, as were differences in resection times (+ 42.1%,  $p = 0.84$ , and + 62.1%,  $p = 0.62$ , respectively).

#### **8.2.3.2 *Impact of 3D freehand ultrasound guidance on resection accuracy and quality***

A reduction in the positive surgical margin rate of 27% was observed and trended towards significance ( $p = 0.09$ , Table 8.2.1). The use of 3D freehand ultrasound guidance was also found to improve the quality of resection with a 31.2% reduction in the resection ratio, although this reduction failed to reach significance ( $p = 0.24$ ).

#### **8.2.3.3 *Sub analysis by surgeon***

When the data was sub-analysed by surgeon, differing performance was seen (Figure 8.2.5 – Figure 8.2.8). One surgeon was noted to have significantly improved the quality of their resection with 3D guidance in contrast to the other two surgeons, in whom no significant improvement was seen ( $p = 0.03$  versus  $p = 0.22$  and  $p = 0.89$ , Figure 8.2.1). In addition, planning time was also found to be significantly reduced through the use of 3D reconstruction for one of the surgeons ( $p = 0.03$ ).



	US (IQR)	3D (IQR)	% change	p-value
Planning time (secs)	103 (83)	66 (81)	-35.9	0.08
Processing time (secs)		105 (24.5)		
Resection time	185 (233)	300 (269)	62.1	0.62
Time to task completion	282 (286)	401 (320)	42.1	0.84
Resection ratio	1.09 (3.65)	0.75 (1.34)	-31.2	0.24
% Positive margins	40	13	-27	0.09

Table 8.2.1 – Freehand registered 3D ultrasound versus conventional 2D ultrasound guided resection. *Where not stated numbers are medians.*

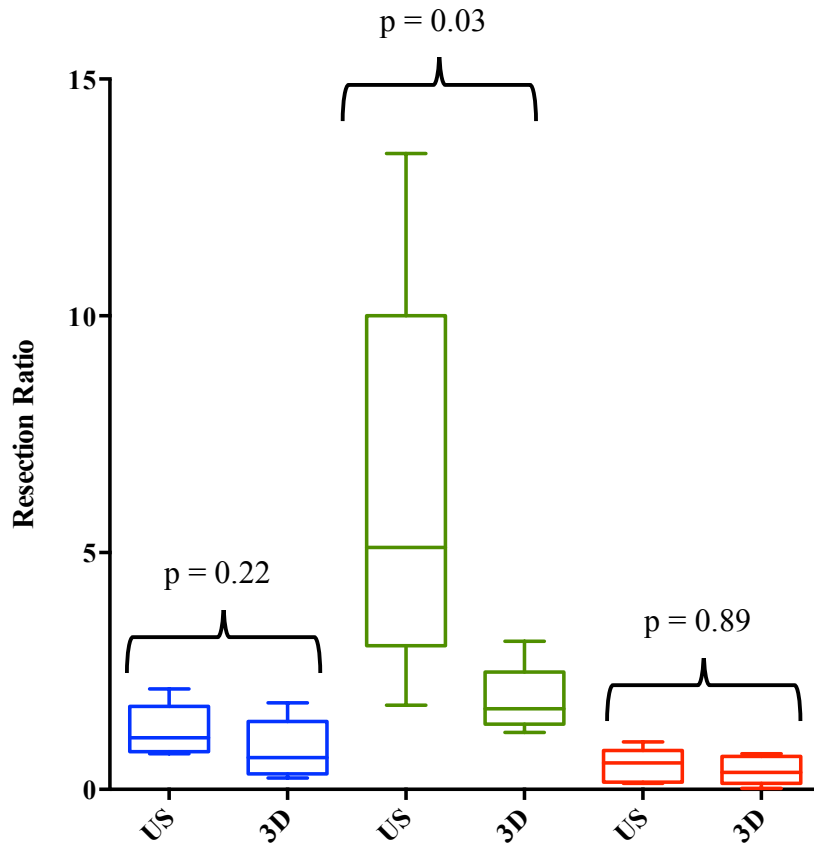


Figure 8.2.5 – Resection ratios by participant (each colour representing a different surgeon)

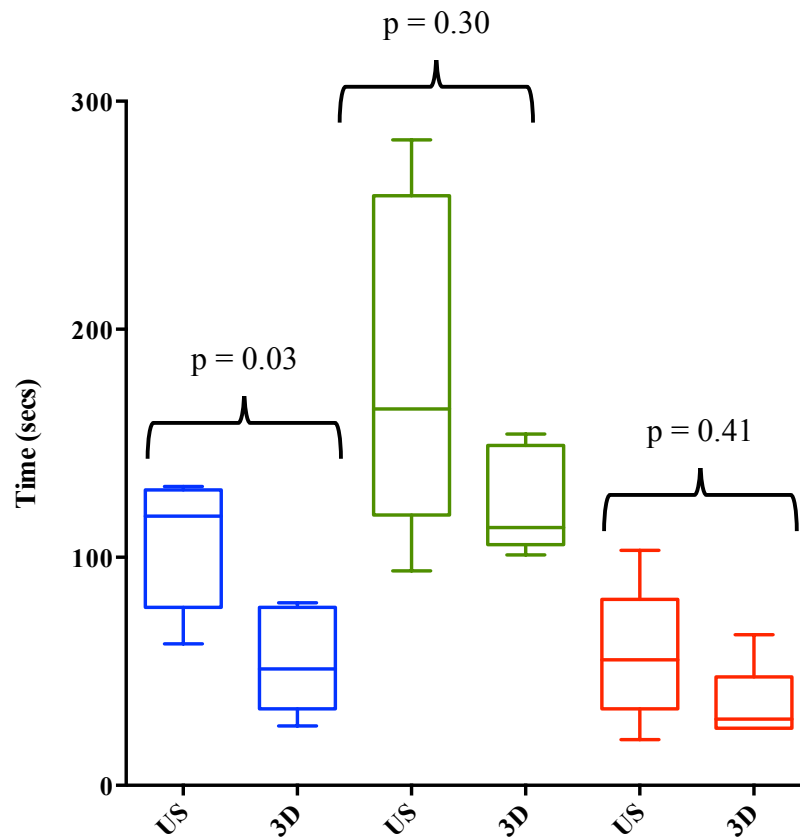


Figure 8.2.6 – Planning time by surgeon (each colour representing a different surgeon)

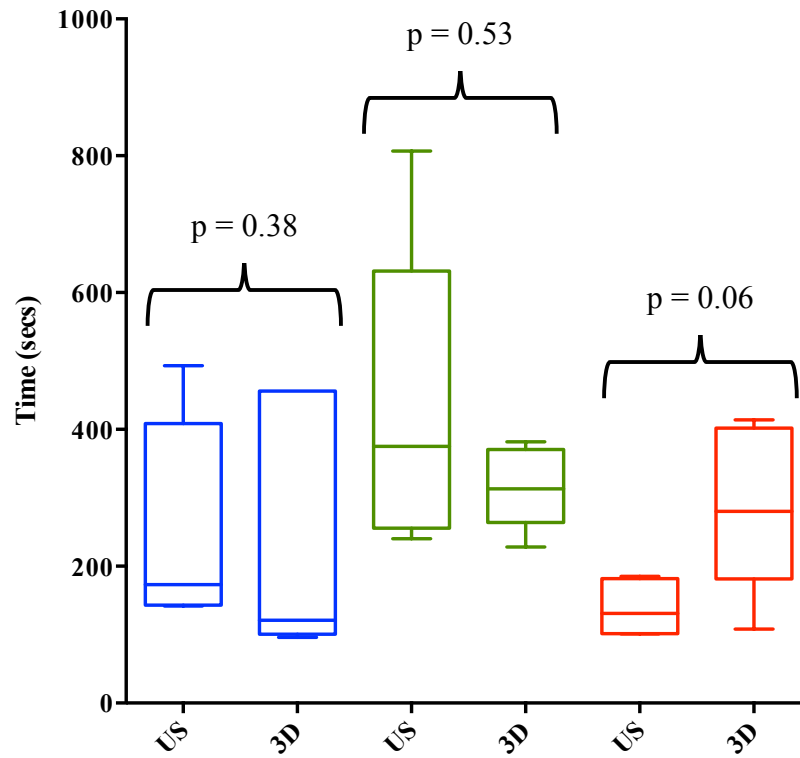


Figure 8.2.7 – Resection time by surgeon (each colour representing a different surgeon)

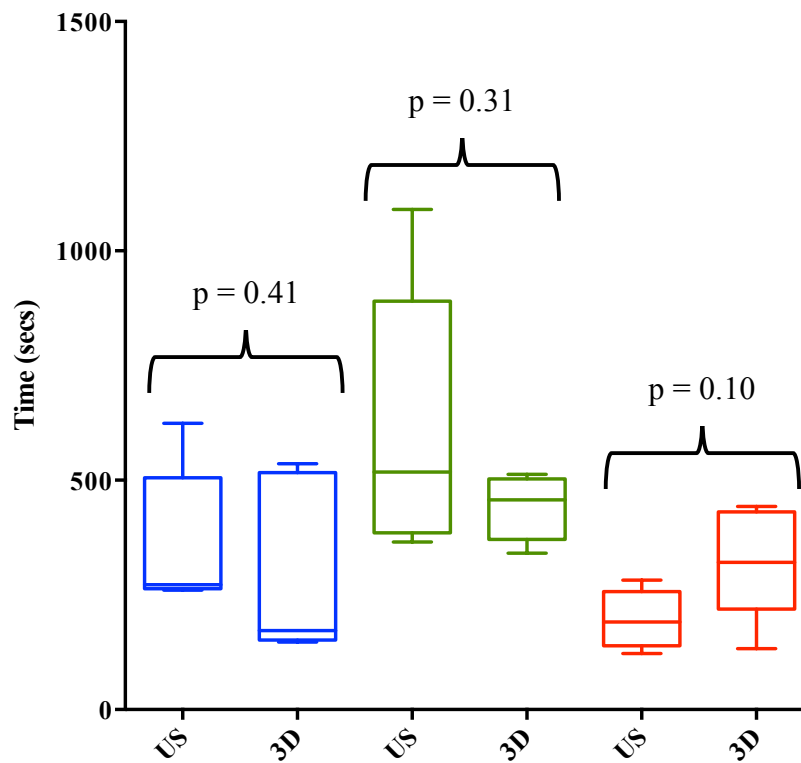


Figure 8.2.8 – Time to task completion (not including processing time) by surgeon (each colour representing a different surgeon)

## 8.2.4 Discussion

### 8.2.4.1 *Principal findings*

The findings of the *ex-vivo* study outlined in this chapter suggest that tracked 3D freehand ultrasound in combination with dense stereo scene reconstruction is safe and feasible, and in the case of one surgeon improved the quality of resection. In addition, the study demonstrates that this potential improvement in quality can be achieved with no increase in positive surgical margins or time taken. The positive margin rates were in fact found to be reduced when compared to conventional ultrasound, with a finding trending towards but failing to reach statistical significance (27% decrease,  $p = 0.09$ ). Crucially, in the context of RAPN, the time taken to perform the tumour resection was not significantly increased.

The potential implications of these findings are not insignificant. If greater efficiency in resection can be achieved with no increase in positive surgical margins, a corresponding improvement in patient's post-operative renal function might be expected, with the added benefits in mortality and morbidity that this improvement entails.<sup>189</sup>

### 8.2.4.2 *Comparison to other studies*

The majority of work to date surrounding image-guided tumour resection in renal oncology and beyond, has focused on the use of registered preoperative datasets. Although these offer the advantage of being able to give the surgeon a broad sense of the subsurface anatomical detail they lack deformation modelling and the quality of registration required for sufficiently accurate tumour resection. Two approaches have been taken to solve this problem.<sup>7</sup> The first has been to utilise tissue deformation modelling in an attempt to predict how the kidney will respond to deforming forces, such as surgical manipulation and pneumoperitoneum.<sup>28</sup> Although theoretically possible the challenge of producing a working model has, as yet, remained unmet due to the number of factors that must be measured and accounted for in the generation of an accurate model.<sup>7</sup> The second approach has been to utilise intraoperative imaging to garner an understanding of anatomical relationships.<sup>93,94,100</sup>

The use of intraoperative image guidance in partial nephrectomy has focused around the use of cone beam CT or intraoperative ultrasound. In the *ex-vivo* study of Teber *et al.* a cone beam CT and reconstruction were performed on the fly. In order to register the images to the endoscopic, view barbed fiducials were planted in the kidney surface and a semi-automated registration was performed using these (Figure 6.3.5).<sup>91</sup> Although feasibility was demonstrated in an *ex-vivo* environment it is perhaps unsurprising that this technique has failed to translate into practice due to the need for barbed fiducials to be inserted into the diseased kidney. In addition to this criticism, the system also necessitates the exposure of both patient and operating staff to significant doses of radiation.

Intra-operative ultrasound is used routinely for partial nephrectomy<sup>178</sup>, with two other groups having utilised it to create a surgical augmented reality.<sup>93,190</sup> In the first of these studies, Harms *et al.* utilised a EM-tracked laparoscopic probe *in-vivo* to scan and subsequently generate 3D reconstructions of colorectal cancer liver metastases. The time taken to generate the volume rendered reconstructions was considerably longer than that seen herein, standing at between 10 and 15 minutes, perhaps relating to the increase in computer processing power since 2001. No attempt at registration or image overlay was made.<sup>190</sup> Cheung *et al.*'s paper used a similarly EM tracked ultrasound probe to aid in the resection of simulated endophytic renal lesions.<sup>93</sup> In contrast to the previous study by Harms *et al.*<sup>190</sup> no attempt was made to reconstruct the images but rather the raw US data was registered and overlaid onto the operative view. The group saw a significant reduction in planning time when compared to a control undertaking the task with conventional ultrasound guidance. In addition, a reduction in margin thickness was observed. Neither of these metrics met the criteria to meet statistical significance but this may have been secondary to under-powering of the data.

The platform in question builds on that proposed earlier in the chapter and addresses a number of the shortcomings of the systems proposed by Harms *et al.*<sup>190</sup> and Cheung *et al.*<sup>93</sup>. Firstly, it removed the need for EM tracking, which is often unreliable in the ferromagnetically rich environment of an operating theatre.<sup>7</sup> In addition, it combined and built on the facets of both previously proposed platforms<sup>93,190</sup>, utilising probe tracking in combination with a dense surface reconstruction to generate a 3D representation of the tumour and its relationship to the renal surface.

### 8.2.4.3 *Future work*

Although the platform appears to offer an advantage over the status quo there are still significant improvements that could be made to its design. These centre around three facets: deformation modelling, tracking, and user-interface.

#### 8.2.4.3.1 *Deformation modelling*

A perfect ultrasound scan, in the context of tumour definition in RAPN, is one in which the ultrasound probe is passed across the surface of the kidney with minimal force exerted on the tissue. This balance is necessary to prevent deforming forces being placed on the kidney and tumour during scanning. Although necessary it is difficult to achieve due to the lack of haptic feedback in the currently available iterations of the da Vinci robotic platform. In future iterations of the system proposed herein the scene reconstruction could be used to define the location of the organ surface allowing haptic and or visual feedback to be given when this surface is infringed by the probe.

#### 8.2.4.3.2 *Tracking*

The current platform gives an accurate representation of the surface and subsurface anatomy at the time of scanning but once the surgeon moves the kidney or camera the registration of the two datasets becomes invalid, thereby limiting the efficacy of the system. This said, the platform is at its most useful in the marking out of the resection boundary and at this point the kidney is likely to be stationary and as such the registration will be correct. In addition, the surgeon is able to manipulate the image to a new viewing angle, allowing them to match the VR view to their current real camera pose; although this registration is manual and therefore has significant limitations.<sup>7,126</sup> Through the use of point-based surface tracking algorithms, such as those proposed by Yip *et al.*,<sup>156</sup> organ tracking can be achieved; an attempt to implement these or similar algorithms will be made in future iterations of the platform.

#### 8.2.4.3.3 *Interface*

Currently, the platform proposed requires a significant amount of engineering input during use. If it is to be widely adopted by the surgical community the steps that need to be undertaken prior to the display of image guidance need to be largely automated and the interface needs to amount to something the surgeon can control from the console, with minimal cognitive load induced.<sup>177</sup>

#### **8.2.4.4 Study limitations**

In addition to the limitations imposed by the platform there were also a number of limitations with the study itself. The first of these relates to the kidney phantom used. As can be seen from the results, higher positive margin rates were seen in both the conventional and 3D ultrasound groups than those that would be expected *in-vivo*,<sup>191</sup> suggesting the task may have been more difficult than that routinely faced in a real world scenario. Although this may have been the case, the study was designed in order to maximise difficulty using entirely endophytic lesions, in order to garner a reciprocal maximum efficacy. As such, it is perhaps unsurprising that higher positive margin rates than reported in the literature were observed.

In addition to the high positive margin rates, the phantom was also limited by the fact that an artificial plane existed on the boundary between the tumour and normal parenchyma. This allowed the tumour to be enucleated, thereby leading to an artificially 'perfect' resection ratio, in order to combat this, participants were asked to undertake sharp dissection leaving a margin. However once the enucleation plane was discovered participants tended to continue in it, perhaps explaining the lack of significant difference in resection ratios achieved by participants one and three. Finally, as the phantom itself is only an approximation of a real world scenario, although a validated one<sup>192</sup>, it cannot be assumed that the same results would be observed *in-vivo*.

The use of expert robotic surgeons also represents a further limitation. Historically the benefits of image guidance have been assumed to be greatest amongst novice surgeons, although this is a limitation it is one that maintains the clinical relevance of the study with only experienced robotic surgeons tending to undertake RAPN.

Lastly, the data was powered according to previous work by Cheng *et al.* utilising planning time. The study may therefore have been underpowered with regards resection ratios and positive surgical margin rates, perhaps further explaining the failure to meet the criteria for overall significance for these two variables.

#### **8.2.5 Conclusions**

This study has demonstrated that a novel system utilising freehand 3D ultrasound in association with dense stereo scene reconstruction was both safe and feasible, and may

improve the quality of tumour resection. In the future more work needs to be done in order to improve the robustness of the platform to allow clinical randomised control trials to be undertaken.



## CHAPTER 9: CONCLUSIONS AND FUTURE WORK<sup>†</sup>

---

<sup>†</sup> Content from this chapter was published as:

Pratt, P., **Hughes-Hallett, A.**, Zhang, L., Patel, N., Mayer, E., Darzi, A., & Yang, G. Z. (2015). Autonomous Ultrasound-Guided Tissue Dissection. In *Medical Image Computing and Computer-Assisted Intervention--MICCAI 2015* (pp. 249-257).

## 9.1 Summary of achievements

This thesis has made a number of significant contributions to the literature and scientific understanding. These contributions have been focused around the aims laid out at its commencement, and are summarised below according to these aims.

### 9.1.1 To define of the window of opportunity for the development of an image guidance platform for intra-abdominal MIS.

The first chapter of the thesis introduced an entirely novel metric for innovation in surgical technology. Subsequent to its development the metric was applied to innovation in surgical image guidance, demonstrating it lies in a phase of innovation growth.<sup>118</sup> The knowledge that this technology cluster lies in a phase of innovation growth maximises the potential for the translation of any developed technology into widespread clinical practice.

### 9.1.2 To establish whether there is a user need for image guidance in RAPN.

Subsequent to establishing the readiness of the market, the potential adopters of the technology were canvassed in the largest survey of its kind to date, this established that image guidance for RAPN was a felt by the urological community to be of potential benefit.<sup>178</sup> In addition, the study highlighted that RAPN can be divided into an intraoperative *planning phase* involving anatomy definition and localization, and a subsequent *execution phase* of tumour resection.<sup>7,178</sup>

### 9.1.3 To better understand the fundamental safety and behavioural implications of the implementation of an IEOE.

For the first time the impact of image guidance and cognitive load on inattention blindness have been examined.<sup>111,177,193</sup> Herein cognitive load was shown to be the driving factor, but with the important caveat that the use of an image overlay impacted on the participants' subjective appreciation of the relevant anatomy, as such the use of image overlay was limited to the minimum in the subsequently developed guidance platform.<sup>177</sup>

In addition, it has been demonstrated that segmented, cross sectional, pre-operative imaging is insufficiently accurate to provide guidance for high precision tasks, such as the guidance of tumour resection, with poor inter-rater reliability demonstrated. The

major implication of this finding being that segmented anatomical reconstructions may only be safe to use for the appreciation of gross anatomical relationships, even in an idealised setting where the problems surrounding registration, tracking, deformation and display have been solved.<sup>29</sup>

#### **9.1.4 To develop and validate a novel approach to image guidance in robot assisted partial nephrectomy, utilising the preceding evidence base to inform this development.**

Perhaps the most significant achievements of the thesis relate to the approach to guidance taken, and the constituent elements of IEOE proposed. As previously mentioned historically image guidance platforms have tended to adopt a *one-size-fits-all* approach, utilising a single modality of imaging to try and solve to plethora of problems faced in developing an image guidance platform for intra-abdominal MIS. In this thesis a novel dual modality approach was taken capitalising on the respective advantages of pre-operative cross section imaging and intraoperative ultrasound for the phases of *planning* and *execution* respectively. Subsequent to the development of these platforms evidence was collected to demonstrate their safety and feasibility. The use of image overlay, a feature common in other platforms proposed in the literature, was intentionally limited due to the concerns raised around the resulting impaired appreciation of the operative scene demonstrated in Chapter 4.

The first part of the IEOE, targeted at the planning phase, is based around a tablet interface, with the original 2D axial slices and reconstructed 3D models (both volume rendered and segmented) of the patients' anatomy displayed to the surgeon; both in the TilePro™ view on the console and the tablet screen. This element looks to facilitate the surgeon during the *planning* phase of the procedure. This novel approach to the interactive intraoperative display of imaging demonstrated the safety, feasibility and efficacy of the platform in a clinical environment, using a matched cohort study design.

Leading on from the planning component of the IEOE a novel approach to the use of intraoperative ultrasound was developed, with the aim of improving the surgeons' appreciation of the tumour anatomy prior to a resection. The design approach to this element of the platform was a two-stage process: the first stage was the development of live overlaid ultrasound, and the second was to build on this initial stage to develop

live registered freehand 3D ultrasound. In a subsequent validation study the use of live freehand 3D ultrasound was shown to have the potential to improve the quality of tumour resection, with an additional trend demonstrated towards the reduction of positive surgical margins.

## 9.2 Future work

### 9.2.1 Further development of the image-enhanced operating environment

Although the potential benefits of surgical image guidance for intra-abdominal surgery, and more specifically for partial nephrectomy, have been widely postulated,<sup>7,9,164</sup> real world image guidance solutions with an evidence base behind them are not widely available. This thesis has outlined such a system, drawing on the respective benefits of intra and preoperative imaging, and has along the way highlighted the limitations of the research undertaken in detail. In the future more work needs to be done to further refine the platform, and to build an evidence base behind it beyond that of feasibility and safety.

#### 9.2.1.1 *Image guidance based on preoperative imaging*

As outlined in Chapter seven, this aspect of the IEOE has reached the point of IIS study (Table 9.2.1), demonstrating safety and feasibility in a prospective case series. The platform has also demonstrated efficacy for the index procedure of robot-assisted partial nephrectomy. In the future, building on the work presented herein, the objective efficacy of image guidance platforms such as this needs to be assessed further in larger multicentre randomised control trials.

In addition, further work needs to be undertaken to improve on the platform itself. This improvement needs to be targeted at three specific guidance steps: *image preparation*, *pre-operative planning* and *intraoperative guidance*.

##### 9.2.1.1.1 *Image preparation*

The current preparation of data using the supervised semi-automated segmentation of patient imaging has a significant learning curve, is time consuming, and subjective.<sup>29</sup> For the technology to stand the best chance of being widely adopted into the target community it needs, as established by Everett Rogers, to have a perceived advantage, compatibility with existing technology, minimal complexity, trialability and observability (Table 9.2.2).<sup>13</sup> The image preparation step fails the tests of compatibility and complexity requiring specialised software, having a significant learning curve, and requiring a time investment from the surgeon to prepare the images.<sup>29</sup> Currently, a significant amount of operator input is required to produce the reconstructions; this

process needs to become sufficiently automated so as to allow a surgeon to undertake the reconstructions with minimal impact on the operative workflow. If this aim cannot be achieved, the platform will likely fall at the diffusion chasm (as discussed in Chapter 2) prior to becoming widely disseminated.

<b>IDEA</b> Professional Innovation Database	<b>DEVELOPMENT</b> Prospective Development Studies	<b>EXPLORATION</b> Phase IIS Study	<b>ASSESSMENT</b> Surgical RCT	<b>LONG TERM MONITORING</b> Prospective Registries
Compulsory reporting of all new innovations	Detailed description of selection criteria  Detailed technical description	To evaluate technique prospectively and co-operatively	RCT – question agreed in Phase IIS  Use power calculations from Phase IIS	Should monitor indications as well as outcomes  SPC used for quality control (Shewart charts, CUSUM, VLAD)
Confidential entry allowed to encourage reporting of failed innovations (similar to CHRP system)	Prospective account of ALL cases consecutively, including those NOT treated with new technique/device	To develop a consensus over definition of the procedure, quality standards and indications	Use learning curve data to decide entry points for clinicians  Use phase IIs consensus to define operation, quality control AND outcome measures	
Hospital or institution to be informed separately as a professional duty	Clear STANDARDISED definitions of outcomes reported  Description of ALL modifications, and when they were made during the series  Registration of PROTOCOL before study starts  Use of Statistical Process Control (SPC) methods to evaluate progress	To gather data for power calculations  To evaluate and monitor learning curves  To achieve consensus on the trial question  To develop a multi-centre randomised trial (RCT)	Use modified RCTs or recognised alternative if RCT not feasible:  Feasibility RCT Expertise-based RCT Cohort multiple RCT Step-wedge design Controlled-interrupted time series	

Table 9.2.1 - Key recommendations for research design at each IDEAL phase<sup>11</sup>

An alternative approach to the problem of image preparation is to outsource it to a third party, removing this labour intense task from the already busy surgeon or radiologist, thereby addressing the issues of compatibility and complexity. This is an approach that is currently being trialled at IRCAD (Research Institute Against Cancers of the Digestive System) in France, with the *Visible-Patient* service offered remotely to a small number of partner institutions.<sup>194</sup> Aside from the complexities of the transfer of

confidential patient imaging, concerns must also exist regarding the quality, cost and scalability of such a service. This service is yet to be made more widely available and, as such, it remains to be seen if the above concerns have been sufficiently addressed.

<b>Factor</b>	<b>Definition</b>
<b>Relative advantage</b>	How improved a technological innovation is over the previous generation
<b>Compatibility</b>	The level of compatibility with existing surgical hardware/how easily can the innovation be integrated into the surgical workflow
<b>Complexity</b>	How difficult is the technology to use
<b>Trialability</b>	Can the technology be easily tested
<b>Observability</b>	Is the technological innovation visible to other surgeons (publication, display at conferences etc.)

Table 9.2.2 – Innovation qualities, as defined by Everett Rogers<sup>13</sup> applied to technological innovations in surgery

Although the outsourcing of image preparation mitigates for the problem faced, it does not attempt to solve it, and without doing so the adoption and impact of any platform based on preoperative imaging will be limited. In the future more work needs to be done looking at ways to improve the speed and accuracy of image pre-processing. This development may well be focused on providing more sophisticated region growing segmentation algorithms, combined with better quality source imaging to improve the robustness and speed of segmentation.

#### 9.2.1.1.2 *Pre-operative planning*

The platform proposed within this thesis has focused on the provision of guidance intra-operatively but there is also significant scope for its use prior to the procedure. This scope varies from the simple manipulation and viewing of reconstructions preoperatively through to patient specific pre-procedural simulation.

Areas of future research focus could include a number of measures that might improve a surgeons' ability to plan the procedure. The first of these steps in planning a procedure would want to include an automated processes to help optimise the planning of port placement; taking into account the body habitus of the patient, allowing the surgeon to perform a semi-automated registration of the real and virtual camera views. These could theoretically then be 'locked' together by means of kinematic data from the chosen

robotic platform, resulting in a synchronicity of movement between the virtual camera and the da Vinci endoscope; thereby removing the need for a series of surgeon derived, manual registrations.

#### *9.2.1.1.3 Intraoperative guidance*

The ‘Holy Grail’ of intraoperative surgical image guidance is surely a situation in which a single imaging modality can be used to provide robust and high precision guidance throughout the procedure, which in the case of partial nephrectomy would be represented by the modality accurate enough to guide tumour resection. Assuming the previously mentioned problems regarding image preparation can be overcome, a number of significant hurdles lie between the surgeon and this ultimate aim, namely those of image registration, deformation and display.

Currently, the image guidance solutions available to surgeons based on preoperative imaging, fail to adequately address any of these issues, and are limited to un-deformed, inaccurately registered imaging either overlaid or viewed alongside the operative view. The benefits of these systems are not to be under-estimated, with the findings of this thesis suggesting that they confer an advantage to the operating surgeon.

Future work must focus on a way to solve these problems, to allow the display of true representations of patient sub-surface anatomy intra-operatively, minimising the amount of interpretation required by the surgeon to translate what they see in imaging datasets to what is actually happening in the operative environment. More work is needed to develop robust registration and deformation models to allow accurate guidance to be derived from a single data source.

#### *9.2.1.2 Freehand 3D ultrasound based guidance*

Until the problems of deformation and registration of preoperative imaging can be solved, alternative approaches to image guidance for high precision tasks need to be developed. In chapter seven of this thesis, an alternative solution based on registered 3D ultrasound was proposed. Although this solution demonstrated promise, more work is needed both to establish its efficacy *in-vivo*, and to improve the platform to make it more user friendly for the wider surgical community.



The two most significant engineering problems that need to be addressed in future work in order to make the platform truly viable in theatre are the current lack of organ tracking, and the failure to model for deformation of the tissue.

#### *9.2.1.2.1 Tissue deformation*

Within the operative scene, a multitude of deforming forces apply, ranging from deformation induced by pneumoperitoneum to the more significant deforming forces exerted on the tissue by the surgeon.<sup>27,152</sup> In the of context 3D freehand ultrasound perhaps the most significant of these is the deforming force that the ultrasound probe exerts as it passes over the renal surface.

There are two potential solutions to this problem: the first would utilise a surface-based reconstruction, using this to actively constrain the path of the ultrasound probe, effectively adhering it to the surface of the kidney thereby preventing any significant pressure being exerted. The second approach would be to create a deformation model. This model would be based on the assumption that deformation is a function of the force exerted and the biomechanical properties of the kidney and tumour. Although this second approach may be theoretically possible it is significantly harder to achieve than the first, particularly due the unpredictable structure of tumours leading to equally unpredictable biomechanical models. As such the first approach of minimising the pressure exerted probably represents a more viable research stream.

#### *9.2.1.2.2 Registration*

In addition to the issues of deformation a common complaint of the surgeons utilising the system *ex-vivo* was the lack of organ tracking. This lack of tracking limits the efficacy of the system as once the kidney or endoscope moves, the image guidance viewed on screen becomes redundant. For the platform to have maximum efficacy *in-vivo*, this problem must be solved with an organ-tracking algorithm perhaps using point based registration and tracking, in combination with true and reconstructed surfaces. Although this approach is possible, it is yet to be demonstrated in a clinical environment.

### **9.2.2 Safety and surgical image guidance**

Although the potential benefits of a surgical image guidance platform are significant, there is also a potential negative impact in introducing such systems. These concerns

focused around two specific areas in this thesis: the quality of the source data set and the potential impact on surgical performance that is incurred by removing focus from the operative scene.

Broadly speaking, further research needs to be done into the potential detrimental impact of image guidance platforms. As mentioned early in the thesis this is an underexplored area and is one it is imperative to understand to guide the safe development of further platforms. Although this thesis has begun to explore this there is much work to do in this area. In particular, more work is needed to quantify the effect of image overlay on the appreciation of the operative scene, directly comparing this to the magnitude of improvement in operative quality, allowing an informed decision to be made about the use of augmented reality overlays.

### **9.2.3 Patient specific simulation**

The remit of this thesis was to deliver an evidence based approach to image guidance in partial nephrectomy. Many of the technological solutions developed in the course of meeting this aim could be more widely utilised, creating tangential research streams.

Procedure- or environment-specific simulation is a tool that has been used widely in the aviation, space exploration, military and motor racing in the prevention of injuries for decades.<sup>195</sup> These simulations are in large part based on virtual reality representations of real world environments, producing these are something on which significant time and effort has been expended while developing the IEOE. As such patient specific simulation represents an obvious target for tangential further research offering operators the ability to interact with a virtual or real world simulation of environments and situations that they are either likely to face, or less common scenarios that pose a significant threat to life.

Although the use of situation-specific simulation has been less widely adopted in surgery, examples do exist, with the patient-specific pre-procedural rehearsal having been shown to improve procedural performance in endovascular cases.<sup>196</sup> Beyond this single study, the use of patient-specific imaging has been limited to the demonstration of feasibility; with reports published in the fields of neurosurgery, craniofacial surgery,

colonoscopy, ear nose and throat surgery, as well as a patient specific simulator for renal surgery.<sup>195,197,198</sup>

The main complexities incurred in creating a patient-specific simulator go some way to explaining surgery's tardiness. These complexities relate mainly to the hugely deformable environment of the patient. This is in contrast to the relatively predictable and rigid environments tackled in the other industries mentioned. For a simulator to have significant efficacy, the virtual world anatomy must represent the real patient and the simulator must respond to surgical interaction in the same way. This creates a significant engineering hurdle necessitating high fidelity biomechanical models; it is no surprise therefore that those areas in which patient specific simulation has begun are in environments (craniofacial and vascular surgery) in which tissues deformation is at a minimum, therefore minimising the amount of deformation modelling that needs to be undertaken. For renal surgery specifically, no tissue deformation models of sufficient accuracy have been proposed in the literature,<sup>147</sup> and as such this is an area of significant future research interest, with patient-specific simulation offering the possibility of improved surgical performance.

#### **9.2.4 Surgical automation**

In 1947, 44 years after the Wright brothers first took to the air, a US air force C-54 made a transatlantic flight, including take-off and landing, totally under the control of an autopilot. By the late 1960s this technology had become common place with most commercial airlines having an autopilot. The increasing automation in aircraft control brought with it significant improvements in safety and efficiency (Figure 9.2.1).<sup>199</sup>

These systems direct the plane to follow a set flight path, altering speed and trajectory according to input from various sensors. Given sufficiently accurate source imaging data, as well as accurate registration and deformation of this imaging, this principle could also be applied to some surgical tasks, in particular tumour resection.

Similarly, to patient specific simulation the automation of surgical tasks, in particular for any automation of resection, require a high fidelity model of the operative environment. If developed a supervised autonomous approach to a task such as tumour

resection, for which image guidance is currently under development offers the potential for the same benefits seen with the advent of automation in the aviation industry.

Although similar the challenges in creating such a platform are subtly different and perhaps more challenging to those tackled in this thesis. The data set must be highly accurate, be brought into the same coordinate system as the patient and device tasked with undertaking the automated task, deform to patient factors and iatrogenic manipulation; and finally a process for articulating this information into automated action by a robot must be developed. This presents significant engineering challenges, some of which have been in part tackled in this thesis and in the broader literature, but these will need to be refined and built on if the above vision is to be realised. This potential stream of research offers significant potential benefit to both patient and surgeon.

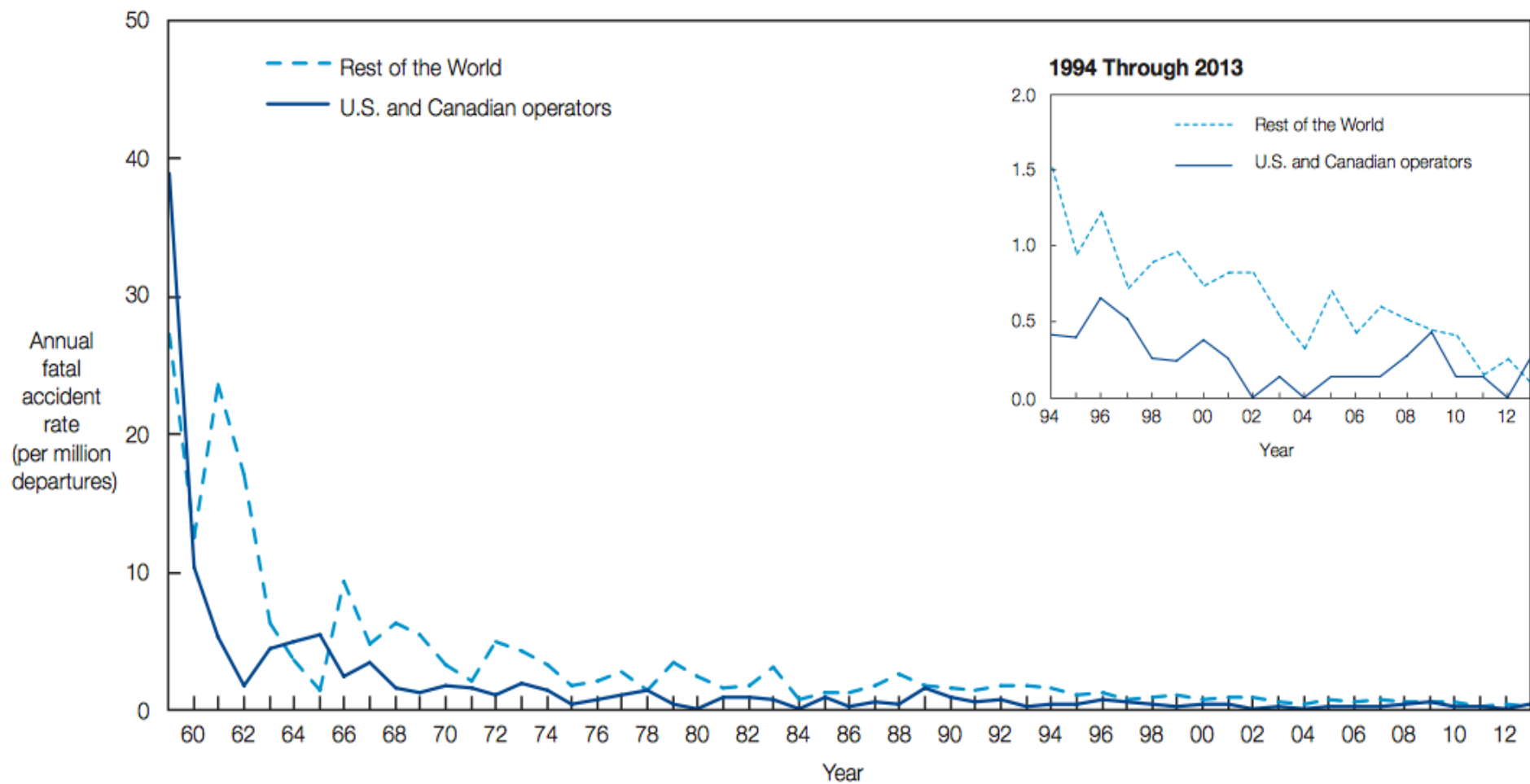


Figure 9.2.1 – Commercial aircraft operator fatal accidents by year. From Statistical summary of commercial jet airplane accidents, 1959 – 2013<sup>200</sup> (Figure courtesy of Boeing, Chicago, USA)

### **9.3 Conclusions**

The gold standard treatment for T1a and b renal cell carcinoma is partial nephrectomy.<sup>201</sup> Although this is the case, the approach is underutilised with more radical nephrectomies undertaken than is probably indicated.<sup>10</sup> A preference for a MIS approach amongst surgeons and patients may well be the driving force behind this with surgeons undertaking a laparoscopic radical nephrectomy rather than the more challenging laparoscopic partial nephrectomy or the more invasive open partial nephrectomy. The preponderance for a laparoscopic radical nephrectomy rather than a nephron-sparing approach has been addressed in part by the advent of robot-assisted laparoscopy but this remains a challenging procedure for complex or endophytic disease, at least in part due to the loss of haptic feedback.

The image-guided approach to robot assisted laparoscopic partial nephrectomy outlined over the course of this thesis has the potential to further redress this balance. Replacing haptic feedback with visual cues to the subsurface anatomy offers a number of direct and indirect potential benefits to the patient. The findings of this thesis would suggest that the use of freehand, registered, 3D ultrasound offers the potential for improved resection quality and a reduction in positive surgical margins. In addition to these direct benefits, the use of an IEOE could potentially influence case selection, with surgeons prepared to take on cases with more challenging anatomy due the improved understanding they are given by the image guidance. This more favourable case selection would translate to more patients undergoing a nephron-sparing rather than radical procedure, thereby acquiring the long-term benefits associated with an organ sparing approach.

## REFERENCES

1. Hopkins HH. Optical system having cylindrical rod-like lenses. USA: United States Patent Office; 3,257,902, 1966. p. 1–9.
2. de Goede B, Klitsie PJ, Hagen SM, et al. Meta-analysis of laparoscopic versus open cholecystectomy for patients with liver cirrhosis and symptomatic cholelithiasis. *Br J Surg*. 2013;100(2):209–16.
3. Wei B, Qi C-L, Chen T-F, et al. Laparoscopic versus open appendectomy for acute appendicitis: a metaanalysis. *Surg Endosc*. 2011;25(4):1199–208.
4. Keus F, de Jong J a F, Gooszen HG, et al. Laparoscopic versus open cholecystectomy for patients with symptomatic cholelithiasis. *Cochrane Database Syst Rev*. 2006;(4):CD006231.
5. Gallagher AG, McClure N, McGuigan J, et al. An ergonomic analysis of the fulcrum effect in the acquisition of endoscopic skills. *Endoscopy*. 1998 Sep;30(7):617–20.
6. Storz P, Buess GF, Kunert W, et al. 3D HD versus 2D HD: surgical task efficiency in standardised phantom tasks. *Surg Endosc*. 2012;26(5):1454–60.
7. Hughes-Hallett A, Pratt PJ, Mayer EK, et al. Augmented Reality Partial Nephrectomy: Examining the Current Status and Future Perspectives. *Urology*. 2014 Oct 19;83(2):266–73.
8. Teber D, Guven S, Simpfendorfer T, et al. Augmented Reality: A New Tool To Improve Surgical Accuracy during Laparoscopic Partial Nephrectomy? Preliminary In Vitro and In Vivo Results. *Eur Urol*. 2009;56(2):332–8.
9. Nicolau S, Soler L, Mutter D, et al. Augmented reality in laparoscopic surgical oncology. *Surg Oncol*. 2011 Sep;20(3):189–201.
10. Hollenbeck BK, Taub D, Miller DC, et al. National utilization trends of partial nephrectomy for renal cell carcinoma: a case of underutilization? *Urology*. 2006 Mar;67(2):254–9.
11. McCulloch P, Altman DG, Campbell WB, et al. No surgical innovation without evaluation: the IDEAL recommendations. *Lancet*. 2009 Sep 26;374(9695):1105–12.
12. Ryan B, Gross N. The diffusion of hybrid seed corn in two Iowa communities. *Rural Sociol*. 1943;8(1):15–24.
13. Rogers E. *Diffusion of Innovations*. 5th ed. New York: Free Press; 1962.

14. Nelson AJ. Measuring knowledge spillovers: What patents, licenses and publications reveal about innovation diffusion. *Res Policy*. 2009 Jul;38(6):994–1005.
15. Huebner J. A possible declining trend for worldwide innovation. *Technol Forecast Soc Change*. 2005 Oct;72(8):980–6.
16. Meade N, Islam T. Modelling and forecasting the diffusion of innovation – A 25-year review. *Int J Forecast*. 2006 Jan;22(3):519–45.
17. Chagpar AB, Edgar J. Poth Memorial Lecture. Innovation in surgery: from imagination to implementation. *Am J Surg*. Elsevier Inc.; 2011 Dec;202(6):641–5.
18. Sodergren M, Darzi A. Surgical innovation and the introduction of new technologies. *Br J Surg*. 2013;100:12–3.
19. Campbell B. How to judge the value of innovation. *BMJ*. 2012;1457(March):10–1.
20. King CH, Culjat MO, Franco ML, et al. Tactile feedback induces reduced grasping force in robot-assisted surgery. *IEEE Trans Haptics*. 2009;2(2):103–10.
21. Pacchierotti C, Prattichizzo D, Kuchenbecker KJ. Cutaneous Feedback of Fingertip Deformation and Vibration for Palpation in Robotic Surgery. *IEEE Trans Biomed Eng*. 2015;PP(99):1–10.
22. Koehn JK, Kuchenbecker KJ. Surgeons and non-surgeons prefer haptic feedback of instrument vibrations during robotic surgery. *Surg Endosc*. 2014;
23. Bark K, McMahan W, Remington A, et al. In vivo validation of a system for haptic feedback of tool vibrations in robotic surgery. *Surg Endosc*. 2013 Feb;27(2):656–64.
24. Hughes-Hallett A, Mayer E, Pratt P, et al. Quantifying innovation in robotic surgery. In: Yang G-Z, Darzi A, editors. *The Hamlyn Symposium on Medical Robotics*. 2014. p. 1–2.
25. Saddik A El, Orozco M, Eid M, et al. *Haptics Technologies: Bringing Touch to Multimedia*. Springer Science & Business Media; 2011. 220 p.
26. Lee S-L, Lerotic M, Vitiello V, et al. From medical images to minimally invasive intervention: Computer assistance for robotic surgery. *Comput Med Imaging Graph*. 2010 Jan;34(1):33–45.
27. Schneider C, Member S, Nguan C, et al. Motion of the Kidney Between Preoperative and Intraoperative Positioning. *IEEE Trans Biomed Eng*. 2013;1–



- 9.
28. Altamar HO, Ong RE, Glisson CL, et al. Kidney deformation and intraprocedural registration: A study of elements of image-guided kidney surgery. *J Endourol.* 2011;25(3):511–7.
29. Hughes-Hallett A, Pratt P, Mayer E, et al. Using preoperative imaging for intraoperative guidance: a case of mistaken identity. *Int J Med Robot.* 2015;
30. Fadden S, Wickens CD, Vevers P. Costs and Benefits of Head up Displays: An Attention Perspective and a Meta Analysis. *World Aviation Congress.* 2000.
31. Williams LJ. Cognitive Load and the Functional Field of View. *Hum Factors J Hum Factors Ergon Soc .* 1982 Dec 1;24(6):683–92.
32. Fischer E, Haines R. Cognitive issues in head-up displays. *NASA Tech Pap* 1711. 1980;
33. Simons DJ, Chabris CF. Gorillas in our midst: sustained inattention blindness for dynamic events. *Perception.* 1999 Jan;28(9):1059–74.
34. Mack A, Rock I. *Inattention blindness.* 1st ed. Cambridge, MA: MIT Press; 1998.
35. Warfield S, Zou K, Wells W. Simultaneous Truth and Performance Level Estimation (STAPLE): An Algorithm for the Validation of Image Segmentation. *IEEE Trans Med Imaging.* 2004;23(7):903–21.
36. Hoyte L, Ye W, Brubaker L, et al. Segmentations of MRI images of the female pelvic floor: a study of inter- and intra-reader reliability. *J Magn Reson Imaging.* 2011 Mar;33(3):684–91.
37. Barone DG, Lawrie TA, Hart MG, et al. Image guided surgery for the resection of brain tumours. *Cochrane database Syst Rev.* 2014;1(1):CD009685.
38. Mezger U, Jendrewski C, Bartels M. Navigation in surgery. *Langenbeck’s Arch Surg.* 2013;398(4):501–14.
39. Altamar HO, Ong RE, Glisson CL, et al. Kidney deformation and intraprocedural registration: a study of elements of image-guided kidney surgery. *J Endourol.* 2011;25(3):511–7.
40. Ljungberg B, Cowan NC, Hanbury DC, et al. EAU guidelines on renal cell carcinoma: the 2010 update. *Eur Urol.* 2010 Sep;58(3):398–406.
41. Novick AC, Campbell S, Beldegrun A, et al. Guideline for Management of the Clinical Stage 1 Renal Mass. *Am Urol Assoc.*
42. Nguyen MM, Gill IS. Halving ischemia time during laparoscopic partial

- nephrectomy. *J Urol*. 2008 Feb;179(2):627–32.
43. Sun M, Bianchi M, Hansen J, et al. Chronic kidney disease after nephrectomy in patients with small renal masses: a retrospective observational analysis. *Eur Urol*. 2012 Oct;62(4):696–703.
  44. Go AS, Chertow GM, Fan D, et al. Chronic kidney disease and the risks of death, cardiovascular events, and hospitalization. *N Engl J Med*. 2004 Sep 23;351(13):1296–305.
  45. Levey AS, Coresh J. Chronic kidney disease. *Lancet*. Elsevier Ltd; 2012 Jan 14;379(9811):165–80.
  46. Zini L, Perrotte P, Capitanio U, et al. Radical versus partial nephrectomy: effect on overall and noncancer mortality. *Cancer*. 2009 Apr 1;115(7):1465–71.
  47. Thompson RH, Boorjian S a, Lohse CM, et al. Radical nephrectomy for pT1a renal masses may be associated with decreased overall survival compared with partial nephrectomy. *J Urol*. 2008 Feb;179(2):468–71.
  48. Huang WC, Elkin EB, Levey AS, et al. Partial Nephrectomy vs. Radical Nephrectomy in Patients With Small Renal Tumors: Is There a Difference in Mortality and Cardiovascular Outcomes? *J Urol*. 2009;181(1):55–62.
  49. Tan H-J, Norton EC, Ye Z, et al. Long-term survival following partial vs radical nephrectomy among older patients with early-stage kidney cancer. *JAMA*. 2012 Apr 18;307(15):1629–35.
  50. Antonelli A, Cozzoli A, Nicolai M, et al. Nephron-sparing surgery versus radical nephrectomy in the treatment of intracapsular renal cell carcinoma up to 7cm. *Eur Urol*. 2008 Apr;53(4):803–9.
  51. Ficarra V. Open radical nephrectomy versus open partial nephrectomy: is it still an issue? *Eur Urol*. 2007 Mar;51(3):593–5.
  52. Gill IS, Kavoussi LR, Lane BR, et al. Comparison of 1,800 laparoscopic and open partial nephrectomies for single renal tumors. *J Urol*. 2007 Jul;178(1):41–6.
  53. Yohannes P, Rotariu P, Pinto P, et al. Comparison of robotic versus laparoscopic skills: Is there a difference in the learning curve? *Urology*. 2002;60(1):39–45.
  54. Link RE, Bhayani SB, Allaf ME, et al. Exploring the learning curve, pathological outcomes and perioperative morbidity of laparoscopic partial nephrectomy performed for renal mass. *J Urol*. 2005 May;173(5):1690–4.
  55. Benway BM, Wang AJ, Cabello JM, et al. Robotic partial nephrectomy with

- sliding-clip renorrhaphy: technique and outcomes. *Eur Urol*. 2009 Mar;55(3):592–9.
56. Marcus HJ, Hughes-Hallett A, Cundy TP, et al. Not everything that counts can be easily counted. *BMJ*. 2013 Apr 24;346.
  57. Dev HS, Sooriakumaran P, Stolzenburg J-U, et al. Is robotic technology facilitating the minimally invasive approach to partial nephrectomy? *BJU Int*. 2012 Mar;109(5):760–8.
  58. Miller DC, Hollingsworth JM, Hafez KS, et al. Partial nephrectomy for small renal masses: an emerging quality of care concern? *J Urol*. 2006 Mar;175(3 Pt 1):853–7; discussion 858.
  59. M. H, F. K, S. F, et al. Partial versus radical nephrectomy for T1 renal tumours: An analysis from the British Association of Urological Surgeons Nephrectomy Audit. *Eur Urol Suppl*. 2014;13(1):e1039.
  60. Baker SR. The diffusion of high technology medical innovation: The computed tomography scanner example. *Soc Sci Med*. 1979;13:155–62.
  61. Rogers W, Lotz M, Hutchison K, et al. Identifying Surgical Innovation: A Qualitative Study of Surgeons' Views. *Ann Surg*. 2013 Jun 19;
  62. Trajtenberg M. A penny for your quotes : patent citations and the value of innovations. *RAND J Econ*. 1990;21(1):172–87.
  63. Riskin DJ, Longaker MT, Gertner M, et al. Innovation in surgery: a historical perspective. *Ann Surg*. 2006 Nov;244(5):686–93.
  64. Daim TU, Rueda G, Martin H, et al. Forecasting emerging technologies: Use of bibliometrics and patent analysis. *Technol Forecast Soc Chang*. 2006 Oct;73(8):981–1012.
  65. Bengisu M, Nekhili R. Forecasting emerging technologies with the aid of science and technology databases. *Technol Forecast Soc Chang*. 2006 Sep;73(7):835–44.
  66. Sanson-Fisher RW. Diffusion of innovation theory for clinical change. *Med J Aust*. 2004 Mar 15;180(6):55–6.
  67. Barkun JS, Aronson JK, Feldman LS, et al. Evaluation and stages of surgical innovations. *Lancet*. 2009 Sep 26;374(9695):1089–96.
  68. Fleuren M, Wiefferink K, Paulussen T. Determinants of innovation within health care organizations: literature review and Delphi study. *Int J Qual Heal Care*. 2004 May;16(2):107–23.

69. Berwick D. Disseminating Innovations in Health Care. *JAMA*. 2003;289(15):1969–75.
70. General Information Concerning Patents [Internet]. The United States Patent and Trademark Office. 2011 [cited 2013 Sep 20].
71. Steurer M, Hill RJ, Zahrnhofer M, et al. Modelling the Emergence of New Technologies using S-Curve Diffusion Models. *Graz Economic Papers*. Graz: University of Graz, Department of Economics; 2012. 1-27 p.
72. Røttingen J-A, Regmi S, Eide M, et al. Mapping of available health research and development data: what's there, what's missing, and what role is there for a global observatory? *Lancet*. 2013 Oct 12;382(9900):1286–307.
73. EPO patent information resource DOCDB [Internet]. European Patent Office. 2008 [cited 2013 Sep 23].
74. Zeebroeck N Van. The puzzle of patent value indicators. *Econ Innov New Technol*. 2011;20:33–62.
75. Hall B, Jaffe A, Trajtenberg M. Market value and patent citations: A first look. *Natl Bur Econ Res*. 2000;w7741:1–40.
76. Robicsek F. The birth of the surgical stapler. *Surg Gynecol Obs*. 1980;150(4):579–83.
77. Tamai S. History of Microsurgery- From the beginning until the end of the 1970s. *Microsurgery*. 1993;14:6–13.
78. Twiss BC. *Forecasting for Technologists and Engineers: A Practical Guide for Better Decisions (IEE Management of Technology)*. 1st ed. London: Peter Peregrinus Ltd; 1992. 236 p.
79. Maciunas RJ, Galloway RL, Fitzpatrick JM, et al. A universal system for interactive image-directed neurosurgery. *Stereotact Funct Neurosurg*. 1992 Jan;58(1–4):108–13.
80. Marcus HJ, Hughes-hallett A, Kwasnicki RM, et al. Technological innovation in neurosurgery: a quantitative study. *J Neurosurg*. 2015;1–8.
81. Wilson CB. Adoption of new surgical technology. *BMJ*. 2006 Jan 14;332(7533):112–4.
82. Denis J-L, Hébert Y, Langley A, et al. Explaining diffusion patterns for complex health care innovations. *Health Care Manag Rev*. 2002 Jan;27(3):60–73.
83. Cain M, Mittman R. *Diffusion of innovation in health care*. California Healthcare Foundation; 2002.

84. Trajtenberg M. Economic analysis of product innovation: The case of CT scanners. 1st ed. Harvard: Harvard University Press; 1990.
85. Waarts E, Everdingen YM, Hillegersberg J. The dynamics of factors affecting the adoption of innovations. *J Prod Innov Manag*. 2002 Nov;19(6):412–23.
86. Foo J-L, Martinez-Escobar M, Juhnke B, et al. Evaluating mental workload of two-dimensional and three-dimensional visualization for anatomical structure localization. *J Laparoendosc Adv Surg Tech A*. 2013 Jan;23(1):65–70.
87. Sridhar AN, Hughes-Hallett A, Mayer EK, et al. Image-guided robotic interventions for prostate cancer. *Nat Rev Urol*. 2013 Jun 18;10(8):452–62.
88. Cohen D, Mayer E, Chen D, et al. Augmented reality image guidance in minimally invasive prostatectomy. *Lect Notes Comput Sci*. 2010 Sep;6367:101–10.
89. Simpfendörfer T, Baumhauer M, Müller M, et al. Augmented reality visualization during laparoscopic radical prostatectomy. *J Endourol*. 2011 Dec;25(12):1841–5.
90. Teber D, Simpfendorfer T, Guven S, et al. In-vitro evaluation of a soft-tissue navigation system for laparoscopic prostatectomy. *J Endourol*. 2010;24(9):1487–91.
91. Teber D, Guven S, Simpfendörfer T, et al. Augmented reality: a new tool to improve surgical accuracy during laparoscopic partial nephrectomy? Preliminary in vitro and in vivo results. *Eur Urol*. 2009;56(2):332–8.
92. Pratt P, Mayer E, Vale J, et al. An effective visualisation and registration system for image-guided robotic partial nephrectomy. *J Robot Surg*. 2012 Jan 13;6(1):23–31.
93. Cheung CL, Wedlake C, Moore J, et al. Fused video and ultrasound images for minimally invasive partial nephrectomy: A phantom study. *Med Image Comput Comput Assist Interv*. 2010;13(Pt 3):408–15.
94. Hughes-Hallett A, Pratt P, Mayer E, et al. Intraoperative Ultrasound Overlay in Robot-assisted Partial Nephrectomy: First Clinical Experience. *Eur Urol*. 2013 Nov 12;65(3):671–2.
95. Eysenbach G. Improving the quality of Web surveys: the Checklist for Reporting Results of Internet E-Surveys (CHERRIES). *J Med Internet Res. Journal of Medical Internet Research*; 2004 Sep 29;6(3):e34.
96. Edwards PJ, Roberts I, Clarke M, et al. Methods to increase response to postal

- and electronic questionnaires ( Review ). *Cochrane Collab.* 2010;(1).
97. Nakamura K, Naya Y, Zenbutsu S, et al. Surgical navigation using three-dimensional computed tomography images fused intraoperatively with live video. *J Endourol.* 2010;24(4):521–4.
  98. Ukimura O, Gill IS. Imaging-assisted endoscopic surgery: Cleveland clinic experience. *J Endourol.* 2008;22(4):803–9.
  99. Ukimura O, Nakamoto M, Gill IS. Three-dimensional reconstruction of renovascular-tumor anatomy to facilitate zero-ischemia partial nephrectomy. *Eur Urol.* 2012;61(1):211–7.
  100. Pratt P, Hughes-Hallett A, Di Marco A, et al. Multimodal Reconstruction for Image-Guided Interventions. *Hamlyn Symposium.* 2013.
  101. Mayer EK, Cohen D, Chen D, et al. Augmented Reality Image Guidance in Minimally Invasive Prostatectomy. *Eur Urol Supp.* 2011 Mar;10(2):300.
  102. Thompson S, Penney G, Billia M, et al. Design and evaluation of an image-guidance system for robot-assisted radical prostatectomy. *BJU Int.* 2013 Jun;111(7):1081–90.
  103. Panebianco V, Salciccia S, Cattarino S, et al. Use of Multiparametric MR with Neurovascular Bundle Evaluation to Optimize the Oncological and Functional Management of Patients Considered for Nerve-Sparing Radical Prostatectomy. *J Sex Med.* 2012 Aug;9(8):2157–66.
  104. Rai S, Srivastava A, Sooriakumaran P, et al. Advances in imaging the neurovascular bundle. *Curr Opin Urol.* 2012 Mar;22(2):88–96.
  105. Sfakianos GP, Frederick PJ, Kendrick JE, et al. Robotic surgery in gynecologic oncology fellowship programs in the USA : a survey of fellows and fellowship directors. *Int J Med Robot Comput Assist Surg.* 2010;6:405–12.
  106. Shaligram A, Meyer A, Simorov A, et al. Survey of minimally invasive general surgery fellows training in robotic surgery. *J Robot Surg.* 2013 May 13;7(2):131–6.
  107. Robinson M, Macneily A, Goldenberg L, et al. Status of robotic-assisted surgery among Canadian urology residents. *Can J Urol.* 2012 Jun;6(3):160–7.
  108. Mccann RS, Foyle DC. Attentional limitations with heads up displays. In: Jensen R, editor. *Proceedings of the Seventh International Symposium on Aviation Psychology.* 1993. p. 70–5.
  109. Wickens CD, Alexander AL. Attentional Tunneling and Task Management in

- Synthetic Vision Displays. *Int J Aviat Psychol*. 2009 Mar 27;19(2):182–99.
110. Marcus HJ, Pratt P, Hughes-hallett A, et al. Comparative effectiveness and safety of image guidance systems in neurosurgery: a preclinical randomized study. *J Neurosurg*. 2015;1–7.
  111. Dixon BJ, Daly MJ, Chan H, et al. Surgeons blinded by enhanced navigation: the effect of augmented reality on attention. *Surg Endosc*. 2013 Feb;27(2):454–61.
  112. Luz M, Manzey D, Modemann S, et al. Less is sometimes more: a comparison of distance-control and navigated-control concepts of image-guided navigation support for surgeons. *Ergonomics*. 2014 Oct 24;58(3):383–93.
  113. Dixon BJ, Daly MJ, Chan H, et al. Augmented image guidance improves skull base navigation and reduces task workload in trainees: a preclinical trial. *Laryngoscope*. 2011 Oct;121(10):2060–4.
  114. Dixon BJ, Chan H, Daly MJ, et al. The effect of augmented real-time image guidance on task workload during endoscopic sinus surgery. *Int Forum Allergy Rhinol*. 2012;2(5):405–10.
  115. Haerle SK, Daly MJ, Chan H, et al. Localized intraoperative virtual endoscopy (LIVE) for surgical guidance in 16 skull base patients. *Otolaryngol Head Neck Surg*. 2015 Jan;152(1):165–71.
  116. Theodoraki MN, Ledderose GJ, Becker S, et al. Mental distress and effort to engage an image-guided navigation system in the surgical training of endoscopic sinus surgery: a prospective, randomised clinical trial. *Eur Arch Oto-Rhino-Laryngology*. 2014;272(4):905–13.
  117. Cartwright-Finch U, Lavie N. The role of perceptual load in inattention blindness. *Cognition*. 2007 Mar;102(3):321–40.
  118. Hughes-Hallett A, Mayer EK, Marcus HJ, et al. Quantifying Innovation in Surgery. *Ann Surg*. 2014 Aug;260(2):205–11.
  119. Hart S, Staveland L. Development of NASA-TLX (Task Load Index): Results of empirical and theoretical research. In: Hancock A, Meshkati N, editors. *Human Mental Workload*. Amsterdam: North Holland Press; 1988. p. 139.-183.
  120. Healey a N, Sevdalis N, Vincent C a. Measuring intra-operative interference from distraction and interruption observed in the operating theatre. *Ergonomics*. 49(5–6):589–604.
  121. Guru K a, Esfahani ET, Raza SJ, et al. Cognitive Skills Assessment during

- Robot-Assisted Surgery: Separating Wheat from Chaff. *BJU Int.* 2014 Jan 28;115(1):166–74.
122. Liu D, Jenkins S a, Sanderson PM, et al. Monitoring with head-mounted displays: performance and safety in a full-scale simulator and part-task trainer. *Anesth Analg.* 2009 Oct;109(4):1135–46.
  123. Bressan P, Pizzighello S. The attentional cost of inattentive blindness. *Cognition.* 2008 Jan;106(1):370–83.
  124. Lavie N. Distracted and confused?: selective attention under load. *Trends Cogn Sci.* 2005 Mar;9(2):75–82.
  125. Levoy M. Display of surfaces from volume data. *IEEE Comput Graph Appl.* 1988 May;8(3):29–37.
  126. Hughes-Hallett A, Pratt PJ, Mayer EK, et al. Image guidance for all – TilePro™ display of three-dimensionally reconstructed images in robotic partial nephrectomy. *Urology.* 2014;84(1):237–42.
  127. Famaey N, Vander Sloten J. Soft tissue modelling for applications in virtual surgery and surgical robotics. *Comput Methods Biomech Biomed Engin.* 2008;11(4):351–66.
  128. Chen Y, Li H, Wu D, et al. Surgical planning and manual image fusion based on 3D model facilitate laparoscopic partial nephrectomy for intrarenal tumors. *World J Urol.* 2013 Dec 12;(253):1493–9.
  129. Yushkevich PA, Piven J, Hazlett HC, et al. User-guided 3D active contour segmentation of anatomical structures: significantly improved efficiency and reliability. *Neuroimage.* 2006 Jul 1;31(3):1116–28.
  130. Galton F. Vox Populi. *Nature.* 1949;75:450–1.
  131. Vemuri AS, Wu JC-H, Liu K-C, et al. Deformable three-dimensional model architecture for interactive augmented reality in minimally invasive surgery. *Surg Endosc.* 2012 Dec;26(12):3655–62.
  132. Shuhaiber J. Augmented Reality in Surgery. *Arch Surg.* 2004;139:170–4.
  133. Kawamata T, Iseki H, Shibasaki T, et al. Endoscopic augmented reality navigation system for endonasal transsphenoidal surgery to treat pituitary tumors: technical note. *Neurosurgery.* 2002 Jun;50(6):1393–7.
  134. Huang Q, Dom B. Quantitative methods of evaluating image segmentation. *Image Processing.* Washington: IEEE; 1995. p. 53–6.
  135. Popovic A, Fuente M, Engelhardt M, et al. Statistical validation metric for



- accuracy assessment in medical image segmentation. *Int J Comput Assist Radiol Surg.* 2007 Jul 28;2(3–4):169–81.
136. Zijdenbos a P, Dawant BM, Margolin R a, et al. Morphometric analysis of white matter lesions in MR images: method and validation. *IEEE Trans Med Imaging.* 1994 Jan;13(4):716–24.
  137. Autorino R, Zargar H, White WM, et al. Current applications of near-infrared fluorescence imaging in robotic urologic surgery: a systematic review and critical analysis of the literature. *Urology.* 2014 Oct;84(4):751–9.
  138. Fitzpatrick JM, Hill DL, Maurer CR. Image Registration. In: Beutel J, Sonka M, editors. *Handbook of Medical Imaging Medical Image Processing and Analysis.* Washington: SPIE; 2000. p. 447–513.
  139. Lam JS, Bergman J, Breda A, et al. Importance of surgical margins in the management of renal cell carcinoma. *Nat Clin Pr Urol.* 2008 Jun;5(6):308–17.
  140. Sutherland SE, Resnick MI, Maclennan GT, et al. Does the size of the surgical margin in partial nephrectomy for renal cell cancer really matter? *J Urol.* 2002 Jan;167(1):61–4.
  141. Volonté F, Pugin F, Buchs NC, et al. Console-Integrated Stereoscopic OsiriX 3D Volume-Rendered Images for da Vinci Colorectal Robotic Surgery. *Surg Innov.* 2013 May 1;20(2):158–63.
  142. Ukimura O, Gill IS. Imaging-assisted endoscopic surgery: Cleveland Clinic experience. *J Endourol.* 2008 Apr;22(4):803–10.
  143. Herrell SD, Kwartowitz DM, Milhoua PM, et al. Toward image guided robotic surgery: system validation. *J Urol.* 2009;181(2):783–90.
  144. Kwartowitz DM, Herrell SD, Galloway RL. Update: Toward image-guided robotic surgery: determining the intrinsic accuracy of the daVinci-S robot. *Int J Comput Assist Radiol Surg.* 2007 Feb 18;1(5):301–4.
  145. Kwartowitz DM, Miga MI, Herrell SD, et al. Towards image guided robotic surgery: multi-arm tracking through hybrid localization. *Int J Comput Assist Radiol Surg.* 2009 May;4(3):281–6.
  146. Nakamoto M, Ukimura O, Gill I. Realtime organ tracking for endoscopic augmented reality visualization using miniature wireless magnetic tracker. *Medical imaging and augmented reality : 4th International Workshop.* 2008. p. 359–66.
  147. Benincasa AB, Clements LW, Herrell SD, et al. Feasibility study for image-

- guided kidney surgery: Assessment of required intraoperative surface for accurate physical to image space registrations. *Med Phys*. 2008;35(9):4251–61.
148. Denavit J, Hartenberg R. A kinematic notation for lower- pair mechanisms based on matrices. *Trans ASME J Appl Mech*. 1955;23:215–21.
  149. Kwartowitz DM, Herrell SD, Galloway RL. Toward image-guided robotic surgery: determining intrinsic accuracy of the da Vinci robot. *Int J Comput Assist Radiol Surg*. 2006 Oct 11;1(3):157–65.
  150. Glisson C, Ong R, Simpson A, et al. The use of virtual fiducials in image-guided kidney surgery. *SPIE Med Imaging*. 2011 Mar 3;796402–9.
  151. Ukimura O, Nakamoto M, Gill IS. Surgical Navigation Using Three-Dimensional Computed Tomography Images Fused Intraoperatively with Live Video. *Eur Urol*. 2011/09/23. Switzerland: Center for Image-Guided Surgery and Center for Advanced Robotic and Laparoscopic Surgery, USC Institute of Urology, Keck School of Medicine, University of Southern California, Los Angeles, CA 90089, USA. ukimura@usc.edu; 2012 Jan;61(1):211–7.
  152. Baumhauer M, Simpfendorfer T, Muller-Stich BP, et al. Soft tissue navigation for laparoscopic partial nephrectomy. *Int J Med Robot Comput Assist Surg*. 2008 May 29;3(3–4):307–14.
  153. Su L-M, Vagvolgyi BP, Agarwal R, et al. Augmented reality during robot-assisted laparoscopic partial nephrectomy: toward real-time 3D-CT to stereoscopic video registration. *Urology*. 2009 Apr;73(4):896–900.
  154. Zhang Z. Flexible camera calibration by viewing a plane from unknown orientations. *Proc IEEE Int Conf Comput Vis*. 1999;1:666–73.
  155. Stoyanov D, Scarzanella MV, Pratt P, et al. Real-time stereo reconstruction in robotically assisted minimally invasive surgery. *Med Image Comput Comput Assist Interv*. 2010 Jan;13(Pt 1):275–82.
  156. Yip M, Lowe D, Salcudean S, et al. Tissue Tracking and Registration for Image-Guided Surgery. *IEEE Trans Med Imaging*. 2012;31(11):2169–82.
  157. Glisson C, Ong R, Simpson A, et al. Registration methods for gross motion correction during image guided kidney surgery. *Int J Comput Assist Radiol Surg*. 2011;Conference:Computer Assisted Radiology and Surgery-25th Int.
  158. Ong RE, Herrell S. Duke, Miga MI, et al. A kidney deformation model for use in non-rigid registration during image-guided surgery. *Medical Imaging*. 2008. p. 69180W.

159. Biot M. General theory of three-dimensional consolidation. *J Appl Phys.* 1941;12(2):155–64.
160. Orth RC, Wallace MJ, Kuo MD. C-arm cone-beam CT: general principles and technical considerations for use in interventional radiology. *J Vasc Interv Radiol.* 2008 Jun;19(6):814–20.
161. Rafferty MA, Siewerdsen JH, Chan Y, et al. Intraoperative cone-beam CT for guidance of temporal bone surgery. *Otolaryngol Head Neck Surg.* 2006 May 1;134(5):801–8.
162. Daly MJ, Siewerdsen JH, Moseley DJ, et al. Intraoperative cone-beam CT for guidance of head and neck surgery: Assessment of dose and image quality using a C-arm prototype. *Med Phys.* 2006;33(10):3767–80.
163. Yamamoto T, Abolhassani N, Jung S, et al. Augmented reality and haptic interfaces for robot-assisted surgery. *Int J Med Robot Comput Assist Surg.* 2012;8(November 2011):45–56.
164. Diana M, Marescaux J. Robotic surgery. *Br J Surg.* 2015;102:e15–28.
165. Volonté F, Pugin F, Bucher P, et al. Augmented reality and image overlay navigation with OsiriX in laparoscopic and robotic surgery: not only a matter of fashion. *J Hepatobiliary Pancreat Sci.* 2011 Jul;18(4):506–9.
166. Horn BKP. Closed-form solution of absolute orientation using unit quaternions. *J Opt Soc Am A.* 1987;4(April):629–42.
167. Huynh DQ. Metrics for 3D Rotations: Comparison and Analysis. *J Math Imaging Vis.* 2009 Jun 18;35(2):155–64.
168. Rosset A, Spadola L, Ratib O. OsiriX: an open-source software for navigating in multidimensional DICOM images. *J Digit Imaging.* 2004 Sep;17(3):205–16.
169. Ficarra V, Novara G, Secco S, et al. Preoperative aspects and dimensions used for an anatomical (PADUA) classification of renal tumours in patients who are candidates for nephron-sparing surgery. *Eur Urol.* 2009 Nov;56(5):786–93.
170. Dindo D, Demartines N, Clavien P-A. Classification of Surgical Complications. *Ann Surg.* 2004 Aug;240(2):205–13.
171. R Core Team. *R: A language and environment for statistical computing.* R Foundation for Statistical Computing. Vienna: R Foundation for Statistical Computing; 2013.
172. Taylor R. Interpretation of the Correlation Coefficient: A Basic Review. *J Diagnostic Med Sonogr.* 1990;6(1):35–9.

173. Volonté F, Buchs N. Augmented reality to the rescue of the minimally invasive surgeon. The usefulness of the interposition of stereoscopic images in the Da Vinci™ robotic console. *Int J Med Robot*. 2013;9(3):e34–8.
174. Lasser MS, Doscher M, Keehn A, et al. Virtual surgical planning: a novel aid to robot-assisted laparoscopic partial nephrectomy. *J Endourol*. 2012 Oct;26(10):1372–9.
175. Isotani S, Shimoyama H, Yokota I, et al. Feasibility and accuracy of computational robot-assisted partial nephrectomy planning by virtual partial nephrectomy analysis. *Int J Urol*. 2015;Epub ahead of print.
176. Herrell SD. Toward image-guided robotic surgery: Determining intrinsic accuracy of the da Vinci robot. *Urol Oncol*. 2007;25(2):175–6.
177. Hughes-Hallett A, Mayer EK, Marcus HJ, et al. Inattention blindness in surgery. *Surg Endosc*. 2015;
178. Hughes-Hallett A, Mayer EK, Pratt PJ, et al. The current and future use of imaging in urological robotic surgery: a survey of the European Association of Robotic Urological Surgery. *Int J Med Robot Comput Assist Surg*. 2015;11:8–14.
179. Hughes-Hallett A, Mayer EK, Pratt PJ, et al. Quantitative analysis of technological innovation in minimally invasive surgery. *Br J Surg*. 2015;102:151–7.
180. Pratt P, Di Marco A, Payne C, et al. Intraoperative ultrasound guidance for transanal endoscopic microsurgery. *Med Image Comput Comput Assist Interv*. 2012 Jan;15(Pt 1):463–70.
181. Pratt P, Jaeger A, Hughes-Hallett A, et al. Robust Ultrasound Probe Tracking: Initial Clinical Experiences During Robot-Assisted Partial Nephrectomy. 6th International Conference on Information Processing in Computer-Assisted Interventions. 2015.
182. Kaehler A, Gary B. *Learning OpenCV*. O’Rielly Media Inc; 2013.
183. Suzuki S, be K. Topological structural analysis of digitized binary images by border following. *Comput Vision, Graph Image Process*. 1985 Apr;30(1):32–46.
184. Fernandez A, Chen E, Moore J, et al. Preliminary assessment of a renal tumor materials model. *J Endourol*. 2011 Aug;25(8):1371–5.
185. Surry KJM, Austin HJB, Fenster a, et al. Poly(vinyl alcohol) cryogel phantoms for use in ultrasound and MR imaging. *Phys Med Biol*. 2004 Dec

- 21;49(24):5529–46.
186. Hirschmüller H. Stereo processing by semiglobal matching and mutual information. *IEEE Trans Pattern Anal Mach Intell.* 2008;30(2):328–41.
  187. Hoppe H. New quadric metric for simplifying meshes with appearance attributes. *Proc IEEE Int Conf Comput Vis.* IEEE Computer Society; 1999.
  188. Krekel NM a, Haloua MH, Lopes Cardozo AMF, et al. Intraoperative ultrasound guidance for palpable breast cancer excision (COBALT trial): a multicentre, randomised controlled trial. *Lancet Oncol.* 2013 Jan;14(1):48–54.
  189. Volpe A, Blute ML, Ficarra V, et al. Renal Ischemia and Function After Partial Nephrectomy: A Collaborative Review of the Literature. *Eur Urol.* 2015;68(1):61–74.
  190. Harms J, Feussner H, Baumgartner M, et al. Three-dimensional navigated laparoscopic ultrasonography: First experiences with a new minimally invasive diagnostic device. *Surg Endosc.* 2001;15(12):1459–62.
  191. Benway BM, Bhayani SB. Surgical outcomes of robot-assisted partial nephrectomy. *BJU Int.* England; 2011 Sep;108(6 Pt 2):955–61.
  192. Fernandez A, Chen E, Moore J, et al. A phantom model as a teaching modality for laparoscopic partial nephrectomy. *J Endourol.* 2012 Jan;26(1):1–5.
  193. Marcus HJ, Pratt P, Hughes-Hallett A, et al. Comparative effectiveness and safety of image guidance systems in surgery: a preclinical randomised study. *Lancet.* 2015;385:S64.
  194. Soler L, Nicolau S, Pessaux P, et al. Real-time 3D image reconstruction guidance in liver resection surgery. *Hepatobiliary Surg Nutr.* 2014;3(2):73–81.
  195. Willaert WIM, Aggarwal R, Van Herzeele I, et al. Recent advancements in medical simulation: patient-specific virtual reality simulation. *World J Surg.* 2012 Jul;36(7):1703–12.
  196. Willaert WIM, Aggarwal R, Daruwalla F, et al. Simulated procedure rehearsal is more effective than a preoperative generic warm-up for endovascular procedures. *Ann Surg.* 2012 Jun;255(6):1184–9.
  197. Makiyama K, Yamanaka H, Ueno D, et al. Validation of a patient-specific simulator for laparoscopic renal surgery. *Int J Urol.* 2015;
  198. Makiyama K, Nagasaka M, Inuiya T, et al. Development of a patient-specific simulator for laparoscopic renal surgery. *Int J Urol.* 2012 Sep;19(9):829–35.
  199. Wilpert B, Qvale TU. Safety in Flight Operations. *Reliability and Safety in*

- Hazardous Work Systems: Approaches to Analysis and Design. Psychology Press; 1993. p. 171–94.
200. Boeing. Statistical Summary of Commercial Jet Airplane Accidents. Worldwide Operations | 1959 – 2013. Seattle; 2013.
  201. Volpe A, Cadeddu J a, Cestari A, et al. Contemporary management of small renal masses. *Eur Urol*. 2011 Sep;60(3):501–15.

## APPENDICES

## Appendix 1. – The use of imaging in robotic surgery questionnaire

Question Asked	Question Type
<b>Demographics</b>	
In which country do you usually practise?	Single best answer
Which robotic procedures do you perform?*	Single best answer
<b>Current Imaging Practice</b>	
What preoperative imaging modalities do you use for the staging and surgical planning in renal cancer?	Multiple choice
How do you typically view preoperative imaging in theatre for renal cancer surgery?	Multiple choice
Do you use intraoperative ultrasound for partial nephrectomy?	Yes or No
What preoperative imaging modalities do you use for the staging and surgical planning in prostate cancer?	Multiple choice
How do you typically view preoperative imaging in theatre for prostate cancer?	Multiple choice
Do you use intraoperative ultrasound for robotic partial nephrectomy?	Yes or No
Which preoperative imaging modality do you use for staging and surgical planning in muscle invasive TCC?	Multiple choice
How do you typically view preoperative imaging in theatre for muscle invasive TCC?	Multiple choice
Do you routinely refer to preoperative imaging intraoperatively?	Yes or No
Do you routinely use Tilepro intraoperatively?	Yes or No
<b>Augmented Reality</b>	
Do you feel there is a role for augmented reality as a navigation tool in robotic surgery?	Yes or No
Do you feel there is a role for augmented reality as a training tool in robotic surgery?	Yes or No
In robotic partial nephrectomy which parts of the operation do you feel augmented reality image overlay technology would be of assistance?	Multiple choice
In robotic nephrectomy which parts of the operation do you feel augmented reality image overlay technology would be of assistance?	Multiple choice
In robotic prostatectomy which parts of the operation do you feel augmented reality image overlay technology would be of assistance?	Multiple choice
Would augmented reality guidance be of use in lymph node dissection in robotic prostatectomy?	Yes or No
In robotic cystectomy which parts of the operation do you feel augmented reality image overlay technology would be of assistance?	Multiple choice
Would augmented reality guidance be of use in lymph node dissection in robotic cystectomy?	Yes or No



## **Appendix 2. – Ethics Documentation**

### **A2.1 Study Protocol**

#### Improving Outcomes in Robotic and Endoscopic Surgery using Augmented Reality Guidance

##### **Background**

The purpose of this research is to establish the feasibility and utility of a system for guidance during robotic and endoscopic surgery. There are three clinical exemplars for this research – urological, transanal, gynaecological. The guidance is based on preoperative and intraoperative imaging aligned to the patient on the operating table and presented to the surgeon as graphics overlaid onto or displayed alongside the endoscopic view. This mixing of a real and virtual views is often termed “augmented reality”. It is hoped and anticipated that in the longer term this guidance will help achieve more accurate surgery, leading to a better rate of full lesion extraction, whilst minimising damage to surrounding tissue.

In the case of urological surgery this should result in improved continence and potency for patients with prostate cancer, and improve tissue preservation and reduce recurrence in patients with cancer of the kidney. For transanal interventions, this should result in more accurate intraoperative visualisation of rectal lesions, specifically their depth of penetration and lateral spread, thereby facilitating complete excision, while minimising the risks of bowel wall perforation and blood loss from concealed, subsurface vessels. In gynaecological interventions it is hoped the technology will assist in more accurately locating lymph nodes during lymph node sampling for gynaecological malignancy.

This research aims to combine improved alignment and visualisation in augmented reality image guidance for robotic and endoscopic surgery with its initial evaluation in the operating theatre. The technical improvements will be led by clinical requirements as established by evaluation in the clinical environment. In this way we can ensure that technological research is closely focused on the needs of the surgeon. We have previously found that this methodology leads to rapid convergence to a system that can be clinically useful.

## Patient Recruitment

The participants will be scheduled to undergo robotic or endoscopic surgery. Any patient who is to undergo such procedures could be recruited. The initial approach will be from the consultant or other member of the surgical team who are managing the patient care.

## Preoperative Imaging

The patient will have had prior diagnostic imaging. This will be made anonymous (coded) and transferred to the imaging database at Imperial College. Depending on the quality of these images the patient may also be asked to have a further MRI scan prior to surgery. This will be a high-resolution scan of the relevant anatomical region.

From these images a 3D surface model of the patient's anatomy will be created. Structures to be identified will include the target lesion and surrounding tissue, nerves or blood vessels. The method of model building is the subject of ongoing research, but volume rendering and segmental reconstruction will be used in the first instance.

Figures 1 and 2 illustrate typical preoperative scans and corresponding 3D models.

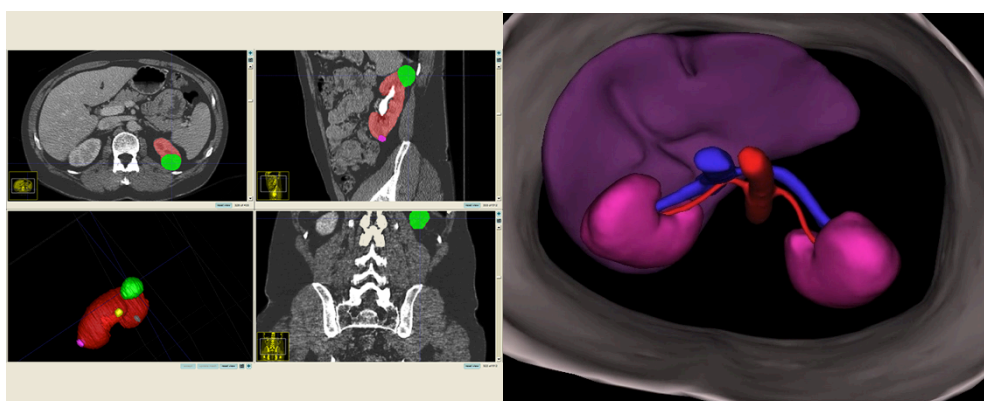


Figure 1 – Segmented CT scan and 3D model of kidneys, tumour, vessels and liver



Figure 2 – Segmented scan and model of rectal wall and embedded lesion

### **Intraoperative Data Collection**

During the operation, video captured through the stereo endoscope will be gathered. This will happen for brief periods at several stages throughout the operation, or the entire operation may be recorded. Initially after placement of the endoscope, but before resection begins, the visible surface and features for registration will be imaged. This will enable rigid registration of the preoperative model by hand and by stereo reconstruction of the visible surface. For pelvic surgery, the pelvic arch can generally be seen and the position of the pubic symphysis can be inferred. For partial nephrectomy, the surface of the kidney itself can be used, since this is a fairly rigid structure. For transanal resections the bony landmarks of the symphysis pubis and anterior superior iliac spines can be utilised.

As well as intraoperative video collection, data may be gathered about the endoscope and instrument kinematics. In the case of the da Vinci system, this can be achieved by connecting the data collection computer to the robot master via an Ethernet link. There is no possibility of control of the robot or alterations in its function and the system will simply record the positions of the robot arm encoders passively. In the non-robotic case, the location and orientation of the endoscope are captured using electromagnetic or optical tracking technology. This data is vital to the development of automated alignment and tracking methods.

As the surgery proceeds, further video images will be taken. These will allow the accuracy of overlay to be assessed. Different structures will be overlaid and the surgeon will be asked to assess which preoperative data is most useful and to estimate the accuracy of alignment. Other

landmarks from the preoperative images and further structures will also be used to judge accuracy.

If intraoperative tracked ultrasound is available, this will also be utilised and collected. It provides real-time 2D and 3D imaging during the operation. This can be used to examine how the soft tissue is deforming during surgery and help to develop methods for non-rigid alignment of the preoperative model. The ultrasound probe itself will be held in a custom designed cobalt chrome alloy clip allowing it to be grasped by the instrument being used.

### **Storage and Analysis of Retrospective Data**

The preoperative imaging data, intraoperative video, and any ultrasound images will be stored on the Imperial College network. This data will enable development and testing of methods and algorithms for alignment and visualisation in the laboratory.

All data will be anonymised and the patient name will be replaced by a code. The cross-reference between this code and the participant's identification will be stored only within the radiology department at St Mary's Hospital. Should any unexpected pathology be discovered the code can be used to inform the medical team managing the patient's care, and ultimately the patients themselves.

### **Intraoperative Display**

Once the equipment is in place to provide overlays on the surgeon's view during the operation these will be displayed during the procedure. The aim will be to examine different display strategies. As well as deciding what structures are useful to visualise, we will aim to optimise different display parameters, for example the mixing level, colour and image orientation (Figure 3). This should enable us to specify an overlay strategy that provides good visualisation. This specification will continue to be updated in response to clinical feedback. The clinical evaluation of the full display system will also enable us to incorporate guidance into the clinical workflow in an ergonomic fashion. The system will be utilised to assist the surgeon in appreciating the surrounding subsurface anatomy but will not be used for the live intraoperative guidance of tumour resection.

Figures 4, 5 and 6 illustrate typical usage scenarios in two of the exemplar application areas.

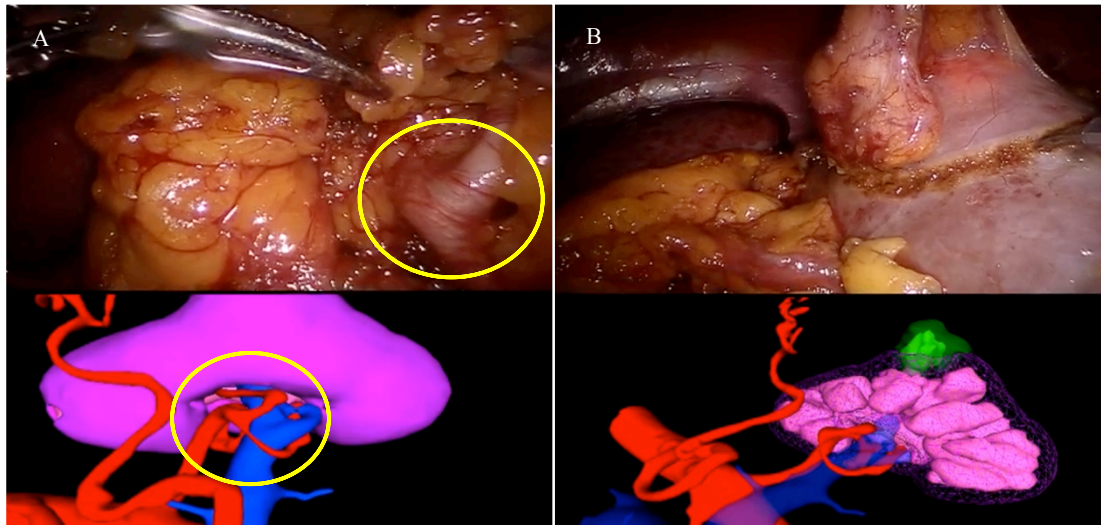


Figure 3 – The console view with TilePro™ enabled. a) The complex hilar vascular anatomy is seen within the image allowing the surgeon to better appreciate the anatomy seen in the operative view. b) The surgeon is able to plan tumour resection by making the surface of the kidney a polygon mesh while keeping the tumour solid

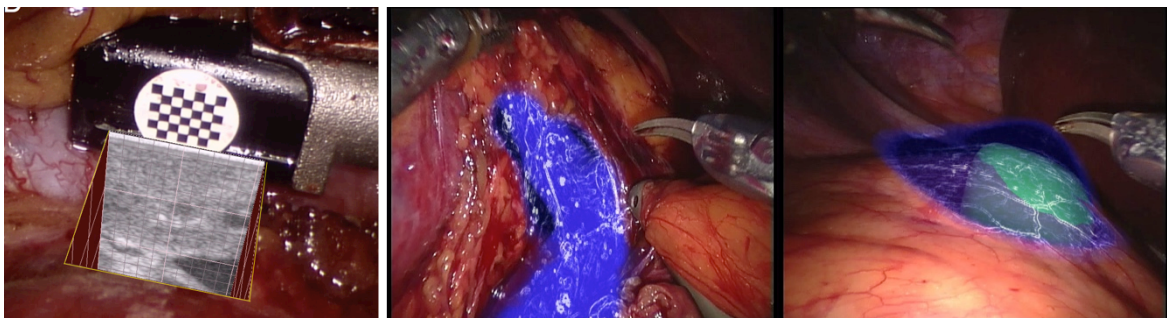


Figure 5 – 2D ultrasound overlay and preoperative imaging overlays showing inferior vena cava (blue) and target lesion (green)

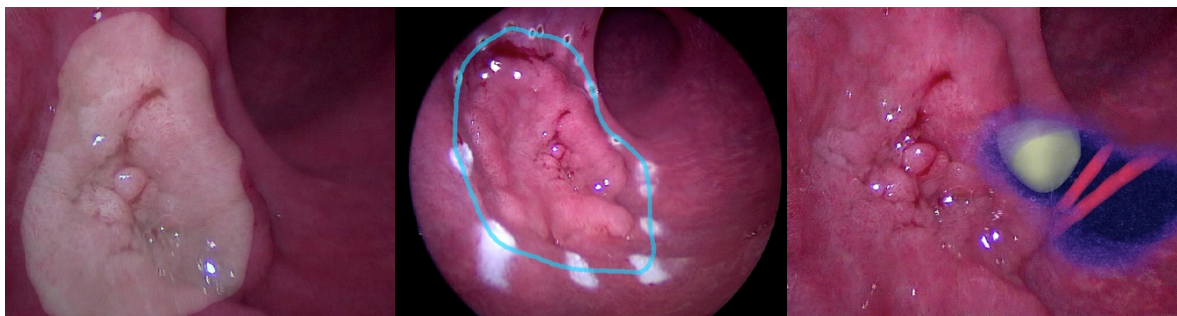


Figure 6 – Overlays showing target lesion, marked excision boundary and structures beneath surface of rectal wall

## **Postoperative Follow-up**

Limited follow-up information will be gathered, consisting of any immediate complications as well as tumour recurrence and postoperative function. Only data already being gathered as part of an audit or as clinical routine will be included. There will be no contact between the patient and the research team for this data collection.

## **Analysis of Results**

The results will be an initial evaluation of the system in terms of accuracy, 3D perception, clinical utility and an initial assessment of outcome. Reports will be written detailing the initial clinical evaluation of the system and giving assessment of the accuracy and improvements to visualisation. There will be no significant statistical analysis, as we are not testing a specific hypothesis. Rather we are using clinical data and experience to drive technological research in a direction that is heavily focused on the surgical application. The results will be reported in peer-reviewed journals and academic conference.

## **A2.2 Participant information sheet**

### Improving Outcomes in Robotic and Endoscopic Surgery using Image guidance Technology

#### Participant Information Sheet

You are invited to take part in a research study. Before you decide, it is important for you to understand why the research is being done and what it will involve. Please take the time to read this information sheet carefully and if you have any questions, please contact the researcher (*contact details at bottom of sheet*).

What is the purpose of this study?

There is increasing interest in the use of graphical overlays to help guide surgeons during a number of different operations. In this study we are interested in any surgery performed using the “da Vinci” robot, but specifically surgical removal of the prostate and partial nephrectomy. The use of a surgical robot enables accurate surgery to be performed through small incisions. We are also interested in transanal endoscopic microsurgery for the removal of tumours in the rectum, and minimally invasive surgery for gynaecological malignancy. However, as with all such surgery, there are small risks of complications due to failure to fully remove the diseased tissue, or from damage to surrounding healthy anatomy. The aim of this work is to investigate whether surgery can be made more accurate and safe by overlaying graphics on the surgeon’s view, showing the target area and surrounding structures. These graphics come from scans taken before or during the operation.

The research will involve development of the methods for aligning the graphics accurately, identifying what information is the most useful and defining how this information should be displayed. The data from your operation will help us to develop this technique and to establish whether it is likely to be of use to the surgeon.

Why have I been chosen?

You have been chosen because you are due to undergo surgery within Imperial NHS trust either with the “da Vinci” surgical robot, or you are due to have transanal or minimally invasive gynaecological surgery.

Do I have to take part?

No - it is entirely up to you whether or not you participate. If you choose to take part, you will be given this information sheet to keep and will be asked to sign a consent form. You are free to withdraw at any time and a decision not to take part will NOT affect the standard of care that you receive. You may also choose not to be included in any specific part of the study.

What will happen to me if I take part?

If you decide to take part, a doctor from your surgical care team will then ask you to sign a consent form. You will be asked to allow us access to your scan data and you may be asked to have a further MRI scan to help us define your anatomy accurately. These are the only parts of the study that occur outside the operation.

During the operation, video images through the endoscope that the surgeon uses to perform the operation will be gathered along with positional data. These will be stored and used at a later time to test the accuracy of different methods of alignment.

The graphical overlays may also be displayed during your operation. This will help us test different methods of display and for the surgeon to assess what types of display are most likely to be useful, it will also help the surgeon to better understand the parts of your anatomy that they cannot see.

Further images from intraoperative and ultrasound scans may also be gathered during your operation. The probe will be used to gather and overlay images showing the position and shape of your anatomy as the operation proceeds. This again will be used to help the surgeon understand the anatomy not directly visible to them.



Finally, we would also like to gather information on how successful the surgery was. This will be stored in an anonymous form and will not require any further correspondence with you.

It will be made very clear by the doctor asking you to take part in this study and on the consent form which parts of this process you are being asked to take part in. You can choose to agree or not to agree to any of these stages.

This study is unlikely to affect your treatment or to have therapeutic benefit to you, but may help improve the surgical treatment of patients in the future.

#### Risks and disadvantages of taking part

It is highly unlikely that this study will pose any risks or disadvantages to you. The system merely adds some graphical information to the surgeon's view for periods during your operation. This information will not be used to help the surgeon understand the anatomy that surrounds them but should have little effect how he performs the operation.

#### Possible benefits of taking part

The surgeon will have a better appreciation of the target organ and surrounding anatomy. This will potentially lead to improved surgical dissection, resulting in potentially quicker recovery times, lower rates of complication, and to potentially more accurate local tumour excision.

#### What do I have to do next?

Once you have consented to take part in the study you may be asked to have a further MRI scan. After this, any additional information is gathered during surgery so you do not have to do anything. After surgery, information will be obtained from the medical team in charge of your care about the success of the operation, but again this will not require your involvement.

What will happen to the information I give?

The information produced is confidential and will be stored anonymously and your name will be replaced by a code. It will be kept in a database at Imperial College. It will not be made available to anyone outside of the research group or used for any other purpose without the prior approval of the Research Ethics Committee. All information about you will be kept confidential.

It is very unlikely, but in some cases another problem or illness may be detected in your scans that was not apparent at the time it was taken. In this case, the code that replaced your name can be used to trace your identity so we can contact you and your doctor to inform you of these findings.

We will keep the database of information for a minimum of 5 years. This will allow us to develop methods to improve alignment and visualisation in the future, and means that any results that may have been published can be verified. We may want to use the information for further research projects, but only if they are approved by the Research Ethics Committee.

What will happen to the results of the research study?

The results may be published in peer-reviewed journals, which will be available to your doctor and surgeon, and may aid in the future management of your disease. Results may also be presented at conferences or internal meetings within St Mary's Hospital or Imperial College, London. Your name will not be disclosed in any of the results. At the end of the study, a summary of the results will be available for you.

Who has reviewed the study?

The Research Ethics Committee has reviewed this study, and has given ethical approval.

## Contact Details

Erik Mayer

Clinical Lecturer in Surgery

Department of Surgery and Cancer

Imperial College, London,

10<sup>th</sup> Floor QEQM Wing,

St. Mary's Hospital,

Praed Street,

London W2 1NY

e.mayer@imperial.ac.uk

**Thank you for taking time to read this information sheet. A copy of the consent form is included in this pack.**

### A2.3 Consent form

Centre: St. Mary's Hospital NHS Trust

Study Number:

Patient Identification Number for this trial:

## CONSENT FORM

**Title of Project: Improving Outcomes in Robotic and Endoscopic Surgery using Augmented Reality Guidance**

Name of Researcher: Mr Erik Mayer

Please initial any boxes that have not been crossed out

I confirm that I have read and understand the information sheet for the above study. I have had the opportunity to consider the information, ask questions and have had these answered satisfactorily.

I understand that my participation is voluntary and that I am free to withdraw at any time, without giving any reason, without my medical care or legal rights being affected.

I consent to the recording of endoscopic video and the collection of tracking data during my operation.

I agree to intraoperative internal or external ultrasound image collection during my operation.

I consent to the display of graphical overlays on the surgeon's view.

I understand that all information, including images and information about surgical outcome will be stored in an Imperial College database in an anonymous form.

I agree to take part in the above study.

\_\_\_\_\_  
Name of participant

\_\_\_\_\_  
Signature

\_\_\_\_\_  
Date

\_\_\_\_\_  
Name of person taking consent

\_\_\_\_\_  
Signature

\_\_\_\_\_  
Date

When completed, 1 copy for patient; 1 copy for researcher site file; and 1 copy (original) to be kept in medical notes

## 1.1 Appendix 3. – Inattention blindness in surgery data collection tool

**Imperial College  
London**

Cognitive load in augmented reality - Mesh control

0%  100%

General questions

\* What is your name?

\* Are you male or female?  
Choose one of the following answers

Male  
 Female

\* How old are you?  
Only numbers may be entered in this field.

\* How many years post graduation are you?  
Only numbers may be entered in this field.

\* Have you ever utilised an augmented reality or surgical image guidance platform before? (if yes please give details in the comments box)  
Choose one of the following answers

Yes  
 No

Please enter your comment here:

Exit and clear survey Next >

Page 1. Demographic data - Shown to all participants



Page 2. Operative video, participants were only allowed to view this a single time (type of overlay varied depending on randomisation group)

The image shows a survey form interface. At the top left is the Imperial College London logo. At the top right, the title 'Cognitive load in augmented reality - Mesh control' is displayed above a progress bar showing 0% to 100%. Below the title is the text 'Post video group'. The main area contains a question: 'How many instrument movements were there? (if you were not asked to count instrument movements leave this blank)'. Below the question is a text input field. A note below the question reads 'Only numbers may be entered in this field.' The form has a light gray background.

Page 3. Instrument movement count - Shown to all participants

**\***

Please rate your agreement with the following statement:

**'I believe image overlay would improve the accuracy of tumour resection'**

*Choose one of the following answers*

Strongly agree

Agree

Slightly agree

Undecided

Slightly disagree

Disagree

Strongly disagree

**\***

Please rate your agreement with the following statement:

**'The image overlay impaired my ability to appreciate all features in the operative environment.'**

*Choose one of the following answers*

Strongly agree

Agree

Slightly agree

Undecided

Slightly disagree


Disagree

Strongly disagree

Page 4. Subjective effect of image overlay - Only shown to participants who were shown video with image overlay

**Imperial College London**

Cognitive load in augmented reality - Mesh control

0%  100%

Post video group 2

\* Did you see any items in the operative field other than the robotic surgical instruments or assistant's suction device (i.e foreign bodies, other surgical instruments or devices)?


Yes  No

If so what did you see?

Page 5. Inattention blindness assessment - Shown to all participants

**Imperial College London**

Cognitive load in augmented reality - Mesh control

0%  100%

Post video group 3


\* Did you see a swab in the operative field of view?

Yes  No

Page 6. Shown to all participants

**Imperial College London**

Cognitive load in augmented reality - Mesh control

0%  100%

Post video group 4

\* Did you see a suture and thread in the operative field of view?

Yes  No

Page 7. Inattention blindness assessment - Shown to all participants





## **1.2 Appendix 4. – Creation of a high fidelity kidney phantom for simulating ultrasound guided partial nephrectomy**

### **A4.1 Renal Cast production**

For the kidney mould a 3D model of an undiseased kidney was 3D printed from segmentations derived from a patients CT scan. Subsequent to this the 3D printed kidney was used to cast a silicone mould from which multiple versions of the same kidney could be created.

### **A4.2 Cryogel**

A PVA solution was created based on the technique described by Fernandez *et al.*<sup>184,192</sup> A solution of 10% PVA, by mass, in water was created by mixing 100g of PVA (Sigma-Aldrich) with 900g of distilled water. Once mixed, the PVA granules were brought into solution by holding the mixture at 85°C for one hour with occasional agitation. The liquid was then checked by eye to ensure that there was no residual PVA out of solution. If any PVA granules remained the solution was held at 85°C for a further 30 minutes at which point the procedure was repeated.

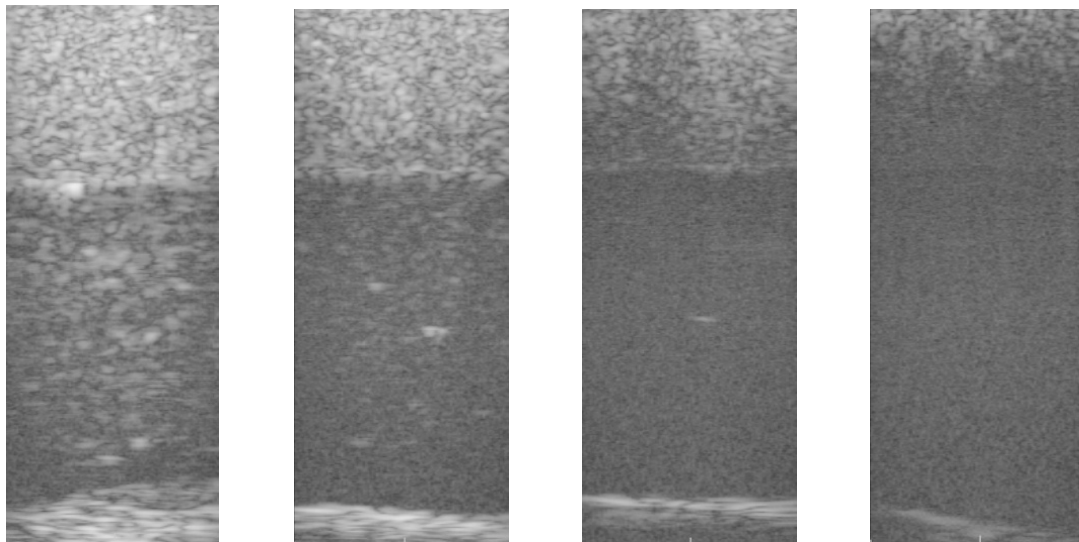
Once the solution had been formed, it was allowed to settle for 24 hours order to allow any air bubbles to rise to the surface. Once cooled, the solution was made back up to 1000g using distilled water to ensure a concentration of 10%. Subsequently, 0.8% by weight of red enamel paint was then added to the solution – this has been shown to have a minimal effect of the acoustic properties of the cryogel.<sup>185</sup> The solution was then kept at room temperature until needed.

This 10% PVA cryogel (PVA-C) was used as the basis for both the tumour and normal parenchyma within the phantom.

### A4.3 Creation of partial nephrectomy phantom

Initially a tumour-specific PVA-C was created by adding 2% (by weight) cellulose powder in order create a well-defined echogenic border between the ‘normal parenchyma’ and ‘tumour tissue’ (Figure A3.3.1).

The tumour PVA-C was then cast into 2.5ml spheres. These were subsequently subjected to a single freeze thaw cycle. Subsequent to this, two spheres were suspended in the kidney (Figure A3.3.2), this was then filled with PVA-C and subjected to a further freeze thaw cycle. This results in a phantom in which the kidney has been subjected to a single freeze thaw cycle and a tumour that has been subjected to two (Figure A3.3.3).



Figure

A3.3.1 – Different % of cellulose by weight over 0% cellulose to establish echogenic properties of differing mixes. From left to right 2%, 4%, 6%, 8%. All cryogels were subjected to two freeze thaw cycles.



Figure A3.3.2 – Tumour phantoms in place prior to filling of renal mould



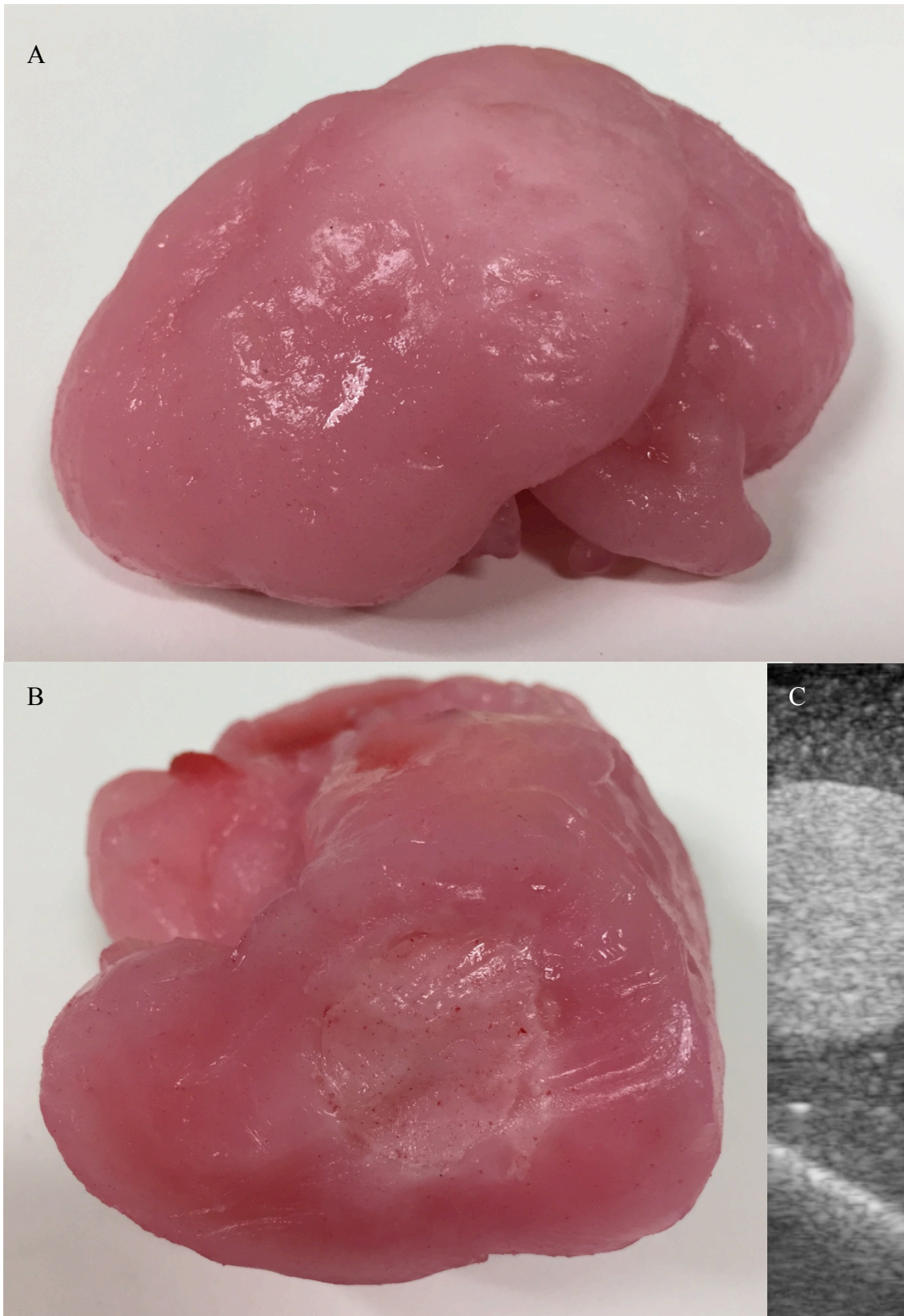


Figure A3.3.3 - High fidelity phantom for the simulation of partial nephrectomy. A) Phantom B) Axial section through phantom, phantom tumour can be seen in the centre of the section C) Ultrasound view of tumour within kidney phantom.